ort No. FHWA-RD-77-111

# SIGN OF ZERO-MAINTENANCE PLAIN JOINTED CONCRETE PAVEMENT

## Vol. I-Development of Design Procedures

June 1977

Final Report





Prepared for

FEDERAL HIGHWAY ADMINISTRATION
Offices of Research & Development
Washington, D.C. 20590

## FOREWORD

Volume I presents the development of comprehensive procedures for the structural design of "Zero-Maintenance" plain jointed concrete pavements for heavily trafficked roadways. These design procedures are based upon results from long-term field studies, comprehensive mechanistic analysis, and laboratory studies.

This report completes a set of three prepared by the University of Illinois under research contract with the Structures and Applied Mechanics Division, Office of Research of the Fed ·al Highway Administration. The first report is FHWA-RD-76-105, "Zero-Maintenance Pavements: Results of Field Studies on the Performance Requirements and Capabilities of Conventional Pavement Systems."

Procedures and specifications for designing the concrete slab, subbase, shoulders, joints, and subsurface drainage are presented in FHWA-RD-77-112, Volume II, Design Manual.

The report is intended primarily for research and development audiences. Copies are being distributed accordingly by transmittal memorandum.

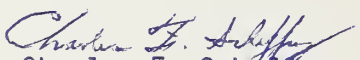

Charles F. Scheffey
Director, Office of Research
Federal Highway Administration

## NOTICE

Technical Report Documentation Page

| 1. Report No. | 2. Government Accession No. | 3. Recipient's Catalog No. |
|---|---|---|
| FHWA-RD-77-111 | | |

| 4. Title and Subtitle | 5. Report Date |
|---|---|
| Design of Zero-Maintenance Plain Jointed Concrete Pavement, Vol. I - Development of Design Procedures | 8 June 1977 |
| | 6. Performing Organization Code |
| 7. Author(s) | 8. Performing Organization Report No. |
| Michael I. Darter | FHWA-RD-77-111 |
| 9. Performing Organization Name and Address | 10. Work Unit No. (TRAIS) |
| Department of Civil Engineering<br>University of Illinois at Urbana-Champaign<br>Urbana, Illinois 61801 | FCP 35E2012 |
| | 11. Contract or Grant No. |
| | DOT-FH-11-8474 |
| 12. Sponsoring Agency Name and Address | 13. Type of Report and Period Covered |
| Federal Highway Administration<br>U.S. Department of Transportation<br>Office of Research<br>Washington, D.C. 20590 | Final, 1975-1976 |
| | 14. Sponsoring Agency Code |
| | 50787 |

15. Supplementary Notes

FHWA Project Monitors: Floyd J. Stanek, Contract Manager
Thomas J. Pasko
William J. Kenis

16. Abstract

Comprehensive procedures for the structural design of "zero-maintenance" plain jointed concrete pavements for heavily trafficked roadways are developed. The term "zero-maintenance" refers to the structural adequacy of the pavement lanes and shoulder. Thus, a "zero-maintenance" pavement would not require maintenance such as patching, joint repair, crack repair, grinding, and overlays. The design procedures are based upon results from long-term field studies, comprehensive mechanistic analyses, and laboratory studies. Both a serviceability-performance analysis and a concrete fatigue analysis are used in the structural design. Procedures are developed for designing the concrete slab, subbase, shoulders, joints and subsurface drainage. Example designs are included with sensitivity and incremental cost analyses. A computer program, JCP-1, was written to assist in the design calculations. A design manual (Vol. II) was developed based upon the results documented herein.



| 17. Key Words | 18. Distribution Statement |
|---|---|
| Pavement, design, concrete, fatigue, serviceability, performance, maintenance, distress | No restrictions. This document is available to the public through the National Technical Information Service, Springfield, Virginia 22161 |

| 19. Security Classif. (of this report) | 20. Security Classif. (of this page) | 21. No. of Pages | 22. Price |
|---|---|---|---|
| Unclassified | Unclassified | 261 | |

# PREFACE

"Design of Zero-Maintenance Plain Jointed Concrete Pavement, Vol. I - Development of Design Procedures" provides documentation of the development of procedures for the design of heavily trafficked highway pavements. The objective of the design is to provide pavements which will perform relatively maintenance-free over a selected design period. The term "zero-maintenance" refers only to structural maintenance such as patching, crack filling, slab replacement, and overlay. Procedures are developed for designing the following components of plain jointed concrete pavements: Portland cement concrete slab, subbase, shoulders, joints, and subsurface drainage. A computer program, called JCP-1, is used to provide serviceability/performance and fatigue damage data for structural design of the pavement. Manual procedures are also included to structurally design the pavement based on serviceability/performance.

This study was conducted at the Department of Civil Engineering, University of Illinois at Urbana-Champaign under sponsorship of the U.S. Department of Transportation, Federal Highway Administration. The principal investigators of the study are Dr. Michael I. Darter and Dr. Ernest J. Barenberg. The author wishes to sincerely thank the several persons who contributed directly to the development of this manual, including: Mr. Jihad Sawan, Miss H. S. Yuan, Mr. Amir M. Tabatabaie, Mr. Clive Campbell, Professor Marshall R. Thompson, and Professor Barry J. Dempsey. Thanks are also due to numerous state highway engineers from many states for providing considerable data and other assistance. Thanks are also due the FHWA project monitors Mr. William J. Kenis, Mr. Thomas Pasko, and Dr. Floyd Stanek, for their assistance and encouragement throughout the study. A special note of thanks to Mrs. Karon Webb for typing and editing this manuscript.

TABLE OF CONTENTS

# LIST OF ABBREVIATIONS

## Pavement Section

| | |
|---|---|
| AC | Asphalt Concrete |
| ADT | Two-directional Average Daily Traffic |
| ATB | Asphalt Treated Base |
| CJS | Contraction Joint Spacing |
| CTB | Cement Treated Base |
| EJS | Expansion Joint Spacing |
| ESAL | Equivalent Single Axle Loads |
| GR.B. | Granular Base of Subbase |
| JCP | Jointed Concrete Pavement (Non-reinforced) |
| JRCP | Jointed Reinforced Concrete Pavement |
| LTD | Load Transfer Device |
| PCC | Portland Cement Concrete |
| SM | Select Material |

---

## Maintenance

| | |
|---|---|
| CF | Crack Filling |
| JF | Joint Filling |
| P | Patching with AC or PCC |

## Distresses

| | |
|---|---|
| JF | Joint Faulting |
| JS | Joint Spalling |
| CF | Crack Faulting |
| CS | Crack Spalling |

Distresses (Continued)

| | |
|---|---|
| TC | Transverse Cracking |
| B | Blowups |
| CC | Corner Cracking |
| LC | Longitudinal Cracking |
| D | "D" Cracking |
| PU | Pumping |
| DC | Diagonal Cracking |

Climatic Region

| | |
|---|---|
| WF | Wet-freeze Region |
| W | Wet-nonfreeze Region |
| DF | Dry-freeze Region |
| D | Dry-nonfreeze Region |

CONVERSION FACTORS, U. S. CUSTOMARY TO METRIC (SI)
UNITS OF MEASUREMENT

U. S. customary units of measurement used in this report can be converted to metric (SI) units as follows:

| MULTIPLY | BY | TO OBTAIN |
|---|---|---|
| inches | 2.54 | centimeters |
| feet | 0.3048 | meters |
| square inches | 6.4516 | square centimeters |
| square yards | 0.83612736 | square meters |
| knots | 0.5144444 | meters per second |
| pounds | 0.45359237 | kilograms |
| kips | 0.45359237 | metric tons |
| pounds per cubic foot | 16.018489 | kilograms per cubic meter |
| pounds | 4.448222 | newtons |
| kips | 4.448222 | kilonewtons (kN) |
| pounds per square inch | 6.894757 | kilopascals |
| pounds per cubic inch | 2.7144712 | kilopascals per centimeters |
| gallons (U. S. liquid) | 3.785412 | cubic decimeters |
| Fahrenheit degrees | 5/9 | Celsius degrees of Kelvins* |

---

* To obtain Celsius (C) temperature readings from Fahrenheit (F) readings, use the following formula: $C = (5/9)(F-32)$. To obtain Kelvin (K) readings, use: $K = (5/9)(F-32) + 273.15$.

# CHAPTER 1

# INTRODUCTION

This report describes the development of comprehensive procedures for the design of "zero-maintenance" plain jointed Portland cement concrete pavement. Based upon the work described herein, a design manual, Volume II (Ref. 1), was written which gives step by step procedures for designing zero-maintenance plain jointed concrete pavements (JCP). The term "zero-maintenance" refers to the structural adequacy of the pavement travel lanes and shoulders. Thus, a zero-maintenance pavement would not require maintenance such as: patching, joint repair, crack repair, grinding, and overlays. However, activities such as mowing, guard rail repair, stripping, providing skid resistance, wear from studded tires, geometric obsolescence, and subsequent widening to increase capacity are not included in the definition of maintenance in this report.

## 1.1 BACKGROUND

Many highways in urban and suburban areas are being subjected to heavy traffic volumes which cause rapid deterioration and premature failure of pavements. Hence, considerable maintenance is required, but scheduling of remedial and preventative maintenance is almost impossible without closing lanes and producing massive traffic jams, accidents, and delays to the traveling public. Often routine maintenance is completely neglected, thus causing even more accelerated deterioration of pavements. When maintenance is performed, it is usually during off-hours or at nights. Under such conditions, repairs are often rushed and/or performed with inadequate equipment and with inadequate room to manuever. The repairs are often inefficiently

done because of logistics, traffic interference, and workers toiling under hazardous conditions. The cost of traffic control is a major item in any maintenance budget, but especially under the conditions described, and the cost of delays to the motorist because of lane closure or detours from the expressway for maintenance operations accumulates at a fantastic rate.

The fundamental question which underlies this research is: "how to design and build conventional pavements (or optimized conventional pavements in which inherent weaknesses are eliminated) to serve exceptionally heavy traffic without requiring maintenance and providing satisfactory 'rideability' for twenty years, and with only routine maintenance for an additional 10 years?" Initially five types of conventional pavements were considered including: jointed reinforced concrete, continuously reinforced concrete, flexible (including thick asphalt layers and full depth asphalt), composite (asphalt over concrete), and jointed plain concrete pavements. The first phase of the study included extensive field surveys and evaluations of over 70 heavily trafficked pavements, and the following was determined:

1. Types and causes of distress and maintenance applied on heavily trafficked pavements;
2. Adequacy of commonly used design procedures to obtain maintenance-free pavements;
3. Limiting criteria for use in designing maintenance-free pavements; and
4. Maximum maintenance-free lives of conventional pavements.

These results were documented in a report by Darter and Barenberg (Ref. 2). The second phase of the study involved the development of zero-maintenance design procedures for jointed plain concrete pavements which is contained in this report.

## 1.2 RESEARCH APPROACH

The research approach used to develop the design procedures is illustrated in Figure 1.1. Field studies were conducted and plain joined concrete pavements were examined in 10 highway agencies and extensive data collected. The types, causes, and ways to eliminate or minimize the significant distresses were identified based upon the experience of local pavement engineers and project staff, previous research studies, and analytical studies conducted as part of the project. Existing design procedures were critically evaluated as to their ability to provide zero-maintenance pavements and their limitations determined. Limiting criteria were determined for zero-maintenance design (including terminal serviceability and allowable fatigue consumption). All available long term performance data of plain jointed concrete pavements were complied which included 25 sections from the original AASHO Road Test that have been under regular traffic since 1962 on I-80 in Illinois and 12 other projects located in various climatic regions which vary in age from 6 to 34 years. Analytical models and procedures for slab stress/strain computation and fatigue damage were developed, and a new serviceability/performance model was derived. A comprehensive fatigue analysis procedure was developed and verified that gives accumulated fatigue damage at the most critical point in the slab considering both traffic load applications and curling of the slab. A comprehensive yet practical design procedure was developed that considers both fatigue damage and serviceability loss in selection of the final pavement structure. Design recommentations were also developed for other components of the pavement system, including shoulders, joints, subbase, and subsurface drainage based upon results from the overall study and other research results.

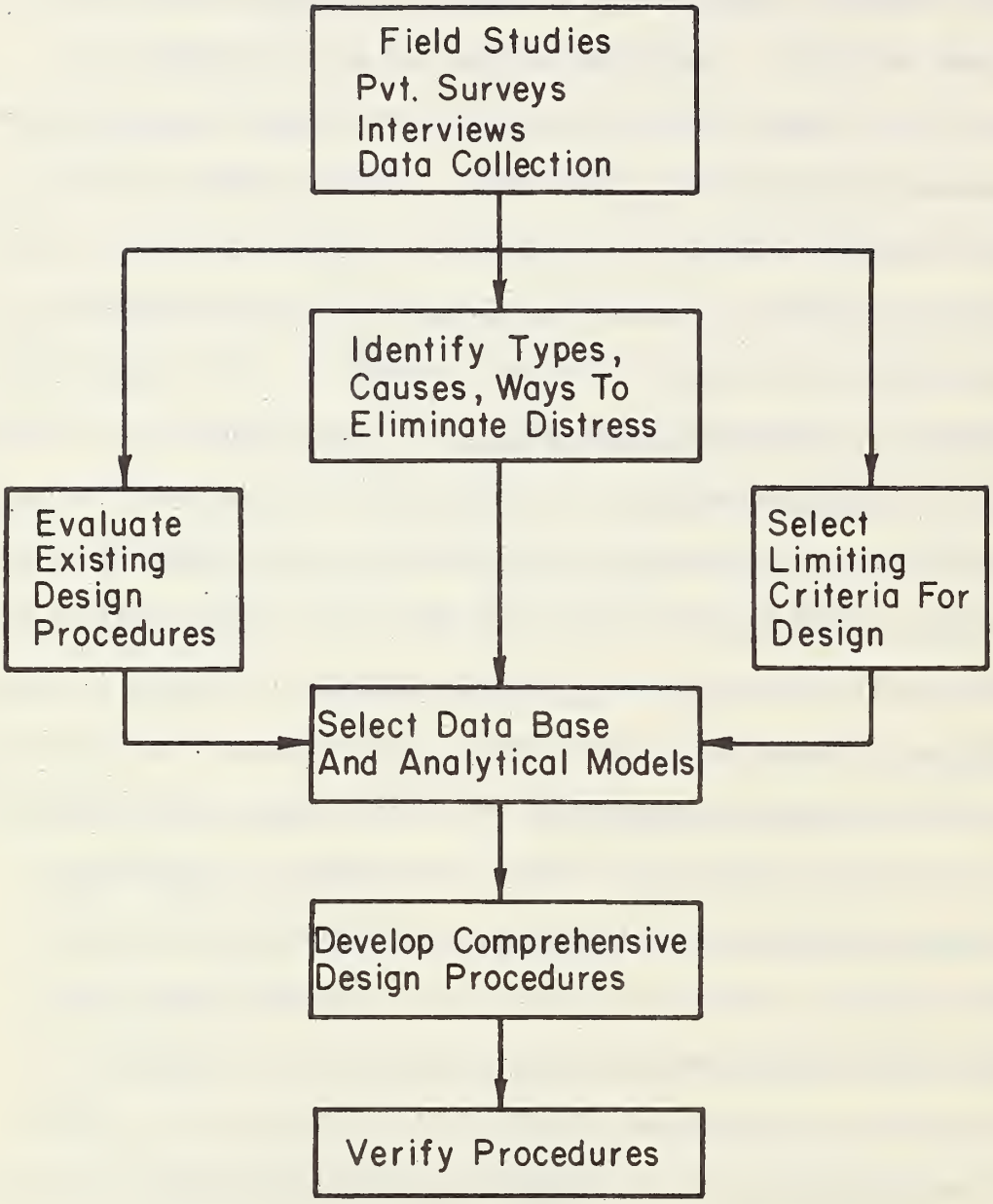


Figure 1.1. Research Approach to Develop Zero-Maintenance Design Procedures for Plain Jointed Concrete Pavements.

## 1.3 GENERAL DESIGN APPROACH

The general design approach consists of (1) determination of material properties and structural thicknesses of the PCC slab and the subbase, (2) selection of joint spacing, configuration, load transfer, and sealant, (3) determination of shoulder type and dimensions, and (4) subsurface drainage provisions. These components are designed as a system to ensure compatibility. A flow diagram showing the major design steps is shown in Figure 1.2.

The structural design procedures consist of both a slab fatigue analysis and also a serviceability/performance analysis. The final structure design is based upon both of these considerations to ensure more comprehensive analysis of pavement performance. A computer program is included that provides fatigue damage and serviceability/performance data used for selection of the structural design. The program is named JCP-1 and is written in FORTRAN. A manual procedure is also included to determine structural design based on serviceability/performance.

The procedure shown in Figure 1.2 is iterative, indicating that there are, of course, more than one zero-maintenance design alternative. The design that gives the minimum construction cost is generally selected as the optimum design as long as it meets all of the limiting design criteria.

The justification for construction of a zero-maintenance design is based upon an economic analysis. The increased costs to construct a zero-maintenance pavement over that of a conventional pavement must be compared with the costs resulting from maintenance, rehabilitation, and user delay if a conventional pavement is constructed. These costs must be computed over a given analysis period such as 20 years. Procedures have been developed by

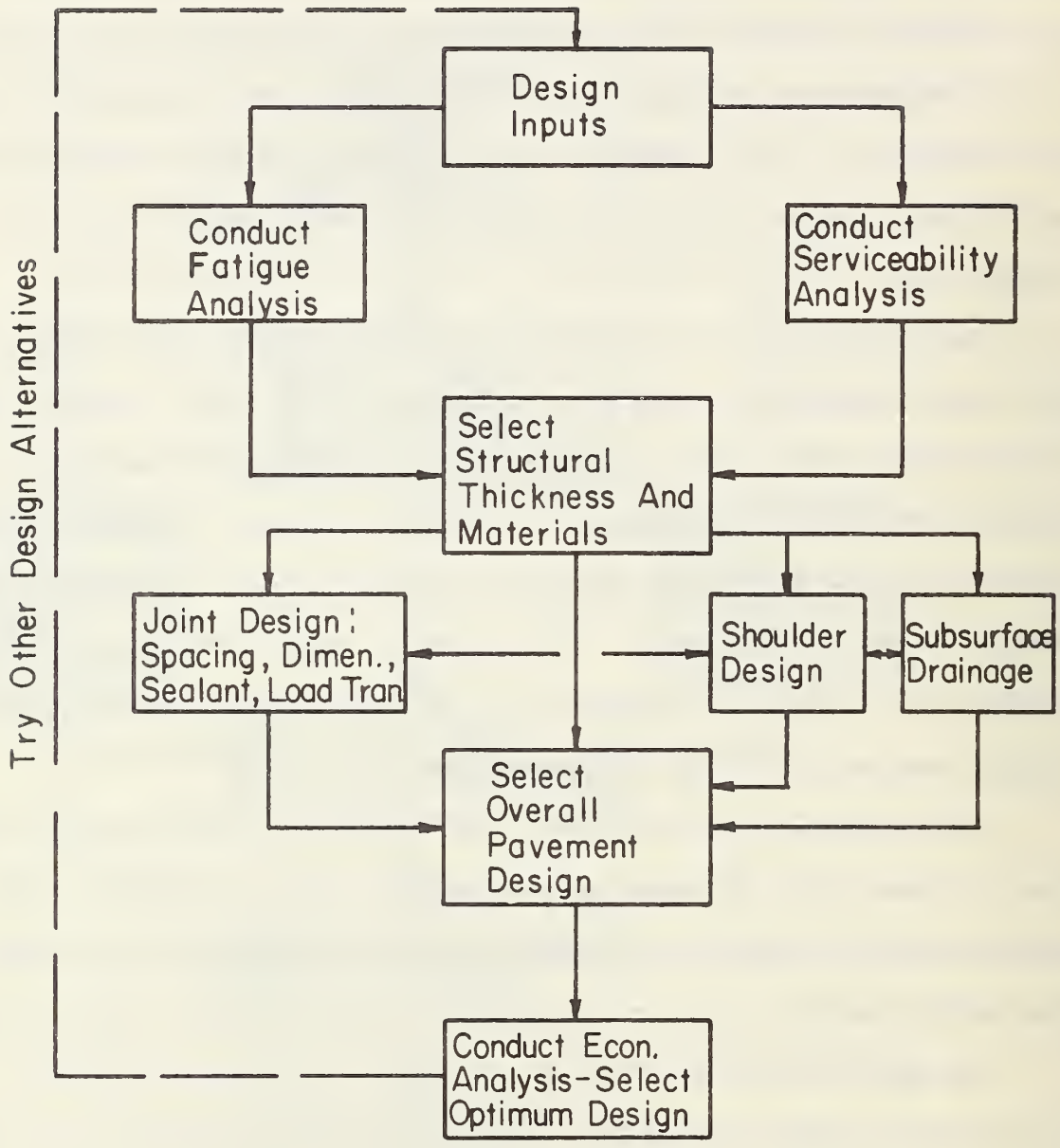


Figure 1.2. Zero-Maintenance Design Procedure for Plain Jointed Concrete Pavements.

Butler (Ref. 3) for FHWA to estimate the maintenance, rehabilitation, and user delay costs of conventional pavements.

## 1.4 LIMITATIONS

An important question that was posed many times during the development of these procedures is: Can a pavement be constructed that actually lasts 20 or more years without requiring structural maintenance such as crack repair, overlay, grinding, joint repair, patching, etc.? The field survey revealed that there are several plain jointed concrete and other pavement types that have performed maintenance-free for 15 to 27 years under heavy traffic. Therefore, it is possible to design and construct a pavement with this performance requirement. It requires, however, a most comprehensive and thorough design approach that considers all significant details to tailor the design to local conditions unique to the project. Although detailed recommendations are provided which are useful to most design situations, there is no substitute for engineering experience, which in certain instances may overrule specific recommendations given herein.

The design procedures contained herein have been developed using the most comprehensive mechanistic models available, and also long term measured pavement performance data. They have been verified using all data available to the project staff and found to give reasonable results. However, there are several aspects that are not as fully reliable as others due to lack of data and technology and these limitations must be carefully considered.

1. PCC Durability - The deterioration of PCC from any of several causes will cause a reduction of pavement maintenance-free life. Although

specific recommendations are given to minimize the occurrence, it may not be possible in some regions to prevent deterioration with existing materials.

2. Pavement Growth - The infiltration of a considerable amount of incompressibles into joints may result in pavement growth at bridge ends. Therefore, high type joint sealants with long performance life must be provided to minimize this occurrence.

3. Joint Faulting - Recommendations herein specify that dowel bars must be used in most all pavements, with the possible exception of pavements with very low truck volumes and pavements located in warm dry climates. If dowels are not used in other conditions, joint faulting may occur which would reduce the maintenance-free life of the pavement.

4. Construction - The failure to achieve construction quality as required in the specifications may have a serious effect on reducing the maintenance-free life of the pavement. A thorough inspection of the pavement should be conducted after construction to ascertain if any deficiencies exist, which would result in a reduced maintenance-free life. These should be corrected, if possible.

5. Design in Various Climates - Results from field surveys indicate that plain jointed concrete performs differently in different climates. Some climatic effects can be quantified directly herein, but an empirical climatic factor is still needed to help adjust for the difference in performance. This factor is not sufficiently verified and should be adjusted if it does not provide reasonable results in certain climates.

6. Traffic Estimation - A considerable effort has been made to specify how to obtain reasonable traffic estimates for design. The most crucial factor being the axle load distribution. The designer must carefully estimate all

traffic inputs using the best sources of data available. Underestimation of traffic to a significant degree may result in a pavement structure not capable of lasting throughout the design period in a maintenance-free condition.

The results of this study are presented in the following sequence:

Chapter 2 - Description of the field survey and distress in JPCP.

Chapter 3 - Development of a new serviceability-performance design model.

Chapter 4 - Development of a comprehensive fatigue analysis procedure.

Chapter 5 - Design recommendations for joints, shoulders, and subsurface drainage.

Chapter 6 - Verification of zero-maintenance design procedures.

Chapter 7 - Conclusions and recommendations for implementation of design procedures.

# CHAPTER 2

# FIELD SURVEY AND DISTRESS

## 2.1 FIELD SURVEY

Field surveys of heavily trafficked plain jointed concrete pavements were conducted in the U.S. and in one Canadian province. Extensive interviews, condition surveys, and data collection were made in 11 highway agencies where 37 projects were selected over a variety of climatic conditions. These projects were used for detailed performance evaluation and other analyses. The general location of these projects is shown in Figure 2.1.

Discussions with agency personnel and condition surveys were conducted in each area visited as described below:

1. Detailed discussions were held with administration, design, construction, and maintenance personnel of the agency. Subjective information was thus gathered for pavement performance, types of distress, recommended design practices, critical design limits, and construction and maintenance practices in the area. Some of this information is contained in a previous report (Ref. 2).

2. Condition surveys were conducted on several projects in each area, some of which were selected for inclusion in the project analyses. Attempts were made to collect data from each project as follows:

   a. A surface condition survey was conducted over a typical 2000 ft (610 m) portion of the pavement and all distress was recorded. The outer traffic lane was surveyed in all cases since this was the lane having the highest truck volume.

   b. Present Serviceability Rating (PSR) was estimated by the

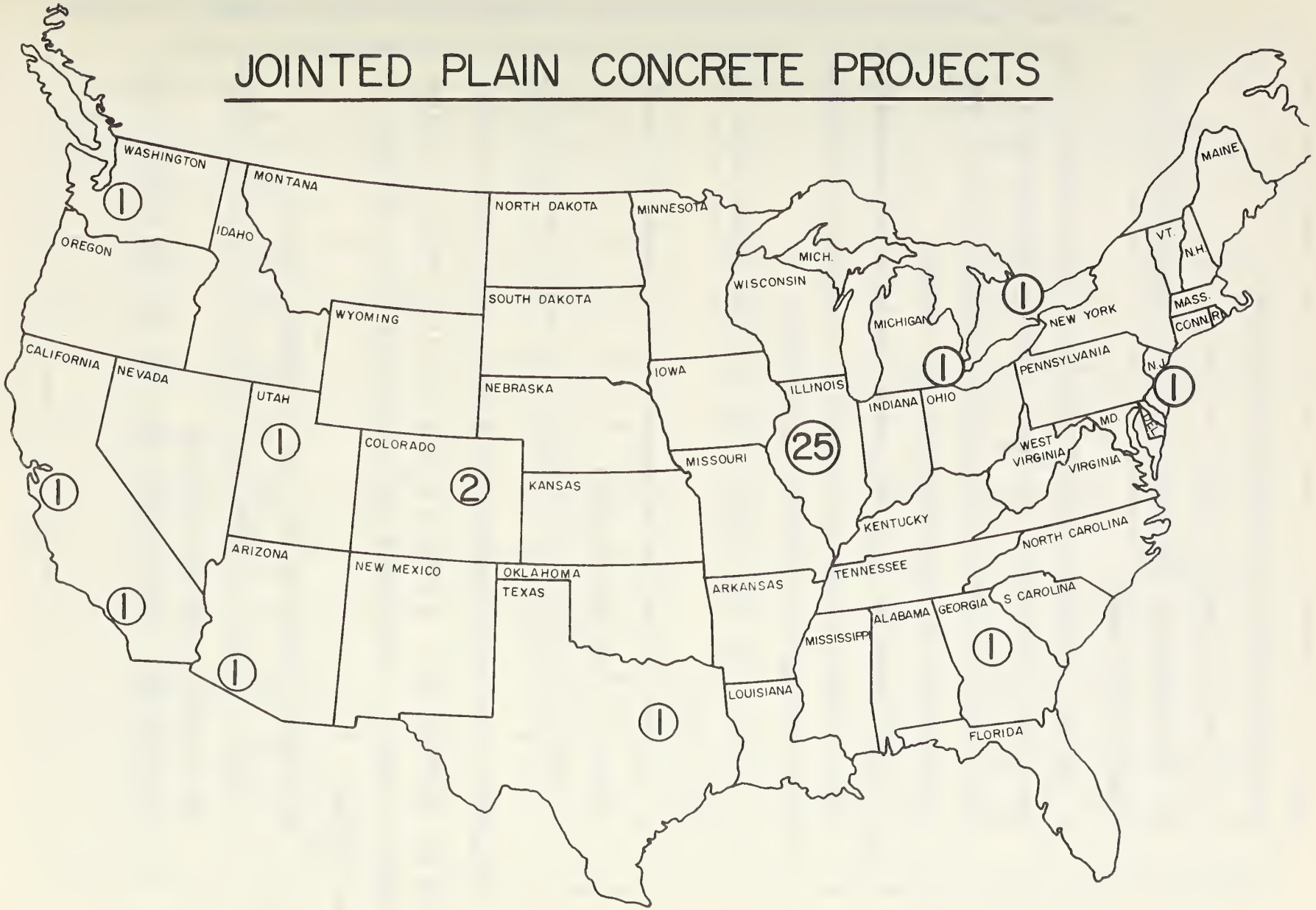


Figure 2.1. Location of 37 Projects Surveyed and Analyzed.

project staff member(s), or when available, the Present Serviceability Index (PSI) was obtained from the agency.

c. A general drainage evaluation was made.

d. The pavement was photographed both with 35 mm camera and with a Super-8 movie camera.

e. The date of opening to traffic and the original pavement cross section were obtained from the agency. Any available material data for various layers and the subgrade measured during or after the construction of the project were also obtained.

f. Traffic data including ADT, percent trucks, axle load distributions, lane distributions, directional distribution, and average axles per truck were obtained from the agency.

g. Climatic data were obtained from published Weather Bureau and other sources.

h. Opinions of the local engineers as to the reasons for pavement distress, if any, were obtained.

i. Previous maintenance performed on the section was determined.

All agencies were very cooperative and helpful in collecting and providing the requested data. A summary of data for all 37 projects is given in Tables 2.1 and 2.2. Performance data for each project are contained in other chapters.

3. The following guidelines were used in project selection:

a. Age - Longevity was important in that generally only projects over 10 years in age were selected.

b. Maintenance - Only projects which had not been overlayed were

Table 2.1. Summary of General Data Relative to 25 Sections of Plain Jointed Concrete Pavements Constructed for the AASHO Road Test (1958-60) and Then Subjected to Regular Mixed Traffic on I-80 (1962-74).

| Project No. | Loop/ Location | Route/ Section | Date Opened | Axle Load (kips) | ADT 1962-74* | | No. Lanes | Percent Trucks | Million 18-kip ESAL | Pavement Section | | | Transverse Joints |
|---|---|---|---|---|---|---|---|---|---|---|---|---|---|
| | | | | | Mean over Life | 1974 | | | | Slab | Subbase | Subgrade | |
| JCP-1 | Loop 4, Ottawa, IL | I-80 672 | 1958 | 32 TA | 11,100 | 18,900 | 4 | 32 | 11.16** | 8 in. PCC | 3 in. GR.B. | Clay | CJS = 15 ft. 1 in. dowels |
| JCP-2 | Loop 4, Ottawa, IL | I-80 658 | 1958 | 32 TA | 11,100 | 18,900 | 4 | 32 | 11.16 | 8 in. PCC | 6 in. GR.B. | Clay | CJS = 15 ft. 1 in. dowels |
| JCP-3 | Loop 4, Ottawa, IL | I-80 652 | 1958 | 32 TA | 11,100 | 18,900 | 4 | 32 | 11.16 | 8 in. PCC | 9 in. GR.B. | Clay | CJS = 15 ft 1 in. dowels |
| JCP-4 | Loop 4, Ottawa, IL | I-80 676 | 1958 | 32 TA | 11,100 | 18,900 | 4 | 32 | 11.32 | 9.5 in. PCC | 3 in. GR.B. | Clay | CJS = 15 ft. 1 1/4 in. dowels |
| JCP-5 | Loop 4, Ottawa, IL | I-80 702 | 1958 | 32 TA | 11,100 | 18,900 | 4 | 32 | 11.32 | 9.5 in. PCC | 6 in. GR.B. | Clay | CJS = 15 ft. 1 1/4 in. dowels |
| JCP-6 | Loop 4, Ottawa, IL | I-80 690 | 1958 | 32 TA | 11,100 | 18,900 | 4 | 32 | 11.32 | 9.5 in. PCC | 9 in. GR.B. | Clay | CJS = 15 ft. 1 1/4 in. dowels |
| JCP-7 | Loop 5, Ottawa, IL | I-80 552 | 1958 | 40 TA | 11,100 | 18,900 | 4 | 32 | 13.75 | 9.5 in. PCC | 0 in. GR.B. | Clay | CJS = 15 ft. 1 1/4 in. dowels |
| JCP-8 | Loop 5, Ottawa, IL | I-80 512 | 1958 | 40 TA | 11,100 | 18,900 | 4 | 32 | 13.75 | 9.5 in. PCC | 3 in. GR.B. | Clay | CJS = 15 ft. 1 1/4 in. dowels |
| JCP-9 | Loop 5, Ottawa, IL | I-80 542 | 1958 | 40 TA | 11,100 | 18,900 | 4 | 32 | 13.75 | 9.5 in. PCC | 3 in. GR.B. | Clay | CJS = 15 ft. 1 1/4 in. dowels |
| JCP-10 | Loop 5, Ottawa, IL | I-80 528 | 1958 | 40 TA | 11,100 | 18,900 | 4 | 32 | 13.75 | 9.5 in. PCC | 6 in. GR.B. | Clay | CJS = 15 ft. 1 1/4 in. dowels |
| JCP-11 | Loop 6, Ottawa, IL | I-80 352 | 1958 | 48 TA | 11,100 | 18,900 | 4 | 32 | 17.82 | 9.5 in. PCC | 3 in. GR.B. | Clay | CJS = 15 ft. 1 1/4 in. dowels |
| JCP-12 | Loop 6, Ottawa, IL | I-80 368 | 1958 | 48 TA | 11,100 | 18,900 | 4 | 32 | 17.82 | 9.5 in. PCC | 6 in. GR.B. | Clay | CJS = 15 ft. 1 1/4 in. dowels |

* Two directional

** Total in heaviest traveled lane in one direction.

1 in = 25.4 mm
1 ft = 0.30 m

Table 2.1. Summary of General Data Relative to 25 Sections of Plain Jointed Concrete Pavements Constructed for the AASHO Road Test (1958-60) and Then Subjected to Regular Mixed Traffic on I-80 (1962-74).(Continued)

| Project No. | Loop/ Location | Route/ Section | Oate Opened | Axle Load (kips) | ADT 1962-74 | | No. lanes | Percent Trucks | Million 18 kip ESAL | Pavement Section | | | Transverse Joints |
|---|---|---|---|---|---|---|---|---|---|---|---|---|---|
| | | | | | Mean over Life | 1974 | | | | Slab | Subbase | Subgrade | |
| JCP-13 | Loop 6, Ottawa, IL | I-80 390 | 1958 | 48 TA | 11,100 | 18,900 | 4 | 32 | 17.82 | 9.5 in. PCC | 6 in. GR.B. | Clay | CJS = 15 ft. 1 1/4 in. dowels |
| JCP-14 | Loop 6, Ottawa, IL | I-80 376 | 1958 | 48 TA | 11,100 | 18,900 | 4 | 32 | 17.82 | 9.5 in. PCC | 9 in. GR.B. | Clay | CJS = 15 ft. 1 1/4 in. dowels |
| JCP-15 | Loop 5, Ottawa, IL | I-80 530 | 1958 | 40 TA | 11,100 | 18,900 | 4 | 32 | 14.09 | 11 in. PCC | 3 in. GR.B. | Clay | CJS = 15 ft. 1 3/8 in. dowels |
| JCP-16 | Loop 5, Ottawa, IL | I-80 498 | 1958 | 40 TA | 11,100 | 18,900 | 4 | 32 | 14.09 | 11 in. PCC | 6 in. GR.B. | Clay | CJS = 15 ft. 1 3/8 in. dowels |
| JCP-17 | Loop 5, Ottawa, IL | I-80 510 | 1958 | 40 TA | 11,100 | 18,900 | 4 | 32 | 14.09 | 11 in. PCC | 9 in. GR.B. | Clay | CJS = 15 ft. 1 3/8 in. dowels |
| JCP-18 | Loop 6, Ottawa, IL | I-80 364 | 1958 | 48 TA | 11,100 | 18,900 | 4 | 32 | 18.94 | 11 in. PCC | 3 in. GR.B. | Clay | CJS = 15 ft. 1 3/8 in. dowels |
| JCP-19 | Loop 6, Ottawa, IL | I-80 378 | 1958 | 48 TA | 11,100 | 18,900 | 4 | 32 | 18.94 | 11 in. PCC | 3 in. GR.B. | Clay | CJS = 15 ft. 1 3/8 in. dowels |
| JCP-20 | Loop 6, Ottawa, IL | I-80 388 | 1958 | 48 TA | 11,100 | 18,900 | 4 | 32 | 18.94 | 11 in. PCC | 6 in. GR.B. | Clay | CJS = 15 ft. 1 3/8 in. dowels |
| JCP-21 | Loop 6, Ottawa, IL | I-80 398 | 1958 | 48 TA | 11,100 | 18,900 | 4 | 32 | 18.94 | 11 in. PCC | 6 in. GR.B. | Clay | CJS = 15 ft. 1 3/8 in. dowels |
| JCP-22 | Loop 6, Ottawa, IL | I-80 366 | 1958 | 48 TA | 11,100 | 18,900 | 4 | 32 | 18.94 | 11 in. PCC | 9 in. GR.B. | Clay | CJS = 15 ft. 1 3/8 in. dowels |
| JCP-23 | Loop 6, Ottawa, IL | I-80 396 | 1958 | 48 TA | 11,100 | 18,900 | 4 | 32 | 19.47 | 12.5 in. PCC | 3 in. GR.B. | Clay | CJS = 15 ft. 1 5/8 in. dowels |
| JCP-24 | Loop 6, Ottawa, IL | I-80 350 | 1958 | 48 TA | 11,100 | 18,900 | 4 | 32 | 19.47 | 12.5 in. PCC | 6 in. GR.B. | Clay | CJS = 15 ft. 1 5/8 in. dowels |
| JCP-25 | Loop 6, Ottawa, IL | I-80 380 | 1958 | 48 TA | 11,100 | 18,900 | 4 | 32 | 19.47 | 12.5 in. PCC | 9 in. GR.B. | Clay | CJS = 15 ft. 1 5/8 in. dowels |

1 in = 25.4 mm
1 ft = 0.30 m

Table 2.2. Summary of General Data Relative to 12 Plain Jointed Concrete Pavements Surveyed.

| Project No. | General Location | Route | Date Opened | ADT** | | No. of Lanes | Percent Trucks | Million 18-kip ESAL* | Pavement Section | | | | | Transverse Joints*** |
|---|---|---|---|---|---|---|---|---|---|---|---|---|---|---|
| | | | | Average over life | 1974 | | | | Slab | Subbase | Subbase | Subbase | Subgrade | |
| JCP-26 | Tacoma, Wash. | I-5 | 1962 | 36,750 | 57,250 | 6 in '62<br>8 in '71 | 12 | 5.42 | 9 in. PCC | 2 in. GR.B. | 7 in. GR.B. | - | Glacial Till | CJS = 15 ft. |
| JCP-27 | San Francisco, California | I-80 | 1955 | 35,750 | 55,000 | 6 | 13 | 14.57 | 8 in. PCC | 4 in. C.T.B. | 12 in. GR.B. | - | Sand, Clay and Silt | CJS = 15 ft. |
| JCP-28 | Los Angeles, California | I-5 | 1954-1958 | 67,500 | | 4 | 12 | 39.65 | 8 in. PCC | 4 in. C.T.B. | 4 in. GR.B. | 8 in. Sand | Sand-Silt | CJS = 15 ft. |
| | | | 1959-1974 | 113,500 | 129,000 | 6 | | | | | | | | |
| JCP-29 | Dallas, Texas | I-35 | Dec. 1960 | 12,000 | 19,300 | 4 | 16 | 3.60 | 10 in. PCC | 6 in. GR.B. | 4 in. AC Old Pavement | - | Austin Chalk | CJS = 15 ft. |
| JCP-30 | Salt Lake City Utah | I-15 | 1965 | 76,500 | 102,000 | 8 | 8 | 5.12 | 9 in. PCC | 4 in. C.T.B. | 2 in. GR.B. | - | Imported Borrow Fill | CJS = 12-19 ft. skewed |
| JCP-31 | Phoenix, Arizona | I-17 | 1960 | 41,500 | 75,000 | 6 | 25 | 30.23 | 9 in. PCC | 4 in. GR.B. | 6 in. S.M. | - | Clay | CJS = 15 ft. skewed |
| JCP-32 | New Brunswick, New Jersey | Rt. 130 | 1949 | 12,850 | 17,100 | 4 | 44 | 35.93 | 10 in. PCC | 12 in. GR.B. | 6 in. S.M. | - | Silt and Clayey Silt | CJS = 15 ft. |
| JCP-33 | Atlanta, Georgia | I-75 & I-85 | 1950 | 100,000 | 170,000 | 6 | 9 | 21.74 | 8 in. PCC | 6 in. GR.B. | - | - | Silty Clay | CJS = 30 ft.<br>EJS = 50[illegible] |
| JCP-34 | Denver, Colorado | I-70 | 1964 | 37,250 | 50,800 | 6 | 25 | 6.45 | 8 in. PCC | 6 in. GR.B. | 14 in. GR.B. | - | Sand-Gravel | CJS = 12-19 ft. skewed |
| JCP-35 | Denver, Colorado | I-25 | 1964 | 56,300 | 75,000 | 6 | 25 | 8.83 | 8 in. PCC | 6 in. GR.B. | - | - | Sand-Gravel | CJS = 15 ft. skewed |
| JCP-36 | Detroit, Michigan | Davison Exp. | 1942 | 44,300 | 61,600 (1976) | 6 | 8 | 18.73 | 10 in. PCC | 5 in. GR.B. | - | - | Clay | CJS = 25 ft. |
| JCP-37 | Toronto, Ontario | Hwy 27 | 1970 | 65,000 | 80,000 (1976) | 6 | 12 | 6.53 | 9 in. PCC | 6 in. C.T.B. | - | - | Clay | CJS = 12-19 ft. skewed/dowels |

** Two directional

* Total in heaviest traveled lane in one direction.

*** No dowels at joints unless indicated.

1 in = 25.4 mm

1 ft = 0.30 m

selected. Past routine maintenance was not a consideration and both pavements performing maintenance-free and those receiving maintenance were selected.

c. Traffic - Pavements that were heavily trafficked were given preference in selection. All of the projects are heavily trafficked urban or rural freeways.

d. Data Sample - The project sample represents only a small portion of all heavily trafficked plain jointed concrete pavements in the U.S. However, many of the projects are representative of others in the general area. JCP-28 in Los Angeles is typical of many pavements in that area that have been constructed for many years (others in this category include JCP-26, 27, 31, 34, and 35). The 25 sections in Illinois (JCP-1 to 25) are from the original AASHO Road Test that were left inservice on I-80 from 1962 to 1974. Three projects represent "one of a kind" constructed in a given area such as JCP-36 in Detroit (the first freeway constructed in 1942), JCP-32 in New Jersey, and JCP-29 near Dallas, Texas. Various plain jointed concrete projects in other states were observed including Nebraska, Wyoming, Florida, Ohio, and Pennsylvania but no data were collected. Available literature on the performance of plain jointed concrete pavement was also reviewed.

Four general climatic regions were selected as defined in Table 2.3 and selected climatic data for these locations are given in Table 2.4. The regions are based on moisture and freeze-thaw considerations. Projects were selected within each of the four climatic regions.

Table 2.3. Definition of the Four General Climatic Regions

| Climatic Region | Annual Precipitation (P) and Potential Evapo-transpiration (E) | Frost Heave and/or Freeze-Thaw Damage |
|---|---|---|
| Wet/Freeze (WF) | $P \geq E$ or<br>$P \geq 30$ ins (0.76 m) | Occurs in pavements in region* |
| Wet/Non-freeze (W) | $P \geq E$ or<br>$P \geq 30$ ins (0.76 m) | Does not occur in pavements in region |
| Dry/Freeze (DF) | $P < E$ | Occurs in pavements in region* |
| Dry/Non-freeze (D) | $P < E$ | Does not occur in pavement in region |

*Generally in areas having a mean Freezing Index > 0 (Ref. 64).

Table 2.4. Annual Precipitation, Evapotranspiration, and Freezing Index of Field Project Regions.

| Project Region | Annual[1] Precipitation (ins.) | Precipitation[2] Minus Evaporation (ins.) | Freezing[3] Index |
|---|---|---|---|
| I. WET/FREEZE AREA | | | |
| Ottawa, IL | 30 | + 4* | 700 |
| Detriot, MI | 29 | + 4 | 500 |
| Toronto, ONT | 31 | + 8 | 750 |
| New Brunswick, NJ | 39 | +10 | 100 |
| II. DRY/FREEZE AREA | | | |
| Salt Lake City, UT | 13 | -20** | 250 |
| Denver, CO | 17 | - 8 | 300 |
| III. WET/NO-FREEZE AREA | | | |
| Atlanta, GA | 43 | +12 | 0 |
| Seattle, WA | 30 | +30 | 0 |
| IV. DRY/NO-FREEZE AREA | | | |
| San Francisco, CA | 17 | -10 | 0 |
| Los Angeles, CA | 10 | -30 | 0 |
| Phoenix, AZ | 5 | -65 | 0 |
| Dallas, TX | 28 | -24 | 0 |

* plus means precipitation is more than evaporation
** minus means precipitation is less than evaporation

1 in. = 2.54 cm

1. Ref. 63
2. Ref. 63
3. Ref. 64

## 2.2 ANALYSIS OF DISTRESS

The development of design procedures to provide zero-maintenance performance requires the consideration and prevention of all distresses that require maintenance. Thus, an identification and study of distresses occurring in plain jointed concrete pavement is required. Results from the field study and other data were analyzed to determine distresses occurring in conventional heavily trafficked plain jointed concrete pavements. Eight distress types were identified in the 37 pavements surveyed as summarized in Table 2.5. The "Distressed/Total" column represents the number of pavements containing the indicated distress to the total number surveyed (or 37). The column "Maintained/Distressed" indicates the number of pavements receiving maintenance for the indicated distress to the total number distressed. Thus there were, for example, 12 projects exhibiting transverse cracking, and 10 of these projects received maintenance for this distress. A summary of distress, performance, and maintenance data for each project is given in Table 2.6.

The following conclusions are based on these data:

(1) Joint Faulting - nearly half of all projects had greater than 0.05 in. (1.3 mm) mean joint faulting. Even though only 3 of the 16 received maintenance for this distress, it is considered the most serious distress because when faulting develops to a level greater than about 0.20 in. (5.1 mm) it results in an intolerable ride quality and maintenance is usually performed. Several pavements located in the area surveyed have been overlayed or had fault grinding because of excessive joint faulting. This distress was considered the most serious problem by those engineers interviewed and must be considered in design. Photos of

Table 2.5. Summary of Distress Types Occurring on Plain Jointed Concrete Pavements.

| Type of Distress | Distressed/Total** | Maintained*/Distressed |
|---|---|---|
| 1. Joint Faulting (>0.05 in.) | 16/37 | 3/16 |
| 2. Transverse Cracking | 12/37 | 10/12 |
| 3. Longitudinal Cracking at Joint | 3/37 | 0/3 |
| 4. Corner Cracking | 1/37 | 0/1 |
| 5. "D" Cracking at Joint | 16/37 | 16/16 |
| 6. Joint and Corner Spalling (>3 in. dia.) | 8/37 | 5/8*** |
| 7. Joint Seal Damage | 35/37 | 29/35 |
| 8. Settlement | 27/37 | 3/27 |

1 in = 25.4 mm

* Maintenance applied only to distress indicated.
** Total number of projects included in field study.
*** Spalls and maintenance patches are very small.

Table 2.6. Summary of Project Distress, Performance, and Maintenance Data.

| Project No. | General Location | Transverse Cracking* | Other Cracking | Ave. Joint Faulting-ins. | PSI or PSR-1974 | Maintenance Performed | Joint Spalling >3 in. dia. | Patching** |
|---|---|---|---|---|---|---|---|---|
| JCP-1 | Ottawa, IL | 9 | 0 | 0.24 | 1.7 | P, CF | 1 | 6 |
| JCP-2 | Ottawa, IL | 34 | 0 | 0.27 | 1.7 | P, CF | 0 | 10 |
| JCP-3 | Ottawa, IL | 17 | 0 | 0.23 | 1.7 | P, CF | 1 | 15 |
| JCP-4 | Ottawa, IL | 0 | 0 | 0.06 | 2.7 | P | 0 | 5 |
| JCP-5 | Ottawa, IL | 0 | 0 | 0.06 | 2.9 | P | 1 | 2 |
| JCP-6 | Ottawa, IL | 0 | 0 | 0.04 | 2.9 | -- | 1 | <1 |
| JCP-7 | Ottawa, IL | 0 | 0 | 0.09 | 2.9 | P | 0 | 9 |
| JCP-8 | Ottawa, IL | 0 | 0 | 0.05 | 3.3 | P | 0 | 5 |
| JCP-9 | Ottawa, IL | 9 | 0 | 0.07 | 2.9 | P, CF | 0 | 5 |
| JCP-10 | Ottawa, IL | 0 | 0 | 0.06 | 3.3 | P | 0 | 8 |
| JCP-11 | Ottawa, IL | 17 | 0 | 0.13 | 3.0 | CF | 0 | <1 |
| JCP-12 | Ottawa, IL | 9 | 0 | 0.07 | 3.2 | P, CF | 1 | 5 |
| JCP-13 | Ottawa, IL | 0 | 0 | 0.05 | 3.3 | -- | 0 | <1 |
| JCP-14 | Ottawa, IL | 0 | 0 | 0.06 | 3.4 | -- | 0 | <1 |
| JPC-15 | Ottawa, IL | 0 | 0 | 0.03 | 3.1 | P | 0 | 3 |
| JCP-16 | Ottawa, IL | 0 | 0 | 0.02 | 3.1 | P | 0 | 2 |
| JCP-17 | Ottawa, IL | 0 | 0 | 0.05 | 3.2 | P | 0 | 2 |
| JCP-18 | Ottawa, IL | 0 | 0 | 0.05 | 3.4 | -- | 0 | <1 |
| JCP-19 | Ottawa, IL | 0 | 0 | 0.05 | 3.2 | P | 0 | 2 |
| JCP-20 | Ottawa, IL | 0 | 0 | 0.05 | 3.4 | -- | 0 | 0 |
| JCP-21 | Ottawa, IL | 0 | 0 | 0.05 | 3.4 | -- | 0 | 0 |

1 in = 25.4 mm; 1 ft = 0.30 m

*ft/1000 $ft^2$

**Generally crack, joint, and corner spalls

Table 2.6. Summary of Project Distress, Performance, and Maintenance Data. (Continued)

| Project No. | General Location | Transverse Cracking* | Other Cracking | Ave. Joint Faulting-ins. | PSI or PSR-1974 | Maintenance Performed | Joint Spalling >3 in. dia. | Patching** |
|---|---|---|---|---|---|---|---|---|
| JCP-22 | Ottawa, IL | 0 | 0 | 0.05 | 3.4 | P | 0 | 2 |
| JCP-23 | Ottawa, IL | 0 | 1 LC | 0.03 | 3.5 | -- | 0 | 0 |
| JCP-24 | Ottawa, IL | 0 | 0 | 0.04 | 3.8 | -- | 0 | <1 |
| JCP-25 | Ottawa, IL | 0 | 0 | 0.03 | 3.4 | P | 0 | 2 |
| JCP-26 | Tacoma, WA | 0 | 1 LC | 0.04 | 3.9 | -- | 0 | 0 |
| JCP-27 | San Francisco, CA | 3 | 1 LC | 0.16 | 3.0 | CF, P, JF | 2 | 3 |
| JCP-28 | Los Angeles, CA | 3 | 0 | 0.20 | 3.0 | -- | 0 | 0 |
| JCP-29 | Dallas, TX | 0 | 0 | 0.03 | 3.6 | JF | 0 | 0 |
| JCP-30 | Salt Lake City, UT | 0 | 0 | 0.04 | 4.0 | -- | 0 | 0 |
| JCP-31 | Phoenis, AZ | 0 | 0 | 0.05 | 3.2 | -- | 0 | 0 |
| JCP-32 | New Brunswick, NJ | 0 | 0 | 0.20 | 3.0 | -- | 0 | 0 |
| JCP-33 | Atlanta, GA | 7 | 0 | 0.05 | 3.4 | CF | 0 | 0 |
| JCP-34 | Denver, CO | 17 | 2 CC | 0.16 | 3.4 | CF | 0 | 0 |
| JCP-35 | Denver, CO | 0 | 0 | 0.05 | 3.6 | -- | 0 | 0 |
| JCP-36 | Detroit, MI | 30 | 0 | 0.22 | 2.1 | CF, P, JF | 3 | 16 |
| JCP-37 | Toronto, ONT | 5 | 0 | 0.01 | 3.9 | -- | 0 | 0 |

1 in = 25.4 mm; 1 ft = 0.30 m

* ft/1000 $ft^2$

** Generally crack, joint, and corner spalls

serious joint faulting are shown in Figure 2.2 and 2.3 (further discussion is given in Chapter 5 on causes).

(2) Transverse cracking - occurred on 12 projects, and 10 of these received maintenance. Thus, transverse cracking is a serious distress that usually requires maintenance because of crack spalling and faulting. Transverse cracking therefore must be considered in design (additional information on causes are given in Chapter 4). Photos of typical transverse cracking are shown in Figs. 2.4-2.9.

(3) Longitudinal Cracking - only occurred on three projects and none received maintenance. This crack always occurred at the joint about 1-3 ft. from the slab edge and only extended about 2 ft., as shown in Fig. 2.10 (further discussion is given in Chapter 4). The cracks were all hairline and did not spall.

(4) Corner cracking - only one project (without dowels) exhibited this distress. This project also had skewed joints. Significant faulting and pumping was evident on this project as shown in Fig. 2.11.

(5) "D" Cracking - only occurred on those projects located at the AASHO Road Test site. However, it has been observed to exist throughout the midwestern U.S. and in other areas. "D" Cracking usually results in joint spalling that was subsequently patched on all 16 pavements. This distress must be considered in materials selection and design (See Figs. 2.12-2.14).

(6) Joint and Corner Spalling - occurred on 8 of the pavements to a very small degree. This was generally the result of "D" cracking as shown in Figs. 2.13 and 2.14. It indicates however, that higher quality PCC is needed

Figure 2.2. Joint Faulting on Plain Jointed Concrete Pavement Containing No Dowels (JCP-28-CA, approximately 0.2 in.)

1 in = 25.4 mm

Figure 2.3. Joint Faulting on Plain Jointed Concrete Pavement Containing No Dowels (GA).

Figure 2.4. Transverse Crack on Plain Jointed Concrete Pavement with 15 ft. Joint Spacing (JCP-28-CA).

1 ft = 0.30 m

Figure 2.5. Transverse Crack on Plain Jointed Concrete Pavement with 20 ft. Joint Spacing (GA).

Figure 2.6. Transverse Cracking on Plain Jointed Concrete Pavement with 25 ft. Joint Spacing (JCP-36-MI).

1 ft = 0.30 m

Figure 2.7. Transverse Cracking on Plain Jointed Concrete Pavement with 19 ft. Joint Spacing (JCP-37-Ontario).

Figure 2.8. Transverse Cracking on Plain Jointed Concrete Pavement with 15 ft. Joint Spacing (JCP-27-CA).

1 ft = 0.30 m

Figure 2.9. Transverse Cracking on Plain Jointed Concrete Pavement with 15 ft. Joint Spacing (JCP-1-IL).

Figure 2.10. Longitudinal Cracking on Plain Jointed Concrete Pavement (JCP-26-WA).

Figure 2.11. Corner Cracking Plain Jointed Concrete Pavement without Dowels at Joint (JCP-34-CO).

Figure 2.12. "D" Cracking of Plain Jointed Concrete Slab at Corner (JCP-22-IL).

Figure 2.13. Spalling at Joint Caused by "D" Cracking of Plain Jointed Concrete Slab (JCP-22-IL).

Figure 2.14. Spalling at Joint Caused by "D" Cracking of Plain Jointed Concrete Slab (JCP-21-IL).

to minimize this distress. None of the joints showed significant spalling where "D" Cracking did not exist.

(7) Joint Seal Damage - this distress occurred on nearly every project, however, only a few were maintained. Sealant damage (infiltration of incompressibles) is shown on one 9 year old pavement in Fig. 2.15. The stripping of sealant can also be seen in Figs. 2.13 and 2.14. This indicates that (1) the sealants used are not sufficiently durable, and (2) most agencies do not maintain joints on heavily traveled routes. The longitudinal joint between the PCC traffic lane and asphalt shoulder was usually always open and not sealed and water could freely enter most of the joints.

(8) Settlement - this distress is difficult to observe but did occur at least to some degree on several projects (See Fig. 2.9 for example). Its effect is perhaps most obvious on the thicker slab sections at the AASHO Road Test where no cracking, faulting, or any significant distress of any kind occurred, and yet the serviceability index dropped from about 4.5 to 3.5 due to increased roughness, apparently from non-uniform slab settlement. This indicates the importance of a stable foundation which must be considered in design.

These distresses are all associated with the traveled lanes. The shoulders of most of these pavements showed considerable distress (alligator and linear cracking, settlement, heaving, longitudinal joint widening and spalling, as illustrated in Figs. 2.16-2.17 etc.). Considerable maintenance was applied to the shoulders in several projects. Also, this distress appears to have increased the distress occurring in the traveled lane (i.e. faulting, pumping, and cracking). Hence, the shoulder must also be designed for maintenance-free performance to avoid lane closure due to shoulder maintenance.

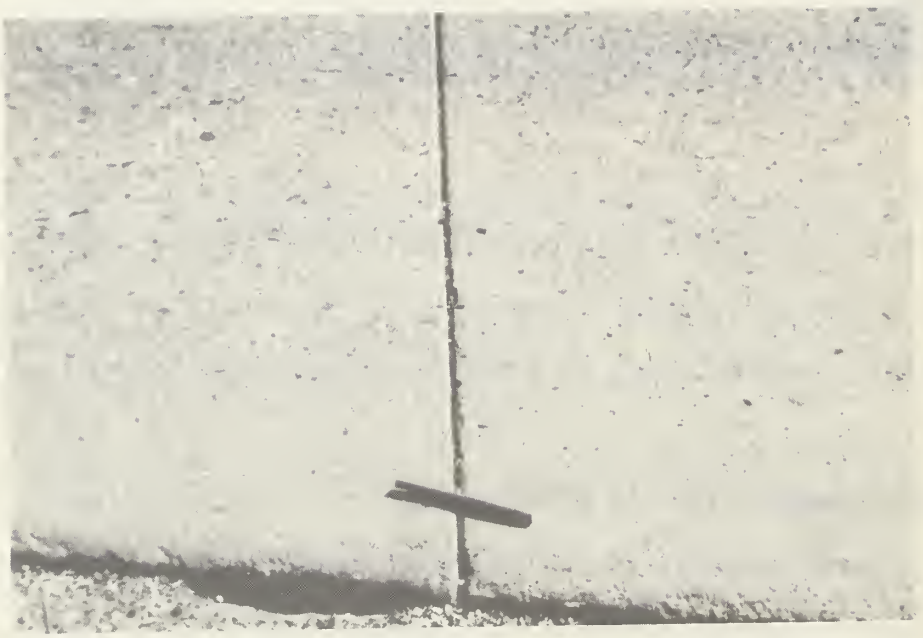

Figure 2.15. Joint Sealant Damage (Stripping and Infiltration of Incompressibles) for 9 Year Heavily Trafficked Freeway (JCP-30UT).

Figure 2.16. Settlement and Spalling of Shoulder (JCP-29-TX).

Figure 2.17. Alligator Cracking in Shoulder near Longitudinal Joint (JCP-30-UT).

In summary, the following distress types commonly occurring in heavily trafficked plain jointed concrete pavements must be considered in design and thereby prevented to provide a zero-maintenance pavement: (1) joint faulting, (2) transverse cracking, (3) "D" cracking, (4) Joint and corner spalling, (5) joint seal damage, (6) settlement of the slab, and (7) shoulder distress. There are obviously other distresses that could occur (i.e. scalling, blowups, longitudinal cracking, etc.), however, these seven are considered the major types presently occurring on conventional plain jointed concrete pavements.

# CHAPTER 3

# STRUCTURAL DESIGN BASED ON SERVICEABILITY/PERFORMANCE

## 3.1 INTRODUCTION

Structural design based upon serviceability/performance permits the general consideration of several distress types since the serviceability index is a function of roughness and distress. The original development of the serviceability index correlated it with roughness, cracking and patching (Ref. 46), and other studies have correlated it with only roughness (Ref. 65) and only distress (Ref. 2). Pavements designed based on serviceability/performance would thus generally consider the following distresses: joint faulting, cracking, joint spalling, and differential settlement of slabs.

The two year AASHO Road Test provided data that were used to derive empirical equations that expressed the relationship between the number of traffic load applications and magnitude, the serviceability index (SI), and slab thickness. This equation was derived by the Road Test staff, and extended by the AASHO Committee on Design of Rigid Pavements (Ref. 60), and has been used extensively in concrete pavement design since 1962. A detailed evaluation of this design equation was conducted by Darter and Barenberg (Ref. 2 ), and several deficiencies were noted. When the equation was used to "redesign" pavements that had provided maintenance-free performance, the results showed that it usually provided inadequate structures.

One of the major deficiencies of the AASHO performance equation is that is is based on only two years data. Since the end of the AASHO Road Test in 1960 the Illinois Department of Transportation (IDOT) has monitored the performance of 25 of the original sections of the Road Test after they were opened to traffic as part of I-80 in 1962. A summary of 25

plain jointed concrete pavement sections and their performance that were monitored from 1962 to 1974 are given in Table 3.1. Slab thickness ranges from 8 to 12.5 inches (203-318 mm). This data, along with the estimated 18-kip (80 kN) equivalent single axle load (ESAL) applications, were used to derive a new performance equation. The data represents 16 years of time and nearly 20 million applied 18-kip (80 kN) (ESAL) applications.

New performance equations were developed using both the same approach applied by the Road Test staff, and a new approach found necessary to provide a more accurate representation of the relationship between the serviceability index, accumulated 18-kip (80 kN) ESALs, and slab thickness. Data was also obtained from 12 other plain jointed concrete projects located in other regions of the U.S. to provide data on the regional or climatic effect on performance. The development of the original AASHO equation is first described, then the development of the new equations based upon the 16 year data is given.

## 3.2 ORIGINAL AASHO MODEL

The Road Test provided data to derive empirical relationships between PCC slab thickness, load magnitude, axle type, number of load applications, and serviceability index of the pavement for Road Test conditions (i.e., specific environment and materials) using multiple regression analyses.

$$\log_{10} W = \log \rho + G/B \qquad (3.1)$$

where

W = axle load applications, for load magnitude L1 and axle type load L2, to a serviceability index of P2.

$$\log \rho = 5.85 + 7.35 \log(H + 1) + 4.62 \log(L1 + L2) + 3.28 \log(L2)$$

Table 3.1. Summary Performance Data for 25 Sections of Plain Jointed Concrete Pavements from AASHO Road Test That Are Inservice on I-80 (1958-1974).*

| Section No. | Slab Thickness (in ) | Subbase Thickness (in ) | SI Data | | | | | |
|---|---|---|---|---|---|---|---|---|
| | | | 1962 | 1968 | 1969 | 1971 | 1972 | 1974 |
| 672 | 8.0 | 3 | 4.10 | 3.44 | 3.21 | 2.61 | 2.76 | 1.69 |
| 658 | 8.0 | 6 | 4.10 | 3.14 | 2.83 | 2.61 | 2.11 | 1.69 |
| 652 | 8.0 | 9 | 4.10 | 3.01 | 3.02 | 2.98 | 2.57 | 1.69 |
| 552 | 9.5 | 0 | 4.30 | 3.36 | 3.52 | 3.14 | 3.14 | 2.87 |
| 676 | 9.5 | 3 | 4.00 | 3.21 | 3.21 | 2.88 | 3.28 | 2.75 |
| 512 | 9.5 | 3 | 4.30 | 3.70 | 3.70 | 3.36 | 3.36 | 3.32 |
| 542 | 9.5 | 3 | 4.20 | 3.36 | 3.12 | 3.21 | 3.01 | 2.88 |
| 352 | 9.5 | 3 | 3.10 | 2.98 | 3.11 | 2.80 | 2.95 | 2.96 |
| 702 | 9.5 | 6 | 4.20 | 3.36 | 3.52 | 3.07 | 3.28 | 2.94 |
| 528 | 9.5 | 6 | 4.30 | 3.79 | 3.61 | 3.28 | 3.36 | 3.27 |
| 368 | 9.5 | 6 | 4.30 | 3.52 | 3.70 | 3.36 | 3.52 | 3.16 |
| 390 | 9.5 | 6 | 4.30 | 4.00 | 3.79 | 3.14 | 3.01 | 3.36 |
| 690 | 9.5 | 9 | 4.20 | 3.21 | 3.52 | 3.21 | 2.85 | 2.95 |
| 376 | 9.5 | 9 | 4.30 | 3.36 | 3.44 | 3.21 | 3.21 | 3.44 |
| 530 | 11.0 | 3 | 4.30 | 3.36 | 3.70 | 3.36 | 3.28 | 3.11 |
| 364 | 11.0 | 3 | 4.30 | 3.79 | 3.78 | 3.21 | 3.28 | 3.44 |
| 378 | 11.0 | 3 | 4.30 | 3.61 | 3.21 | 3.21 | 3.21 | 3.23 |
| 498 | 11.0 | 6 | 4.50 | 3.52 | 3.70 | 3.14 | 3.28 | 3.08 |
| 388 | 11.0 | 6 | 4.30 | 3.44 | 3.52 | 3.28 | 3.61 | 3.44 |
| 398 | 11.0 | 6 | 4.30 | 4.11 | 3.70 | 3.70 | 3.44 | 3.44 |
| 510 | 11.0 | 9 | 4.40 | 3.36 | 3.44 | 3.07 | 3.21 | 3.23 |
| 366 | 11.0 | 9 | 4.30 | 3.89 | 3.21 | 3.29 | 3.34 | 3.39 |
| 396 | 12.5 | 3 | 4.30 | 3.44 | 3.44 | 3.21 | 3.36 | 3.52 |
| 350 | 12.5 | 6 | 4.20 | 3.70 | 3.89 | 3.45 | 3.63 | 3.81 |
| 380 | 12.5 | 9 | 4.20 | 3.36 | 3.35 | 3.06 | 3.28 | 3.39 |

* Determined by Illinois Department of Transportation

1 in = 25.4 mm

$$B = 1.00 + \frac{3.63(L1 + L2)^{5.20}}{(H + 1)^{8.46} L2^{3.52}}$$

$$G = \log\left(\frac{P1 - P2}{P1 - 1.5}\right)$$

H = Pcc slab thickness, inches

L1 = load on a single or a tandem axle, kips

L2 = axle code, 1 for single axels, 2 for tandem axles

P1 = initial serviceability index

P2 - terminal serviceability index

Using the Spangler corner equation, the empirical model given by Equation 3.1 was modified and extended to include material properties: PCC flexural strength (FF), modulus of elasticity (E), and modulus of foundation support (k). The following basic assumptions were made in this extension:

a. The variation in pavement life (W) for different load magnitudes of the same level of the ratio of tensile stress/strength of the PCC slab is accounted for by the basic AASHO Road Test Equation 3.1, and is covered in the design procedure by the traffic equivalence factors, and

b. Any change in the ratio tensile stress/strength resulting from changes in the values of E, k, and F will have the same effect on W as an equivalent change in slab thickness (calculated by Spangler's equation) will have on W as per Equation 3.1.

The resulting final structural design model is given as follows:

$$\log W_{18} = 7.35 \log(H + 1) - 0.06 + \frac{G}{1 + \frac{1.624 \times 10^7}{(H + 1)^{8.46}}} + (4.22 - 0.32\ P2) \log\left[\left(\frac{FF}{215.63J}\right)\left(\frac{H^{0.75} - 1.133}{H^{0.75} - \frac{18.42}{Z^{0.25}}}\right)\right] \quad (3.2)$$

where

$W_{18}$ = number of 18 kip single axle loads to reduce the serviceability index from P1 to P2

FF = flexural strength of the concrete slab (28-day cure, 3rd point loading), psi

H = PCC slab thickness, inches

J = load transfer coefficient

Z = E/k

E = PCC slab modulus of elasticity, pci

k = modulus of foundation support, pci

Detailed derivation of Equation 3.2 is given in Reference 61.

NCHRP Report 128 (Ref. 62) and the AASHO Interim Guides (Ref. 61) suggest that other terms should be added to the equation to permit variation of subbase quality (Q), and also regional factor (R) for climate. The regional factor should be included to account for differences in frost penetration, rainfall, daily temperature variation, and other climatic factors.

An analysis was conducted using 16 years data from the 25 sections to determine the ability of Equation 3.2 to predict long term performance. The number of 18-kip ESAL accumulated to each year (i.e., 1962, 1968, 1969, 1971, 1972, 1974) for each project was calculated based on mixed traffic data measured on the site and computed load equivalency factors. This value was plotted versus the number of predicted 18-kip ESAL that should have passed over the section to cause a loss of serviceability index from 4.5 to the value shown in Table 3.1 according to Equation 3.2. The plot is shown in Figure 3.1.

The standard error of the estimate (standard deviation of residuals) is 0.31 for log W. The plot clearly shows that Equation 3.2 predicts

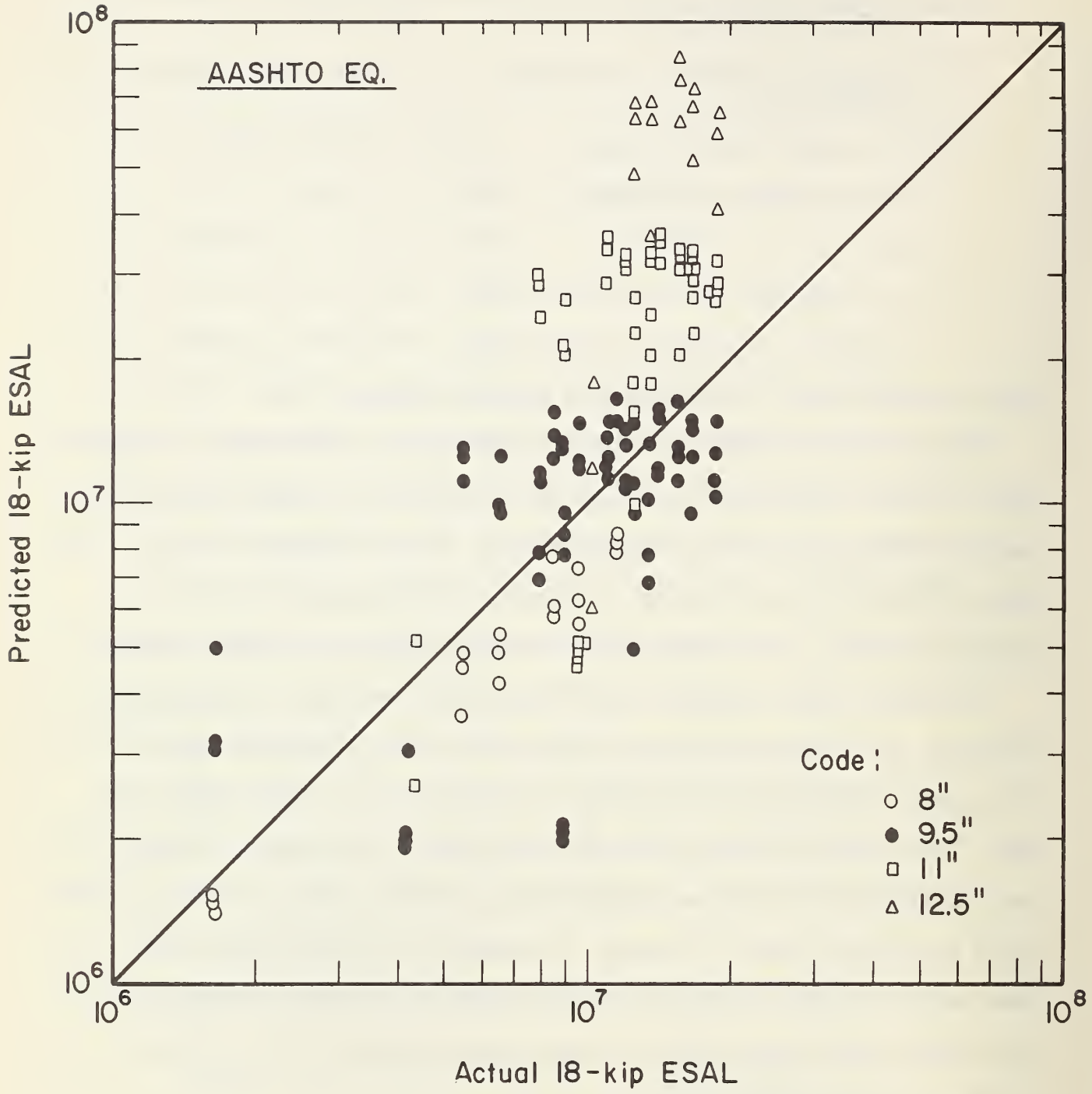


Figure 3.1. Predicted Versus Actual Equivalent 18-kip Single Axle Load Applications using AASHO Equation 3.2 and 16 Years Data From AASHO Road Test Site (1958-1974).

poorly for thick slabs (H $\geq$ 11 inches). For example, the actual 18-kip (80 kN) ESAL for a 12-1/2 inch (318 mm) inch slab is about 18 million, and the computed value according to Equation 3.2 is over 50 million. This standard error is considerably larger than the error based on only the results from the two year Road Test which was 0.22. Additional information is presented later to show that the equation has an incorrect "form" for predicting the performance of thicker slabs.

## 3.3 DEVELOPMENT OF NEW EQUATIONS

3.3.1 Modified AASHO Equation. An approach similar to that used to develop the original AASHO Road Test Equation 3.2 was used to develop a modified equation. Data from the 25 AASHO sections were used in the regression analyses to determine the functions $\beta$ and $\rho$. This equation which is called the "modified AASHO" equation is as follows:

$$\log W_{18} = 1.27\ 61 \log(H + 1) + 5.9802 + \frac{G}{0.00342(H + 1)^{2.574}} \quad (3.3)$$

The standard error of this equation is 0.158. Although Equation 3.3 has a much smaller standard error than Equation 3.2, the form of the equation does not fit the performance data for thicker slabs as is illustrated in Figure 3.2. This plot shows the serviceability index versus accumulated 18-kip (80 kN) ESAL for all data available from the 11 inch (279 mm) PCC slabs. The data shows that although there is a loss of serviceability, the serviceability index levels off, but the new AASHTO Equation 3.3 continues to show a rapid loss. A typical plot for a single 9.5 inch (241 mm) PCC slab is shown in Figure 3.3. The modified AASHO Equation 3.3 cannot fit this type of performance curve because of its mathematical form. Therefore,

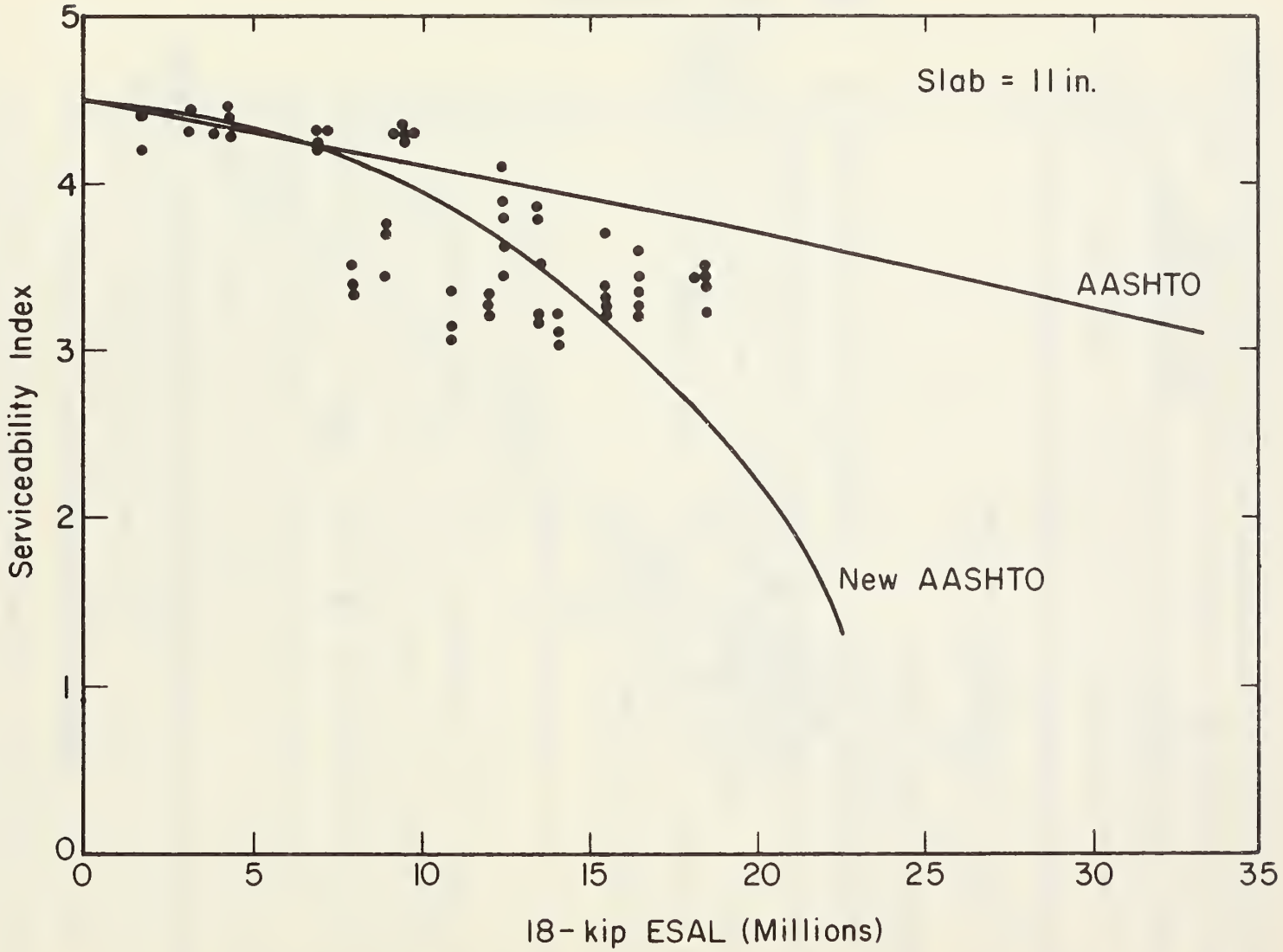


Figure 3.2. Illustration of Original AASHTO and Modified AASHTO Performance Equation (Data from 16 Years Performance at Ottawa, Illinois).

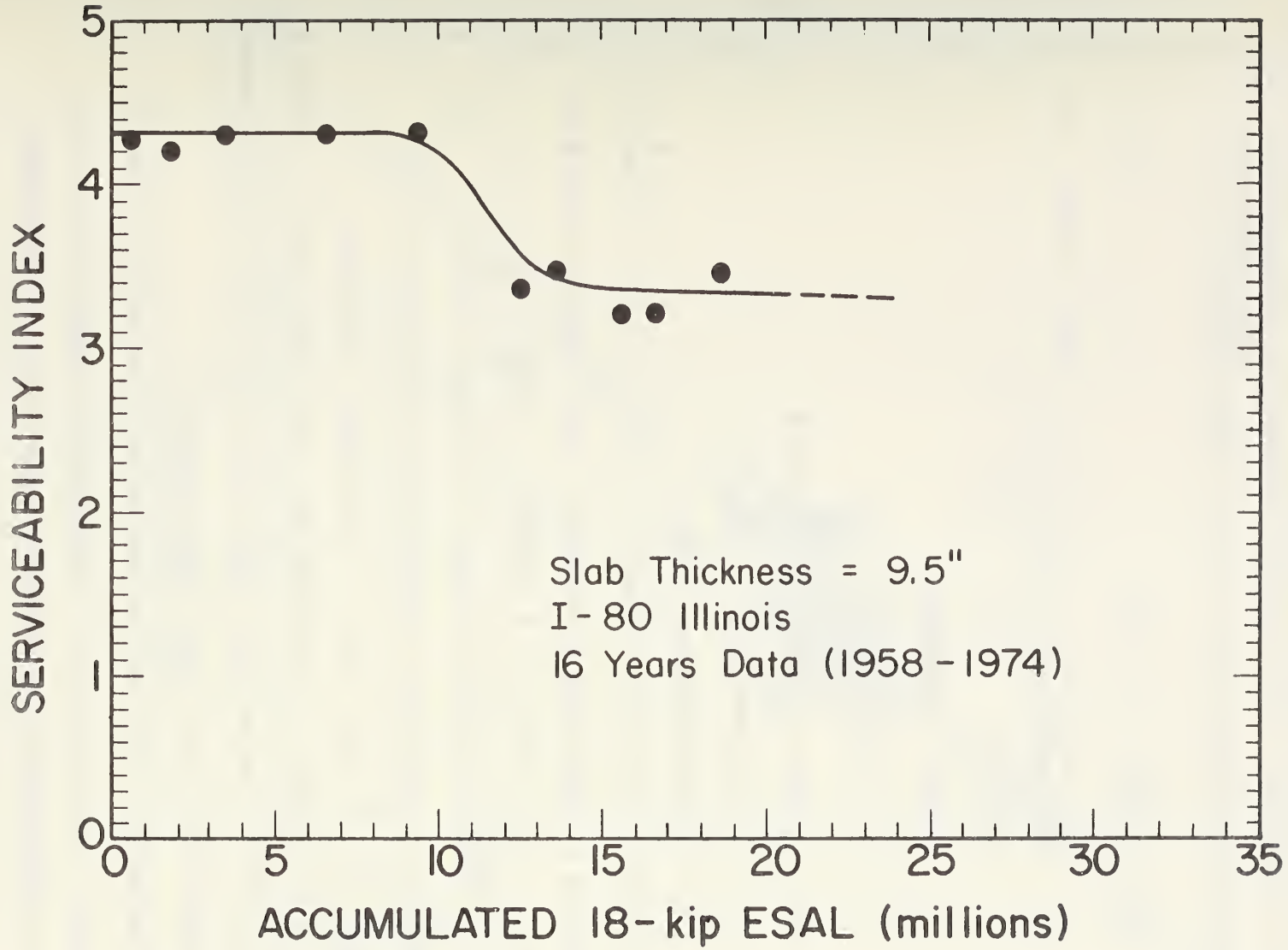


Figure 3.3. Typical Performance Curve for Original AASHO Road Test Sections on I-80 (16 year data).

a new approach based on a different mathematical function is needed to develop an equation that "fits" the form of the performance curve.

3.3.2 New Approach. The following mathematical form better fits the actual measured performance curves for the 25 AASHO sections

$$W'_{18} = [\rho \ln(\frac{3}{y} - 1) + \beta]10^6 \qquad (3.4)$$

where $W'_{18}$ = total equivalent 18-kip single axle loads to reduce the serviceability index from P1 to P2.

$$\beta = -50.08826 - 3.77485H + 30.64386 \sqrt{H}$$

$$\rho = -6.69703 + 0.13879H^2$$

$$y = P2 + \frac{3.0}{(e)^{-\beta/\rho} + 1} - P1$$

P2 = terminal serviceability index

P1 = initial serviceability index.

H = PCC slab thickness, inches

The standard error of the estimate of log $W'_{18}$ is 0.22. The adequacy of Equation 3.4 to predict the performance of the 25 sections over a 16 year period is shown in Figure 3.4 which can be directly compared with Figure 3.1. The data plotted in Figure 3.4 is given in Table 3.2. The new equation has a much smaller standard error (0.22 versus 0.31) and the difference can be seen visually in the figures. Individual plots for the 8, 9.5, 11, and 12.5 inch (203, 241, 274, 318 mm) slabs are given in Figures 3.5-3.8. The new equation 3.4 can be seen to fit the performance data much better than the original AASHO Equation 3.1.

This expression permits only an evaluation of the effect of the PCC slab thickness, terminal and initial serviceability index on equivalent 18-kip load applications. Therefore, the equation was extended so that

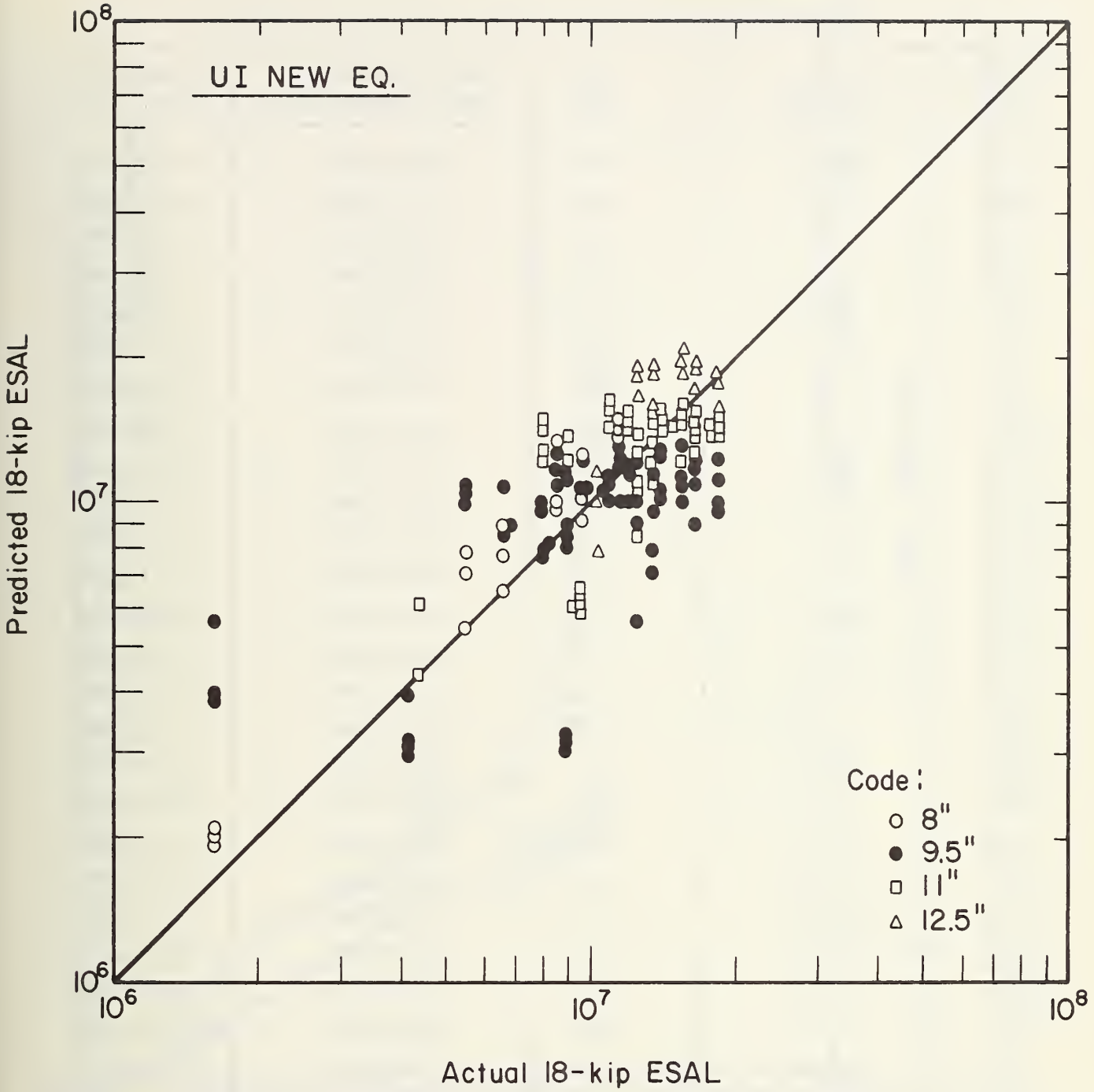


Figure 3.4. Accuracy of New Performance Equation (3.5).

Table 3.2. Performance Data of 25 Sections Computed Using the New Equation 3.5.

| Section No. | Slab Thickness | SI 1974 | 1974 Accumulated Actual 18-kip ESAL* | Computed 18-kip ESAL** |
|---|---|---|---|---|
| 672 | 8.0 | 1.69 | 11,641,421 | 15,976,948 |
| 658 | 8.0 | 1.69 | 11,641,421 | 15,976,948 |
| 652 | 8.0 | 1.69 | 11,641,421 | 15,976,948 |
| 552 | 9.5 | 2.87 | 14,091,699 | 14,358,886 |
| 676 | 9.5 | 2.75 | 11,641,421 | 15,611,260 |
| 512 | 9.5 | 3.32 | 14,091,699 | 10,431,283 |
| 542 | 9.5 | 2.88 | 14,091,699 | 14,260,283 |
| 352 | 9.5 | 2.96 | 18,643,645 | 13,496,459 |
| 702 | 9.5 | 2.94 | 11,641,421 | 13,683,436 |
| 528 | 9.5 | 3.27 | 14,091,699 | 10,833,032 |
| 368 | 9.5 | 3.16 | 18,643,645 | 11,737,991 |
| 390 | 9.5 | 3.36 | 18,643,645 | 10,113,170 |
| 690 | 9.5 | 2.95 | 11,641,421 | 13,589,634 |
| 376 | 9.5 | 3.44 | 18,643,645 | 9,483,560 |
| 530 | 11.0 | 3.11 | 14,091,699 | 20,256,096 |
| 364 | 11.0 | 3.44 | 18,643,645 | 15,124,949 |
| 378 | 11.0 | 3.23 | 18,643,645 | 18,277,072 |
| 498 | 11.0 | 3.08 | 14,091,699 | 20,778,232 |
| 388 | 11.0 | 3.44 | 18,643,645 | 15,124,949 |
| 398 | 11.0 | 3.44 | 18,643,645 | 15,124,949 |
| 510 | 11.0 | 3.23 | 14,091,699 | 18,277,072 |
| 366 | 11.0 | 3.39 | 18,643,645 | 15,848,616 |
| 396 | 12.5 | 3.52 | 18,643,645 | 20,347,888 |
| 350 | 12.5 | 3.81 | 18,643,645 | 14,278,986 |
| 380 | 12.5 | 3.39 | 18,643,645 | 23,286,432 |

* Determined from traffic data in outside traffic lane from 1958 to 1974.

** Computed using new performance equation 3.4 based on loss of serviceability from 4.50 to 1974 SI as given.

1 in. = 2.54 mm

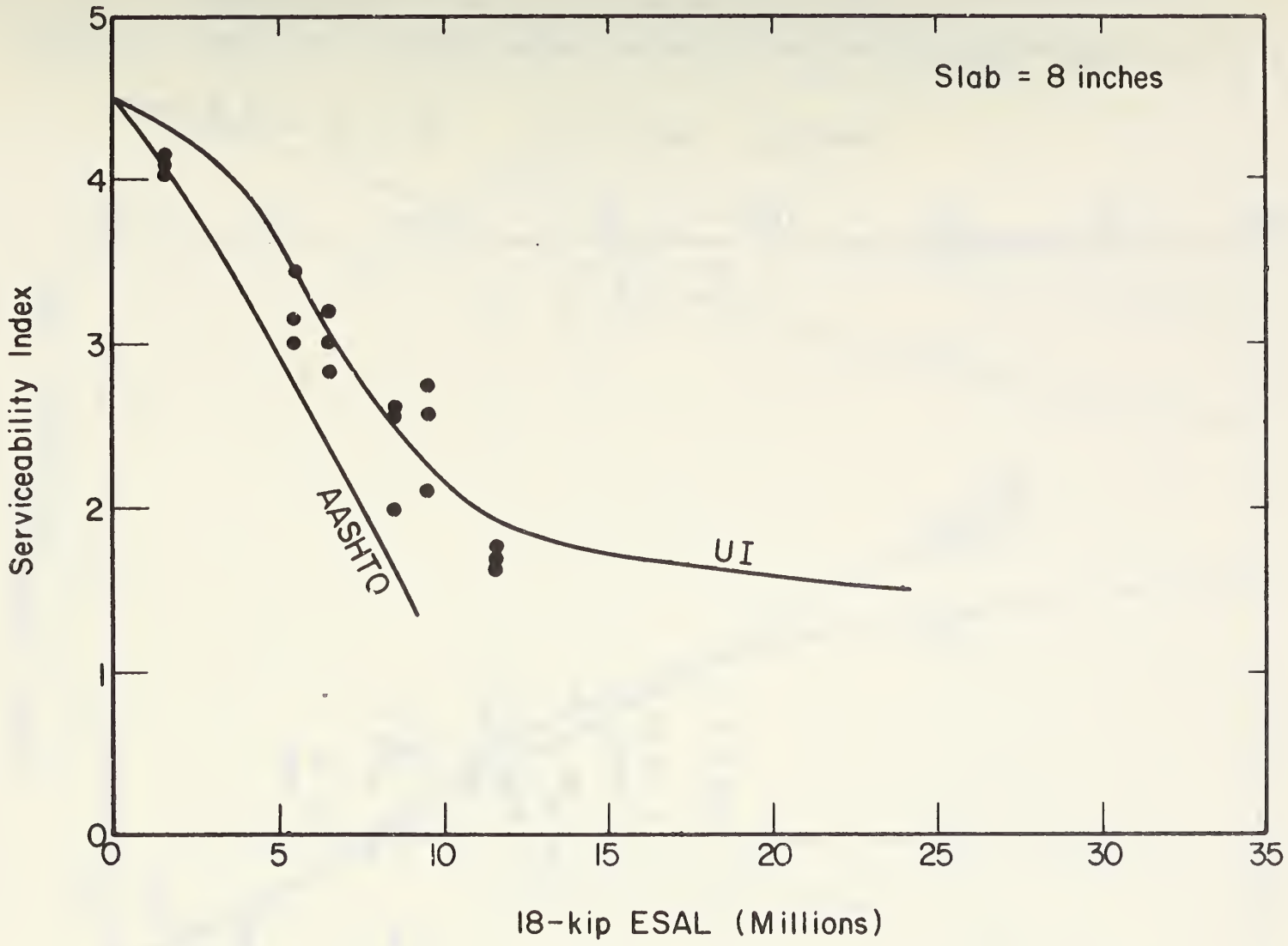


Figure 3.5. Comparison of Original AASHO Performance Equation (Eq. 3.2) and New Performance Equation (Eq. 3.5) for 8 in. (203 mm) Thick Slab.

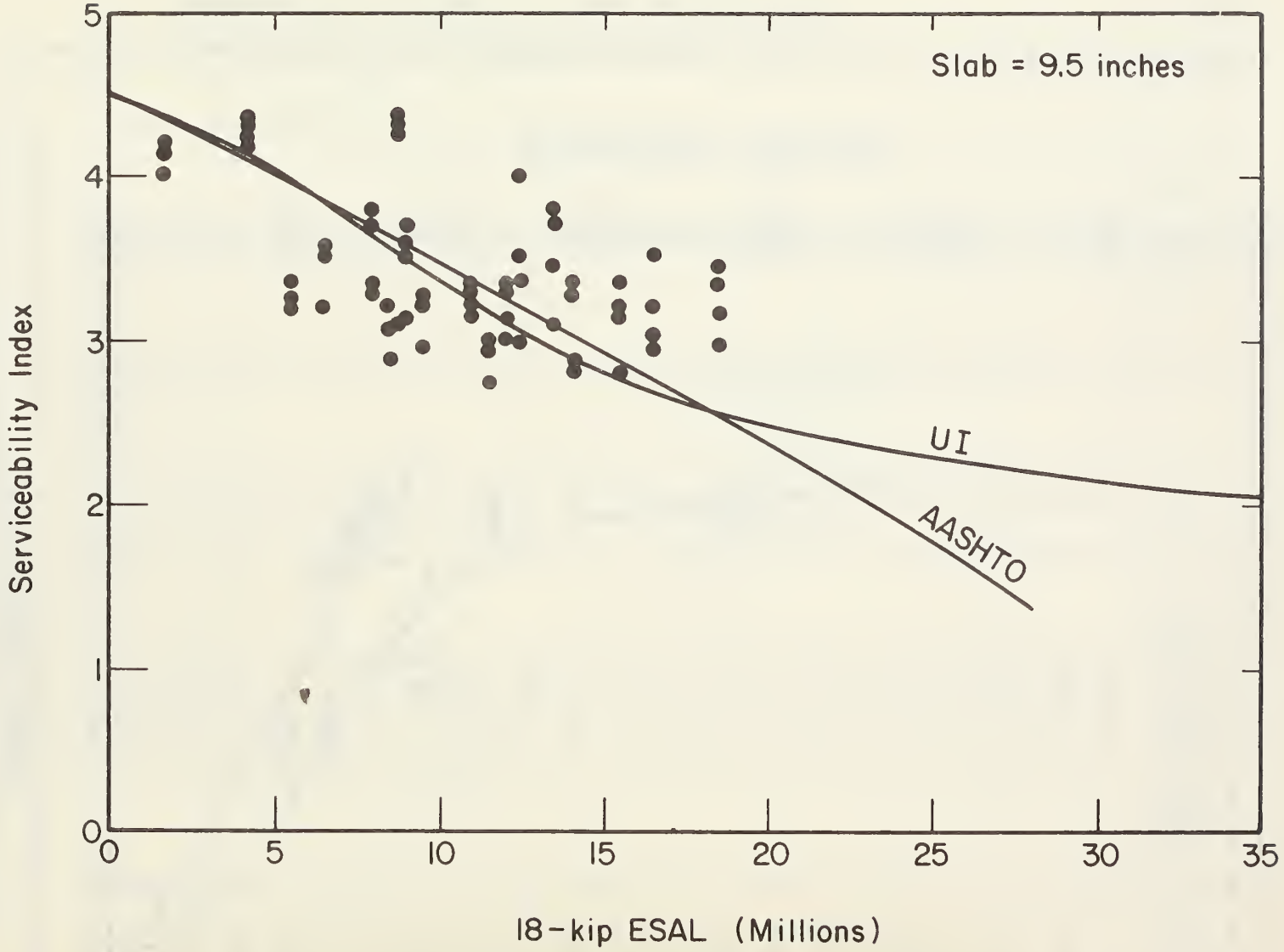


Figure 3.6. Comparison of Original AASHO Performance Equation (Eq. 3.2) and New Performance Equation (Eq. 3.5) for 9.5 in. (241 mm) Thick Slab.

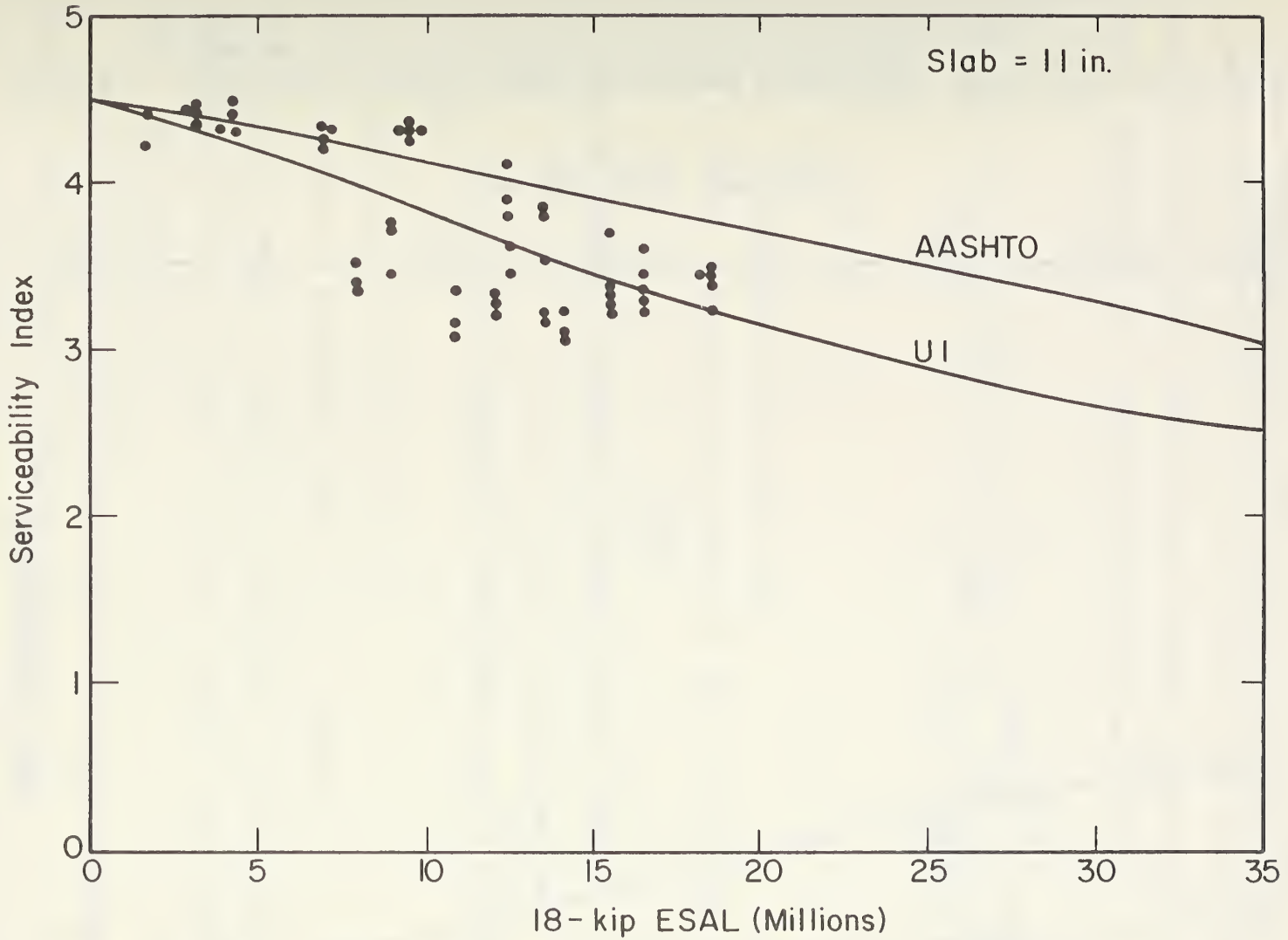


Figure 3.7. Comparison of Original AASHO Performance Equation (Eq. 3.2) and New Performance Equation (Eq. 3.5) for 11 in. (279 mm) Thick Slab.

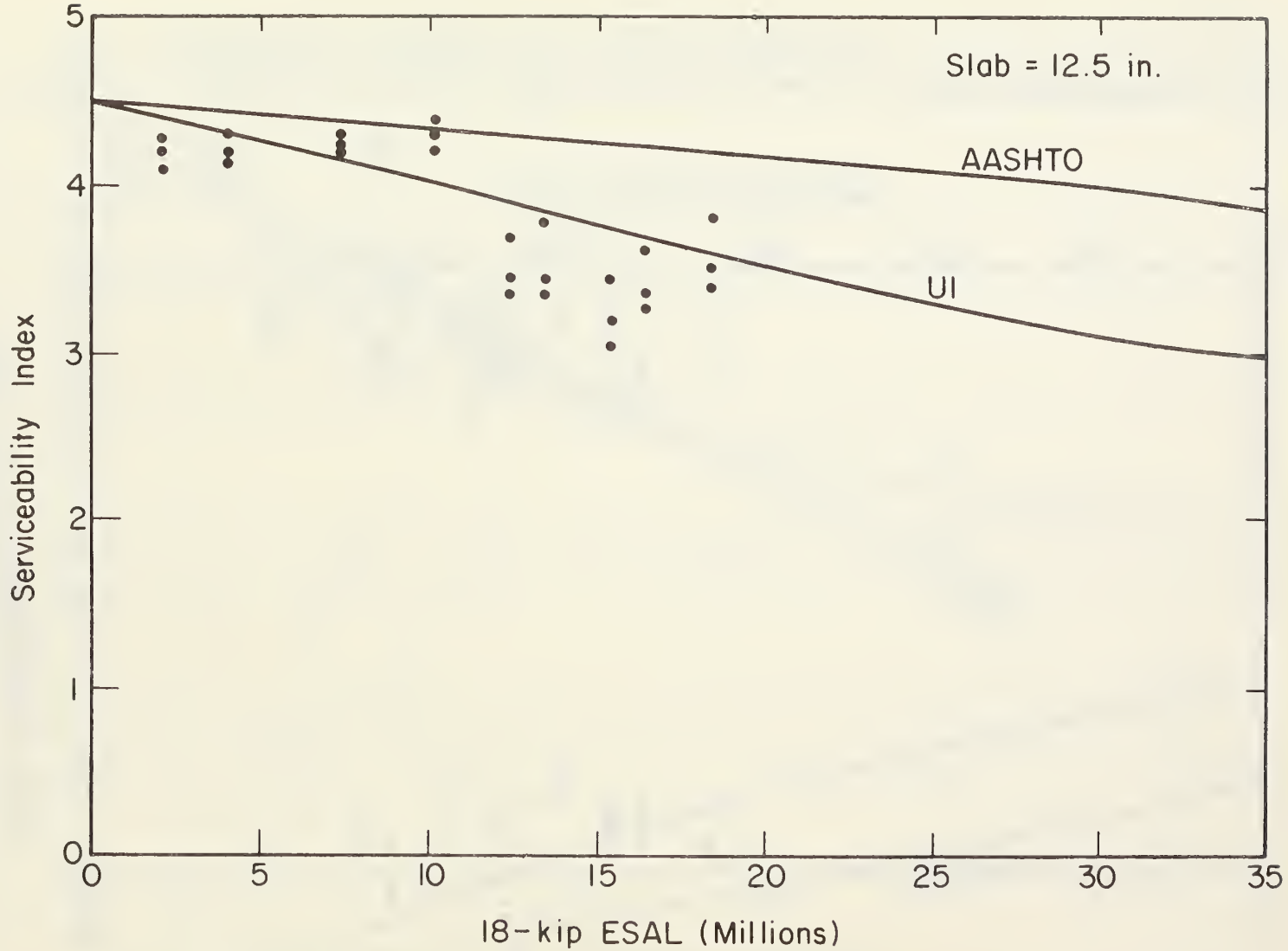


Figure 3.8. Comparison of Original AASHO Performance Equation (Eq. 3.2) and New Performance Equation (Eq. 3.5) for 12.5 in. (318 mm) Thick Slab.

other variables could be included such as the k-value and PCC modulus of rupture. The Equation 3.4 was extended using the Westergaard edge stress equation similar to the way in which the Spangler corner equation was incorporated into the original AASHO Road Test equation as described in the AASHTO Interim Guides (Ref. 61). The following equation was obtained:

$$\log_{10}W_{18} = \log_{10}W'_{18}+(3.892-0.706P2)\log\left[\left(\frac{F28}{690}\right)\frac{4\log\left[\frac{8.789H^{0.75}}{M}\right]+0.359}{4\log\left[\frac{(Z)^{0.25}(0.540H^{0.75})}{M}\right]+0.359}\right] \quad (3.5)$$

in which:

$M = \sqrt{1.6a^2 + H^2} - 0.675H$

a = radius of applied edge load, inches

F28 = modulus of rupture used in design (28 day, 3rd point load adjusted for variability) = $FF - C(\frac{Fcv}{100})FF$

FF = mean modulus of rupture at 28 days, 3rd point load, psi

Fcv = coefficient of variation of modulus of rupture, percent

C = 1.03, a constant representing a confidence level of 85 percent

Z = E/k

E = modulus of elasticity of PCC, psi

k = modulus of foundation support on top of subbase, pci

The Westergaard edge load equation was used because fatigue analysis and field observations of distress as discussed in Chapter 4 show that the slab edge is the critical point.

Based upon these results, Equation 3.5 is the best performance equation derived and is believed to be adequate for design purposes. Its standard error is 0.22 based upon 150 data points from the 25 AASHO sections which is the same as standard error of the original AASHO Equation 3.1.

## 3.4 CLIMATIC FACTOR

Pavement data were collected from 12 plain jointed concrete projects located in eight states. These projects ranged in age from 6 to 34 years and total 18-kip (80kN) ESAL in the heaviest traveled lane up to 39 million.

Analyses were conducted to determine if the pavements from regions different from Illinois showed different performance. Four general climatic regions were chosen based upon precipitation and potential evapotranspiration, and frost heave and freeze thaw damage as defined in Table 2.3. A "climatic factor" is defined as follows:

$$CF = \frac{W_{18(computed)}}{W_{18(actual)}} \tag{3.6}$$

where

$CF$ = climatic factor

$W_{18(computed)}$ = total computed number of equivalent 18,000 pound (80 kN) single axle load applications to reduce serviceability index from an initial value to a terminal value determined from performance Equation 3.5.

$W_{18(actual)}$ = total accumulated number of equivalent 18,000 pound (80 kN) single axle load applications to pass over pavement, determined from traffic data.

If CF equals 1.0 then there is no significant climatic effect for a given pavement. The CF could theoretically range from less than 0.1 to more than 1.0. A computation of CF for each of the pavements is given in Table 3.3. There is considerable scatter in each climatic region, but the results indicate that pavements perform somewhat different in the general climatic regions.

Table 3.3. Data Used to Compute Factors.

| Project No. | Climatic Region | H (in.) | FF (psi) | k* (pci) | SI | Calc.*** $W_{18}(10^6)$ | Act.**** $W_{18}(10^6)$ | CF |
|---|---|---|---|---|---|---|---|---|
| 1-3** | WF | 8 | 690 | 115 | 1.7 | 15.44 | 11.16 | 1.38 |
| 4-6 | WF | 9.5 | 690 | 115 | 2.8 | 15.07 | 11.32 | 1.33 |
| 7-10 | WF | 9.5 | 690 | 115 | 3.1 | 12.25 | 13.75 | 0.89 |
| 11-14 | WF | 9.5 | 690 | 115 | 3.2 | 11.40 | 17.82 | 0.64 |
| 15-17 | WF | 11 | 690 | 115 | 3.1 | 20.42 | 14.09 | 1.45 |
| 18-22 | WF | 11 | 690 | 115 | 3.4 | 15.70 | 18.94 | 0.83 |
| 23-25 | WF | 12.5 | 690 | 115 | 3.6 | 18.62 | 19.47 | 0.96 |
| 32 | WF | 10 | 750 | 197 | 3.0 | 22.83 | 35.93 | 0.64 |
| 36 | WF | 10 | 600 | 115 | 2.5 | 20.87 | 18.73 | 1.11 |
| 37 | WF | 9 | 650 | 400 | 3.9 | 6.11 | 6.53 | 0.94 |
| 26 | W | 9 | 700 | 192 | 3.9 | 6.08 | 5.42 | 1.12 |
| 33 | W | 8 | 707 | 200 | 3.4 | 12.16 | 21.74 | 0.56 |
| 30 | DF | 9 | 675 | 267 | 4.0 | 5.12 | 5.12 | 1.00 |
| 34 | DF | 8 | 707 | 353 | 3.4 | 8.10 | 6.45 | 1.25 |
| 35 | DF | 8 | 707 | 367 | 3.6 | 6.97 | 8.83 | 0.79 |
| 27 | D | 8 | 675 | 450 | 3.0 | 10.29 | 14.57 | 0.71 |
| 28 | D | 8 | 675 | 500 | 3.0 | 11.58 | 39.65 | 0.29 |
| 31 | D | 9 | 725 | 200 | 3.2 | 12.57 | 30.23 | 0.42 |

* Mean of lowest 9 months on top of subbase.
** Pavements from the Road Test site that had similar slab thickness and traffic were combined.
*** Computed from Eq. 3.5.
**** Computed from traffic data.

1 in = 25.4 mm

| Region | CF Range | Mean C F |
|---|---|---|
| Wet/Freeze | 0.64-1.45 | 1.02 |
| Dry/Freeze | 0.79-1.26 | 1.02 |
| Wet/Non-freeze | 0.56-1.12 | 0.84 |
| Dry/Non-freeze | 0.29-0.71 | 0.47 |

These data indicate, for example, that similar plain jointed concrete pavements constructed in dry/non-freeze climates would last about twice as long as those in wet/freeze climates. Additional data are needed to further verify these results however.

The following values are selected for use in design.

| | |
|---|---|
| Wet-freeze (WF) | 1.0 |
| Wet/non-freeze (W) | 0.9 |
| Dry-freeze (DF) | 1.0 |
| Dry/Non-freeze (D) | 0.6 |

A plot showing predicted 18-kip (80 kN) ESAL (by Eq. 3.5) vs. the computed 18-kip (80 kN) ESAL (or actual) for all pavements is given in Figure 3.9. The total 18-kip (80 kN) ESAL data is computed based on the heaviest traveled lane from the time the pavement was opened to traffic unitl the data of the survey when the SI was determined. The computed 18-kip (80 kN) ESAL were adjusted by the recommended climatic factors. The standard error of prediction of Equation 3.5 is 0.175 which is less than the 0.222 for the AASHO equation.

## 3.5 TERMINAL SERVICEABILITY INDEX FOR ZERO-MAINTENANCE DESIGN

A terminal SI must be selected for zero-maintenance design. The value selected has a significant effect on (1) construction cost of the pavement, (2) probability of structural distress occurring that requires

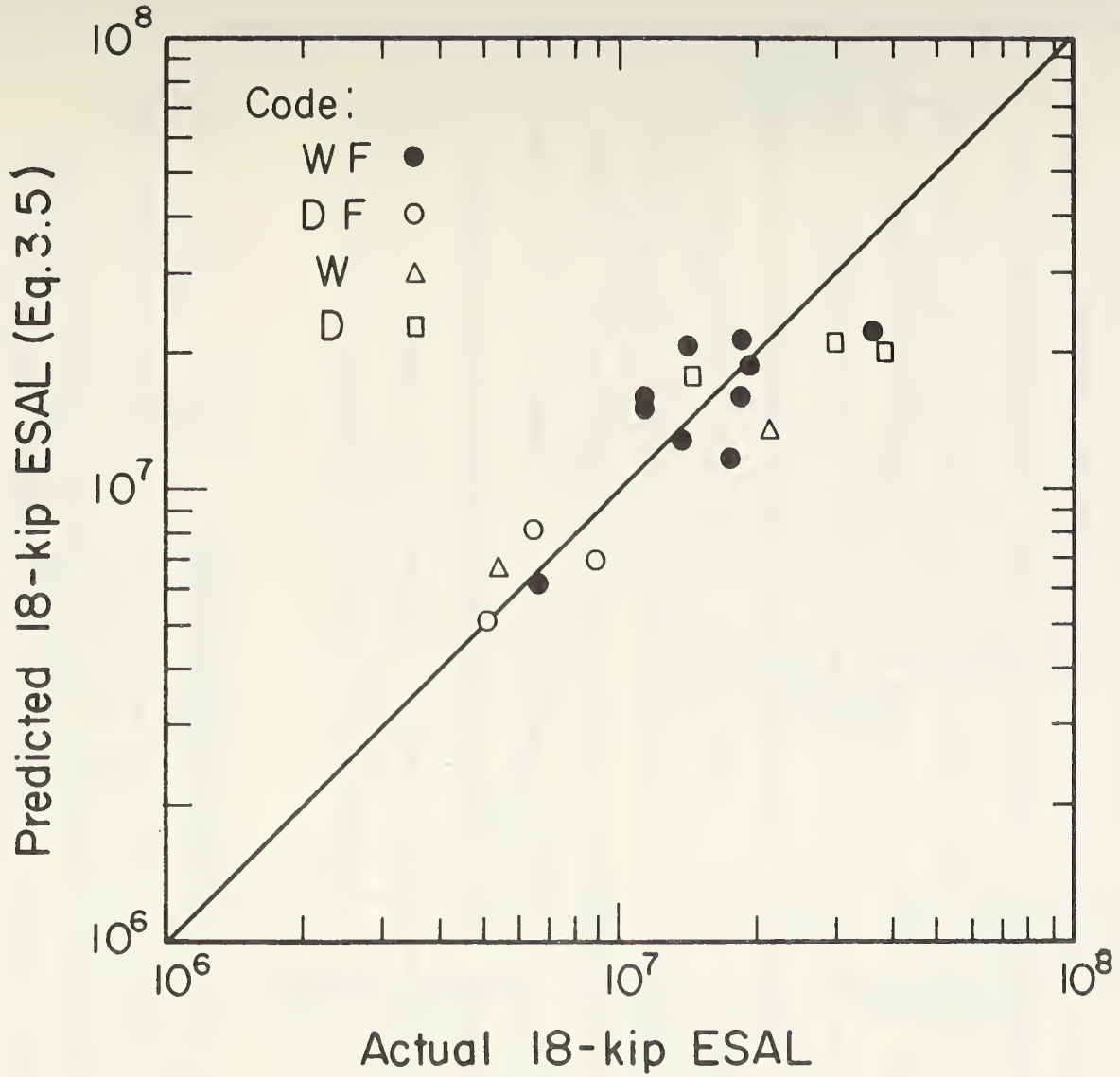


Figure 3.9. Comparison of Actual 18 kip (80 kN) ESAL (Computed from Traffic Data) with Predicted (Computed from Equation 3.5 and Adjusted by Climatic Factors) over Life of Each Project.

maintenance, (3) user costs due to rough pavements. The higher the terminal SI the more substantial the structure must be and therefore the higher the construction cost of the pavement. However, the higher the terminal SI the lower the probability of structural distress and the lower the user costs due to rough pavements as shown in Figure 3.11.

The loss of serviceability of a jointed concrete pavement is caused by several distress types. Previous analysis (Ref. 2) indicated that linear cracking, faulting at joints and cracks, spalling of joints and cracks, and differential settlement of the slabs (causing roughness) are the major causes of loss of serviceability. As the serviceability index drops from its initial value after construction, the probability of the pavement requiring maintenance increases. A plot of serviceability index versus the percentage of projects showing zero-maintenance performance is shown in Figure 3.10 for all 37 projects (Pavements having less than 3 $ft^2$ patching/1000 $ft^2$ were considered to be relatively maintenance-free). Pavements having serviceability indices of 3.6 or higher all showed maintenance-free performance, while pavements having serviceability indices of less than 2.7 all received maintenance. The 50th percentile for receiving maintenance is a serviceability index of 3.0.

## 3.6 SENSITIVITY OF NEW PERFORMANCE EQUATION

A sensitivity analysis of Equation 3.5 is presented to illustrate the effect of the several parameters. The five design parameters included are slab thickness, modulus of rupture of PCC, modulus of subgrade reaction, climatic region, and total 18-kip (80 kN) ESAL application in design lane. The relative effects of these variables are shown in Figures 3.12 to 3.14. All of these curves are developed for a terminal serviceability index of

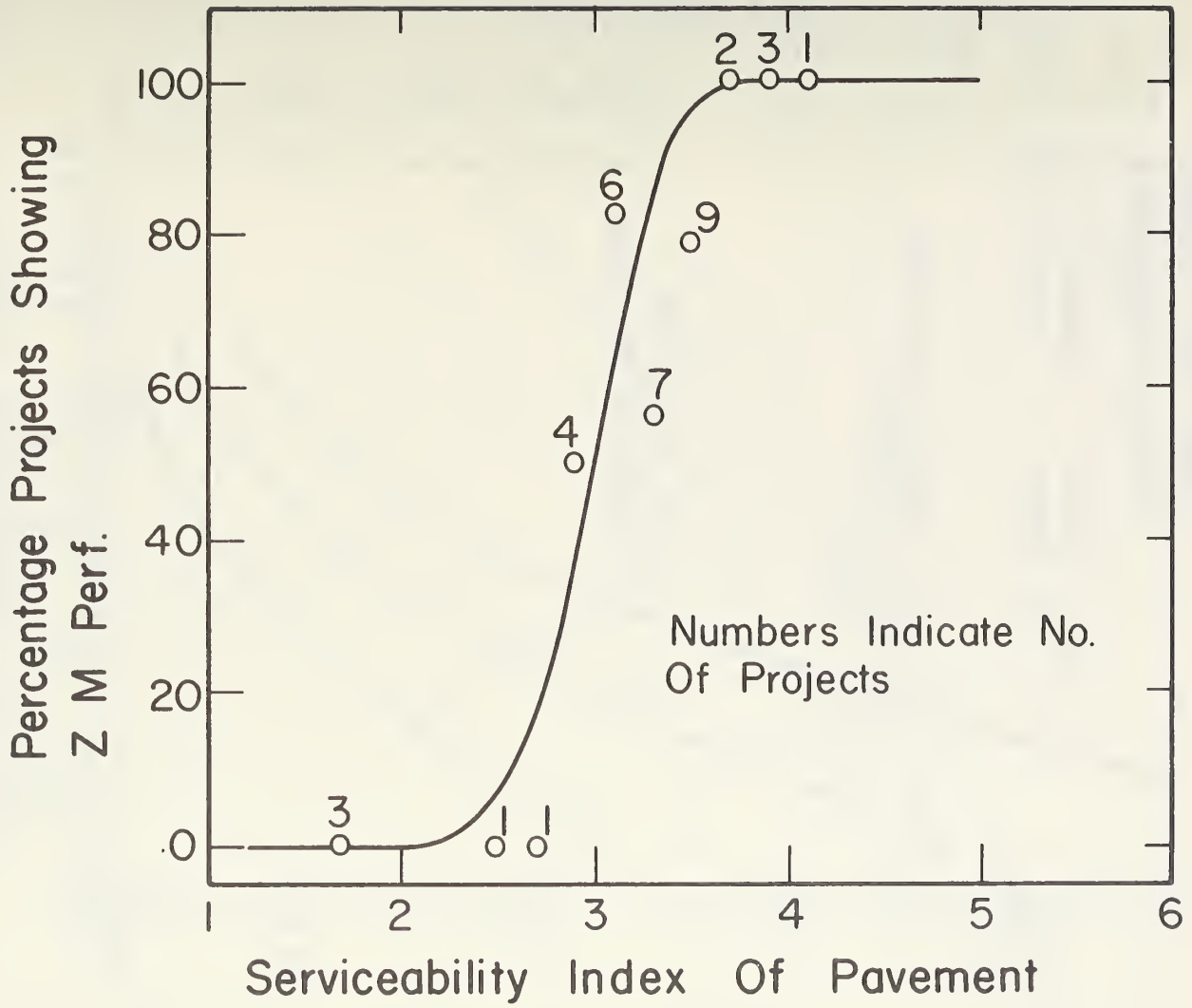


Figure 3.10. Effect of Serviceability on Maintenance Requirements.

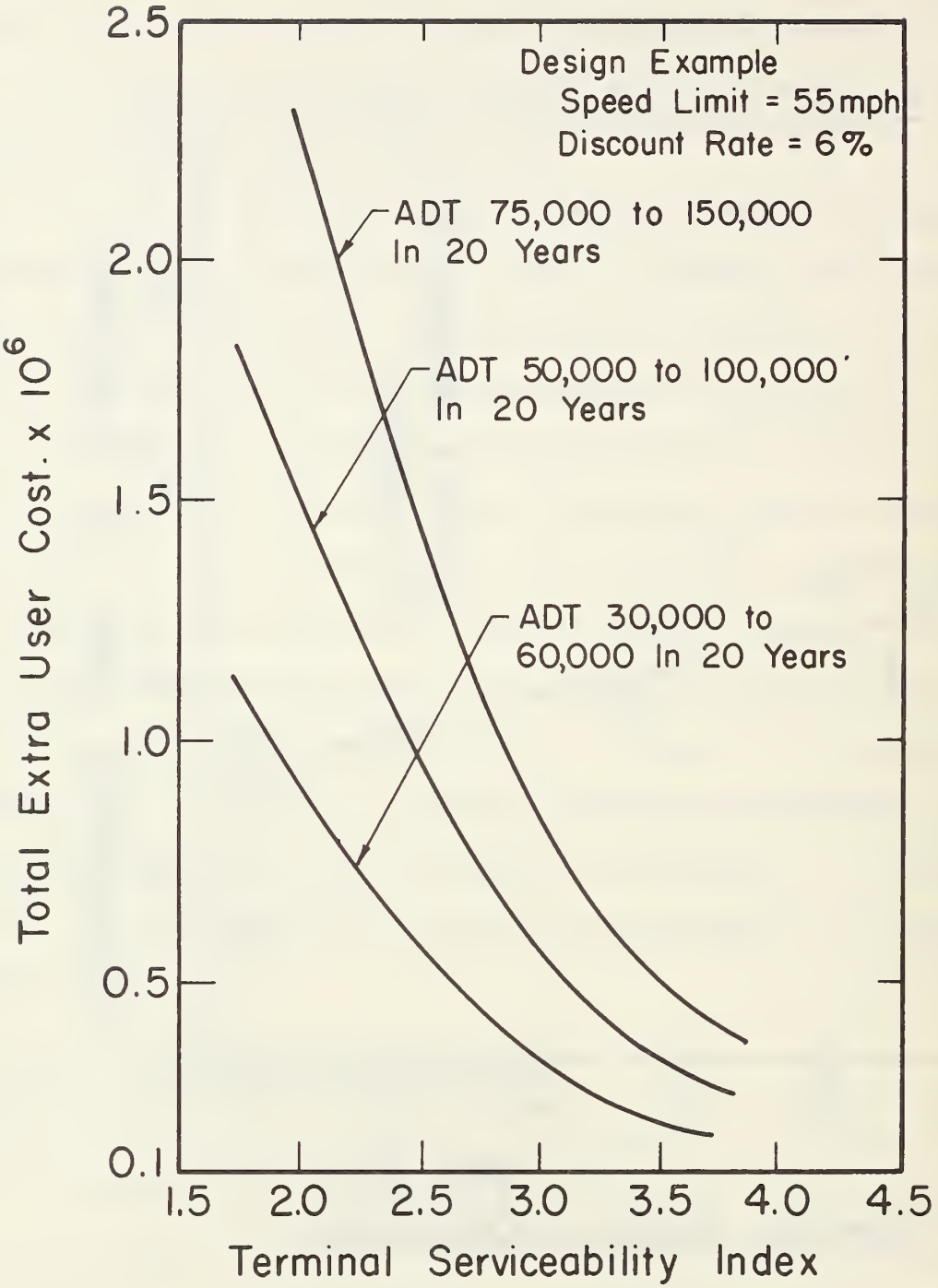


Figure 3.11. Total Extra User Costs vs. Terminal Serviceability for Different Traffic Conditions (from Ref. 2).

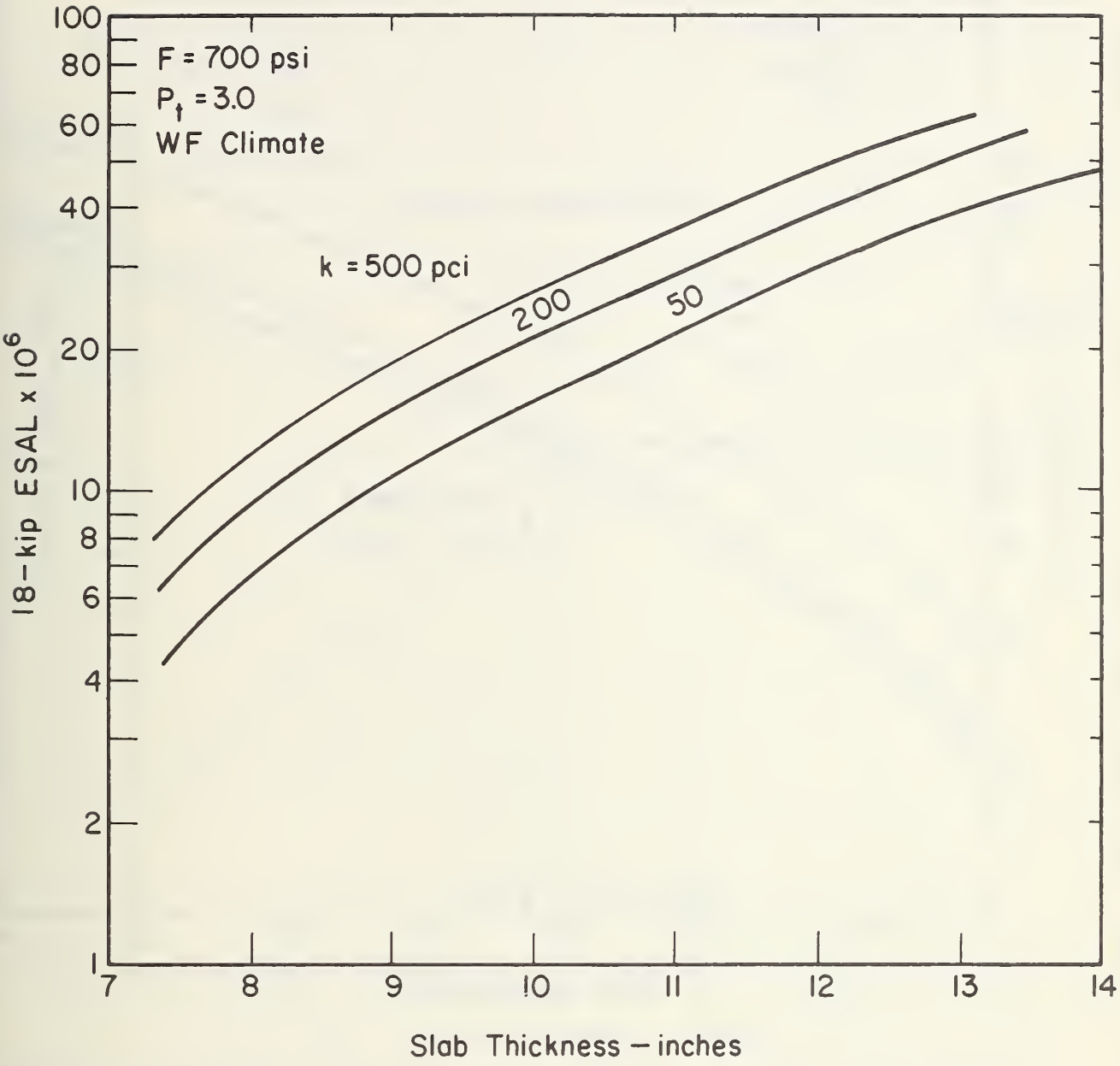


Figure 3.12. Sensitivity of New Performance Equation (Eq. 3.5).

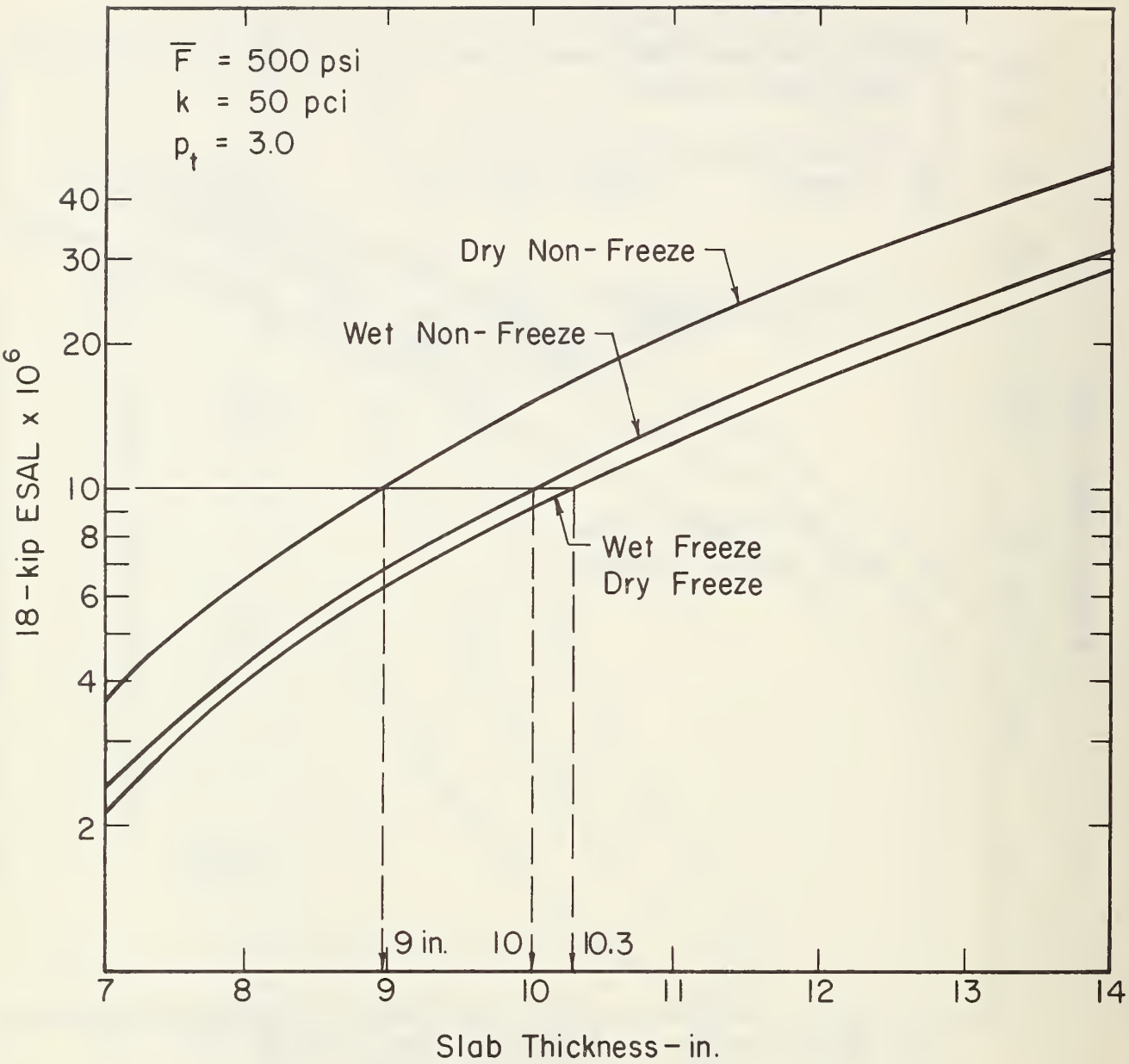


Figure 3.13. Sensitivity of New Performance Eq. 3.5 over Climatic Regions.

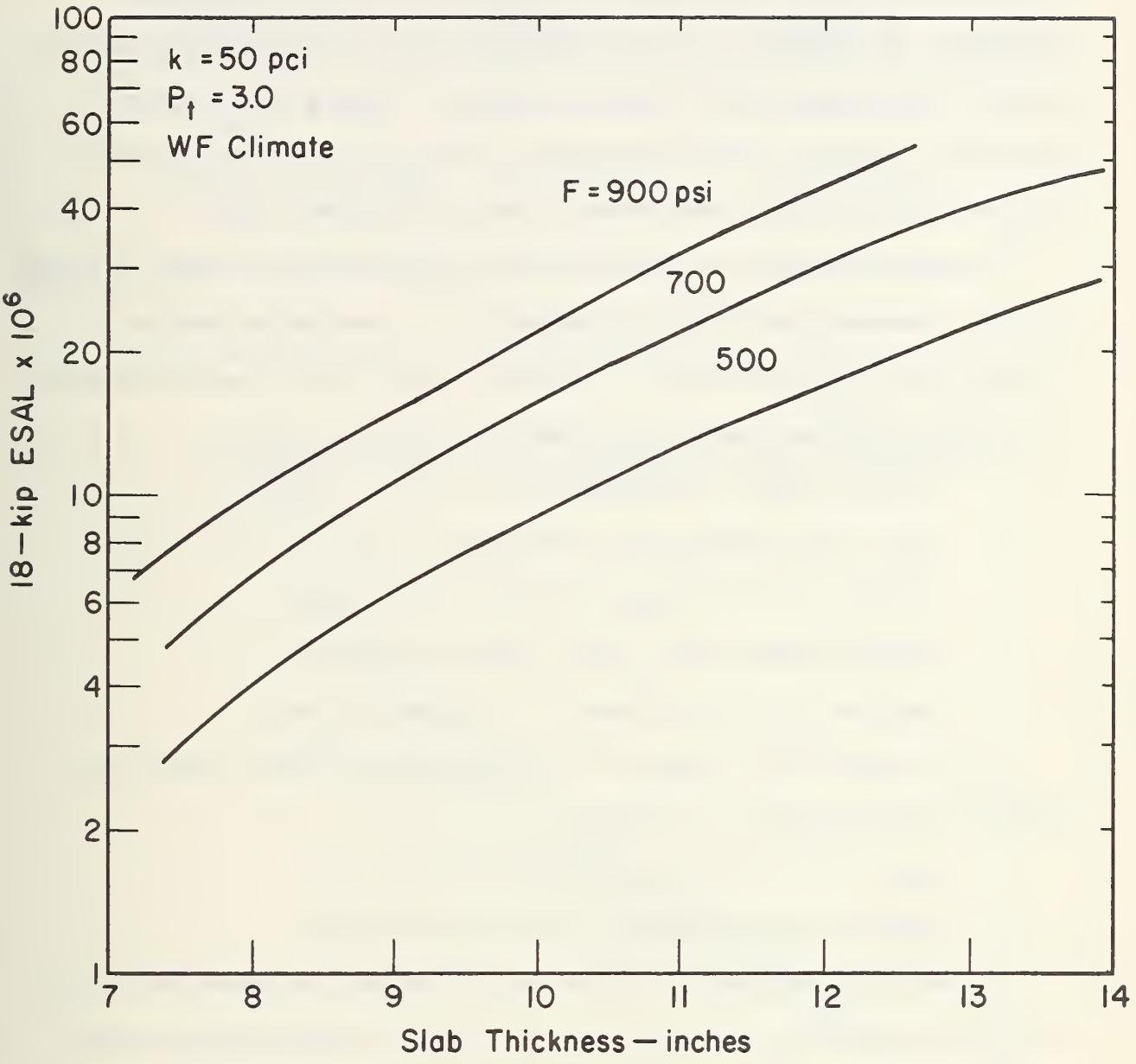


Figure 3.14. Sensitivity of New Performance Equation (Eq. 3.5).

3.0. These plots show that each of the five parameters have a significant effect on pavement life as measured by the 18-kip (80 kN) ESAL. An example of the effect of each parameter is shown in Table 3.4 where the change in 18-kip (80 kN) ESAL is noted due to a change in each of the four other parameters. A significant change in each parameter, produces a significant change in the 18-kip (80 kN) ESAL applications. Since a typical lane loading for a heavily trafficked pavement is one million 18-kip (80 kN) ESAL/year, these could be considered as years of pavement life.

A graphical solution of Equation 3.5 was prepared and is shown in Figure 3.15 for a terminal serviceability index of 3.0. An example is given to illustrate the use of this chart in design. Assume the following parameters and solve for the required slab thickness:

Climatic Region = Wet/freeze

Total 18-kip (80 kN) ESAL (millions) = 20.0

k-value on top of subbase = 100 pci (271 kP/cm)

Working stress of PCC (F28) = 600 psi (4137 kP)

Required PCC slab thickness = 11 inches (279 mm)

If the pavement was located in a dry/non-freeze climatic region the required slab thickness is as follows:

Total 18-kip (80 kN) ESAL = 20.0 x 0.6 = 12.0

Required Slab Thickness = 9.5 inches (241 mm)

The effect of terminal SI on user costs from vehicle operation and travel time was previously analysed (Ref. 2). Results showed that the total user costs over a 20 year life span increases dramatically as the terminal serviceability at the 20th year is decreased from 3.5 to 2.0 as shown in Figure 3.11. The rate of increase is very high for a terminal serviceability less than 3.0.

Table 3.4. Example Sensitivity Analysis of New Performance Design Equation 3.5.

| Design Parameter | Change in Parameter * | Change in 18-kip ESAL (million) |
|---|---|---|
| Modulus of Rupture, psi | 600 to 800 | 9.2 to 15.5 |
| k-value of Foundation, pci | 100 to 500 | 9.2 to 14.5 |
| Slab Thickness, ins. | 9 to 11 | 9.2 to 20.0 |
| Climatic Region | WF to D | 9.2 to 15.3 |

*Values are computed assuming a standard section of 9 in. slab, k-value of 100 pci, modulus of rupture of 600 psi, located in a wet-freeze region.

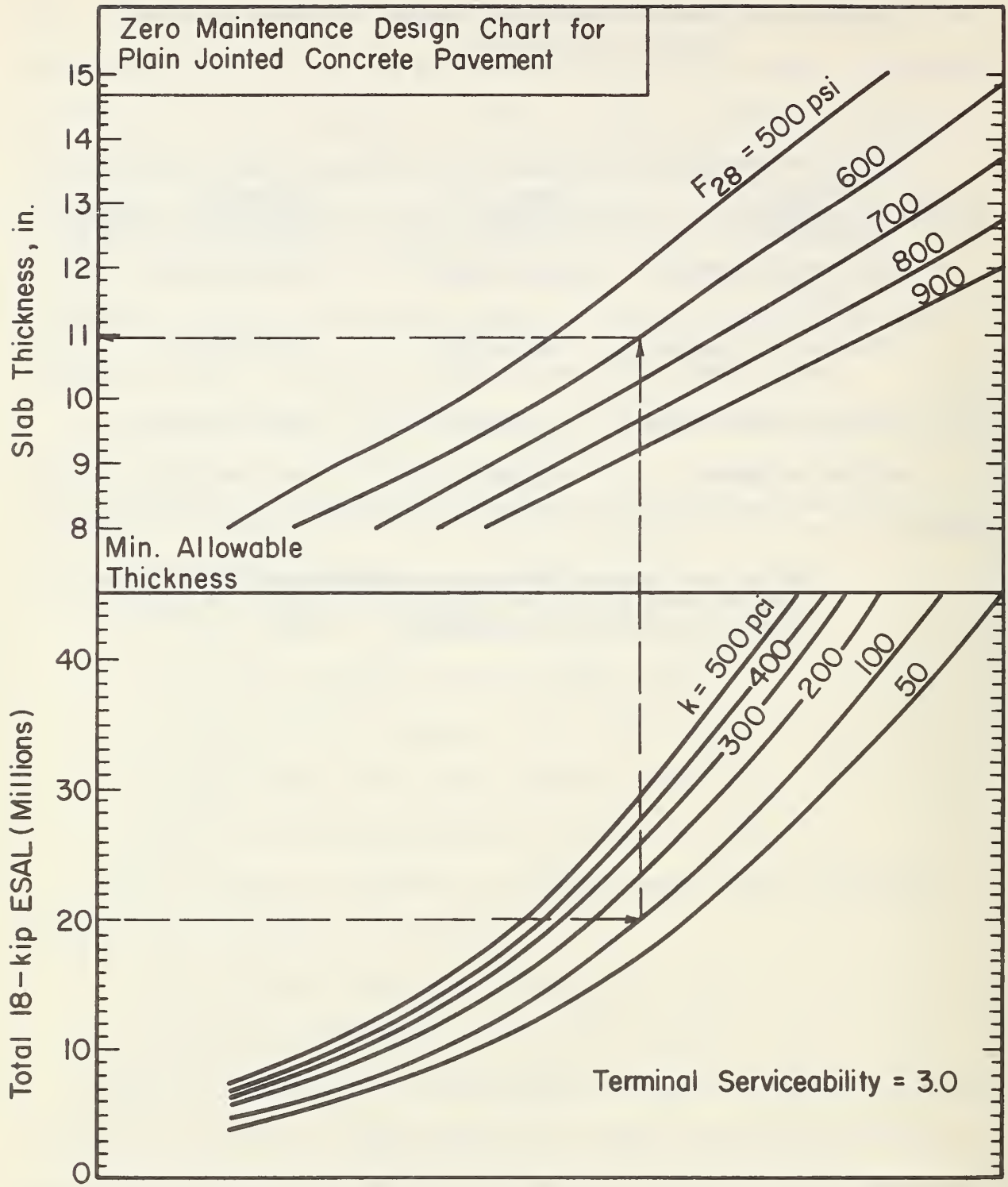


Figure 3.15. Graphical Solution of Equation 3.5 to be Used for Design.

Based upon these results, and the desirability of keeping construction costs as low as possible, a minimum acceptable design terminal SI is in the range of 3.0 to 3.5. A minimum value of 3.0 is selected since it provides a reasonable assurance that no or only minimal maintenance will be required before the pavement reaches this value. Also, user delay costs have not increased dramatically at a SI of 3.0. Much of the loss in SI from its initial value to 3.0 to 3.5 is believed to be from differential settlement or possibly heave of the foundation, hence very little surface deterioration should have taken place.

# CHAPTER 4

# STRUCTURAL DESIGN BASED ON PCC FATIGUE

This chapter discusses the development of a fatigue analysis procedure for plain jointed concrete slabs. The purpose of the fatigue analysis is to prevent cracking of the slabs which is one of the most serious types of distress requiring maintenance.

## 4.1 FINITE ELEMENT MODEL

An evaluation was conducted to determine the best jointed concrete pavement structural analysis program. Several programs were evaluated including the following:

a. Finite Element Program for Concrete Slabs Using Winkler Foundation (Ref. 66).

b. Finite Element Program for Concrete Slabs Using Elastic Solid Foundation (Ref. 67).

c. Concrete Airfield Pavement Design Program (PCA) (Ref. 68).

d. Discrete-Element Method of Analysis for Orthogonal Slab and Grid Bridge Flow Systems Program (Slab 49) (Ref. 4).

e. Finite Element Analysis of Concrete Airfield Pavements Program (Ref. 5).

f. Finite Element Program for Pavement Analysis (Ref. 7).

Results from the evaluation showed that the finite element slab analysis program developed by Y. H. Huang and S. T. Wang (Ref. 66) has the most desirable capabilities for analysis of plain jointed concrete pavement slabs. This program has many important capabilities including the determination

of stresses and deflections in concrete pavement slabs with full or partial subgrade contact, variable load transfer of transverse and longitudinal joints, and the effect of thermal gradients on curling stress both independently and in combination with traffic load. The method is based on the theory of minimum potential energy by dividing the slab into small elements interconnected only at a finite number of nodal points. Other major advantages of the finite element method are that computed stresses agree well with experimental results, elements of varying sizes can be easily incorporated in the analysis, and no special treatment is needed at a free edge.

4.1.1 Description of Finite Element Method. This finite-element method is based on the classical theory of thin plates which assumes that:

(a) The plane before bending remains plane after bending.

(b) The slab is homogeneous, isotropic, and elastic.

(c) The subgrade acts as a Winkler foundation, i.e., the reactive pressure between subgrade and slab at any given point is proportional to the deflection at the point (dense liquid approximation of the subgrade).

A set of simultaneous equations are obtained for solving the unknown nodal displacements of every element in the PCC slab and a force-displacement relationship for all nodes in the pavement model is developed as

$$k[A]\{\delta'\} = \{F\}\ [k]\{\delta\} \qquad (4.1)$$

where k is the modulus of subgrade reaction, [A] is the diagonal matrix representing the area over which subgrade reaction is distributed, $\{\delta'\}$ is the subgrade displacement, {F} is a vector containing all the forces acting on the pavement model, $\{\delta\}$ contains all the nodal displacements, and

[k] is the assembled stiffness matrix of the whole pavement system (for more details see Ref. 66). The first term on the left hand side of Eq. 4.1 represents the nodal forces due to subgrade displacement caused from the resultant of the initial curling of the pavement slab due to a temperature differential between the top and the bottom, and the amount of the initial gaps due to pumping or plastic deformation of the subgrade. The amount of the initial gap as well as the deformed shape of the slabs due to the combined effect of slab weight and warping are determined first. The nodal moments and stresses are then computed from the nodal displacements using the stress matrix tabulated by Zienkiewicz (Ref. 8). Because the stresses at a given node computed by means of one element might be different from that by the neighboring elements, the stresses in all adjoining elements are computed and their average values obtained.

4.1.2 Transverse and Longitudinal Joints. The finite element model provides an effective method for analyzing concrete slabs with doweled transverse joints. First by assuming the discontinuity of the two adjacent slabs at the joint, the equilibrium equations of each slab is developed separately. Assuming there is no moment transfer across the joint (since dowel bars do not transmit much moment from one slab to the other), then dowel bars will effect only those equations that give vertical forces at each node. Therefore, by equating the sum of two equations corresponding to vertical forces at every two adjacent nodes at the joint, to the external forces applied at that node, the number of equations is reduced. However, at every two adjacent nodes at the joint, one equation (the efficiency equation of load transfer) is added to the set of the equilibrium equations which result in the total number of equations remaining unchanged.

4.1.3 Computer Program. The finite element model is programmed for an IBM 360 computer. The program can determine the slab stresses and deflections due to thermal curling (stresses caused only by weight of slabs), applied traffic loads, or the combination of the applied loads and thermal curling of the slab. The program can handle one slab, two slabs connected by a transverse joint, or four slabs connected by a longitudinal and a transverse joint. The efficiency of load transfer at each joint can be specified as the ratio of the deflection of the unloaded slab over the deflection of the loaded slab at the transverse joint, as a percent:

$$\text{Efficiency} = \frac{W_{\text{unloaded}}}{W_{\text{loaded}}} \times 100 \qquad (4.2)$$

The tire imprints of the wheel load are converted to rectangular areas, and the coordinates of their sides must be input so that the program can distribute the wheel loads among adjacent nodes by statics. The program can handle any number of loads at the same time. The additional computer time due to these additional loads is very small because Gauss elimination of the coefficient matrix is carried out only once regardless of the number of loads involved.

Computation of the thermal curling stress of the slab requires input of temperature differential through the slab.

The program can be used to investigate the effect of partial subgrade contact on stress distribution. The nodal numbers at which subgrade reactions resulting from loss of subgrade contact does not exist can be assigned, and the first term on the left side of Equation 4.1 will be automatically eliminated at these nodal points when forming the simultaneous equations.

4.1.4 Comparison of Measured and Computed Load Stress. A comparison is made between the finite-element solutions and experimental measurements so that the validity of the method as applied to actual pavements can be tested. The results of the strain measurements from AASHO Road Test (Ref. 9) provide excellent data for making such comparisons. Tests were conducted on the main traffic loops where the strain due to moving traffic was measured at the slab edge far from any joint. The length of slabs consisted of 15 ft. non-reinforced sections and 40 ft. reinforced slabs and slab thickness ranged from 5 to 12.5 ins.

The finite element program requires the modulus of elasticity and the Poisson's ratio of concrete, the modulus of subgrade reaction, k, and the axle load. The measured dynamic modulus of concrete was $6.25 \times 10^6$ psi, and the Poisson's ratio was 0.28. The determination of the subgrade k-values is much more difficult because it changes appreciably with the time of the year. The elastic k-values on the subbase obtained by the plate bearing test at the AASHO Road Test varied from approximately 85 to 200 $lb/in.^3$ over all of the loops throughout the two years. Two k-values of 108 and 150 pci were used in a F.E. analysis conducted to verify the closeness of the program to the measured values at the AASHO Road Test. The first value (108 pci) is the mean k-value that was measured during the spring trenching program between April 23 and May 25, 1960. The second value (150 pci) is somewhat of an overall average from the loops as indicated from Figure 3-8, Reference 9.

The single and tandem axle loading configurations are shown in Figures 4.1 and 4.2, respectively. The load configuration shown in Figure 4.3 was also used and was found to give the same stresses as the configuration in Figure 4.1.

The stress comparison for single axles is shown in Figure 4.4 and for

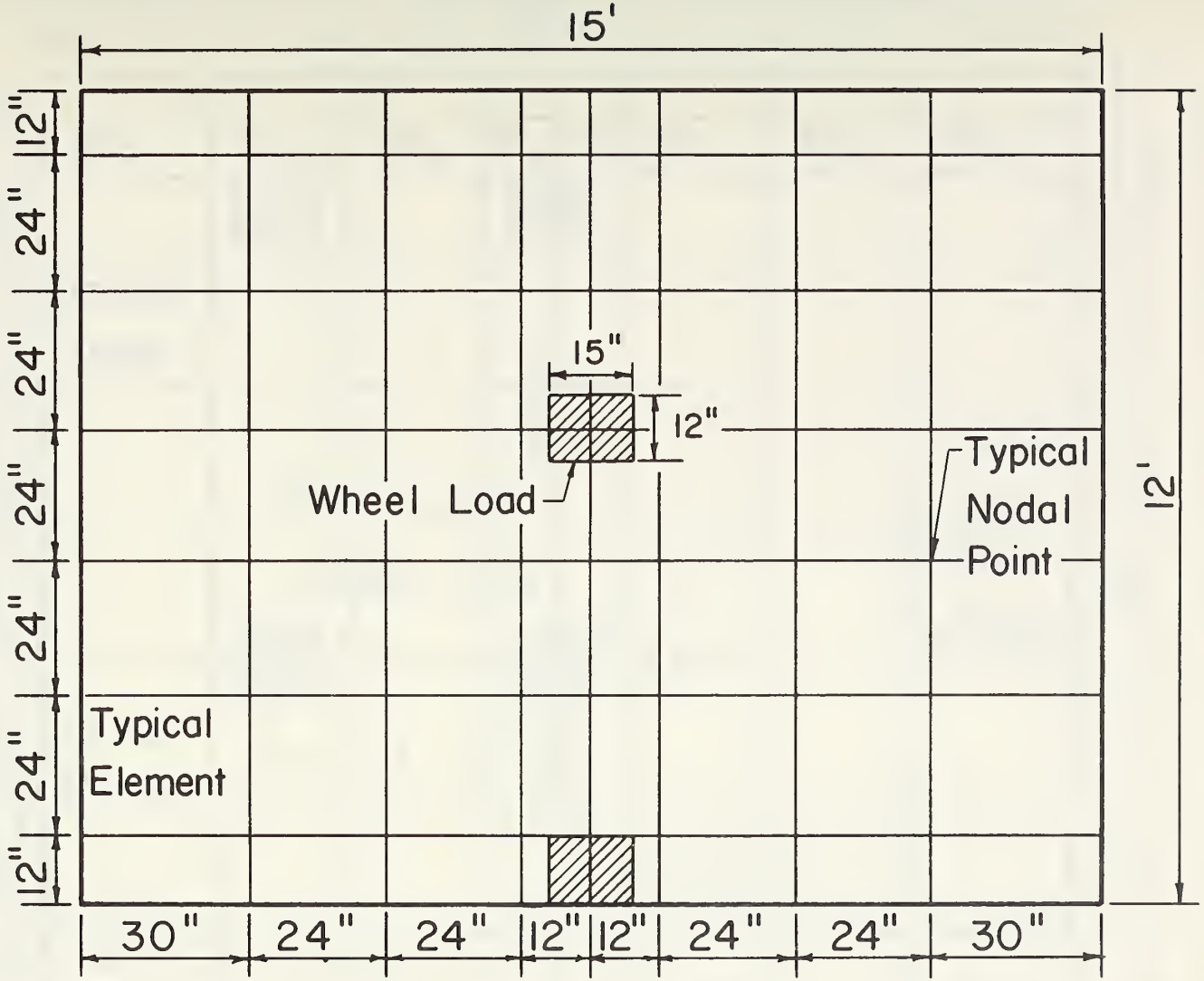


Figure 4.1. Finite Element Slab Layout for Single Axle Load.

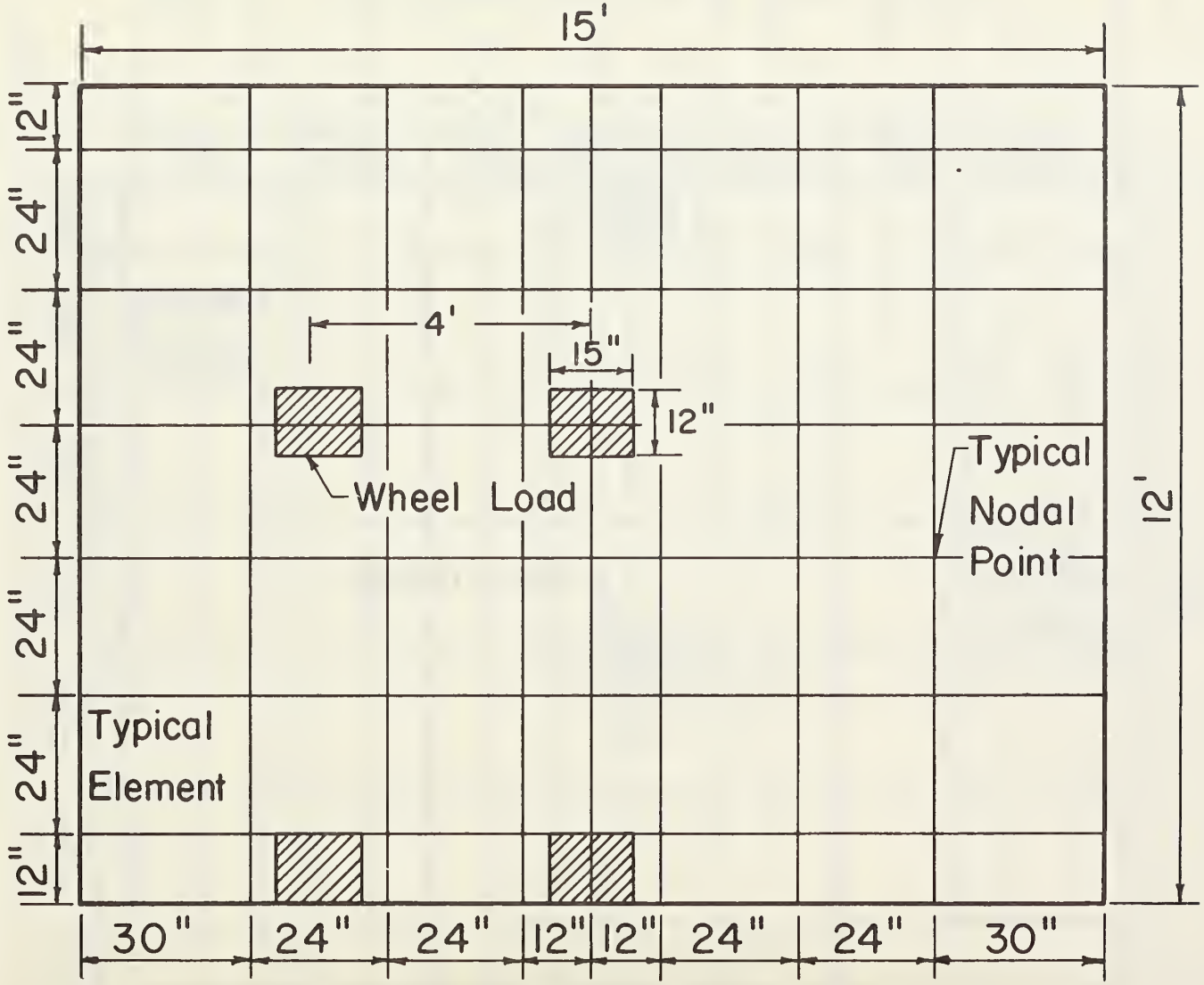


Figure 4.2. Finite Element Slab Layout for Tandem Axle Alternate Configuration.

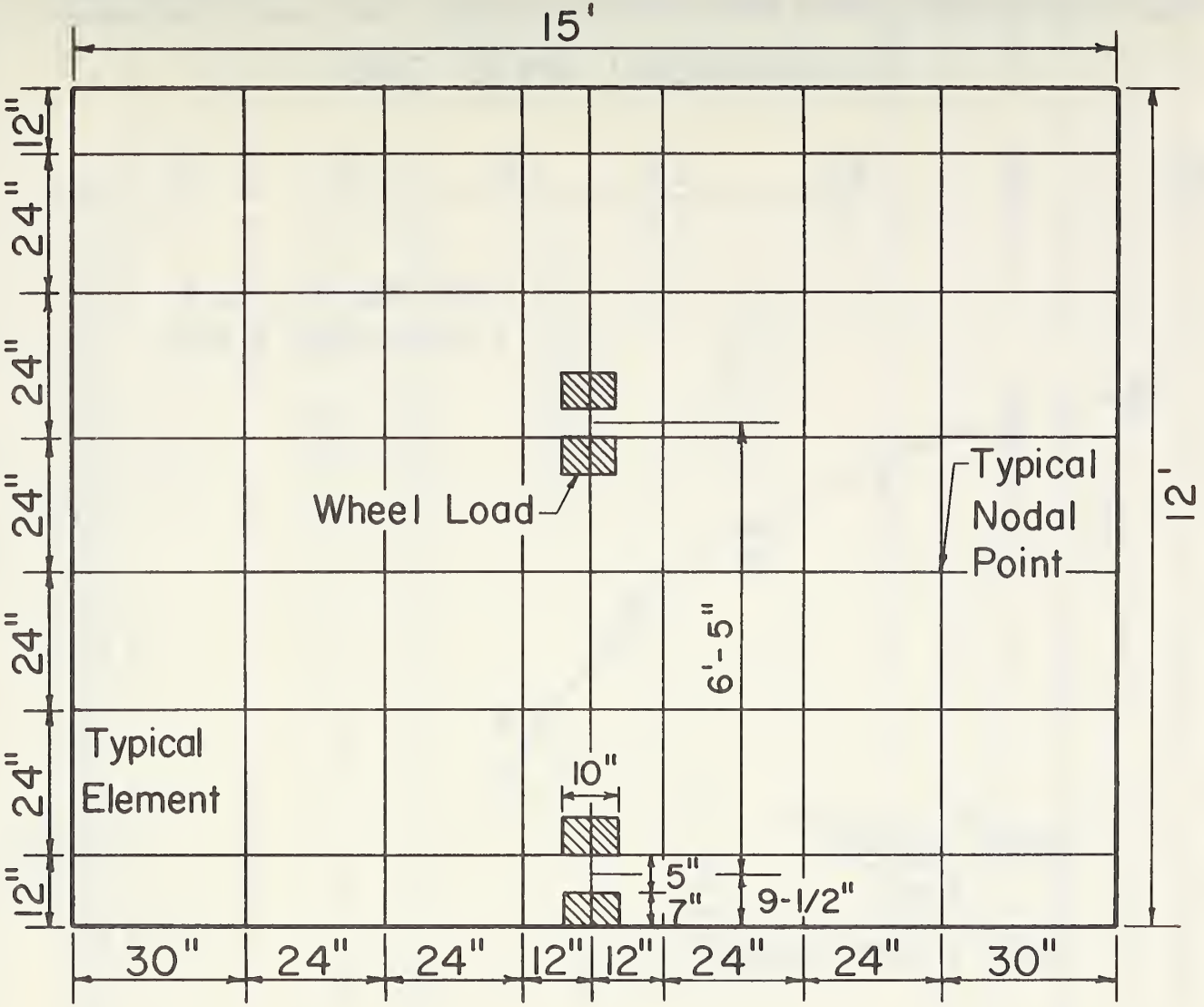


Figure 4.3. Finite Element Slab Layout for Single Axle Load.

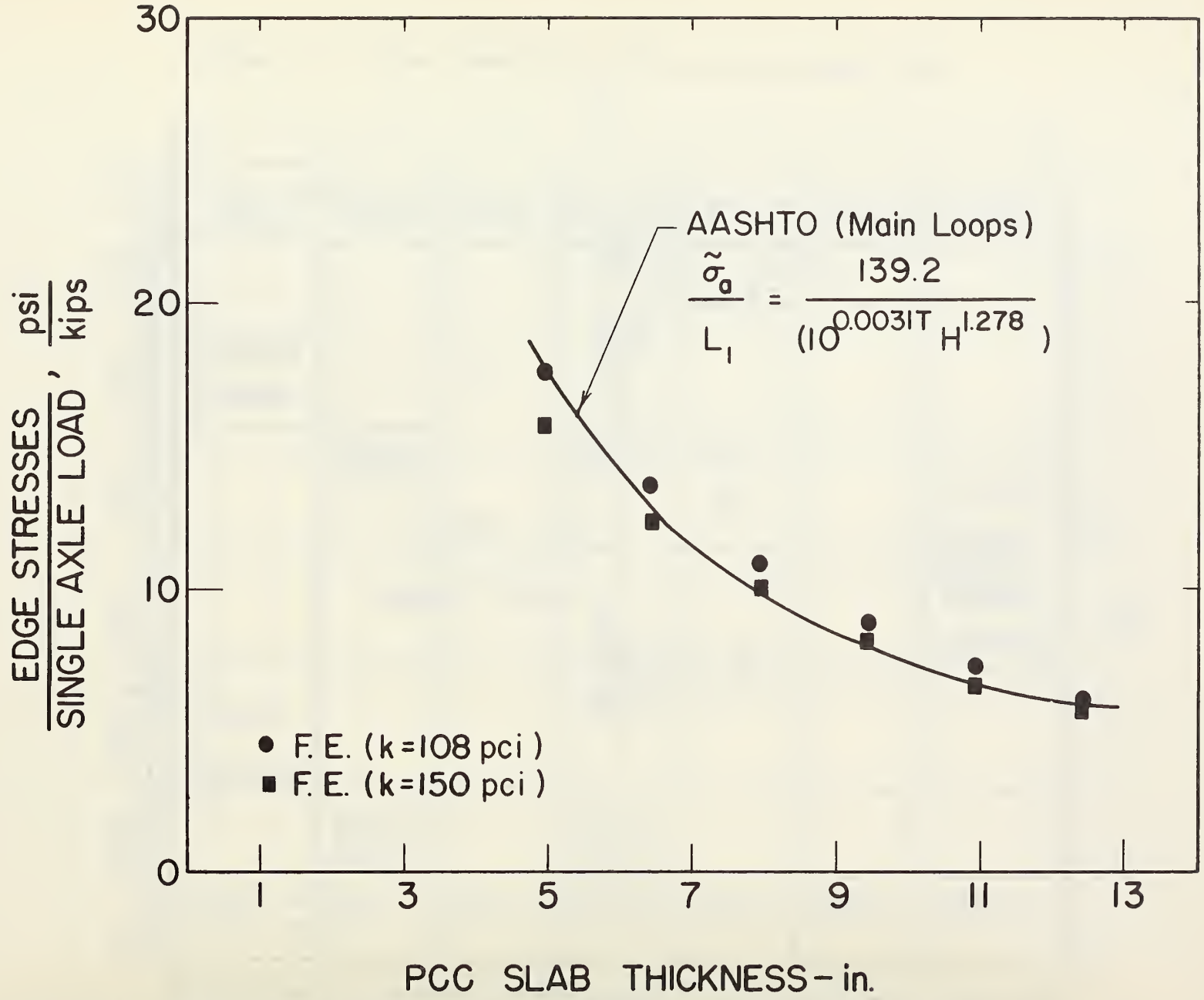


Figure 4.4. Comparison of Edge Stresses Computed with the Finite Element Program and those Measured at the AASHO Road Test for Single Axle Load (load placed 20 in. from edge of slab, but strain measured at edge).

tandem axles is shown in Figure 4.5. The distance from edge of the slab to the center of the wheel load was 20 in. (508 mm) in the F.E. analysis, which is similar to the 17-22 in. (432-559 mm) measured for the actual loadings. Compressive strain at the top of the slab was measured in the longitudinal direction, 1 in. (25 mm) from the edge of the slab. The strain measurements were correlated with axle load, PCC slab thickness, and temperature difference (standard differential) and regression equations were developed (see Eqs. 78 and 79 in Ref. 9). The theory of elasticity was then used to convert the strain equations into stress equations (Ref. 10) as follows:

Single Axles:

$$\sigma_s = \frac{139.2L_1}{10^{0.0031T/(H^{1.278})}} \tag{4.3}$$

Tandem Axles:

$$\sigma_t = \frac{25.87L_1}{10^{0.0035T/(H^{0.8523})}} \tag{4.4}$$

where

$\sigma_s$ = predicted stress at edge of slab for single axle load located 17-22 in. (432-559mm) from edge, psi

$\sigma_t$ = predicted stress at edge of slab for tandem axle load located 17-22 in. (432-559mm) from edge, psi

$L_1$ = axle load of truck (a single axle or a tandem axle set), kips

H = PCC slab thickness, inches

T = the temperature at a point 1/4 inches (6 mm) below the top surface of the 6.5 in. (165 mm) slab minus the temperature at a point 1/2 in. (113 mm) above the bottom surface, determined at the time the strain was measured (called standard differential).

The axle loads used for these plots were 18-kip single and 36-kip tandem.

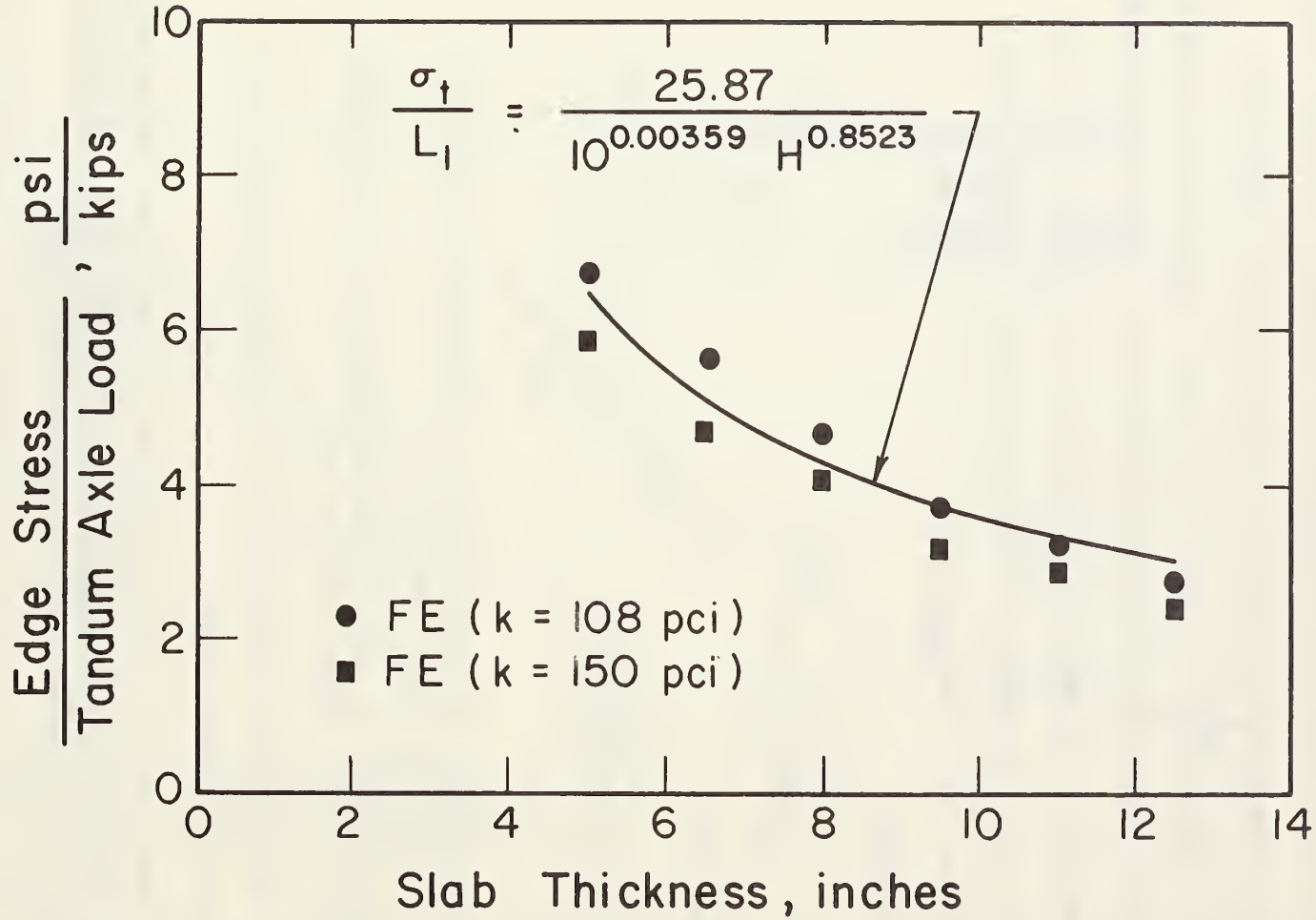


Figure 4.5. Comparison of Edge Stresses Computed with the Finite Element Program and those Measured at the AASHO Road Test for Tandem Axles (placed 20 in. [508 mm] from joint and strain measured at edge).

The results show good correlation between the stresses computed with the finite element program and the stresses computed with the AASHO equations for both single and tandem axles. Thus, the finite element program can be used with confidence to compute stresses caused by axle loads.

4.1.5 Comparison of Computed and Measured Thermal Curl Stress. Results from the tests conducted by Teller and Southerland at Arlington, VA (Refs. 12 and 29) provide "measured" thermal curling stress data (actually computed from measured strains) for plain jointed concrete pavement that can be used for comparison with computed finite element stress. Slabs were 20 ft. (6.1 m ) in length and 10 ft. (3.0 m) wide with one exception, where a 10 ft. (3.0 m ) long slab was obtained after a transverse crack occurred. Longitudinal edge stresses were computed from measured strains during periods of maximum thermal gradients for several days in 1934, A summary of data obtained for 9 and 9-6-9 in. (229-152-229mm) slabs and the computed FE edge stress are given in Table 4.1. Also some data for 15 ft. (4.6 m) slabs as later reported by Southerland (Ref. 29) is given. These data are plotted in Figure 4.6. The results generally agree, however, computed stress using the finite element program is slightly higher than measured stress for the limited data available.

The computation of curling stresses using the finite element (FE) program provides a much more realistic analysis than the Westergaard/Bradbury analysis (Refs. 17 and 18). The FE program allows the slab to curl in a weightless condition, and then the restraining weight of the slab is added. Hence, the slab is restrained by its weight. The Bradbury model assumes full restraint of the slab which should give higher stresses. A comparison of stress computed by each method over a range of slab thickness and foundation modulus values is given in Table 4.2. The thermal curling stress computed

Table 4.1. Measured and Computed Curling Stress at Edge of Slab.*

| Thermal Gradient (°F/in) | Slab Length (ft) | Curling Stress at Edge-psi | | | |
|---|---|---|---|---|---|
| | | Measured 8 in. Slab | Measured 9 in. Slab | Measured 9-6-9 in. Slab | Finite Element Computed Stress (psi) |
| 3.0 | 20 | --- | --- | 316 | 307 |
| 2.3 | 20 | --- | --- | 218 | 235 |
| 3.2 | 20 | --- | --- | 291 | 327 |
| 2.7 | 20 | --- | 191 | 245 | 276 |
| 3.3 | 20 | --- | 298 | 380 | 338 |
| 3.1 | 20 | --- | 306 | 380 | 317 |
| 3.6 | 20 | --- | 302 | 361 | 368 |
| 3.5 | 20 | --- | 329 | 409 | 358 |
| 2.8 | 20 | --- | 213 | 282 | 286 |
| 2.0-3.0 | 10 | --- | --- | 19-68 | 48-72 |
| 2.0-3.0 | 15 | 115-120 | --- | --- | 136-204 |

*From Refs. 12 and 29.
$E = 5 \times 10^6$ psi, $\mu = 0.15$, $k = 200$ pci

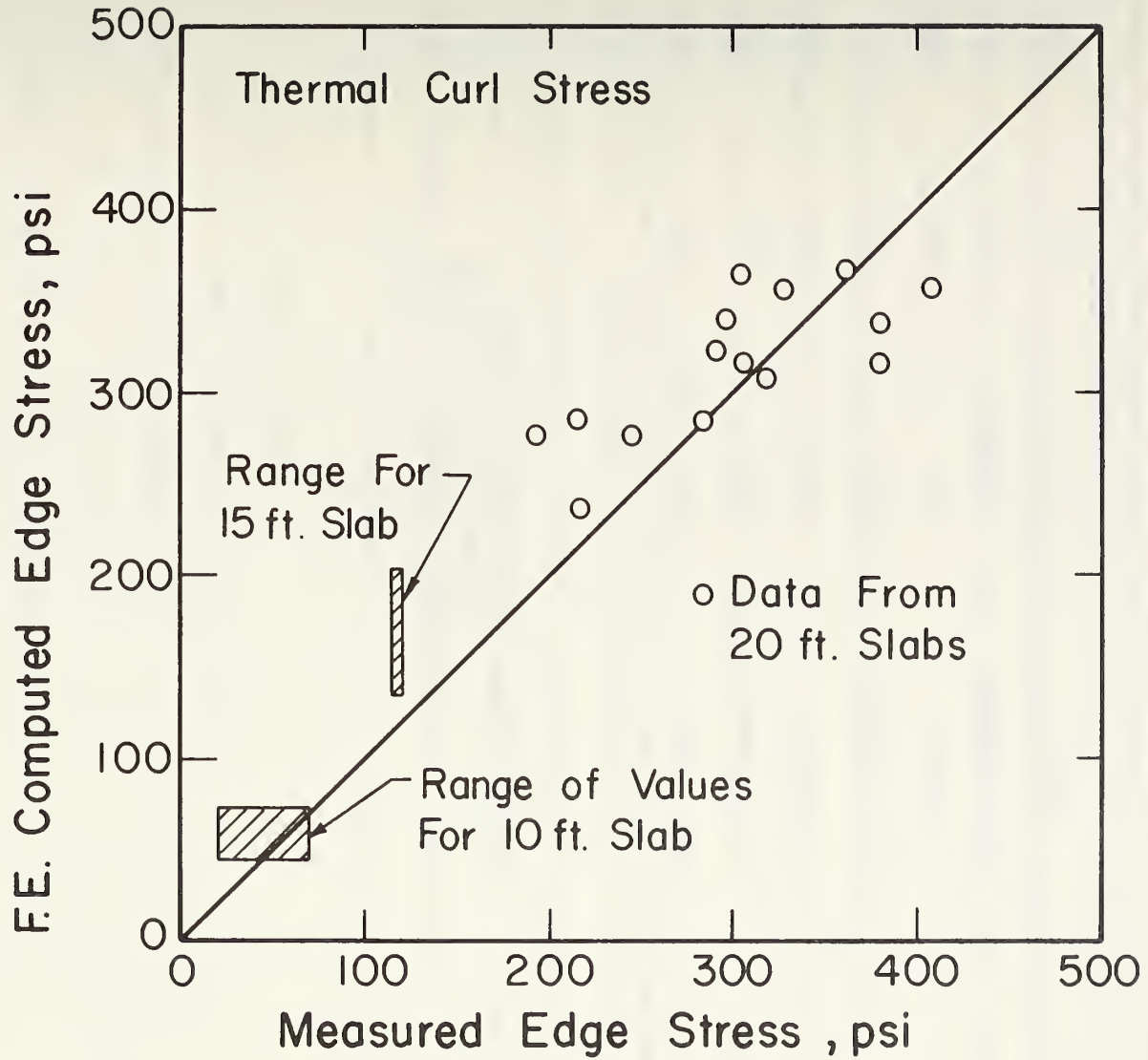


Figure 4.6. Comparison of Measured (Refs. 12 and 29) and Computed Edge Stress (with finite element program for thermal gradients).

Table 4.2. Comparison of Thermal Edge Curling Stresses Computed Using Bradbury (Ref. 18) and Finite Element Models (Ref.66).

| Slab Thick-in | Model | Foundation Modulus (k) - pci 50 | 200 | 500 |
|---|---|---|---|---|
| 8 | Finite Element | 134*psi | 204 | 247 |
| | Bradbury | 144 | 246 | 294 |
| 10 | Finite Element | 105 | 178 | 204 |
| | Bradbury | 98 | 255 | 330 |
| 14 | Finite Element | 66 | 129 | 145 |
| | Bradbury | 100 | 210 | 341 |

Parameters Used: Slab Length = 15 ft.
Thermal Grad = 3° F/in.
Mod. of Elast. = $5 \times 10^6$ psi
Coef. of Exp. = $5 \times 10^{-6}$/°F

from the Bradbury model is on the average 43 percent greater than the stress computed using the finite element model. This result is significant in that most of the comparisons of measured curling stress with Bradbury or Westergaard computed curling stress showed that the measured stress was less than the computed stress (Ref. 29). Hence, the finite element procedure is closer to measured curling stress than the Bradbury procedure. The Bradbury procedure gives much higher stresses for thicker slabs than the finite element model as shown in Table 4.2.

There are at least two reasons why the computed curling stress is less than measured stress. The effect of a moisture gradient through the slab (dryer on top than on bottom) causes stresses of opposite sign to thermal curl stress (when top of slab is warmer than bottom), and hence reduced measured strain. Another reason is some settlement of the subgrade which would reduce curling stress. In summary, considering the hazards in measuring thermal curling strains, computed and measured values are reasonably close. However, the finite element computed thermal edge curling stresses are somewhat higher than the "measured" stresses (computed from strains).

## 4.2 EFFECTS OF PAVEMENT FACTORS

The finite element program (Ref. 66) provides a powerful tool for evaluating the effect of several pavement factors on critical stress in the PCC slab. A sensitivity analysis is provided and the results are used several times throughout the chapter in the development of the fatigue analysis.

The traffic loading includes an 18-kip single axle and a 36-kip tandem axle located at the edge of the slab at midpoint between transverse joints as shown in Figure 4.1 and 4.2. The critical stress for this load position is at the bottom of the slab edge, parallel to the edge beneath the wheel

load. This stress is used in all of the subsequent analyses and is referred to as edge stress. The stress is caused by traffic load (referred to as load stress), thermal gradient through the slab (referred to as curl stress), or a combination of load and thermal gradient (referred to as load and curl stress). The edge load position was used because this position was determined to be the most critical point for fatigue damage in Section 4.3. Stresses were computed for a complete factorial of six factors.

(1) Slab thickness (H): 8, 10, and 14 ins.

(2) Modulus of foundation support (k): 50, 200, and 500 pci

(3) Thermal gradient (G): -1.5 (nighttime where bottom warmer than top of slab), 0, +3.0 (daytime), °F/in.

(4) Slab length (L): 15, 20, 25, and 30 ft.
(width was constant at 12 ft.

(5) Erodability of support (ES): 0, 12, 36, and 60 ins.
(longitudinal strip of width ES along outer slab edge).

A summary of edge stresses for all possible combinations of these factors and levels for an 18-kip (80 kN) single axle load is given in Table 4.3 as computed with the finite element program. Some results for the 36-kip tandem axle load are given in Table 4.4. Results for only thermal curling stress (without traffic load) are shown in Table 4.5. Some of these results are illustrated considering a selected "standard pavement" and then varying each factor over a typical range and plotting the change in edge stress that results. The selected standard pavement is selected as follows:

Slab Thickness (H) = 10 ins.

Modulus of Foundation Support (k) = 200 pci

Table 4.3. Edge Stress Data Computed with Finite Element Program (18 kip Single Axle Loading Shown in Figure 4.1).

Slab Thickness (H) - 8 ins.

| ES | L | k = 50 pci, G = -1.5 °F/in | k = 50 pci, G = 0 | k = 50 pci, G = 3.0 | k = 200, G = -1.5 | k = 200, G = 0 | k = 200, G = 3.0 | k = 500, G = -1.5 | k = 500, G = 0 | k = 500, G = 3.0 |
|---|---|---|---|---|---|---|---|---|---|---|
| 0 in | 15 ft | 318* | 387 | 532 | 206 | 307 | 574 | 144 | 257 | 572 |
| | 20 | 278 | 387 | 648 | 162 | 307 | 633 | 110 | 257 | 602 |
| | 25 | 248 | 387 | 694 | 157 | 307 | 638 | 115 | 257 | 597 |
| | 30 | 227 | 387 | 720 | 153 | 307 | 644 | 120 | 257 | 593 |
| 12 in | 15 | 333 | 397 | 532 | 224 | 322 | 576 | 159 | 275 | 583 |
| | 20 | 293 | 397 | 645 | 176 | 322 | 644 | 124 | 275 | 625 |
| | 25 | 264 | 397 | 697 | 171 | 322 | 652 | 127 | 275 | 618 |
| | 30 | 239 | 397 | 731 | 166 | 322 | 661 | 131 | 275 | 612 |
| 36 in | 15 | 400 | 420 | 531 | 290 | 362 | 570 | 235 | 326 | 570 |
| | 20 | 354 | 420 | 631 | 255 | 362 | 648 | 192 | 326 | 660 |
| | 25 | 322 | 420 | 703 | 240 | 362 | 680 | 185 | 326 | 665 |
| | 30 | 287 | 420 | 757 | 215 | 362 | 700 | 176 | 326 | 670 |
| 60 in | 15 | 520 | 441 | 530 | 375 | 400 | 513 | 318 | 371 | 495 |
| | 20 | 474 | 441 | 620 | 341 | 400 | 651 | 274 | 371 | 688 |
| | 25 | 416 | 441 | 710 | 300 | 400 | 720 | 243 | 371 | 715 |
| | 30 | 376 | 441 | 783 | 261 | 400 | 757 | 229 | 371 | 728 |

*Values in psi

Table 4.3. Edge Stress Data Computed with Finite Element Program (18 kip Single Axle Loading Shown in Figure 4.1) (Continued).

Slab Thickness = 10 ins.

| ES | L | k | 50 pci | | | 200 | | | 500 | | |
|---|---|---|---|---|---|---|---|---|---|---|---|
| | | G | -1.5 °F/in | 0 | 3.0 | -1.5 | 0 | 3.0 | -1.5 | 0 | 3.0 |
| 0 in | 15 ft | | 216* | 269 | 380 | 127 | 222 | 463 | 80 | 187 | 505 |
| | 20 | | 177 | 269 | 515 | 70 | 222 | 578 | 28 | 187 | 590 |
| | 25 | | 133 | 269 | 612 | 41 | 222 | 630 | 10 | 187 | 610 |
| | 30 | | 89 | 269 | 674 | 24 | 222 | 652 | 7 | 187 | 613 |
| 12 in | 15 | | 226 | 273 | 377 | 138 | 230 | 463 | 88 | 197 | 500 |
| | 20 | | 191 | 273 | 511 | 79 | 230 | 583 | 34 | 197 | 593 |
| | 25 | | 147 | 273 | 613 | 50 | 230 | 635 | 12 | 197 | 625 |
| | 30 | | 98 | 273 | 677 | 31 | 230 | 658 | 9 | 197 | 630 |
| 36 in | 15 | | 263 | 286 | 366 | 184 | 251 | 439 | 137 | 225 | 475 |
| | 20 | | 257 | 286 | 480 | 123 | 251 | 563 | 85 | 225 | 594 |
| | 25 | | 212 | 286 | 589 | 91 | 251 | 622 | 55 | 225 | 625 |
| | 30 | | 154 | 286 | 676 | 63 | 251 | 671 | 25 | 225 | 660 |
| 60 in | 15 | | 316 | 302 | 354 | 251 | 270 | 385 | 198 | 251 | 390 |
| | 20 | | 378 | 302 | 449 | 210 | 270 | 512 | 148 | 251 | 569 |
| | 25 | | 350 | 302 | 565 | 157 | 270 | 607 | 100 | 251 | 630 |
| | 30 | | 271 | 302 | 676 | 101 | 270 | 691 | 65 | 251 | 684 |

*Values in psi

Table 4.3. Edge Stress Data Computed with Finite Element Program (18 kip Single Axle Loading Shown in Figure 4.1) (Continued).
Slab Thickness = 14 ins.

| ES | L | k: 50 pci, G: -1.5°F/in | 50 pci, 0 | 50 pci, 3.0 | 200, -1.5 | 200, 0 | 200, 3.0 | 500, -1.5 | 500, 0 | 500, 3.0 |
|---|---|---|---|---|---|---|---|---|---|---|
| 0 in | 15 ft | 113* | 145 | 212 | 58 | 131 | 299 | 27 | 115 | 355 |
| | 20 | 84 | 145 | 333 | -1 | 131 | 455 | -31 | 115 | 512 |
| | 25 | 32 | 145 | 510 | -50 | 131 | 590 | -85 | 115 | 625 |
| | 30 | -28 | 145 | 614 | -105 | 131 | 693 | -138 | 115 | 700 |
| 12 in | 15 | 118 | 147 | 209 | 64 | 134 | 294 | 30 | 119 | 357 |
| | 20 | 92 | 147 | 326 | 5 | 134 | 446 | -29 | 119 | 521 |
| | 25 | 40 | 147 | 505 | -45 | 134 | 585 | -82 | 119 | 632 |
| | 30 | -23 | 147 | 606 | -101 | 134 | 696 | -138 | 119 | 703 |
| 36 in | 15 | 130 | 151 | 200 | 90 | 141 | 280 | 45 | 129 | 312 |
| | 20 | 121 | 151 | 304 | 40 | 141 | 415 | -12 | 129 | 510 |
| | 25 | 80 | 151 | 468 | -12 | 141 | 555 | -42 | 129 | 610 |
| | 30 | 21 | 151 | 521 | -81 | 141 | 680 | -110 | 129 | 698 |
| 60 in | 15 | 154 | 156 | 180 | 139 | 149 | 231 | 93 | 139 | 259 |
| | 20 | 159 | 156 | 252 | 109 | 149 | 328 | 45 | 139 | 426 |
| | 25 | 142 | 156 | 365 | 60 | 149 | 462 | -17 | 139 | 575 |
| | 30 | 108 | 156 | 482 | -22 | 149 | 623 | -79 | 139 | 693 |

*Values in psi

Table 4.4. Edge Stress Data Computed with Field Element Program (36-kip tandem axle loading shown in Figure 4.2).

| ES | H | k | 8 in | | | 10 in | | | 14 in | | |
|---|---|---|---|---|---|---|---|---|---|---|---|
| | | | 50 pci | 200 | 500 | 50 | 200 | 500 | 50 | 200 | 500 |
| | 0 in | | 339* | 259 | 210 | 238 | 190 | 157 | 128 | 116 | 99 |
| | 12 in | | 345 | 264 | 230 | 241 | 193 | 162 | 134 | 117 | 101 |
| | 36 in | | 375 | 305 | 253 | 259 | 215 | 187 | 143 | 126 | 102 |
| | 60 in | | 405 | 348 | 314 | 273 | 239 | 226 | 151 | 138 | 123 |
| | | | | | | | | | | | |
| | | | | | | | | | | | |
| | | | | | | | | | | | |
| | | | | | | | | | | | |
| | | | | | | | | | | | |
| | | | | | | | | | | | |
| | | | | | | | | | | | |
| | | | | | | | | | | | |
| | | | | | | | | | | | |
| | | | | | | | | | | | |
| | | | | | | | | | | | |
| | | | | | | | | | | | |
| | | | | | | | | | | | |

*Values in psi

Table 4.5. Thermal Curling Edge Stress Data Computed with Finite Element Program (without traffic load).

Slab Thickness = 8 ins.

| ES | L | G | k = 50 pci | | | k = 200 | | | k = 500 | | |
|---|---|---|---|---|---|---|---|---|---|---|---|
| | | | -1.5 °F/in | 0 | 3.0 | -1.5 | 0 | 3.0 | -1.5 | 0 | 3.0 |
| 0 in | 15 ft | | -67* | 0 | 134 | -102 | 0 | 204 | -124 | 0 | 247 |
| | 20 | | -118 | 0 | 231 | -161 | 0 | 318 | -150 | 0 | 300 |
| | 25 | | -156 | 0 | 304 | -162 | 0 | 324 | -152 | 0 | 310 |
| | 30 | | -163 | 0 | 329 | -162 | 0 | 330 | -155 | 0 | 316 |
| 12 in | 15 | | -63 | 0 | 126 | -92 | 0 | 195 | -112 | 0 | 235 |
| | 20 | | -116 | 0 | 224 | -159 | 0 | 322 | -150 | 0 | 300 |
| | 25 | | -154 | 0 | 296 | -160 | 0 | 326 | -152 | 0 | 310 |
| | 30 | | -164 | 0 | 328 | -162 | 0 | 330 | -155 | 0 | 316 |
| 36 in | 15 | | -42 | 0 | 98 | -74 | 0 | 160 | -91 | 0 | 195 |
| | 20 | | -90 | 0 | 188 | -140 | 0 | 282 | -160 | 0 | 310 |
| | 25 | | -132 | 0 | 268 | -151 | 0 | 290 | -160 | 0 | 315 |
| | 30 | | -155 | 0 | 313 | -162 | 0 | 327 | -160 | 0 | 319 |
| 60 in | 15 | | -25 | 0 | 72 | -57 | 0 | 128 | -75 | 0 | 160 |
| | 20 | | -68 | 0 | 154 | -122 | 0 | 245 | -140 | 0 | 280 |
| | 25 | | -120 | 0 | 245 | -153 | 0 | 302 | -156 | 0 | 313 |
| | 30 | | -147 | 0 | 298 | -163 | 0 | 325 | -162 | 0 | 325 |

*Values in psi

Table 4.5. Thermal Curling Edge Stress Data Computed with Finite Element Program (without traffic load) (Continued).

Slab Thickness = 10 in.

| ES | L | k | 50 pci | | | 200 | | | 500 | | |
|---|---|---|---|---|---|---|---|---|---|---|---|
| | | G | -1.5 °F/in | 0 | 3.0 | -1.5 | 0 | 3.0 | -1.5 | 0 | 3.0 |
| 0 in | 15 ft | | -53* | 0 | 105 | -89 | 0 | 178 | -105 | 0 | 204 |
| | 20 | | -106 | 0 | 208 | -147 | 0 | 296 | -167 | 0 | 332 |
| | 25 | | -153 | 0 | 317 | -180 | 0 | 360 | -180 | 0 | 385 |
| | 30 | | -192 | 0 | 389 | -203 | 0 | 410 | -200 | 0 | 407 |
| 12 in | 15 | | -47 | 0 | 98 | -79 | 0 | 177 | -98 | 0 | 204 |
| | 20 | | -102 | 0 | 201 | -147 | 0 | 295 | -166 | 0 | 336 |
| | 25 | | -150 | 0 | 300 | -180 | 0 | 368 | -190 | 0 | 386 |
| | 30 | | -191 | 0 | 386 | -203 | 0 | 413 | -200 | 0 | 407 |
| 36 in | 15 | | -26 | 0 | 77 | -66 | 0 | 145 | -79 | 0 | 169 |
| | 20 | | -73 | 0 | 165 | -129 | 0 | 261 | -148 | 0 | 298 |
| | 25 | | -125 | 0 | 264 | -170 | 0 | 346 | -181 | 0 | 370 |
| | 30 | | -170 | 0 | 358 | -200 | 0 | 402 | -200 | 0 | 407 |
| 60 in | 15 | | -8 | 0 | 56 | -53 | 0 | 115 | -62 | 0 | 137 |
| | 20 | | -44 | 0 | 129 | -111 | 0 | 229 | -131 | 0 | 259 |
| | 25 | | -95 | 0 | 225 | -158 | 0 | 327 | -172 | 0 | 350 |
| | 30 | | -146 | 0 | 330 | -198 | 0 | 395 | -202 | 0 | 408 |

*Values in psi

Table 4.5. Thermal Curling Edge Stress Data Computed with Finite Element Program (without traffic load) (Continued).

Slab Thickness = 14 in.

| ES | L | G | k | 50 pci | | | 200 | | | 500 | | |
|---|---|---|---|---|---|---|---|---|---|---|---|---|
| | | | -1.5 °F/in | 0 | 3.0 | -1.5 | 0 | 3.0 | -1.5 | 0 | 3.0 |
| 0 in | 15 ft | | -31* | 0 | 66 | -65 | 0 | 129 | -82 | 0 | 145 |
| | 20 | | -78 | 0 | 152 | -115 | 0 | 225 | -140 | 0 | 275 |
| | 25 | | -122 | | 280 | -182 | 0 | 340 | -195 | 0 | 410 |
| | 30 | | -201 | 0 | 420 | -239 | 0 | 528 | -261 | 0 | 563 |
| 12 in | 15 | | -29 | 0 | 61 | -58 | 0 | 120 | -76 | 0 | 145 |
| | 20 | | -75 | 0 | 146 | -113 | 0 | 222 | -138 | 0 | 275 |
| | 25 | | -120 | 0 | 240 | -180 | 0 | 340 | -205 | 0 | 410 |
| | 30 | | -198 | 0 | 415 | -239 | 0 | 528 | -261 | 0 | 563 |
| 36 in | 15 | | -16 | 0 | 43 | -41 | 0 | 98 | -58 | 0 | 120 |
| | 20 | | -52 | 0 | 114 | -90 | 0 | 186 | -118 | 0 | 239 |
| | 25 | | -92 | 0 | 203 | -160 | 0 | 290 | -180 | 0 | 361 |
| | 30 | | -166 | 0 | 355 | -222 | 0 | 492 | -249 | 0 | 551 |
| 60 in | 15 | | -7 | 0 | 32 | -25 | 0 | 77 | -43 | 0 | 103 |
| | 20 | | -28 | 0 | 82 | -67 | 0 | 150 | -97 | 0 | 202 |
| | 25 | | -58 | 0 | 140 | -114 | 0 | 270 | -157 | 0 | 347 |
| | 30 | | -133 | 0 | 295 | -206 | 0 | 456 | -237 | 0 | 538 |

*Values in psi

Slab Length (L) = 15 ft.

Slab Width = 12 ft.

Thermal Gradient through Slab (G) = 0°F/in.

PCC Modulus of Elasticity = $5 \times 10^6$ psi

PCC Thermal Coefficient of Expansion = $5 \times 10^{-6}$/°F

Erodability of Support (ES) = 0 in.

Data are plotted showing the change in edge stress due to changes in H, k, E, G, and L, and their interactions. Results for edge stress caused by the combination of traffic load and thermal gradients are given Figures 4.7-4.11. Results showing the effect of an edge stress at the slab bottom for only thermal gradients are shown in Figures 4.12-4.15. A comparison of stresses caused by 18-kip single axle and 36-kip tandem axles is shown in Figure 4.16. A brief summary of the most significant results as illustrated in Figures 4.7-4.16 and from the data in Tables 4.3-4.5 is as follows:

(1) As joint spacing (L) increases from 15 to 30 ft. (4.6-9.1 m), edge stress caused by thermal gradients change greatly. Stress increases for daytime gradients (i.e. top of slab warmer than bottom) and decreases for nighttime gradients (i.e. bottom warmer than top) as joint spacing increases (Figure 4.7b shows combined load and curl edge stress, Figure 4.12 shows curl stress only). Joint spacing does not have significant effect when only traffic load is applied (Figure 4.7b).

(2) As slab thickness increases, edge stress caused by either traffic load, thermal gradient, or load and gradient combined, decreases significantly for slabs of about 20 ft. (6.1m) or less (Figure 4.8, 4.13b, Table 4.3). The conbined stress generally increases as slab thickness increases for slabs with length greater than about 20 ft. Slab thickness also interacts with other parameters such as the k-value and erodability. The

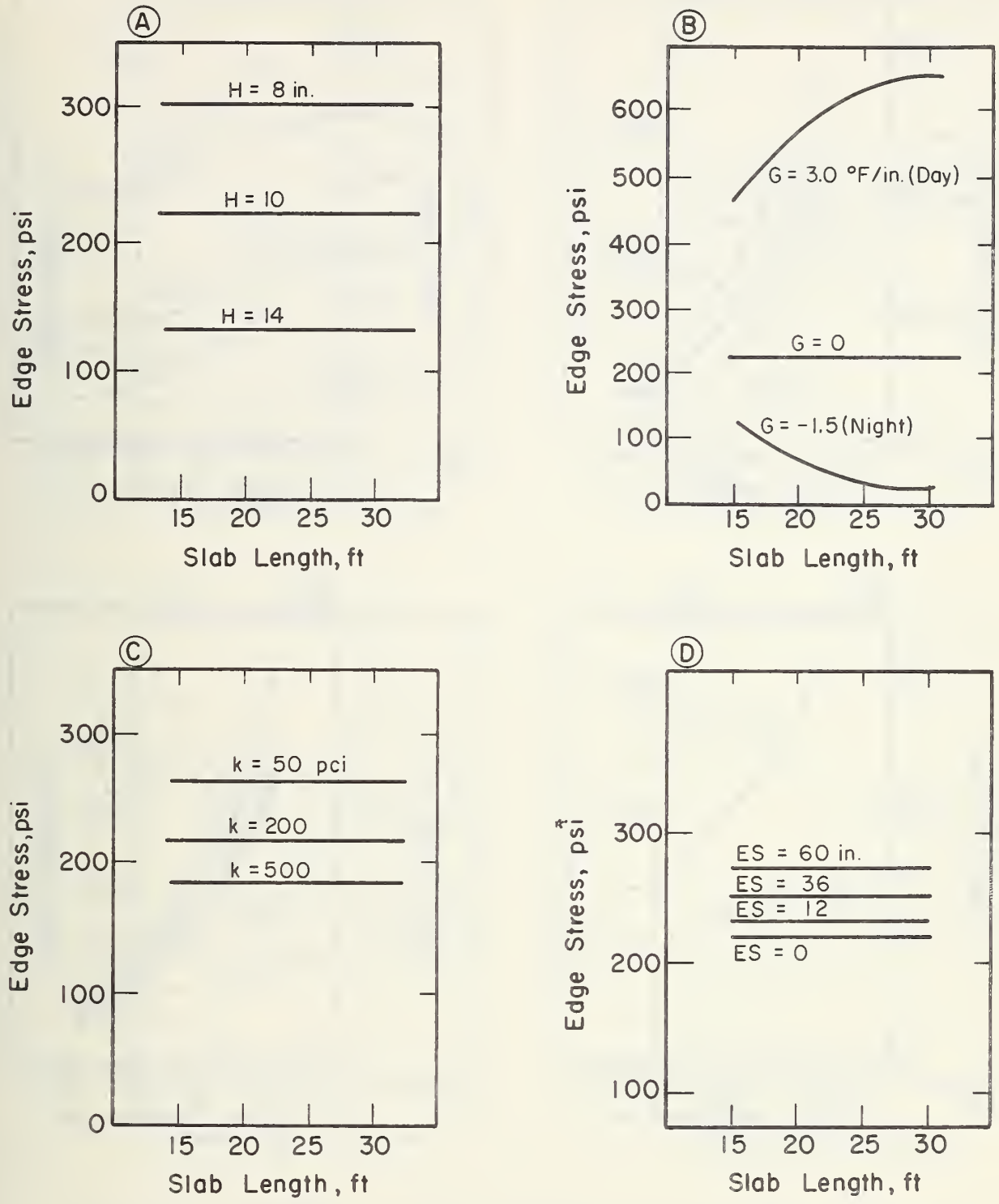


Figure 4.7. Effect of Slab Length on Total Edge Stress (load and curl) for Selected Pavement Single Axle Load.

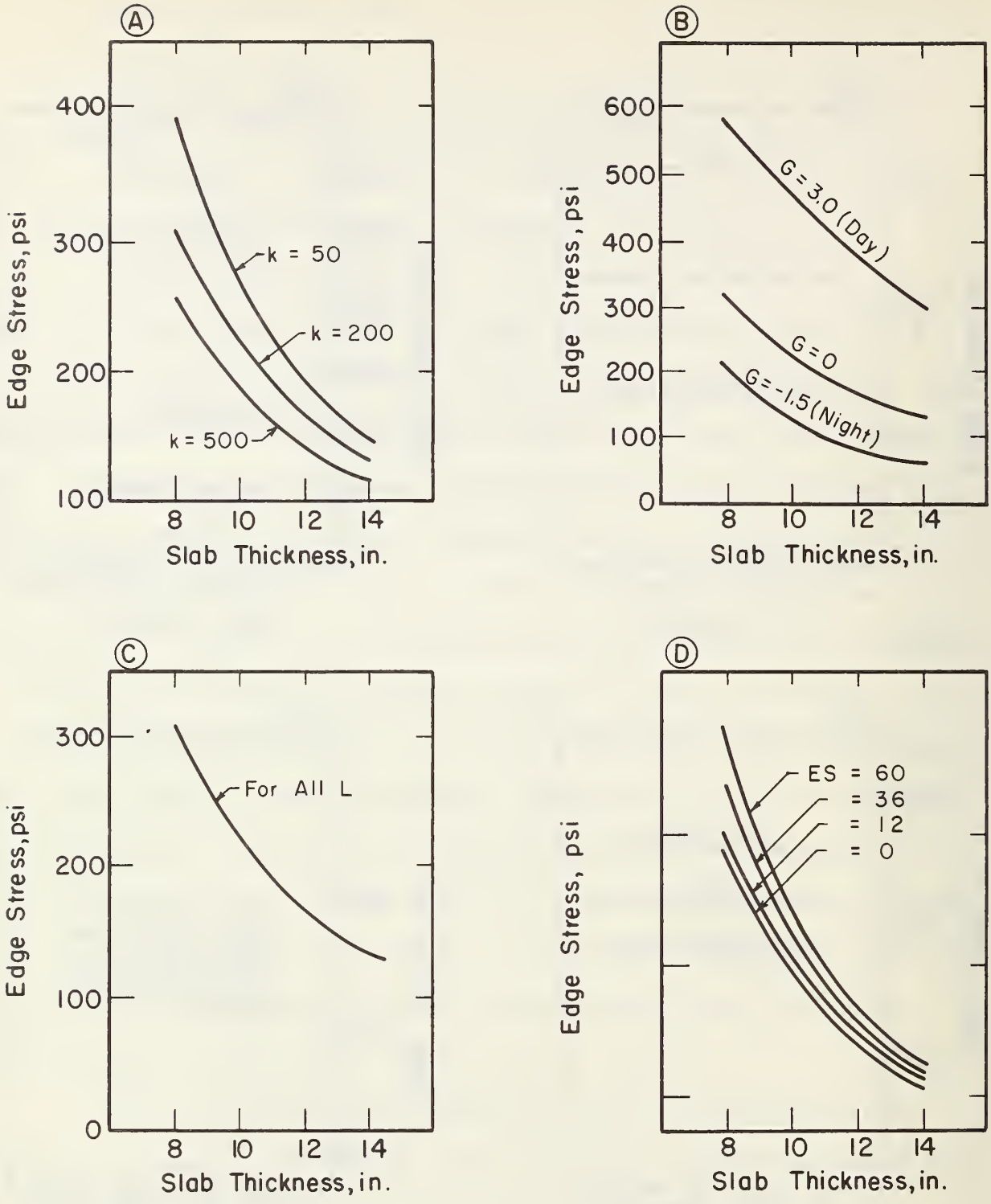


Figure 4.8. Effect of Slab Thickness on Total Edge Stress for Selected Pavement/Single Axle Load.

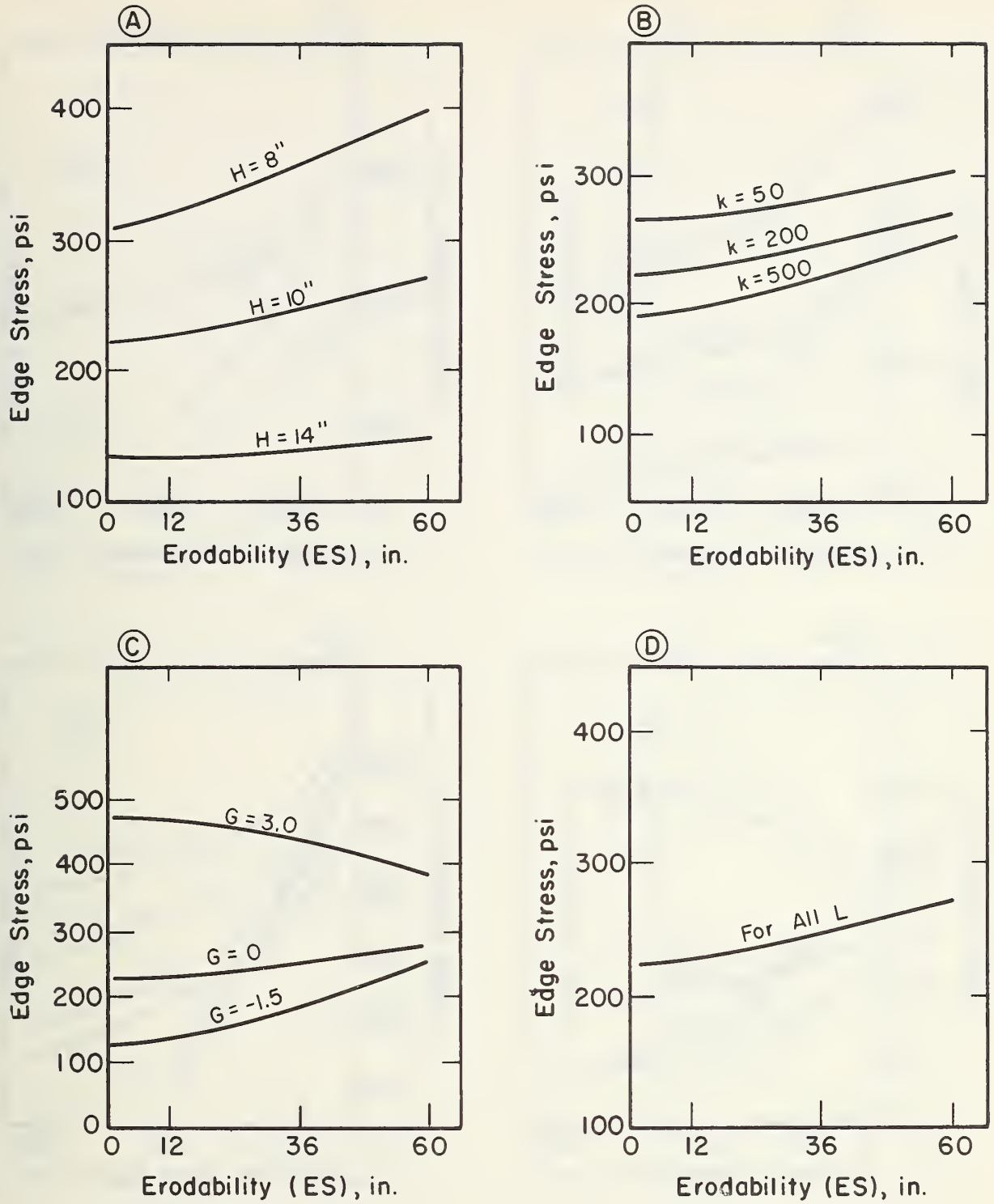


Figure 4.9. Effect of Subbase Erosion on Total Enge Stress for Selected Pavement/Sincle Axle Load.

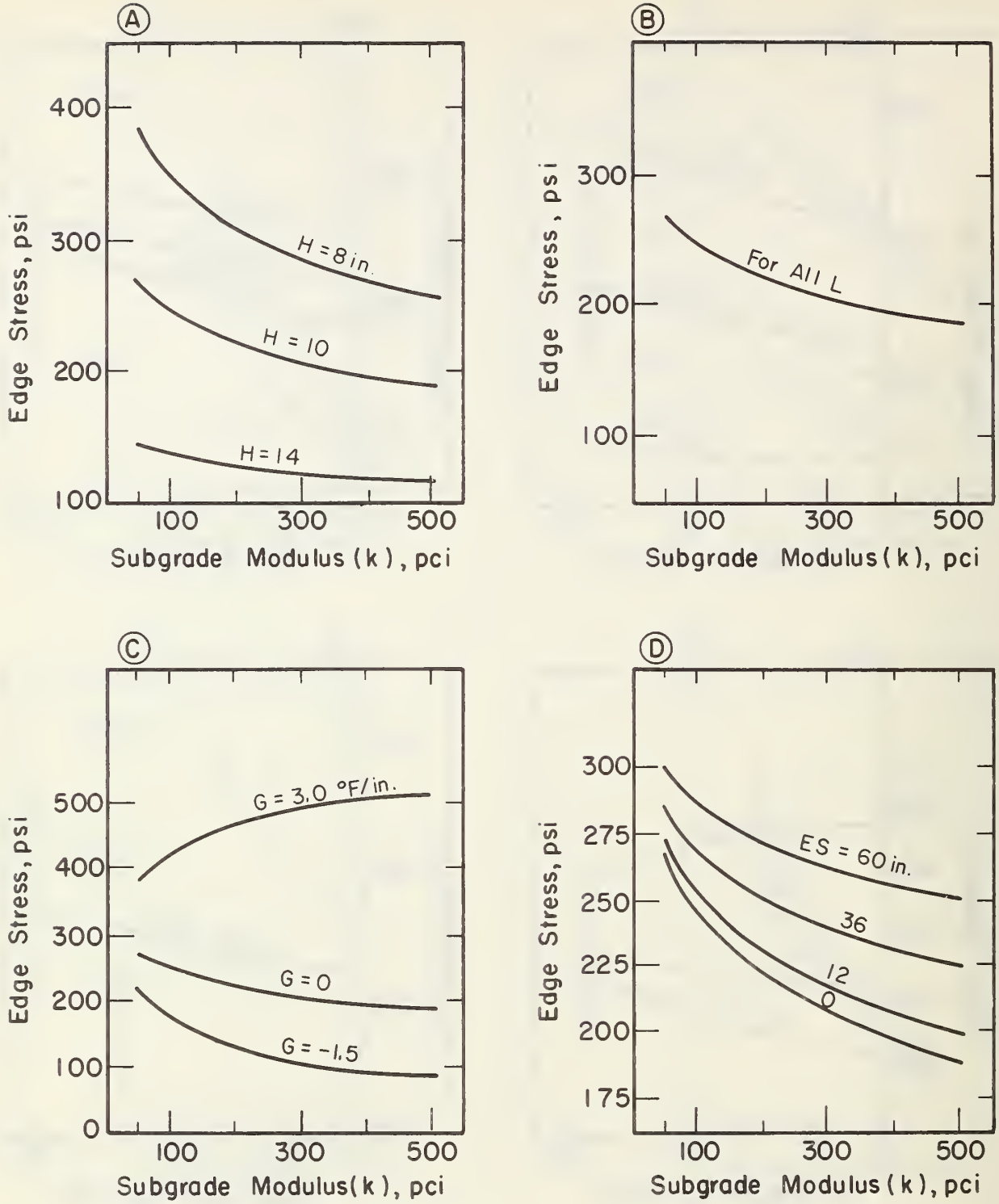


Figure 4.10. Effect of Subgrade Modulus on Total Edge Stress for Selected Pavement/Single Axle Load.

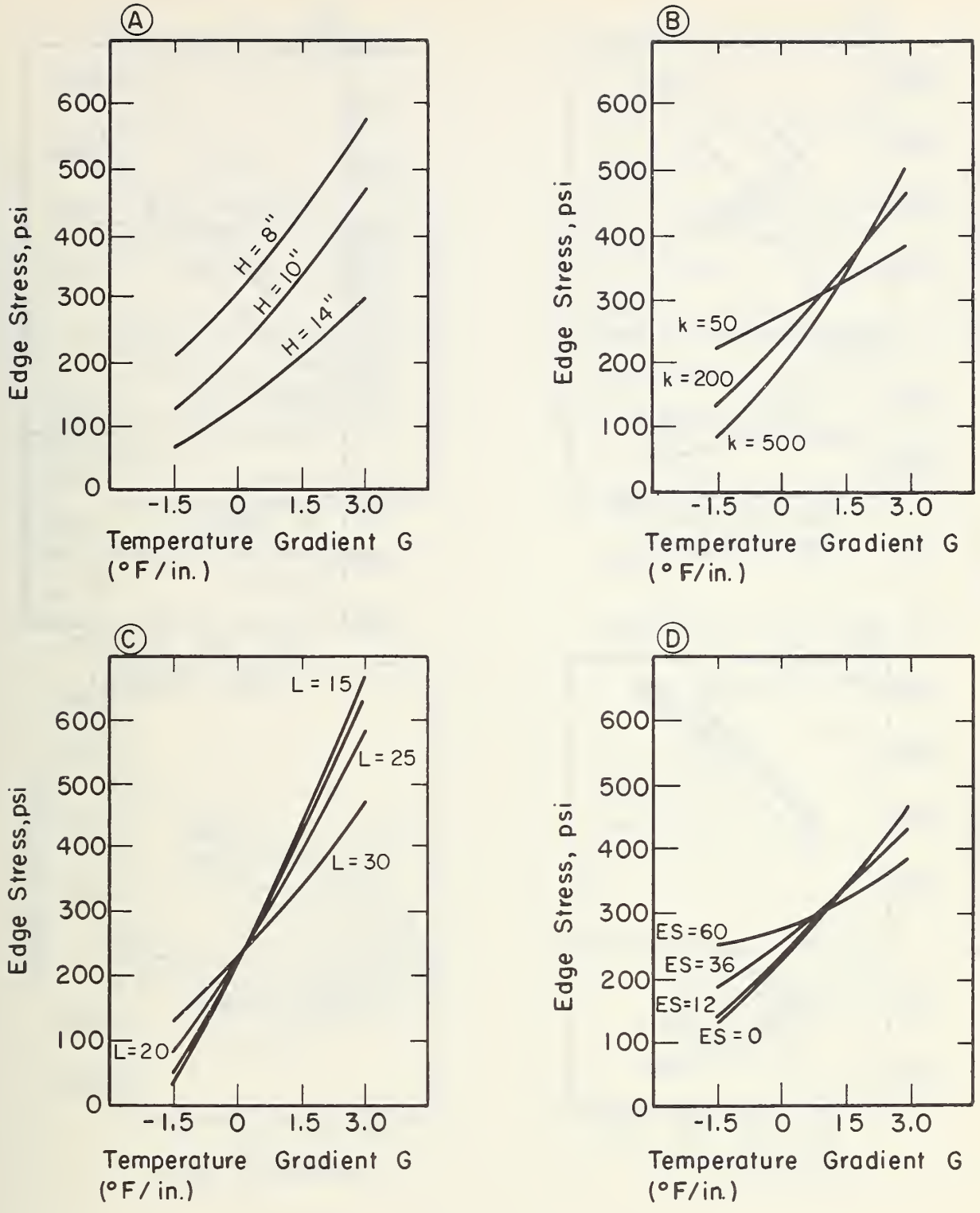


Figure 4.11. Effect of Thermal Gradient on Total Edge Stress for Selected Pavement/Single Axle Load.

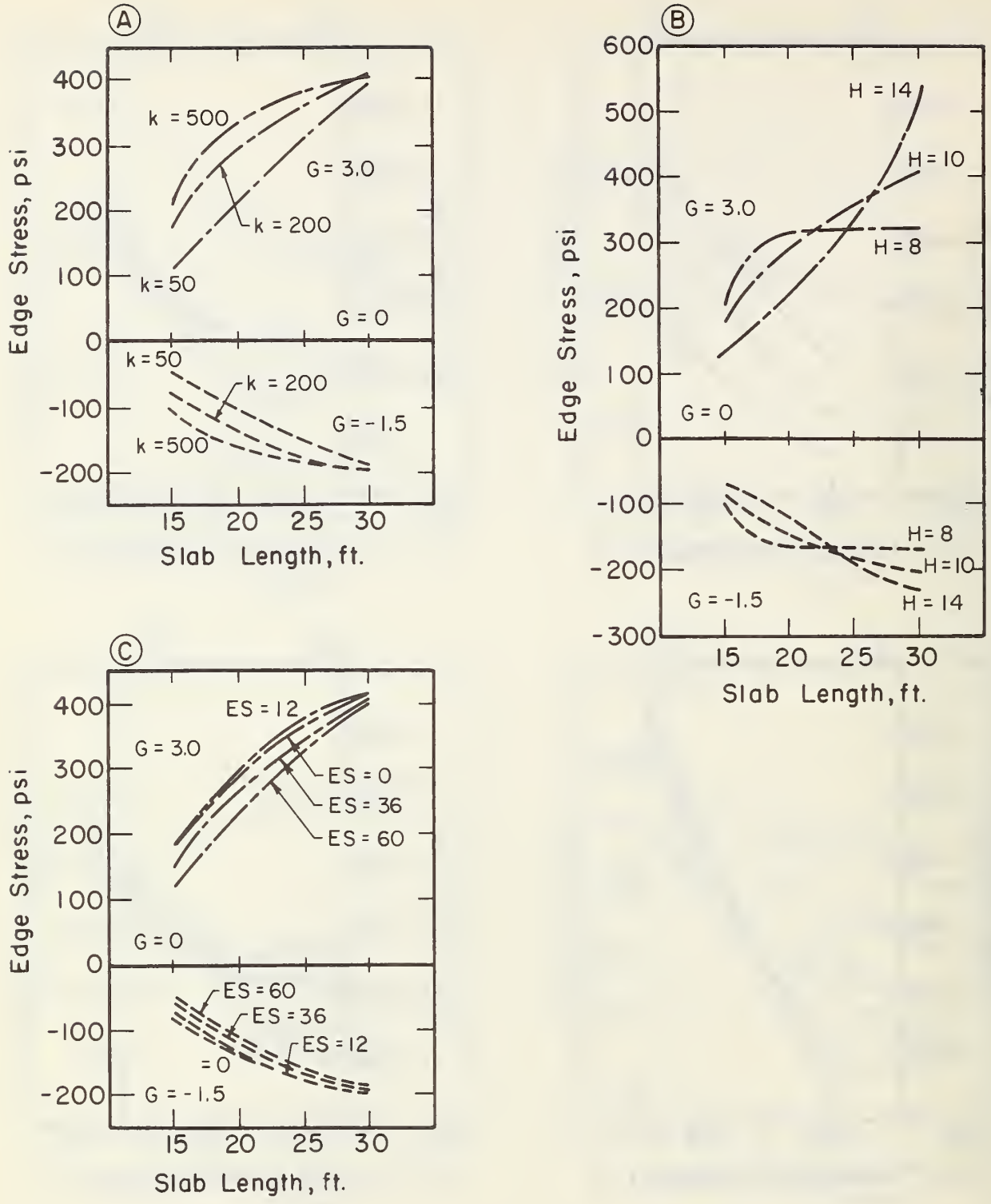


Figure 4.12. Effect of Slab Length on Thermal Curl Edge Stress for Selected Pavement.

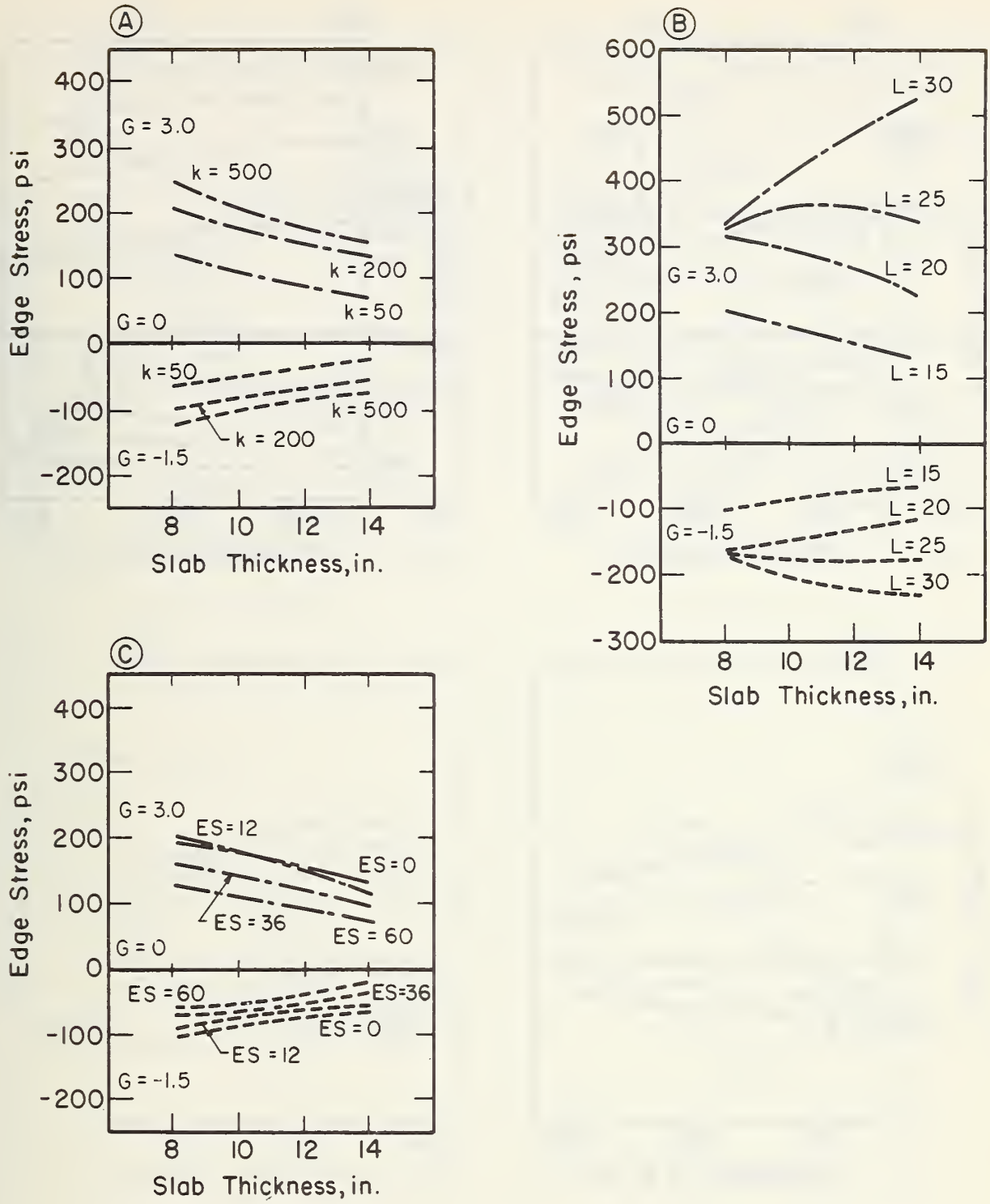


Figure 4.13. Effect of Slab Thickness on Thermal Curl Edge Stress for Selected Pavement.

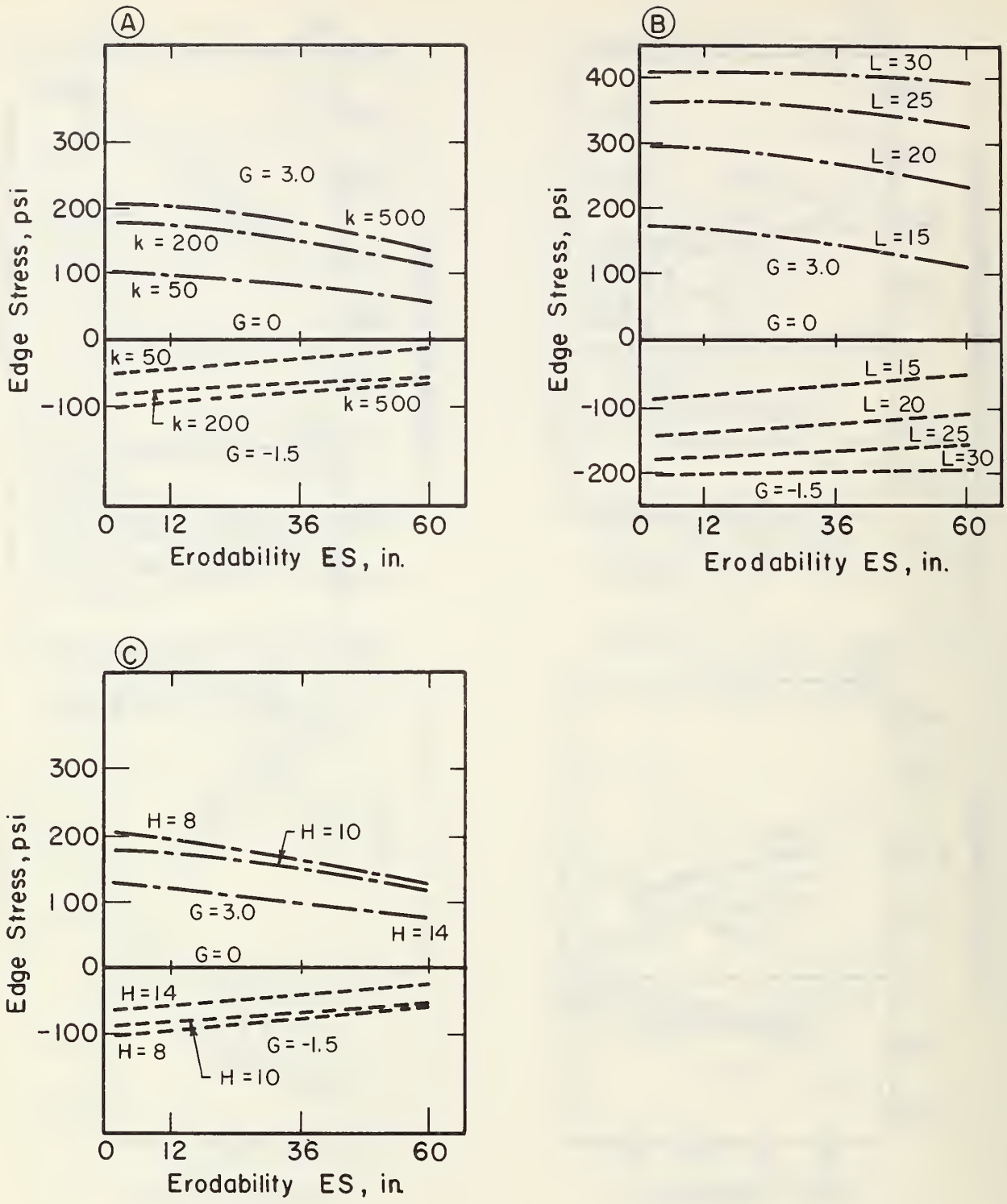


Figure 4.14. Effect of Subbase Erosion on Thermal Curl Edge Stress for Selected Pavement.

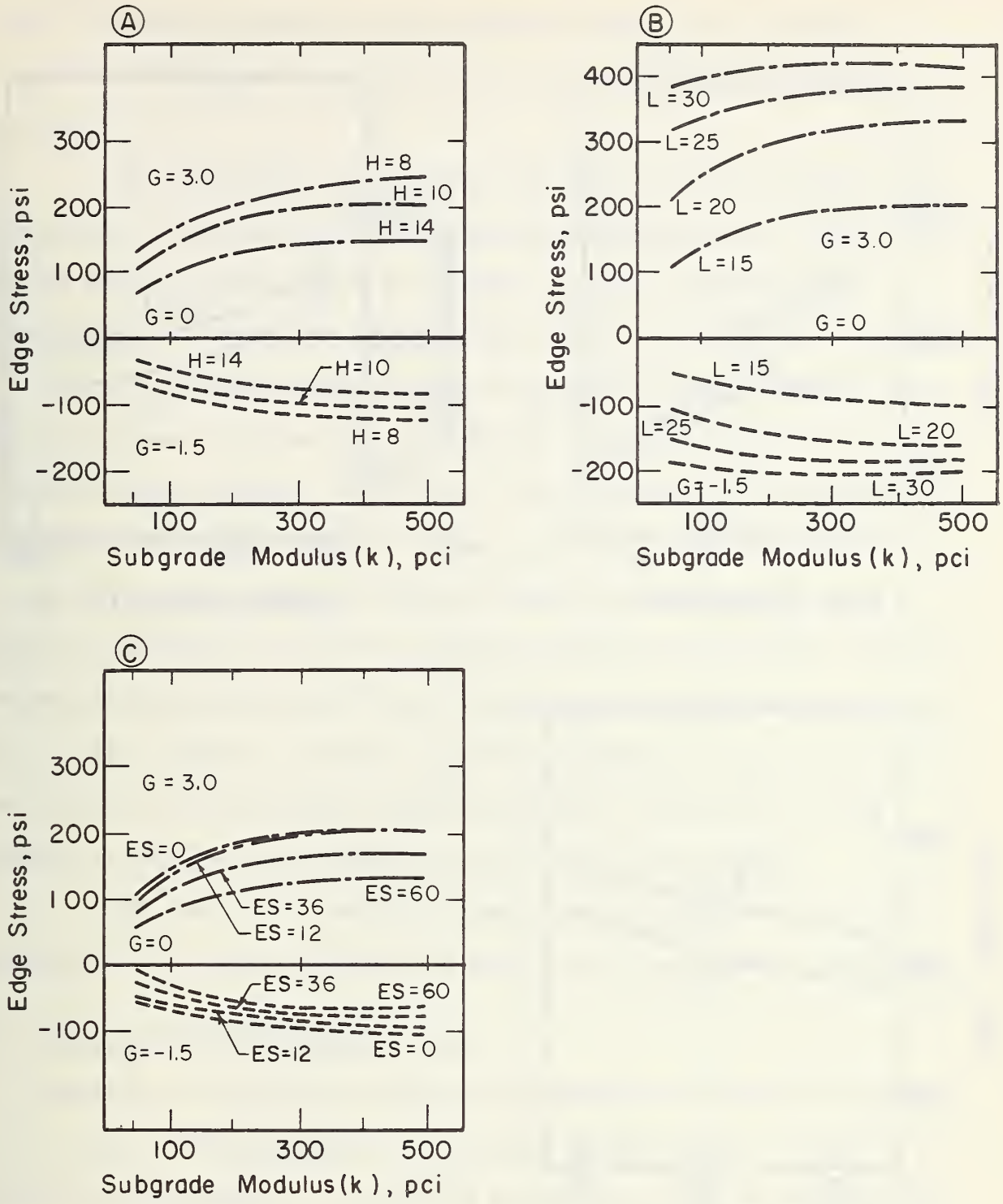


Figure 4.15. Effect of Subgrade Modulus of Thermal Curl Edge Stress for Selected Pavement.

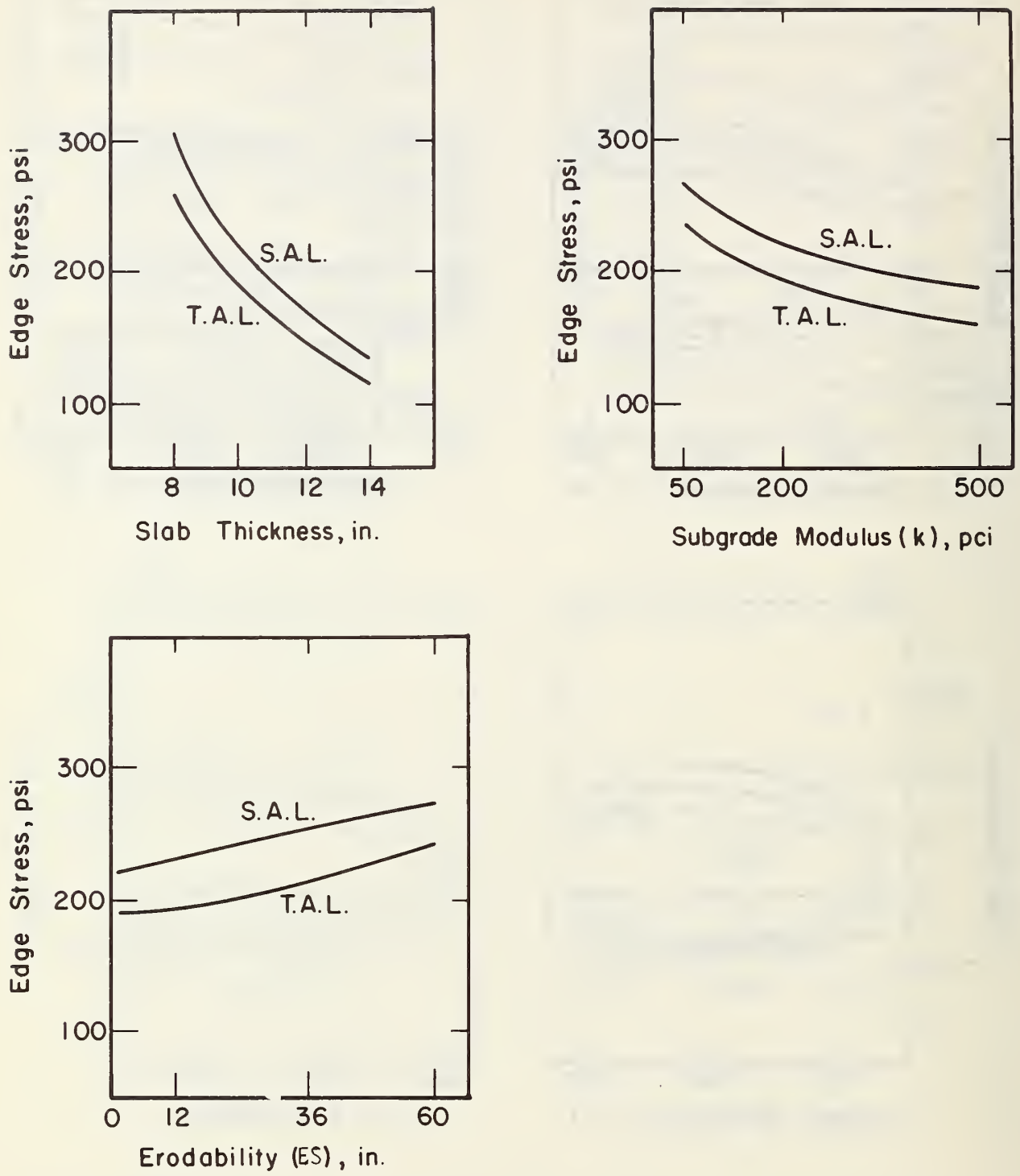


Figure 4.16. Comparison of Single and Tandem Axles (shown in Figs. 4.1 and 4.2) on Edge Stresses in Selected Pavement.

effect of change in stress for thick slabs for changes in k-value or erodability of support is less than it is for thin slabs (Figures 4.8a and 4.8b).

(3) As erodability of support increases, combined load and curl edge stress increase with one exception (Figures 4.9 and 4.14). When a daytime gradient exists, there is a slight decrease in combined edge stress because of reduced restraint of the slab.

(4) As the subgrade modulus of support increases, combined load and curl stresses decrease with one important exception (Figure 4.10). With a daytime thermal gradient (+3.0 °F/in.), the stress generally increases as the k-value increases (Table 4.3, Figure 4.10c).

(5) As the thermal gradient through the slab increases from a negative (nighttime) to positive (daytime) edge stress caused from both the combined load and curl and curl only increases very significantly (Figures 4.11 - 4.15). When the gradient is positive (daytime) the edge stress at the slab bottom caused by only thermal gradient is tensile, but if the gradient is negative (nighttime) the edge stress is compressive.

(6) Edge stress resulting from an 18-kip single axle load is approximately 15 percent greater than edge stress from a 36-kip tandem axle.

## 4.3 CRITICAL FATIGUE LOCATION IN SLAB

Location of the critical point at which cracking initiates in the PCC slab is vital to the development of a fatigue analysis with an objective of preventing slab cracking. The location of the critical point is approached using both field results and a comprehensive slab fatigue analysis.

4.2.1 Initiation of Cracking - Field Results. A few road tests have been conducted where the cracking of plain jointed PCC slabs was carefully recorded. Results from the AASHO and Michigan road tests and also observations made on in-service pavements are presented.

The AASHO Road Test provides data relative to the initiation of cracking. Transverse cracking occurred first on 61 out of 91 plain and reinforced concrete sections and "usually began with a crack originating at a point on the edge of the pavement at least 5 ft. (1.5m) from the transverse joint" (Ref. 9). Although longitudinal cracking initiated first in the other 32 sections, it usually only occurred in thin slabs (2.5-5.0 in., 63-127 mm) and not on thicker slabs of 8 ins. (203 mm) or greater which are under consideration in this study. The location of the first crack in 31 plain jointed concrete sections is as follows:

| Distance From Joint To Transverse Crack, ft. | Number of Failed Section |
|---|---|
| 0 - 5 | 5 |
| 5 - 10 | 20 |
| 10 - 15 | 6 |

An example of crack initiation and progression for an 8 in. (203 mm) plain slab section is shown in Figure 4.27. The initiation of most of the cracking at the slab edge near the midpoint of the slab is apparent.

Results from the Michigan Test Road (Ref. 19) also show transverse cracking to be the dominant type occurring for slabs of 8 in. (203 mm) thickness having joint spacing ranging from 10 to 30 ft. (3 to 9 m). A diagram of the cracking of these slabs after 10 years of traffic is shown in Figure 4.18. Cracking in 1955 per mile is as follows:

| | Joint Spacing, ft. | | |
|---|---|---|---|
| | 30 | 20 | 15 |
| Transverse | 296 | 139 | 50 |
| Diagonal | 7 | 6 | 0 |
| Longitudinal | 4 | 20 | 11 |

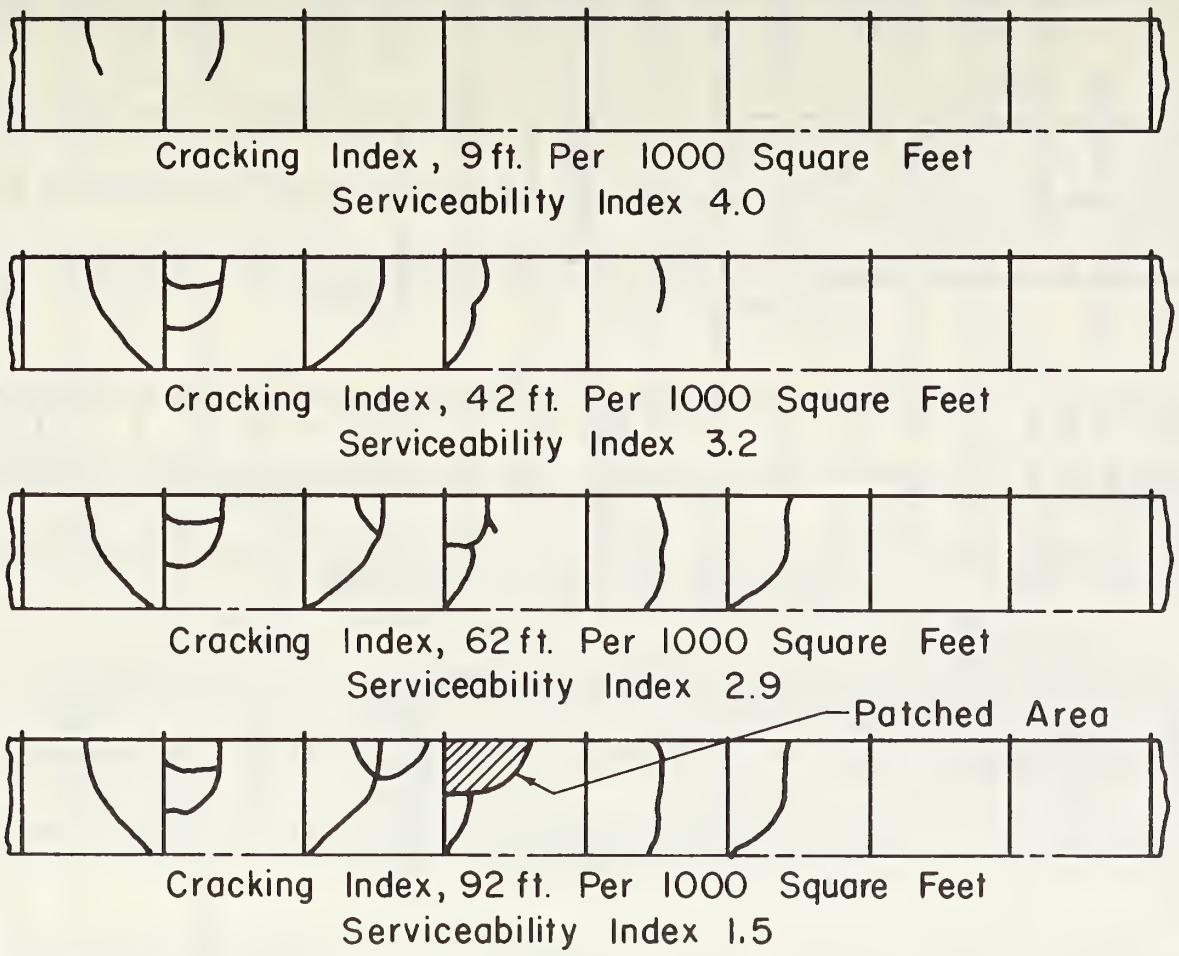


Figure 4.17. Initiation and Progression of Cracking in an 8.0 in. (203 mm) Non-reinforced Section on 3.0 in. (76 mm) Granular Subbase, 30-kip Single Axle Load, AASHO Road Test.

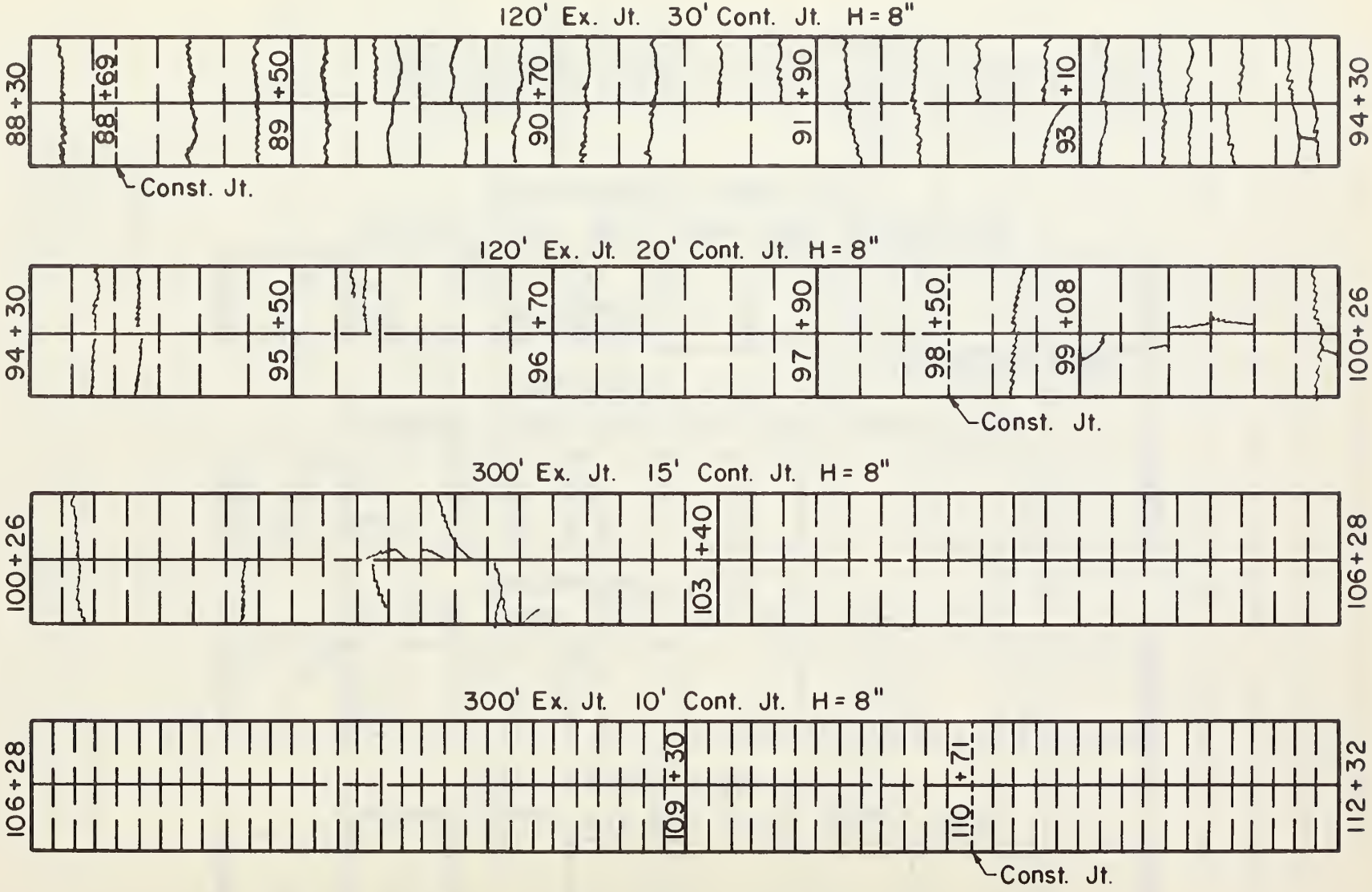


Figure 4.18. Crack Pattern for a Portion of the Michigan Road Test after 10 Years Service (Ref. 19).

Transverse cracking occurred much more than any other type of cracking.

Several heavily trafficked plain jointed concrete pavements were examined during the field survey and the type of cracking noted and summarized in Table 2.6. Transverse cracking was observed in 12 pavements, corner cracking occurred in one, and longitudinal cracking occurred in three projects.

In summary, results from field observations indicate that for slabs of normal thickness (i.e. $\geq$ 8 ins. [203mm]), cracking usually initiates at the slab edge and propagates transversely across the slab. These cracks are usually located in the center third of the slab. Available data indicate that transverse cracking occurs much more often than longitudinal or corner cracking. Longitudinal cracking generally occurs about 24 to 42 ins. [0.6-1.1m] from the slab edge (Ref. 9) and initiates at the transverse joint. Corner cracking occurred at the outer transverse joint corner on one project having skewed joints without any mechanical load transfer device (LTD) and where pumping of the subbase was evident. It was also observed on another project with skewed joints (no LTD) that had severe faulting and pumping at the joints. Corner cracking did not occur on any slab having dowels at the transverse joints.

4.2.2 Initiation of Cracking - Fatigue Analysis. A comprehensive fatigue analysis was conducted using the finite element program and Miner's fatigue damage hypothesis to determine theoretically the critical point in the slab where cracking should initiate. Two general positions in the slab were evaluated based on the results from the field studies:

(1) near the transverse joint where longitudinal cracking initiates (this is the critical fatigue location assumed by PCA in their design procedure, Ref. 49).

(2) at mid-slab between the transverse joints where transverse cracking initiates.

These locations and the direction of critical stresses are shown in Figure 4.19.

A fatigue analysis was conducted by considering typical variations in truck axle weights, axle types, and lateral placement across the slab. The axle load distribution used is given in Table 4.6 which is typical for a major truck route. The lateral truck placement in the outer lane as measured by Emery (Ref. 12) was used. The lateral distance from the edge of the slab to the outside of the truck duals is designated D as shown in Figure 4.20. The lateral placement of trucks in the lane, or D, was found to be approximately normally distributed (see Section 4.5) with a standard deviation of 10 ins. (254 mm). Table 4.7 gives the lateral displacement percentage for every six inch (152 mm) increment across the slab which were computed using a normal distribution for five mean lateral placement positions (i.e. $\overline{D}$ = 12, 24, 36, 42, and 48 ins. [0.3, 0.6, 0.9, 1.1, 1.2m]). The mean lateral displacement of truck traffic probably varies from 12 to 30 ins.(0.3 to 0.8 m) depending on shoulder conditions,existence of curb and gutter,and any lateral obstructions. For example, if the mean lateral placement was $\overline{D}$ = 24 ins. (610 mm) the percent of loads passing between 3 and 9 ins. from the edge of slab is 4.89.

Stresses in the slab were computed using the finite element program for lateral positions of D = 0, 6, 12, 18, 24, 30, 36, 42, and 48 ins.

A typical plot of tensile stress for a 10 in. (254mm) slab placed on a foundation with k = 200 psi and an 18-kip single axle load at mid-slab is shown in Figure 4.21. The highest stress occurs when the load is at the slab edge (D = 0 ins.) and decreases as the

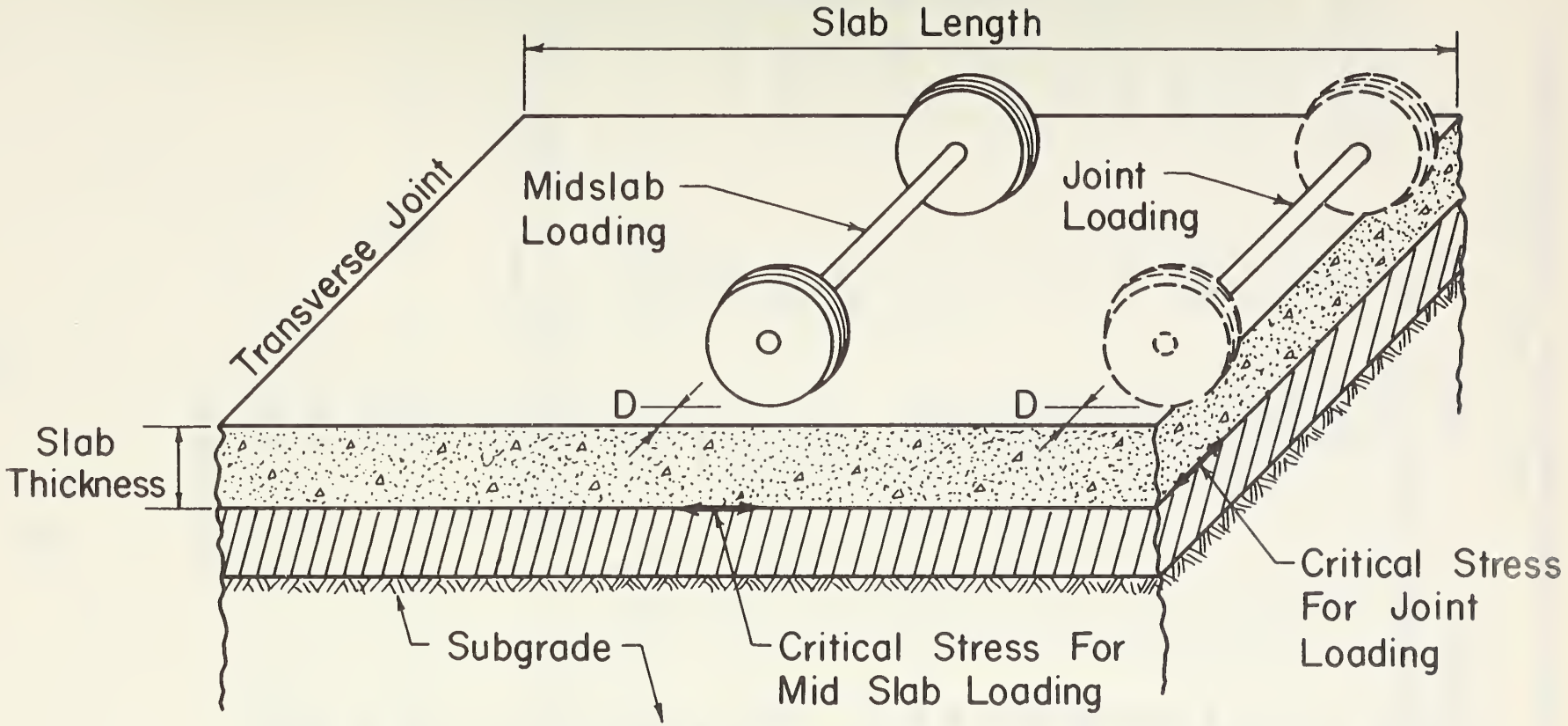


Figure 4.19. Illustration of Load Positions and Stresses Considered in Fatigue Analysis of Critical Points in Slab.

Table 4.6. Axle Load Distribution Used in Fatigue Analysis.

| Axle Load Group (kips) | Percent |
|---|---|
| Single Axle: | |
| <3 | 7.52 |
| 3-7 | 16.82 |
| 7-8 | 8.01 |
| 8-12 | 16.56 |
| 12-16 | 4.92 |
| 16-18 | 2.01 |
| 18-20 | 0.87 |
| 20-22 | 0.20 |
| 22-24 | 0.08 |
| 24-26 | 0.01 |
| 26-30 | 0.01 |
| 30-32 | 0.01 |
| Tandem Axle: | |
| <6 | 0.37 |
| 6-12 | 10.31 |
| 12-18 | 5.36 |
| 18-24 | 5.63 |
| 24-30 | 9.92 |
| 30-32 | 5.90 |
| 32-34 | 3.73 |
| 34-36 | 1.24 |
| 36-40 | 0.45 |
| 41-42 | 0.03 |
| 42-44 | 0.01 |
| 44-46 | 0.01 |
| 46-48 | 0.01 |
| 48-50 | 0.01 |
| Total | 100.00 |

Table 4.7. Percentage of Truck Wheel Loads at Various Lateral Distances from Slab Edge*.

| Position on Slab (or Shoulder), D | Mean Lateral Displacement ($\bar{D}$), ins. | | | | |
|---|---|---|---|---|---|
| | 12 | 24 | 36 | 42 | 48 |
| < -3 ins. | 6.68 | 0.35 | 0.01 | -- | -- |
| -3 to +3 ins. | 11.73 | 1.44 | 0.04 | 0.01 | -- |
| +3 to +9 ins. | 19.80 | 4.89 | 0.30 | 0.04 | 0.01 |
| 9 to 15 ins. | 23.58 | 11.73 | 1.44 | 0.30 | 0.04 |
| 15 to 21 ins. | 19.80 | 19.80 | 4.89 | 1.44 | 0.30 |
| 21 to 27 ins. | 11.73 | 23.58 | 11.73 | 4.89 | 1.44 |
| 27 to 33 ins. | 4.89 | 19.80 | 19.80 | 11.73 | 4.89 |
| 33 to 39 ins. | 1.44 | 11.73 | 23.58 | 19.80 | 11.73 |
| 39 to 45 ins. | 0.30 | 4.89 | 19.80 | 23.58 | 19.80 |
| 45 to 51 ins. | 0.04 | 1.44 | 11.73 | 19.80 | 23.58 |
| 51 ins. | 0.01 | 0.35 | 6.68 | 18.41 | 38.21 |
| | 100.00 | 100.00 | 100.00 | 100.00 | 100.00 |

*Data computed from normal distribution with standard deviation = 10 ins. (254 mm), and mean $\bar{D}$ as indicated.

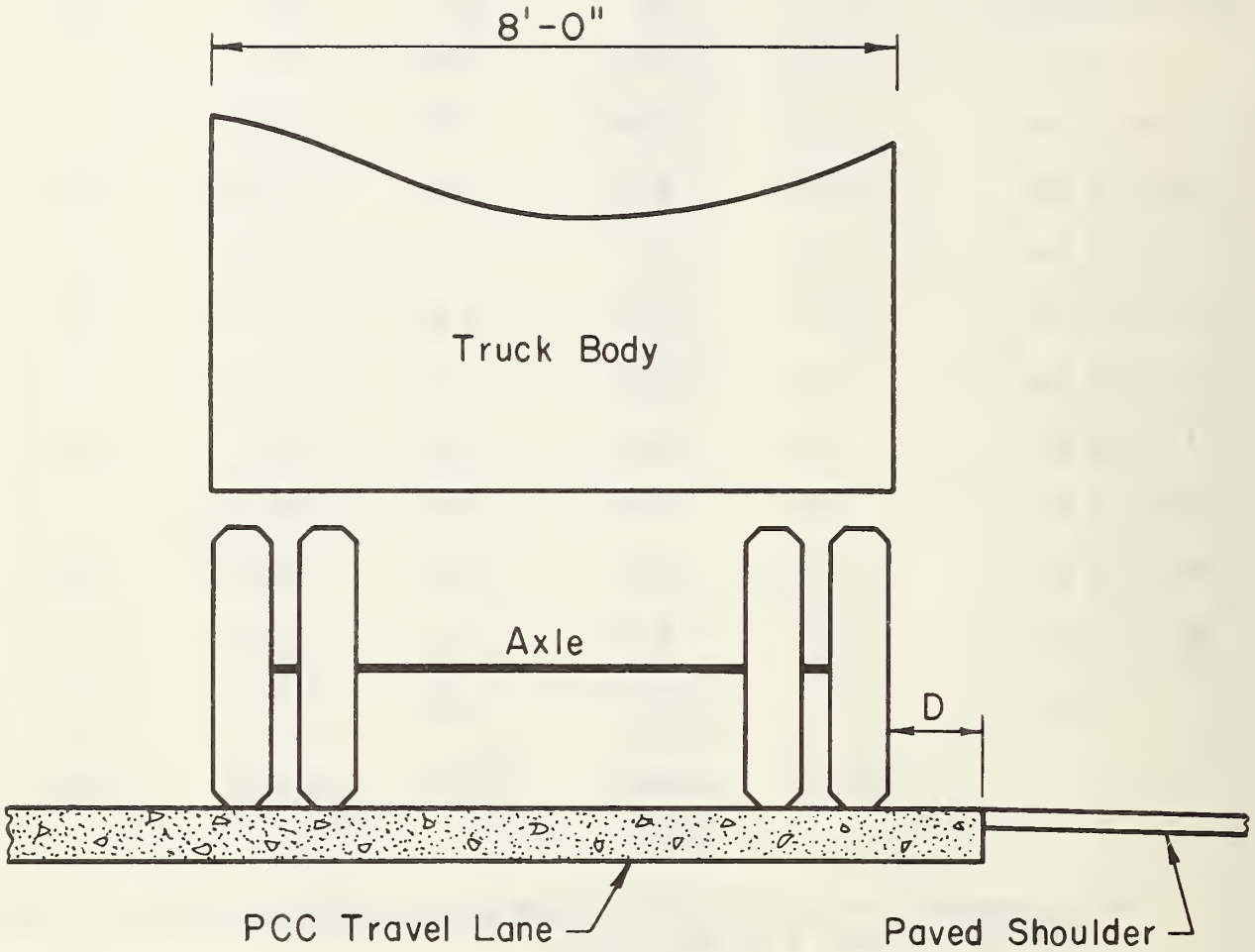


Figure 4.20 Illustration of the Mean Distance from Slab Edge to Outside of Dual Tires.

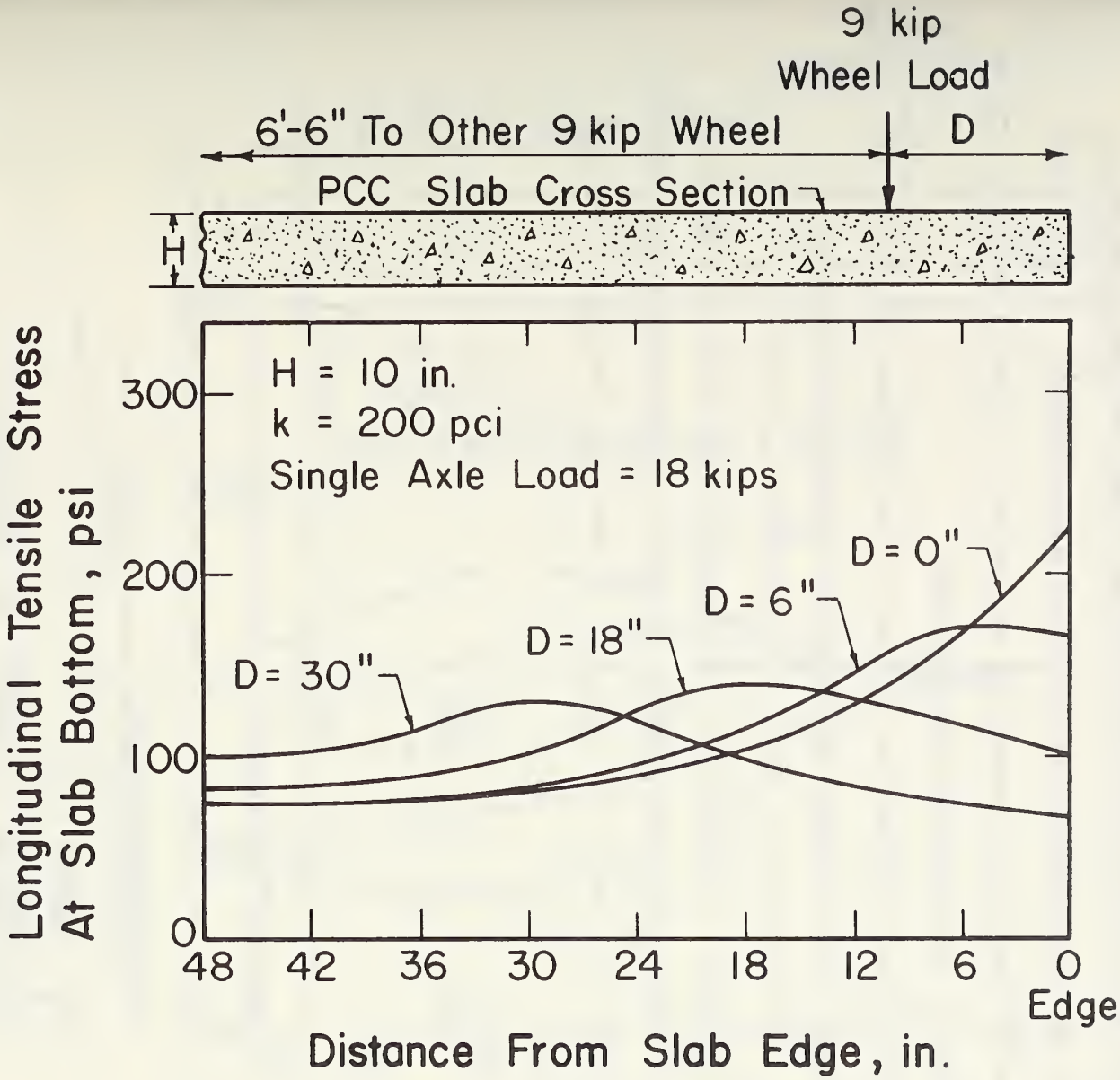


Figure 4.21. Computed Tensile Stresses Across Bottom of PCC Slab at Midpoint between Transverse Joints for Various Transverse Positions of Axle Load.

load is moved inward (D = 6, 18, and 30 ins. [152, 457, 762 mm]). A similar plot is shown in Figure 4.22 for the axle load placed at the transverse joints. Here the transverse stresses are compressive for D = 0, 6, and 18 ins. (0, 152, 457 mm) due to contraflexure at the bottom of the slab. The magnitude of these stresses at the transverse joint are considerably less than for the edge loading position (57 psi versus 225 psi). A joint load transfer efficiency of 50 percent was used which is a typical value as defined by Eq. 42. when dowel bars are used.

Stresses were computed over a range of slab thickness (8, 10, 14 ins. [203, 254, 356 mm]) and modulus of foundation support (50, 200, 500 pci) at every six inch (152 mm) across the slab both at mid-slab and at the transverse joint. Fatigue damage was computed at each 6 in. (152 mm) point across the slab using these stresses and Miner's accumulative damage hypothesis (Ref. 30). Damage at each point was computed using the following expression:

$$\text{Damage} = \sum_{i=1}^{p} \sum_{j=1}^{m} \frac{n_{ij}}{Nij} \qquad (4.5)$$

where

$n_{ij}$ = number of applied axle load applications at $i^{th}$ lateral position and of $j^{th}$ magnitude

Nij = number of allowable axle load applications determined from PCC fatigue curve (Eq. 4.8)

m = total number of $i^{th}$ lateral positions of axle load

p = total number of $i^{th}$ lateral positions of axle load

i = counter for lateral load positions (i = 1 corresponds to D = 0 ins., i = 2 to D = 6 ins. [152 mm], i = 3 to D - 12 ins. [ 305 mm ], . . . i = 6 to D = 48 ins. [1219 mm ]).

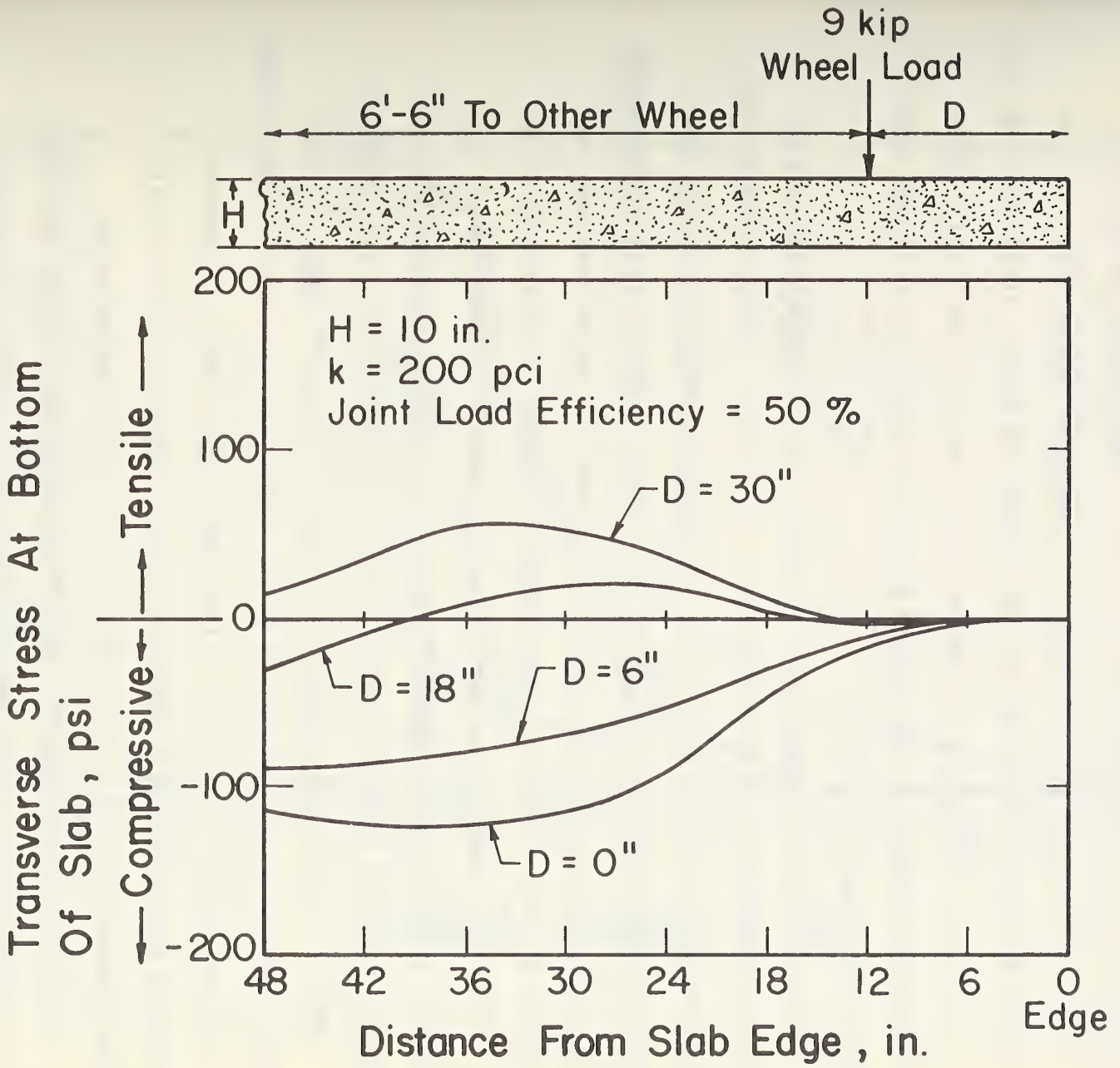


Figure 4.22. Computed Tensile Stress across Bottom of PCC Slab at Transverse Joint for various Transverse Positions of Axle Loads.

j = counter for axle load groups (j = 1 corresponds to 3-kip SA load, j = 2 to 6 kip SA load, etc.).

Damage at a given point is first summed over the axle load distribution considering the load to be located at D = 0 ins. Then the load is shifted to D = 6 ins. (152 mm) and fatigue damage is summed over the axle load distribution, and so on for D = 12, 18, 24, 30, 36, 42, and 48 ins. (0.3, 0.5, 0.6, 0.8, 0.9, 1.1, 1.2 m). The number of applied traffic loads at each load position are computed according to the Table 4.7 based on a total of 10 million axles total to pass over the slab.

The procedure was computerized and results from the analysis for mid-slab are given in Figures 4.23-4.25 for 8, 10, and 14 in. (203, 254, 427mm) slabs with a foundation support of 200 pci. These curves show that when the mean lateral placement ($\bar{D}$) is less than 36 ins. (0.9 m), the critical fatigue damage point is at D = 0 or the slab edge. Similar results are obtained when slab thickness is held constant and the foundation support is varied from 50 to 500. Therefore these fatigue analyses show that at a crosssection at the midpoint, cracking should definitely initiate at the outer edge of the slab. This was observed to occur in the field studies documented in Section 4.2.1.

Results from the analysis at the transverse joint are given in Figures 4.26-4.28 for slab thickness (H) of 8, 10, and 14 ins. (203, 254, 427 mm) placed on a foundation of k = 200 pci. A load transfer efficiency of 0 percent (a free edge) was used to give the most critical situation. The critical fatigue damage location is 24 to 42 ins. (0.6-1.1m) from the corner.

A final important result is the difference in magnitude of damage for the mid-slab location versus the transverse joint location. The mid-slab edge position has a much higher fatigue damage than the transverse joint position when both were subjected to the same average lane traffic. Thus, transverse

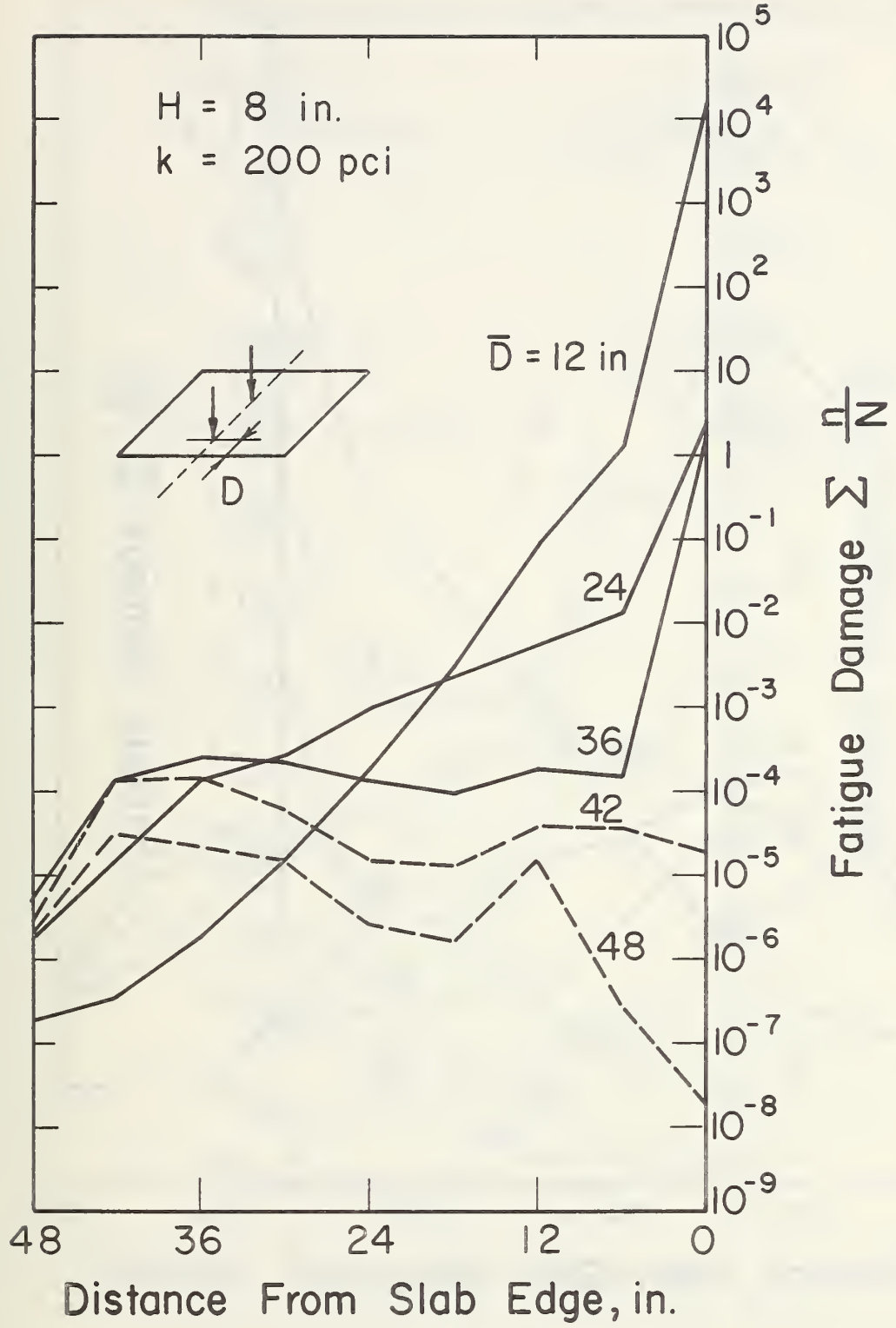


Figure 4.23. Computed Fatigue Damage across Slab Due to Lateral Distribution of Trucks on Lane--at Midpoint between Transverse Joints.

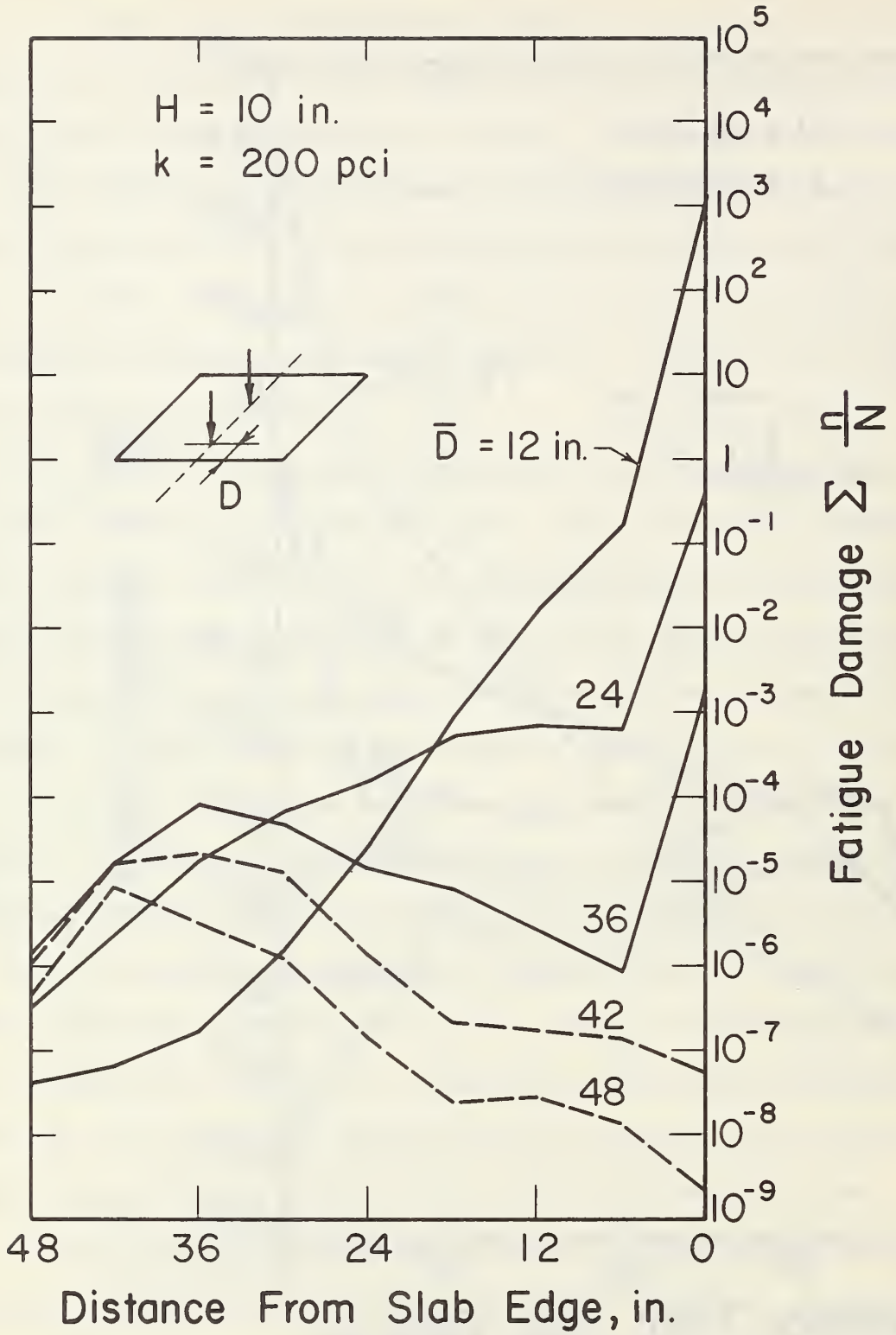


Figure 4.24. Computed Fatigue Damage across Slab Due to Lateral Distribution of Trucks in Lane--at Midpoint between Transverse Joints.

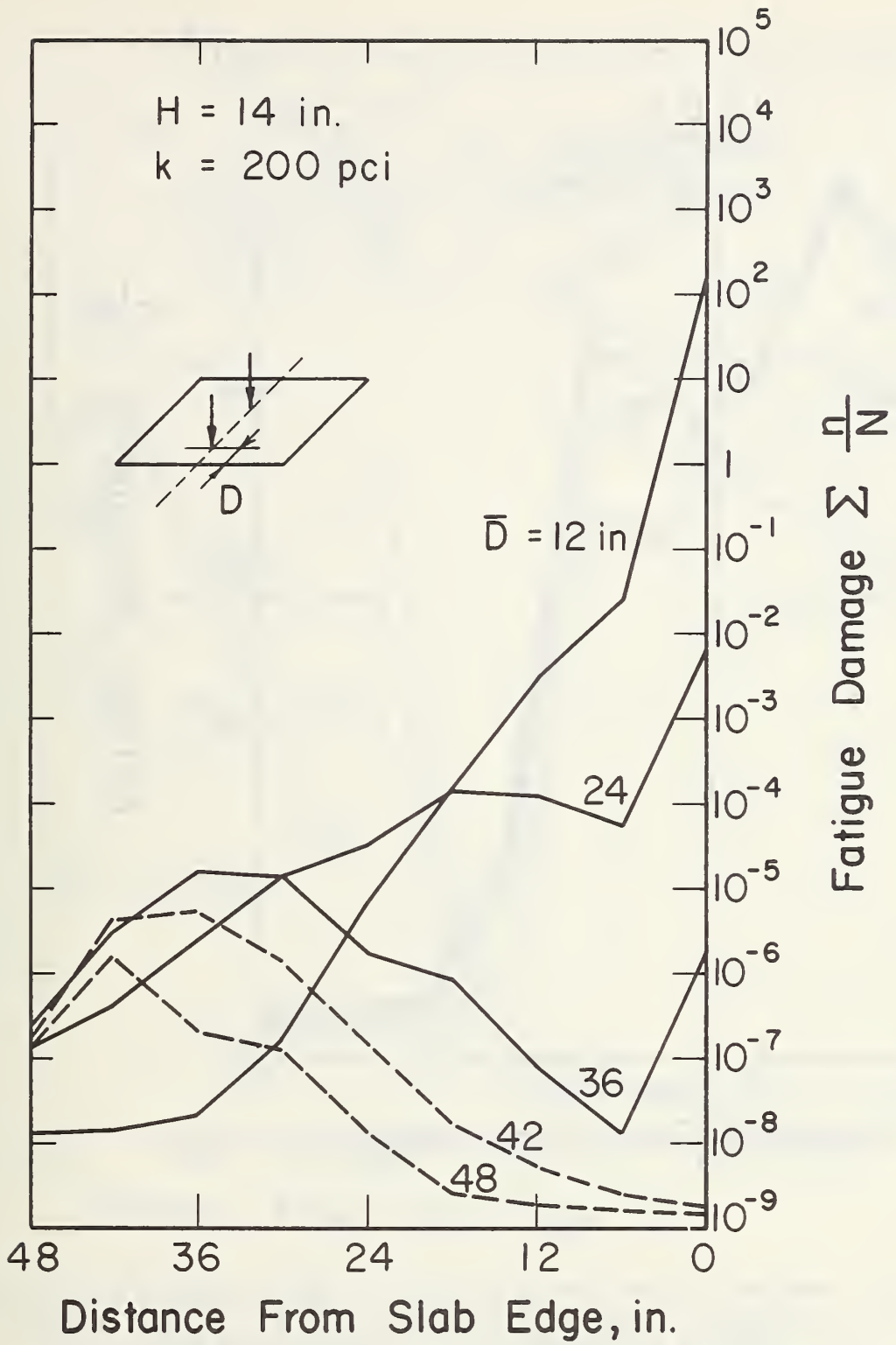


Figure 4.25. Computed Fatigue Damage Across Slab Due to Lateral Distribution of Trucks in Lane--at Midpoint between Transverse Joints.

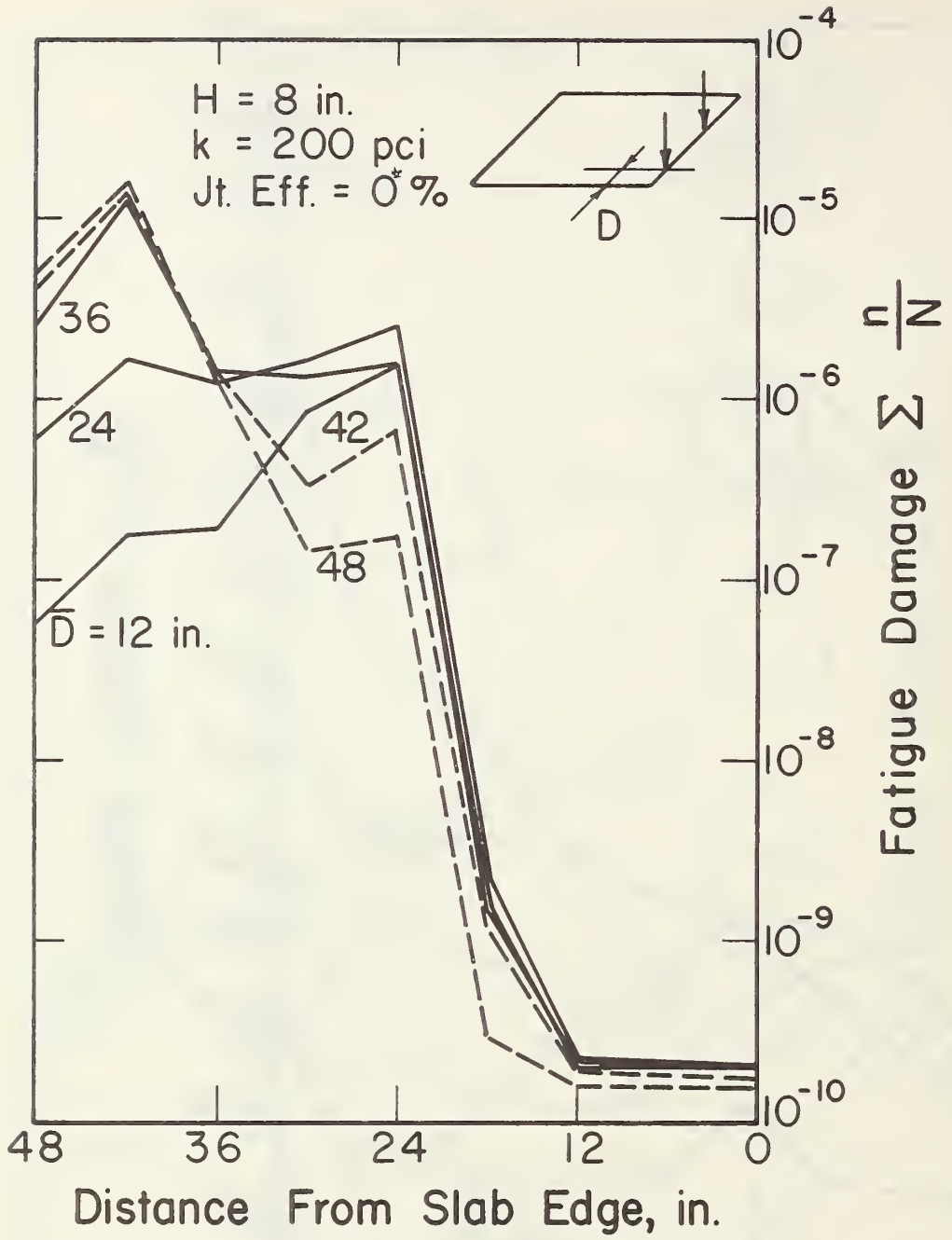


Figure 4.26. Computed Fatigue Damage across Slab Due to Lateral Distribution of Trucks in Lane--at Transverse Joint (H = slab thickness, k = modulus of foundation, D = distance from edge of slab measured toward center of slab).

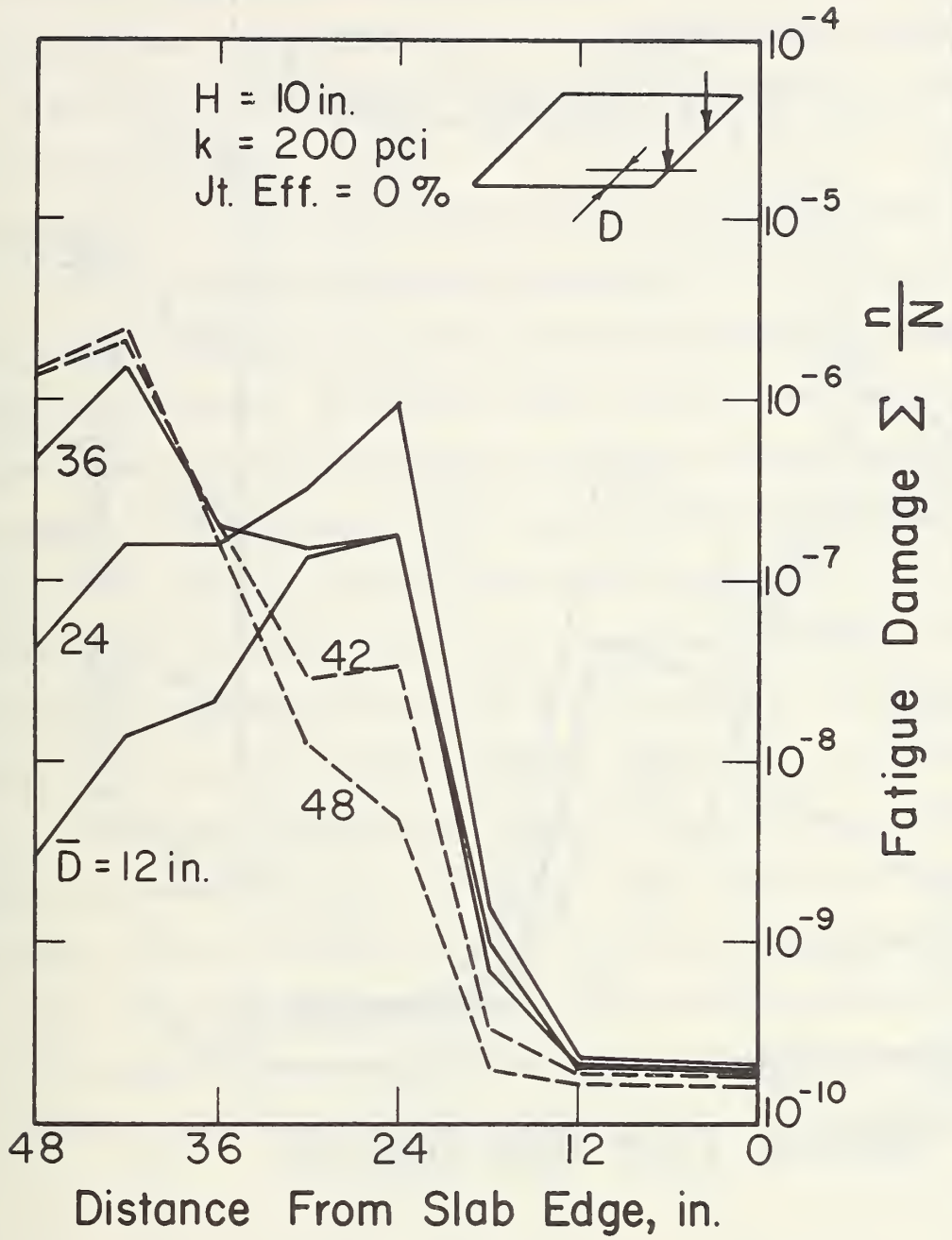


Figure 4.27. Computed Fatigue Damage across Slab Due to Lateral Distribution of Trucks in Lane--at Transverse Joint.

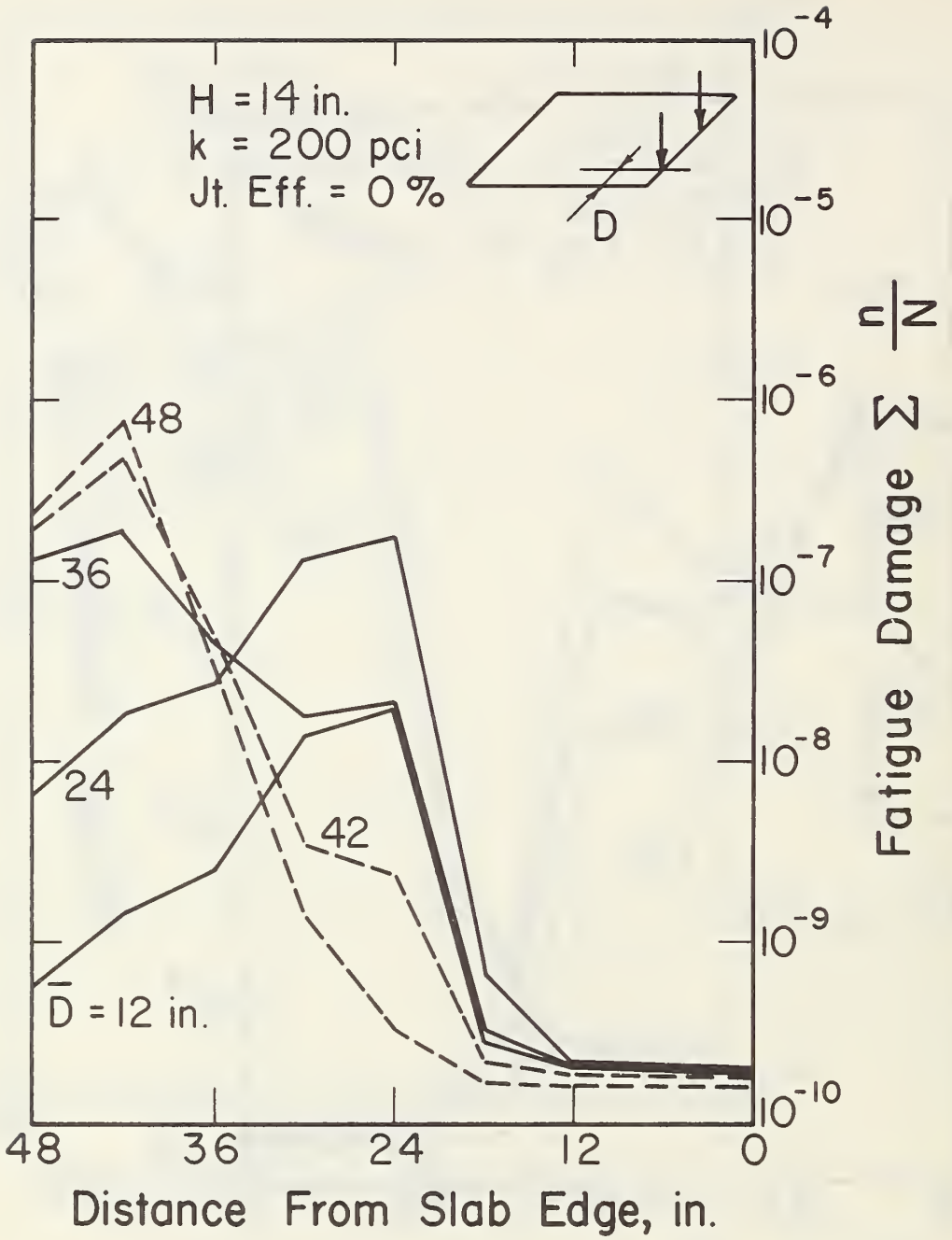


Figure 4.28. Computed Fatigue Damage across Slab Due to Lateral Distribution of Trucks in Lane--at Transverse Joint.

cracking would theoretically be expected to occur long before longitudinal cracking occurred. This result was verified at the AASHO Road Test and from the field survey where transverse cracking occurred much more often than longitudinal cracking. Hence, both field and analytical results indicate that for normal highway loadings and slab widths the critical fatigue damage point is at the slab edge.

An analysis of stresses occurring for slab edge loading and joint loading further illustrates the fatigue damage results. The stresses in Figure 4.29 were computed with the finite element program for the loadings and slab properties indicated. The critical stress (vertical ordinate) represents the maximum stress occurring anywhere in the slab for the given loading. For example, when D = 0 (load at the midslab edge), the critical stress is 390 psi and occurs beneath the load. If the load is moved inward to D = 24 ins. (0.6 m) the critical stress is 190 psi which occurs beneath the wheel load. The critical stresses occurring when the load is at the transverse joint are highly dependent on the joint load transfer efficiency (L). For L = 0 percent no load is transferred across the joint and the joint becomes essentially a free edge transferring no moment or shear. A critical stress of 270 psi occurs when D = 0 and is located at the top of the slab approximately 5 ft. (1.5 m ) from the joint. It is important to note that the maximum critical stress at the mid-slab edge loading (390 psi) is much greater than the maximum critical stress near the joint (270 psi) for any lateral distance, D.

## 4.4 EFFECT OF JOINT SPACING ON CRACKING

Plain jointed concrete pavements have been constructed with joint spacings ranging from 10 to 30 ft. (3 to 9 m). Available field data indicate that

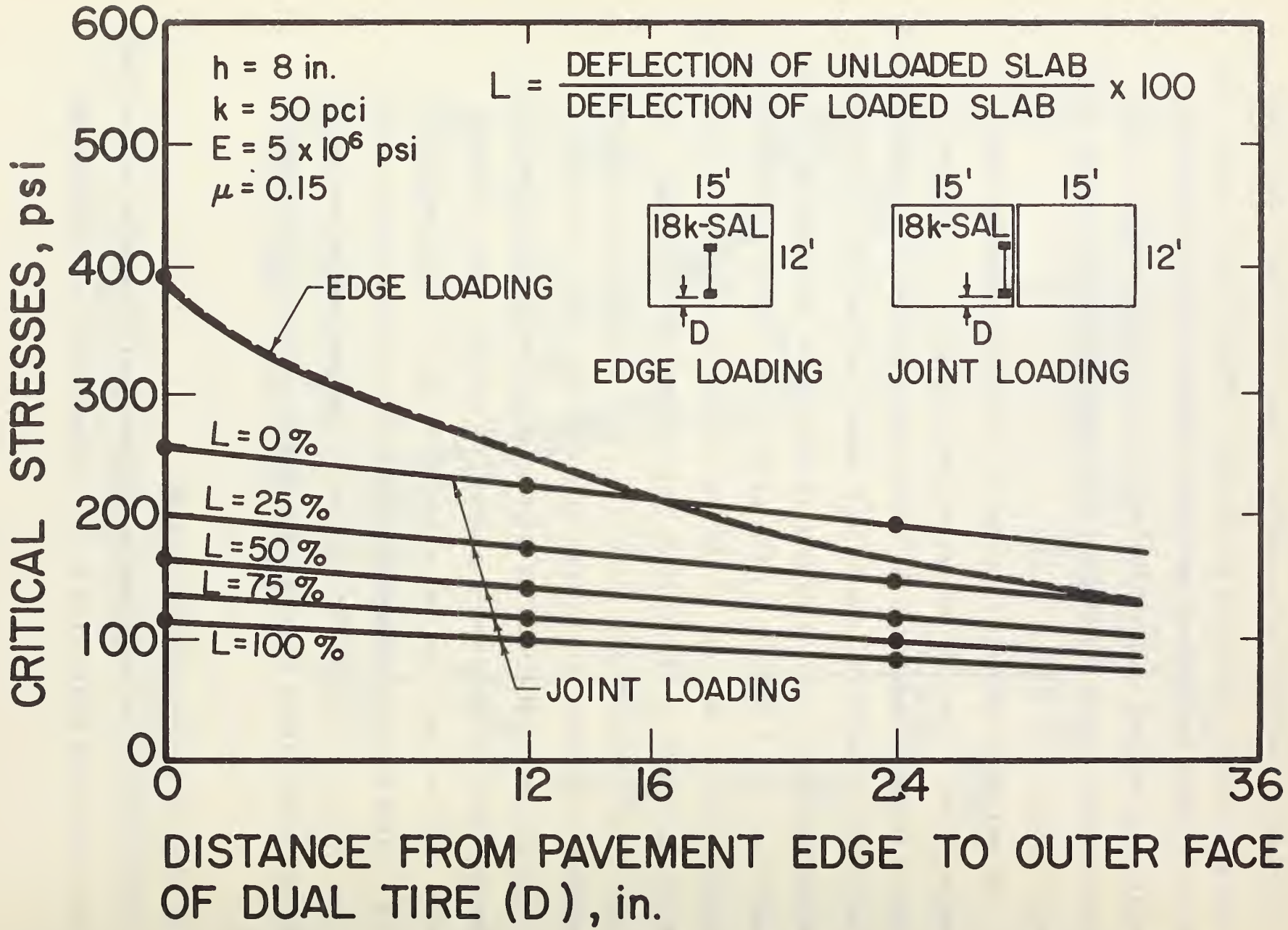


Figure 4.29. Effect of Axle Load Position on Critical Stress in Slab.

joint spacing has a significant effect on transverse cracking of the slabs. Road tests were conducted in Minnesota and Michigan where the transverse joint spacing varied from 15 to 30 ft. (4.6-9.1 m) and 10 to 30 ft. (3.0-9.1 m) respectively. Figure 4.30 shows transverse cracking versus joint spacing after 10-15 years of service for 8 in. (203 mm) slabs. Both road tests show a dramatic increase in transverse cracking with increase in joint spacing with a leveling out after about 25 ft. (7.6 m). The Michigan study concluded that ". . . joint spacing of approximately 10 ft would be necessary to completely prevent transverse slab cracking. The rate of transverse cracking increased approximately in relation to the square of increased slab length over 10 ft" (Ref. 9). The Minnesota study concluded "contraction joints should be placed at intervals of 15 ft. in order to obtain the best overall performance of the pavement slab from the standpoint of joint movement, cracking, warping, faulting, and roughness" (Ref. 10). The effect of joint spacing on transverse cracking was observed in four of the states visited during the field survey (California, Colorado, Washington, and Utah) where in randomly spaced joints of 12 to 19 ft. (3-6 m), the 18-19 ft. (5.5 m) slabs transversely cracked much more than the shorter slabs. Washington reduced their joint spacing to less than 15 ft. (4.6 m) because of transverse cracking on the longer slabs. Colorado reported that about 1/4 slabs that are 18-19 ft. (5.5 m) long crack transversely, but much less cracking occurs on shorter slabs. Numerous projects in California show much greater amounts of transverse cracking in the 18-19 ft. (5.5 m) slabs than the 12-13 ft. (4 m) slab. Transverse cracking was also observed in the 18-19 ft. (5.5 m) slabs in Toronto, Ontario where joint spacing ranged from 12 to 19 ft (3-6 m).

It is very important that the reasons for this occurrence are understood so that it may be considered in design. There are at least four factors which may be contributing to the increase of transverse cracking with increased joint spacing.

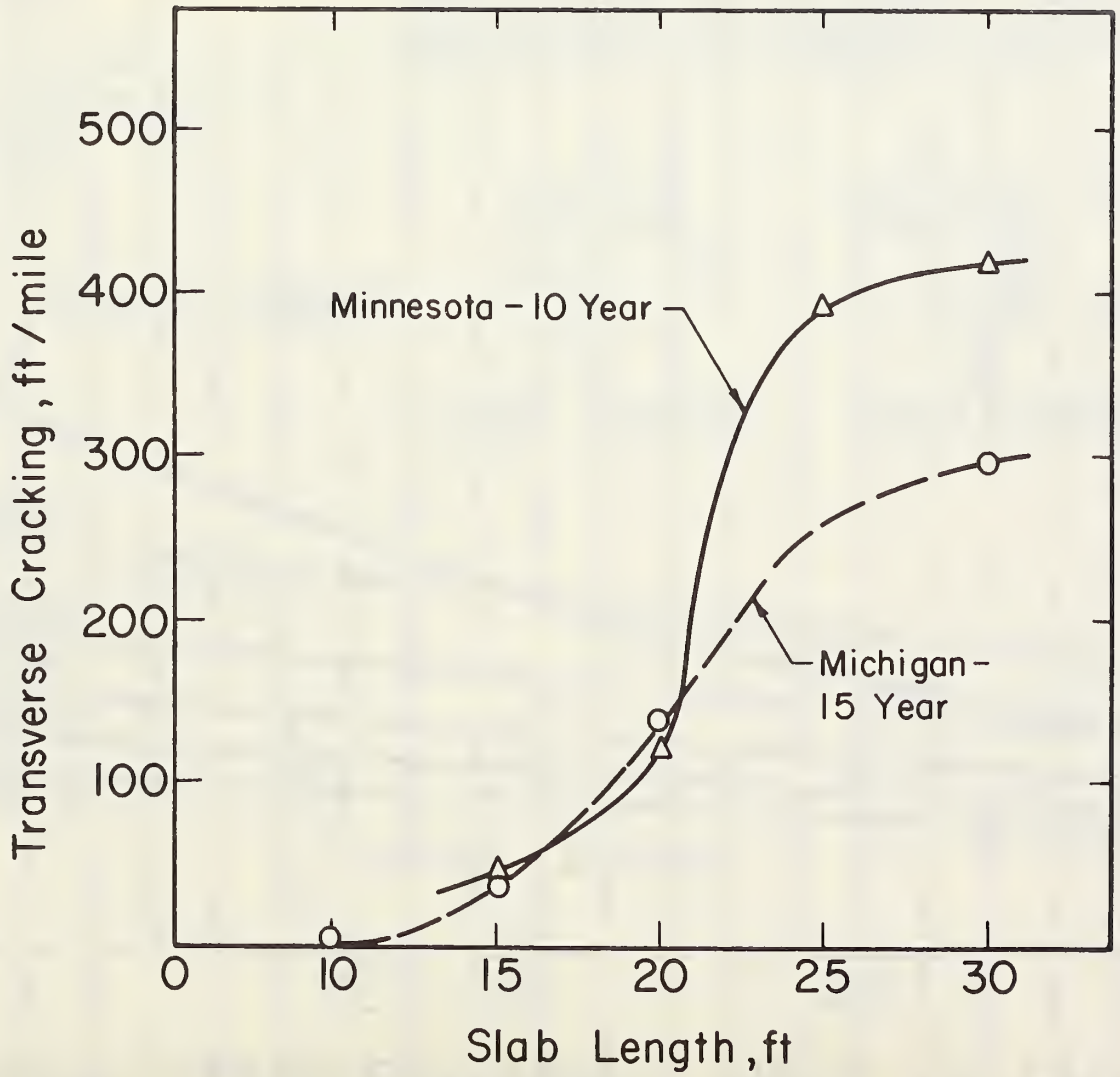


Figure 4.30. Effect of Slab Length on Transverse Cracking of Slabs for Two Road Tests.

1) Concrete Drying Shrinkage. PCC contains considerably more water at placement than is needed to hydrate the cement. With time, the exposed PCC slab loses considerable water which results in shrinkage. Water content, type and gradation of aggregate, chemical admixtures, moisture and temperature conditions have all been found to affect drying shrinkage (Refs. 21, 22, 23). The shrinkage of the PCC slab is resisted by friction at the slab/subbase interface and thus tensile stresses develop in the slab. Also, the temperature of the PCC drops during the first night due to a reduction in hydration rate and lower nighttime temperature resulting in additional tensile stress. Transverse cracks occur generally within the first day after placement ranging from 40 to 150 ft. (12 to 45 m) in slabs that are placed without any joints. However, when joints are placed in the PCC, tensile stresses due to drying shrinkage are reduced due to joint movement and their effect becomes smaller as joint spacing decreases. Many slabs ranging up to 80 ft. (24 m) in length were observed during the field survey that did not have any transverse cracks for pavements ranging up to 25 years in age. Hence, it is believed that for relatively short joint spacings (i.e. $\leq$20 ft.)[6 m] tensile stresses caused by drying shrinkage are mostly relieved through joint opening, and therefore have only minor effect, if any, on transverse cracking.

(2) Concrete Temperature Shrinkage. After the PCC hardens and the temperature drops, both during nighttime and seasonally, tensile stress occurs due to thermal shrinkage of the PCC and subsequent frictional resistance of the subbase. The maximum value of these stresses can be crudely estimated using the "subgrade drag theory" where the slab is pulled over the foundation and the stress required is computed. Frictional resistance tests have been conducted by several researchers (Refs. 24, 12, 25) which show that

the coefficient of frictional resistance is not a constant, but increases with increasing displacement of slab, until a maximum is reached where the slab slides freely. Sliding friction values ranging from less than 1.0 to over 2.0 have been obtained depending on foundation conditions. Stresses computed using conventional subgrade drag theory are given in Table 4.8 for a range of conditions using Equation 4.6 (Ref. 18).

$$S = \frac{Lf\gamma_c}{288} \qquad (4.6)$$

where S = tensile stress in PCC, psi

f = coefficient of frictional resistance

L = slab length, ft.

$\gamma_c$ = unit weight of PCC, pcf

The tensile stress increases linearly with joint spacing which probably contributes somewhat to the increase in cracking with increased joint spacing. These stresses are very small, however, for short joint spacings (i.e. <20 ft. [6 m ]), but are of significant magnitude for longer joint spacings. They are believed to be negligable for relatively short slabs.

(3) Slab Moisture Gradients. Hatt (Ref. 16) reported in 1925 that slab warping was cuased when moisture differences existed between slab surfaces.

> "After curing under water (for 30 days), the slab was dried by circulating air both above the slab and through the subgrade. The more rapid drying of the top surface warped the slab to a maximum upward deflection of 0.12 in. at the corners and 0.05 in. at the unbroken edge during a period of 40 days, after which time upward movement ceases, . . . After 3 months of further drying, the slab had become approximately uniformly dry throughout its depth and substantially level (or flat), . . . In order to saturate the bottom of the slab, water was then introduced to the level of the top of the gravel subgrade (opengraded). During 110 days of saturation the slab again warped upward 0.20 in. at the corners and 0.066 in. at the unbroken edge. . . The surface was (then) covered with saturated burlap to simulate the effect of prolonged rain. . . In 30 days the corner ahd dropped 0.06 in., to a deflection of 0.14 in." (Ref. 16).

Table 4.8. Computed Tensile Stress in PCC Slabs Due to Temperature Reduction and Subbase Frictional Resistance.*

| Joint Spacing (ft) | Coefficient of Frictional Resistance | | |
|---|---|---|---|
| | 1.0 | 1.5 | 2.0 |
| 10 | 5 psi** | 8 | 10 |
| 15 | 8 | 12 | 16 |
| 20 | 10 | 16 | 21 |
| 30 | 16 | 23 | 31 |
| 50 | 26 | 39 | 52 |
| 100 | 52 | 78 | 104 |

* PCC unit wt. = 150 pcf

** Computed from Eq. 4.6.

The weight of the slab, resistance from the subgrade, and any resistance at the slab edges apply restraint to warping of the slab, and thus stresses occur at the top and bottom of the slab. The stresses caused by moisture gradients through the slab are referred to as warping stresses. A field study into the effects of moisture gradients was conducted by the Bureau of Public Roads (Refs. 11-15) in the 1930's. Conclusions reached from these studies are briefly summarized as follows:

> "The data indicate that the curvature caused by moisture is principally an upward warping of the edges caused by a moisture loss from the upper surface of the pavement. The downward warping of the edges, resulting from a condition in which the moisture content in the upper part of the pavement exceeds that in the lower part, seems to be considerably smaller for the conditions of these tests. . . The edges of the slab reach their maximum position of upward warping from this cause during the summer and the maximum position of downward warping during the winter, the extent of the upward movement apparently exceeding that of the downward movement considerably" (Ref. 12).

These results indicate that the warping of a pavement slab from moisture gradients is mostly a seasonal change occurring over a considerable time interval. For example, during the winter months in Phoenix, Arizona, when the relative humidity is very low, the PCC slabs are noticeably warped upward due to the severe drying of their surface. The warp is less during other seasons. The Arlington tests (Ref. 12) also showed that as the seasonal warping occurs, the slab settles somewhat into the subgrade, thus reducing the restraint due to slab weight. Any creep of the concrete would also tend to reduce the stress from moisture warping.

Because of the many difficulties involved (i.e. inability to measure moisture contents in slabs, settlement, creep, etc.) attempts have not yet been successful to compute or measure strains due to moisture gradients, and their relative magnitudes are unknown. However, the following conclusions appear justified based upon the available information:

(a) The top of the slab is usually dryer than the bottom through most of the year, causing some compressive stresses at the bottom of the slab.

(b) These stresses are greater during the warm weather portion of the year becuase of a drier slab surface.

(c) Moisture warping stresses at the slab bottom are generally of opposite sign than load stresses, and hence tend to reduce the combined stresses occurring at the slab edge or interior.

(d) There is not enough information presently available to consider moisture gradient warping stress in design, however, as joint spacing increases, the warping stress will also increase similar to thermal curling stress as subsequently described.

(4) Slab Thermal Gradients. A difference in temperature between the top and bottom of slabs has been shown both experimentally and analytically to cause significant stress in the slabs (Refs. 2, 7, 8, 17, 18, 19). The most recent and accurate analytical method to compute these stresses is the finite element model (Ref. 66). These stresses are referred to as curling stresses. The most critical condition occurs when the top is warmer than the bottom (daytime), which results in tensile stresses at the bottom of the slab that are additive to load stresses. The daytime stresses have been shown to be much larger (about 3 times) than the nighttime stresses. Teller and Southerland (Ref. 12) concluded the following based upon their extensive studies into thermal curling stresses in the 1930's:

> "The data that have just been presented clearly indicate that the stresses arising from restrained temperature warping equal in importance those caused by the heaviest wheel loads. The stresses from this cause are actually large enough to cause failure in concrete of low flexural strength, and since the direction of the stresses is such that they become added to the critical stresses caused by wheel loads, there is little doubt but that warping stress is primarily responsible for much of the cracking in concrete pavements" (Ref. 12).

The effects of joint spacing on thermal gradient curl edge stress as computed with the finite element program was shown in Section 4.2, and is illustrated for a specific slab in Figure 4.31 with slab length varying from

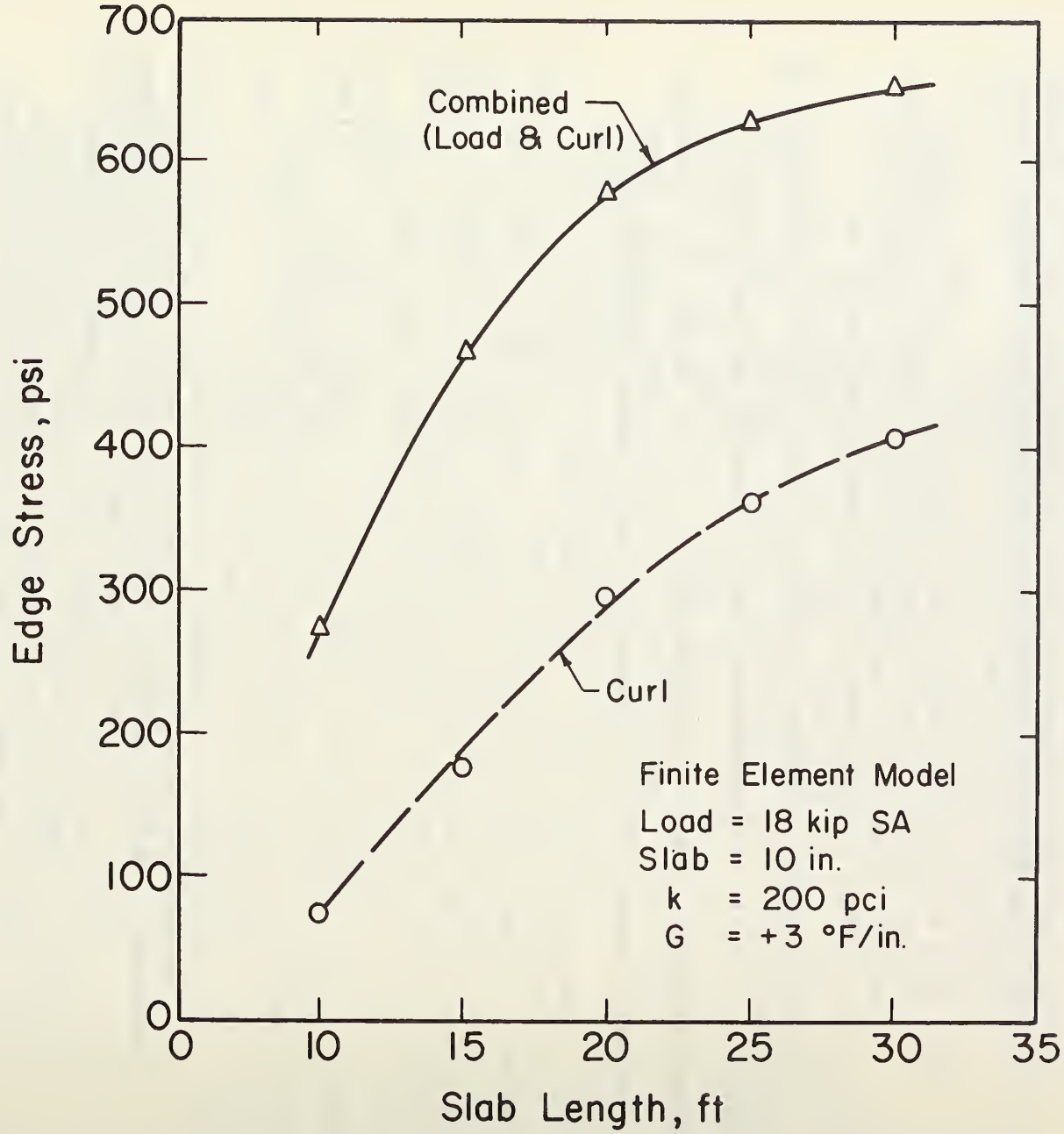


Figure 4.31. Edge Stress Due to Load and Thermal Gradient for Varying Joint Spacing Computed with Finite Element Program.

10 to 30 ft. ( 3 to 9 m ). There is a dramatic increase in edge stress (which is parallel to the longitudinal slab edge) as slab length is increased up to about 25 ft. ( 8 m ). It then levels off as shown. This relationship is similar to Figure 4.31 for transverse cracking of slabs varying from 10 to 30 ft. ( 3 to 9 m). While there may be a basis to conclude that calculated curl stress is not as large as actual curl stress (due to the opposite effect of moisture and slab settlement into subbase), the general trend of curl stress relates very closely to the trend of transverse cracking. But most importantly, the stress resulting from both combined load and curl for a daytime temperature gradient (top warmer than bottom) also shows the same trend as cracking with increasing slab length.

These curl stresses caused by thermal gradients are of sufficient magnitude to cause transverse cracking even independently over a long time period. Loop 1, the non-trafficked loop at the AASHO Road Test, was surveyed after 16 years, and most of the 40 ft. ( 12 m) long slabs were cracked, but none of the 15 ft. ( 5 m) slabs were cracked. Possibly the repeated daily thermal gradient cycles over many years resulted in a thermal curl stress fatigue of the slabs. Other stresses such as temperature shrinkage and moisture gradients may also contribute however. Several researchers have concluded that thermal curling stress is of significant magnitude to contribute to transverse cracking of slabs (Refs. 12, 31, 29). Based upon available results it is concluded that thermal curl stresses are of sufficient magnitude to cause an increase in transverse cracking as joint spacing increases, and must be considered in any design analysis that attempts to prevent slab cracking.

In summary, field experience indicated that as transverse joint spacing increases from 10 to 30 ft. ( 3 to 9 m ), transverse cracking increases

dramatically. The major cause of this increase is increased stress resulting from restrained thermal curling with increased joint spacing. Drying shrinkage and temperature shrinkage do not have a significant effect on short slabs because of stress relief effected by joints. The effect of moisture gradients is not fully known, but is believed to be usually of opposite sign of stresses caused by traffic load for edge and interior slab positions. Thus, it tends to reduce the critical combined stress effect of load and thermal curl (when top is warmer than bottom).

## 4.5 DEVELOPMENT OF FATIGUE DAMAGE ANALYSIS

A comprehensive PCC slab fatigue damage analysis was developed based upon the following:

- -The critical fatigue damage location in the slab is at the slab longitudinal edge midway between transverse joint.
- -Critical edge stresses caused by both traffic loads and thermal gradient curl are considered to prevent transverse cracking.
- -Both load and thermal curl stresses are computed using a finite element program which has been shown to provide accurate results.
- -The proportion of traffic occurring near the slab edge is used in the fatigue analysis.
- -Concrete strength changes with time and thus the fatigue analysis must be time dependent.
- -Fatigue "damage" is computed according to the Miner hypothesis.
- -A correlation between computed fatigue "damage" and measured cracking was determined and limiting "damage" for zero-maintenance design selected.

4.5.1 PCC Fatigue. Several laboratory studies have shown that plain PCC beams experience fatigue failure when subjected to high repetitive flexural stresses (Refs. 32-41). Also, several road tests and many inservice PCC slabs have been observed to experience fatigue failure when subjected to many applications of heavy truck traffic (Refs. 9, 45). However, no

correlation between laboratory and field fatigue results has been attempted.

The results from laboratory studies provide significant information about the fatigue properties of PCC applicable to pavement fatigue conditions.

(1) The number of repeated loads that PCC can sustain in flexure before fracture depends upon the ratio of applied flexural stress to the ultimate static flexural strength or modulus of rupture.

(2) PCC does not have a fatigue limit within 20 million load applications, hence there is no limiting repeated stress below which the life will be infinite (Refs. 32,33, 34). The mean fatigue strength of PCC, which is the strength expressed as a percentage of the static ultimate strength, is approximately 55 percent at 10 million applications of load (Ref. 38).

(3) The range of loading (expressed as the ratio of flexural stress at minimum load divided by stress at maximum load) affects fatigue strength as shown in Figure 4.32. As the range increases the fatigue strength increases (Ref. 38).

(4) Application of varying flexural stress levels gives different fatigue results depending on the sequence of applied loads of varied intensity (Refs. 34, 35). Thus, Miner's damage hypothesis, which assumes linear accumulation of damage, does not give exact prediction of failure of PCC. However, data from recent tests indicate that the inaccuracy of the Miner's hypothesis is not very significant compared to the large variability in strength and fatigue life that is typical of PCC (Ref. 43). Hence, it was concluded that Miner's hypothesis represents the cumulative damage characteristics of concrete in a reasonable manner (Ref. 43).

(5) Variability of fatigue life of PCC is very high with coefficients of variations ranging up to 100 percent. An example of the large variability

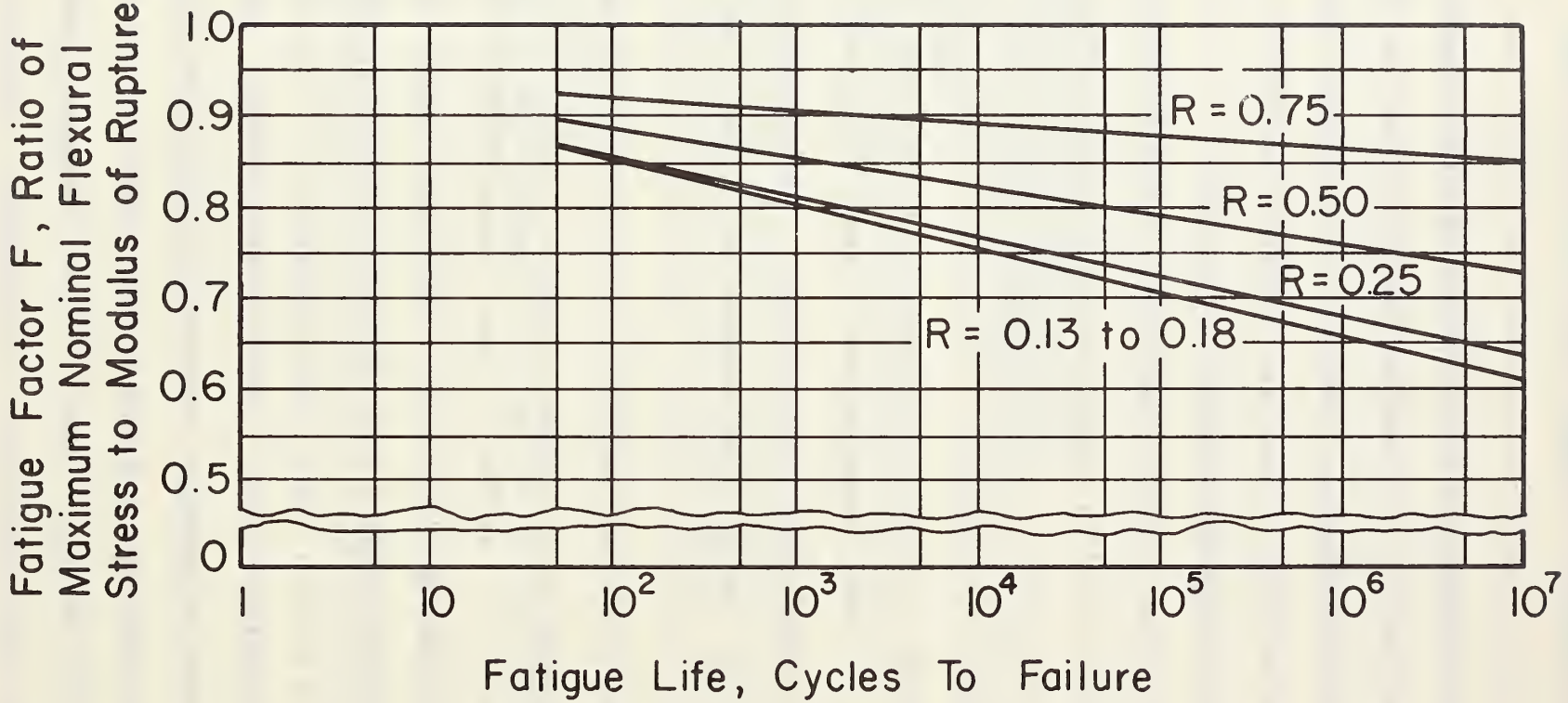


Figure 4.32. Effect of Range of Stress on the Behavior of Plain Concrete under Fatigue Loading (Ref. 38).

of the number of applications to failure of similar specimens tested under the same conditions is shown in Figure 4.33.

(6) Repeated rest periods during a fatigue test increase the fatigue strength, hence some recovery occurs during the rest periods (Ref. 35).

(7) The effect of moisture conditions of PCC under flexural fatigue has not been fully determined. Some limited tests, indicate that high moisture content gives lower fatigue strength (Refs. 34, 44). However, a recent limited study tends to indicate that saturation affects fatigue life, but does not significantly change the fatigue strength (Ref. 42), however, the results are not conclusive.

(8) The increase in modulus of rupture of PCC with time has significant effect on increasing fatigue life, but not on fatigue strength as long as the modulus of rupture at the specific time is used to compute the stress ratio (Ref. 42). This result is shown for PCC ranging in age from 4 weeks to 3 years in Figure 4.34. The various curves for different ages overlap each other.

Fatigue data were obtained for plain PCC beams from three studies (Refs. 33, 42, 43). A S-N plot of 140 tests from these studies is shown in Figure 4.35. The plot shows a large scatter of data, and the data from the three studies generally overlap each other. A least square regression curve was fit through the data as shown.

$$\log_{10} N = 17.61 - 17.61\ (R) \qquad (4.7)$$

where

N = number of stress applications to failure of beam.

R = ratio of repeated flexural stress to modulus of rupture

Standard error = 1.40 (of log N).

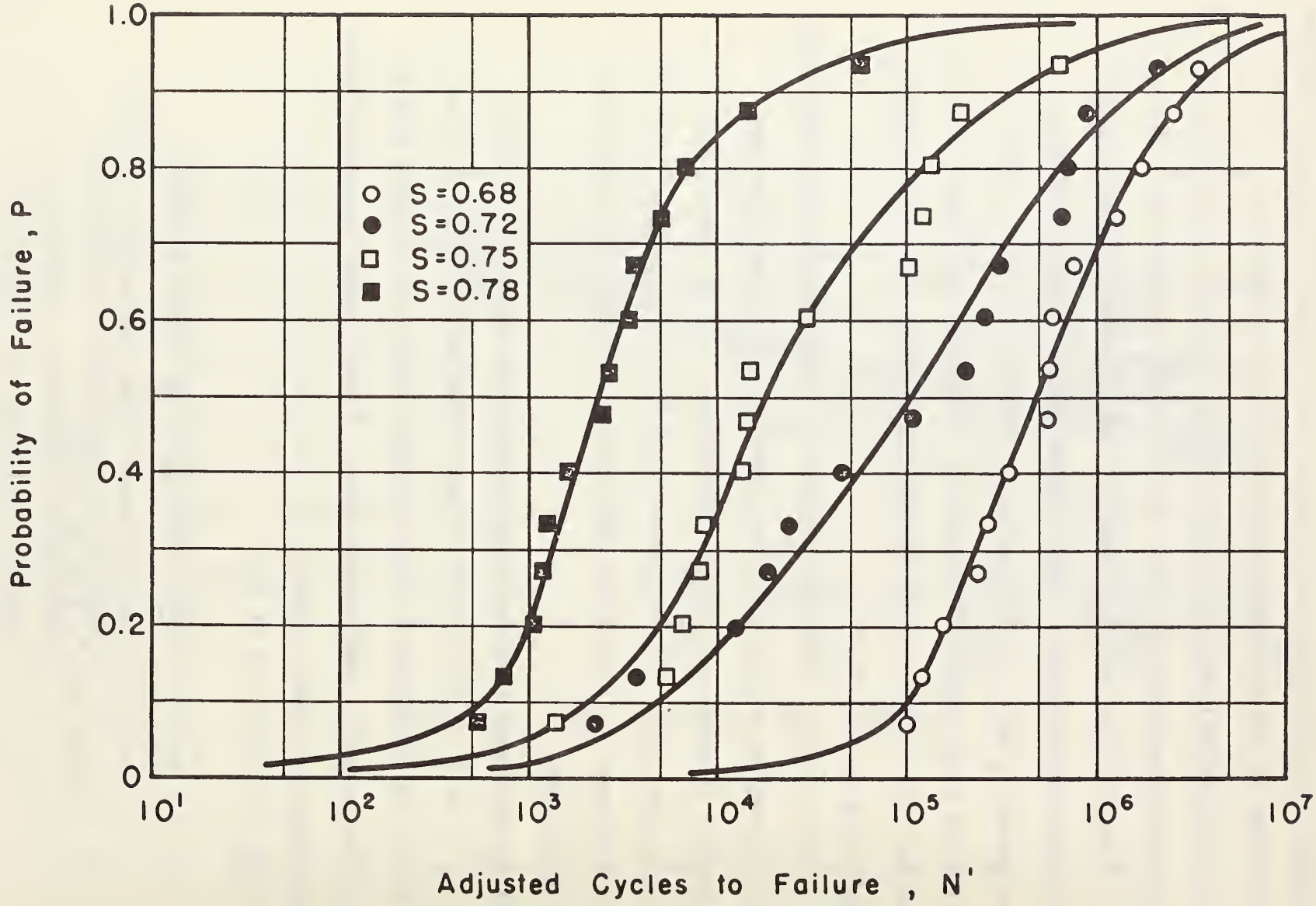


Figure 4.33. Variation of Fatigue Lifes of Flexural Plain Concrete Beam Specimens Subject to Varying Levels of Stress (Ref. 4).

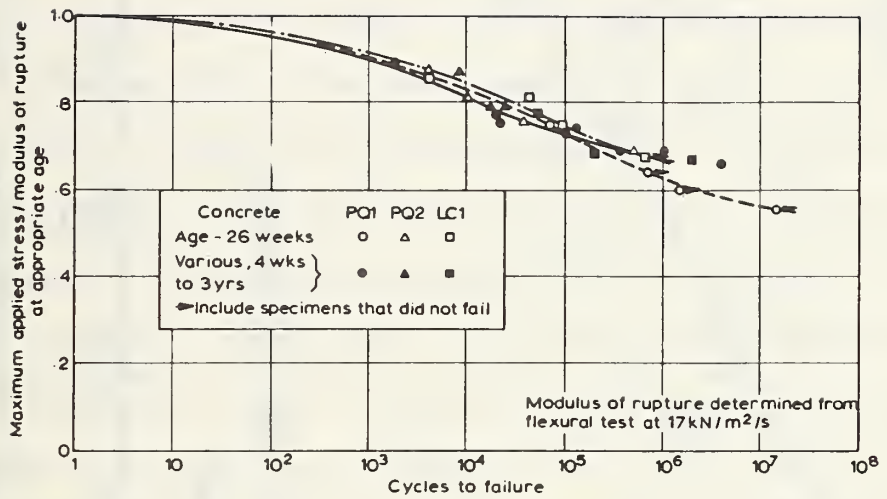


Figure 4.34. Fatigue Performance Related to Modulus of Rupture for Varying Ages (saturated beams) (Ref. 42).

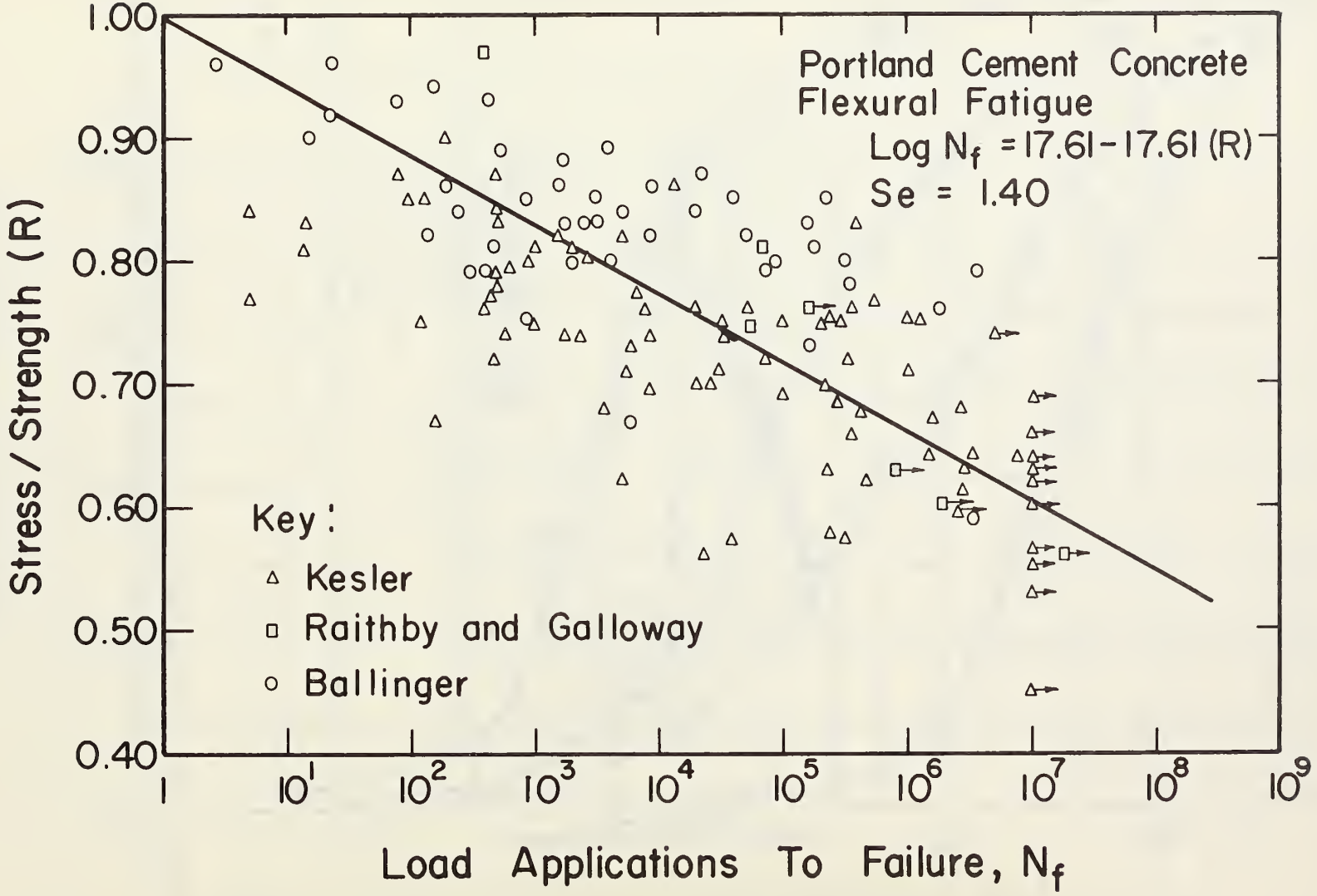


Figure 4.35. Summary of PCC Flexural Fatigue Data.

This equation is a mean regression curve in that it represents a failure probability of 0.50 or 50 percent. Hilsdorf and Kesler (Ref. 35), for example, established curves for various probabilities of failure based upon their data, and the curve for a probability of 0.05 is plotted in Figure 4.36. The fatigue curve used in design by PCA is also shown in Figure 4.36 which is much lower than the P = 0.05 curve for lower stress ratios.

The applicability of these laboratory fatigue results from beam specimens to the fatigue of actual pavement slabs under field conditions has never been established. Many differences exist between laboratory and field conditions that probably result in different fatigue responses. Table 4.9 has been prepared based upon a review of literature to show the probable differences in fatigue life of laboratory beams and of field slabs. For example, the effect of thermal curl which occurs daily in field slabs but not in laboratory beams reduces the fatigue life of slabs due to the additive effect of load and curl stress when the top of the slab is warmer than the bottom of the slab. On the other hand, the effect of age of slab and the corresponding increase in static ultimate strength would cause an increase in fatigue life of the field slab (loaded over many years) over the laboratory beam that is tested in a relatively short time period. The relative significance of each factor is indicated. Several of these factors can be reasonably considered in design including thermal curl, thickness variation, loss of support, age of PCC, and variation of PCC strength. There is not adequate data available to directly consider the other factors, however, several only have minor effects and also since some have beneficial and some detrimental effects they tend to cancel each other out. In summary, the complexities are so great and available information so limited that any laboratory curves used to estimate fatigue damage in field slabs must be

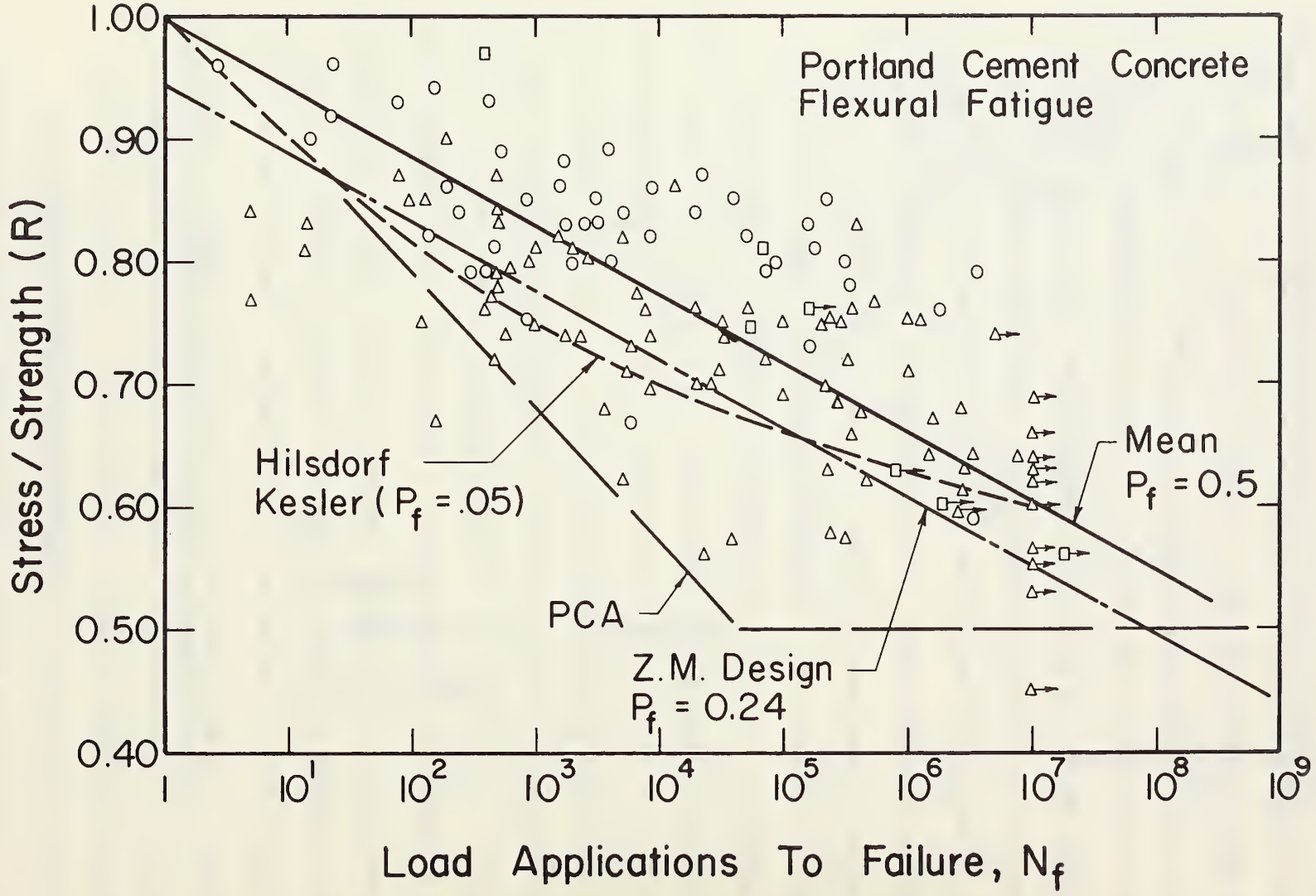


Figure 4.36. PCC Flexural Fatigue Data with Various Curves.

Table 4.9. Differences in fatigue life of PCC beams (Nb) and pavement slabs due to certain slab conditions.

| Field Slab Condition | Fatigue Life | Relative Significance |
|---|---|---|
| Variability of PCC strength | Ns < Nb | *** |
| Thermal Gradient Curl | Ns < Nb | *** |
| Thickness Variations | Ns < Nb | ** |
| Loss of Support | Ns < Nb | ** |
| Durability of PCC | Ns < Nb | ** |
| Thermal Shrinkage | Ns < Nb | * |
| Moisture Gradient Warp | Ns > Nb | ** |
| Rate of Loading | Ns > Nb | ** |
| Rest Periods | Ns > Nb | ** |
| Age of PCC (strength gain) | Ns > Nb | *** |
| Stress Ratio | Ns > Nb | * |
| Moisture of Slab | Unknown | |
| Scale Effects | Unknown | |
| Drying Shrinkage | Unknown | |
| Load Effects (testing machine vs. truck traffic) | Unknown | |

* Minor

** Moderate

*** Major

"calibrated" based on field data as presented in Section 4.6. Additional research on PCC slab fatigue is greatly needed.

A fatigue curve must be selected for design purposes. Figure 4.36 shows four curves plotted with the laboratory fatigue data. The mean regression curve, Eq. 4.7 essentially represents a 50 percent failure probability curve, because approximately one-half of the beams fail before this curve is reached for any given stress ratio. A curve desired by Hilsdorf and Kesler (Ref. 35) for varying flexural stresses representing a probability of failure of 5 percent is shown along with the current PCA design curve. A curve with a fatigue limit such as the PCA curve is not selected since several researchers have concluded that concrete does not have a fatigue limit within 20 million load applications (Refs. 32, 33, 34). After consideration of a number of factors the following curve was selected for design:

$$\log N_d = 16.61 - 17.61\ (R) \qquad (4.8)$$

This expression provides a safety margin of one decade of load application as shown in Figure 4.26, and represents a failure probability of 24 percent. The use of a lower probability of failure curve is not felt justified because much of the variation in fatigue life is due to the inability to predice ultimate static strength. Since the variation of strength will also be considered directly in design, the fatigue curve represented by Eq. 4.8 is believed in reality to represent a much lower failure probability if variation due to concrete strength were removed.

4.5.2 PCC Strength Increase. PCC strength data were obtained from five projects located in as many states (Refs. 46, 47, 48, 50, 51) and also from the Portland Cement Association (Ref. 49). The modulus of rupture at various times ranging from 3 days to 17 years was obtained from tests on beams cast

during construction and then cured over time, and beams cut from slabs over time. The modulus of rupture was also estimated from cylinders cast during construction, and cores cut from the slabs over time. The cylinders and cores were tested for compressive strength and converted to a modulus of rupture using the following relationship (Ref. 52):

$$\text{Mod. of Rupture (psi)} = 10[\text{Comp. strength (psi)}]^{1/2} \quad (4.9)$$

Data were obtained ranging from 3 days to 17 years and many points between as shown in Figure 4.37. The following equation was obtained using multiple regression techniques.

$$F_A = 1.22 + 0.17 \log_{10} T - 0.05(\log_{10} T)^2 \quad (4.10)$$

where

$F_A$ = ratio of the modulus of rupture at time T to the modulus of rupture at 28 days.

T = time since slab construction in years.

The modulus of rupture can be estimated at any time T using the following expression:

$$F = F_A (F_{28}) \quad (4.11)$$

where

F = modulus of rupture at time T

$F_{28}$ = modulus of rupture at 28 days (3rd pt. loading).

Equations 4.10 and 4.11 can be used to estimate the ultimate static modulus of rupture at any time over the life of the pavement for use in the fatigue damage analysis.

4.5.3 Lateral Truck Distribution. The lateral placement of trucks in the traffic lane is very crucial because of the high longitudinal edge stresses that develop when the wheel load is near the edge. The encroachment of loads

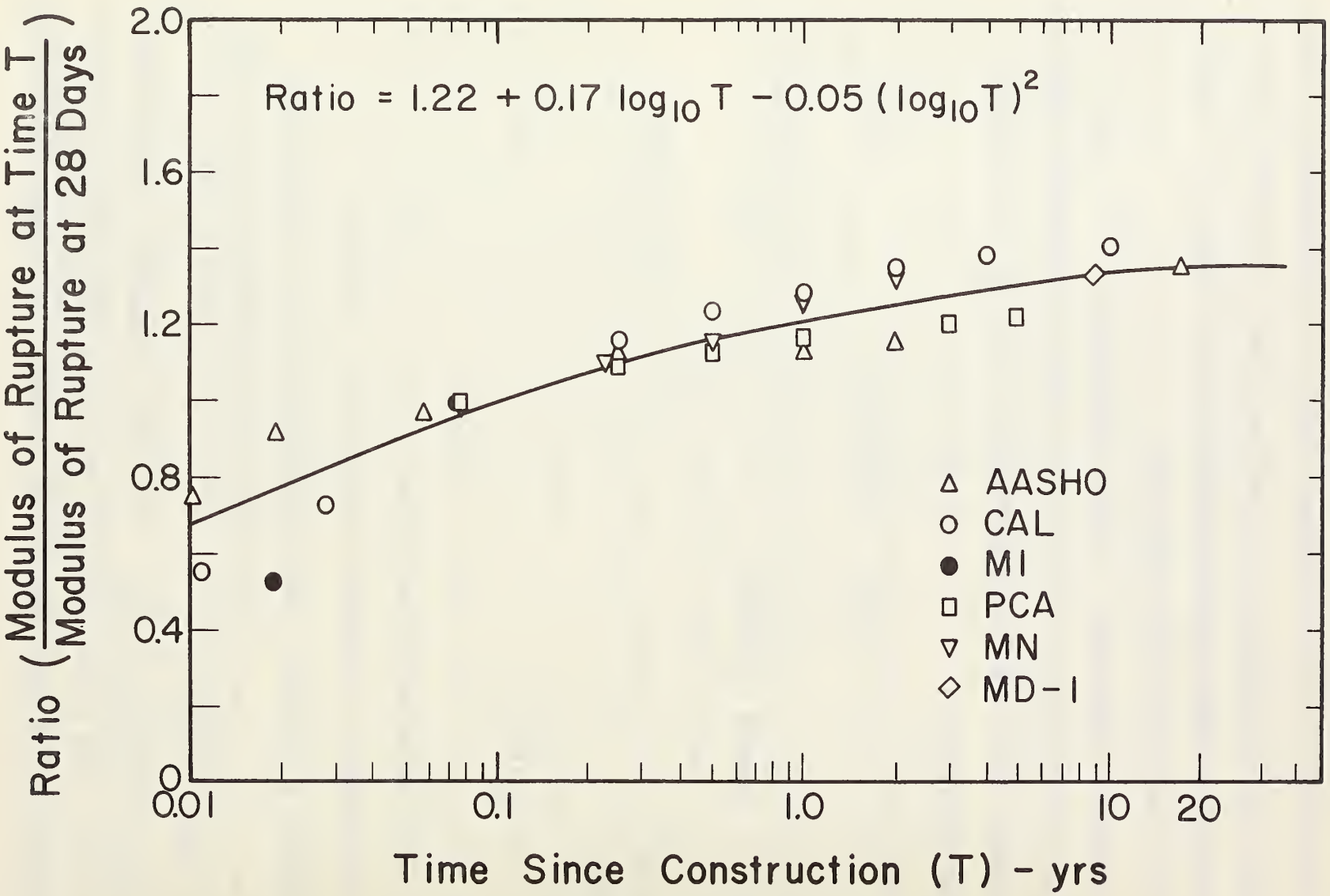


Figure 4.37. Change in PCC Modulus of Rupture with Time.

onto the shoulder is also important in shoulder design. The lateral distribution varies with several factors such as width of traffic lane, location of edge stripe, paved or unpaved shoulders, any edge restraints such as retaining walls, and the existence of curb and gutter.

The lateral distribution should be measured for local conditions, and only general guidelines are given as to the typical range of the mean distance. If heavy trucks travel on the average down the center lane, the mean distance D as shown in Figure 4.20 would be 24 ins. (.7 m ) (for a 12 ft. [3.6 m ] wide lane and an 8 ft. [2.4 m] wide truck). However, available evidence indicates that when there is a paved shoulder and no lateral obstructions, there is a definite tendency of trucks to shift about 3 to 12 ins. (75-305 mm) toward the slab edge, which gives a mean value for D of approximately 12 to 21 ins. (25-533 mm ). Bureau of Public Roads measurements at 15 locations in 1956 for 12 ft. (3.6 m) concrete traffic lanes and paved shoulders on two lane rural highways showed an average of 11 ins. (279mm) (Ref. 53). Studies by Emery in 1975 (Ref. 54) showed a mean of approximately 16 to 18 ins. (406-457 mm) on rural four lane Interstate highways. The lateral distribution obtained from Emery (Ref 54) is approximately normal with a standard deviation of 10 ins. (25 mm) as shown in Figure 4.38.

Data were collected by Taragin (Ref. 53) in 1956 for 12 ft. (3.6 m) concrete traffic lanes with (1) contrasting bituminous shoulders, and (2) grass or gravel shoulders. The average placement from the center of truck to the centerline paint strip was 7.1 ft. (2.1 m ) for bituminous shoulders and 5.9 ft. ( 1.8 m ) for grass or gravel shoulders. These placements correspond to the following mean lateral distances, D:

Bituminous Shoulders = 0.9 ft. or 11 ins. (two lanes)

Grass of Gravel Shoulders = 2.1 ft. or 25 ins. (4 lanes)

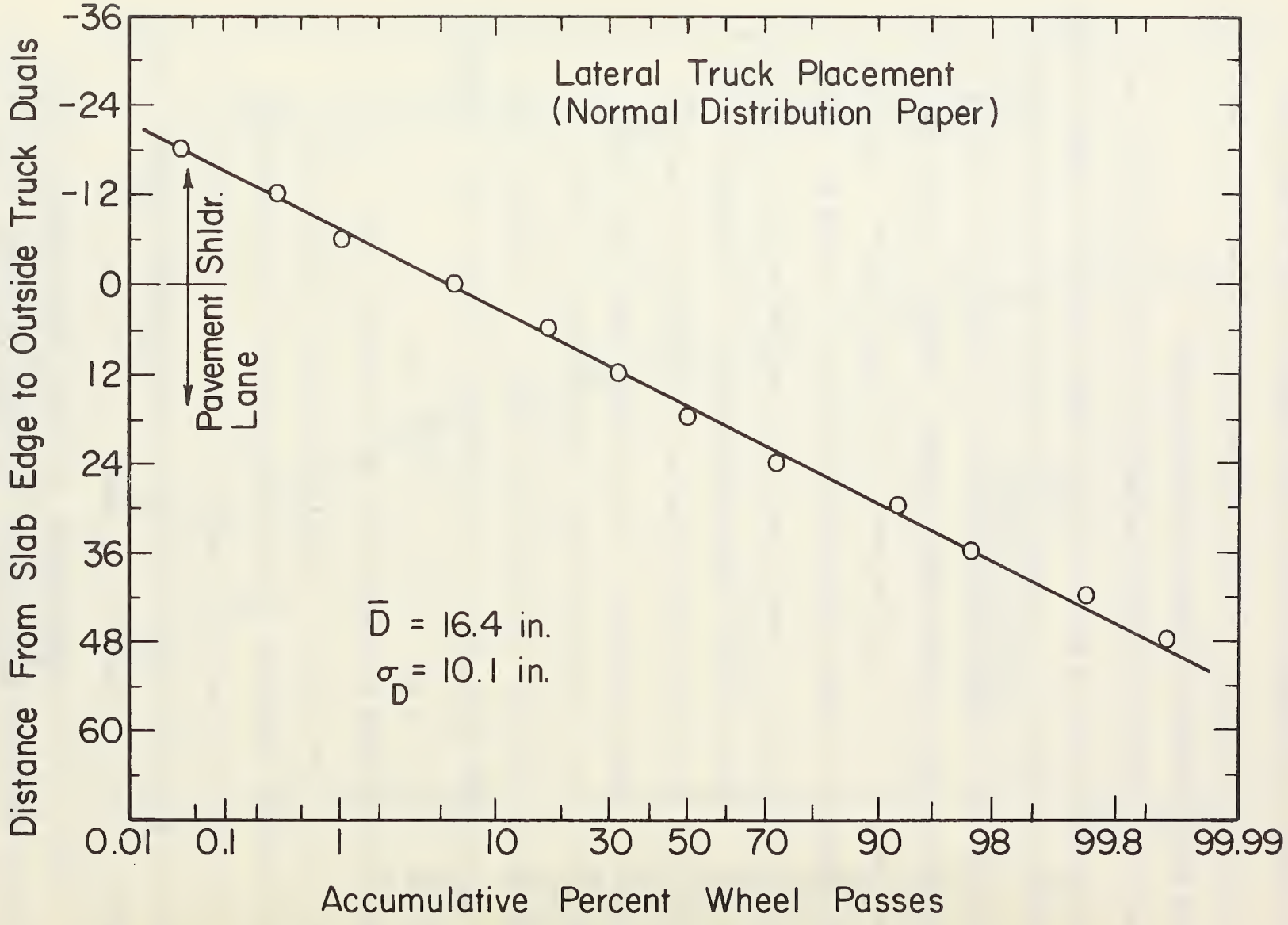


Figure 4.38. Lateral Distribution of Trucks in Outer Lane on 4-lane Freeway.

". . . for traffic lanes of the same width, the placements on sections of bituminous shoulders are considerably farther from the centerline of the pavement than on sections with grass of gravel shoulders. The results of this study confirm the results of earlier studies that bituminous-paved shoulders which appear distinctly different from the traffic lane increase the effective pavement width at least 2 ft., regardless of lane width" (Ref. 53).

Surprisingly, the lateral distribution data from the bituminous shoulders were not used and the general distributions for gravel shoulders was used to program the lateral off-set for the AASHO Road Test. However, nearly all heavily trafficked highways have paved shoulders, and hence the proportion of edge loads and shoulder encroachments are usually much greater than the programed loads at the AASHO Road Test. Results from the study by Emery (Ref. 54) show that approximately 10 percent of loads were within 6 in. (152 mm) of the slab edge on rural Interstate highways with paved shoulders. Several observations made by the author tend to confirm that there are a significant proportion of loads near the edge. Additional data are greatly needed to establish lateral placements of trucks for varying conditions.

4.5.4 Thermal Gradients. The thermal gradient in the PCC slab is defined as follows:

$$G = \frac{T_{top} - T_{bottom}}{H} \tag{4.12}$$

where $G$ = thermal gradient, °F/in.

$T_{top}$ = temperature at the top of the slab, °F

$T_{bottom}$ = temperature at the bottom of the slab, °F

$H$ = PCC slab thickness, inches

A positive gradient indicates the top of the slab is warmer than the bottom which normally always occurs during the daytime. A negative gradient indicates that the bottom is warmer than the top which normally occurs during the

nighttime. A positive gradient results in tensile stress at the bottom of the slab, and a negative gradient results in compressive stress at the bottom of the slab. During times when the gradient is positive (termed daytime) the total combined stress at the bottom of the slab edge midway between the joints under traffic load will be much greater than when the gradient is negative (termed nighttime).

The temperature gradient varies continually throughout a 24-hour daily period and also varies from month to month. A mean monthly positive gradient (called mean daytime gradient) can be used in design. An illustration of the mean daytime and nighttime gradients for northern Illinois is shown in Figure 4.39 for two slab thicknesses. A summary of mean monthly thermal gradients for the four climatic regions is given in Table 4.10. These mean monthly gradients were computed using an accurate temperature model developed by Dempsey (Ref. 55, 56) which has been verified with actual data from several sources. The mean values were determined by calculating the gradient for every three hours throughout the day and night for over a year's time, and then conputing the mean positive and negative gradients. These values are means, and therefore less than the maximum values (of say, 3.0 °F/in.) commonly used. These values may be used for design if measured data are not available. Results show that the thermal gradients can be linearly interpolated for slabs between 8 and 12 ins. (203-304 mm ) in thickness and also for a greater thickness.

4.5.5 PCC Fatigue Computation. A fatigue analysis procedure was developed based upon the results of previous sections to provide a method of estimation of traffic "damage" that could result in cracking of the slabs. The basic fatigue design philosophy for zero-maintenance plain jointed pavements is that

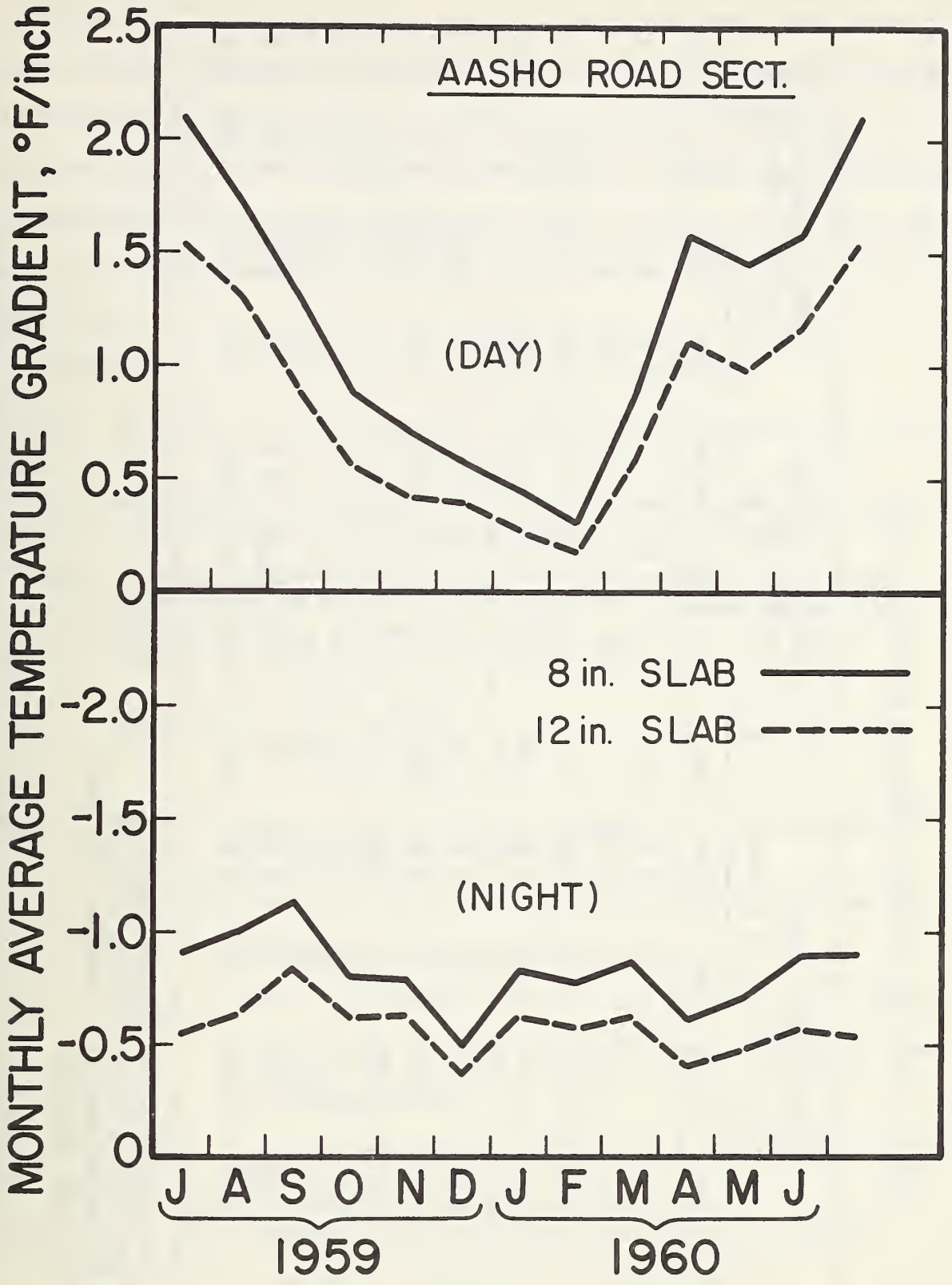


Figure 4.39 Computed Monthly Average Temperature Gradients Through PCC Slabs at AASHO Road Test Site.

Table 4.10. Monthly Average Temperature Gradient (°F/inch)

| | Wet/Non-Freeze Region* | | | | Dry or Wet/Freeze Region** | | | | Dry/Non-Freeze Region*** | | | |
|---|---|---|---|---|---|---|---|---|---|---|---|---|
| | 8 in. | | 12 in.**** | | 8 in. | | 12 in. | | 8 in. | | 12 in. | |
| MONTH | Day | Night | Day | Night | Day | Night | Day | Night | Day | Night | Day | Night |
| JULY | 1.87 | -0.63 | 1.42 | -0.39 | 2.08 | -0.91 | 1.54 | -0.54 | 1.83 | -0.90 | 1.43 | -0.56 |
| AUGUST | 1.47 | -0.87 | 1.15 | -0.56 | 1.73 | -1.00 | 1.32 | -0.63 | 1.62 | -1.10 | 1.24 | -0.76 |
| SEPT | 1.23 | -0.91 | 0.83 | -0.68 | 1.34 | -1.13 | 0.92 | -0.83 | 1.46 | -0.87 | 0.97 | -0.66 |
| OCT | 1.59 | -1.12 | 1.10 | -0.81 | 0.88 | -0.80 | 0.56 | -0.62 | 1.62 | -0.91 | 1.01 | -0.69 |
| NOV | 1.15 | -1.00 | 0.81 | -0.75 | 0.72 | -0.79 | 0.43 | -0.64 | 1.20 | -0.81 | 0.78 | -0.59 |
| DEC | 0.85 | -0.65 | 0.55 | -0.52 | 0.57 | -0.50 | 0.40 | -0.37 | 1.07 | -0.69 | 0.71 | -0.52 |
| JAN | 0.79 | -0.49 | 0.55 | -0.38 | 0.45 | -0.84 | 0.27 | -0.63 | 1.18 | -0.68 | 0.76 | -0.51 |
| FEB | 1.25 | -0.93 | 0.79 | -0.73 | 0.32 | -0.78 | 0.18 | -0.57 | 1.14 | -0.57 | 0.73 | -0.43 |
| MARCH | 1.53 | -0.81 | 1.01 | -0.61 | 0.86 | -0.87 | 0.59 | -0.62 | 1.27 | -0.80 | 0.84 | -0.60 |
| APRIL | 1.75 | -1.02 | 1.29 | -0.70 | 1.59 | -0.62 | 1.11 | -0.41 | 1.49 | -0.99 | 1.12 | -0.70 |
| MAY | 1.70 | -1.01 | 1.33 | -0.65 | 1.46 | -0.72 | 0.99 | -0.49 | 1.47 | -0.89 | 1.13 | -0.61 |
| JUNE | 1.63 | -1.07 | 1.23 | -0.74 | 1.58 | -0.90 | 1.18 | -0.57 | 1.59 | -1.01 | 1.24 | -0.68 |

* Data calculated for Atlanta, Georgia
** Data calculated for Chicago, Illinois
*** Data calculated for Los Angeles, California
**** PCC slab thickness

linear cracking must be prevented. This is possible through direct consideration of traffic loadings, slab curling, joint spacing, and foundation support. The PCC slab is subjected to many applications of heavy traffic loads. At the same time, it is also experiencing stresses due to temperature gradients which have been shown to have significant effect. Curling of the slab also results in "gaps" between the slab and the subbase which increase the stress under load.

The major steps in the fatigue analysis are as follows:

(1) Determine axle applications in each single and tandem axle load group.

(2) Select trial slab/subbase structure, transverse joint spacing, PCC strength, thermal gradients, and other required factors.

(3) Compute fatigue damage occurring at the slab edge for a given month, both day and night using the Miner's accumulative damage hypothesis (Ref. 30) and sum monthly over the entire design period.

$$DAMAGE = \sum_{k=1}^{k=p} \sum_{j=1}^{j=2} \sum_{i=1}^{i=m} \frac{n_{ijk}}{N_{ijk}} \qquad (4.13)$$

where DAMAGE = total accumulated fatigue damage over the design period occurring at the slab edge

$n_{ijk}$ = number of applied axle load applications of $i^{th}$ magnitude over day or night for the $k^{th}$ month

$N_{ijk}$ = number of allowable axle load applications of $i^{th}$ magnitude over day or night for the $k^{th}$ month determined from PCC fatigue curve

i = a counter for magnitude of axle load, both single and tandem axle

j = a counter for day and night (j=1 day and j=2 night)

k = a counter for months over the design period

m = total number of single and tandem axle load groups

p = total number of months in the design period

The fatigue damage is computed at the slab longitudinal edge because results from field observations of many jointed concrete pavements (Sec. 2.2 and 4.3) and analytical fatigue analysis (Sec. 4.3) definitely showed this to be the critical point where cracking initiates.

Applied traffic, $n_{ijk}$. The $n_{ijk}$ is computed using the traffic data for the month under consideration. It is computed using the following expression:

$$n_{ijk} = (ADTm)(T/100)(DD/100)(LD/100)(A)(30)(P/100)(C/100)(DN/100)(TF/100)(CON/100) \quad (4.14)$$

where

ADTm = average daily traffic at the end of the specific month under consideration

T = percent trucks of ADT

DD = percent traffic in direction of design lane

LD = land distribution factor, percent trucks in design lane in one direction

A = mean number of axles per truck

P = percent axles in $i^{th}$ load group

C = percent of total axles in the lane that are within 6 in. (152 mm) of edge

DN = percent of trucks during day or night

TF = factor to either increase of decrease truck volume for the specific month

CON = 1 for single axles, 2 for tandem axles

Allowable Traffic, $N_{ijk}$. The $N_{ijk}$ is computed from PCC fatigue considerations. First the total stress occurring at the edge of the slab for a given axle load is computed considering both traffic load and slab curling for the given month for either day or night conditions as illustrated in Figure 4.40. The stress is computed for edge loading of both single and tandem axles using models developed from the finite element program that realistically considers

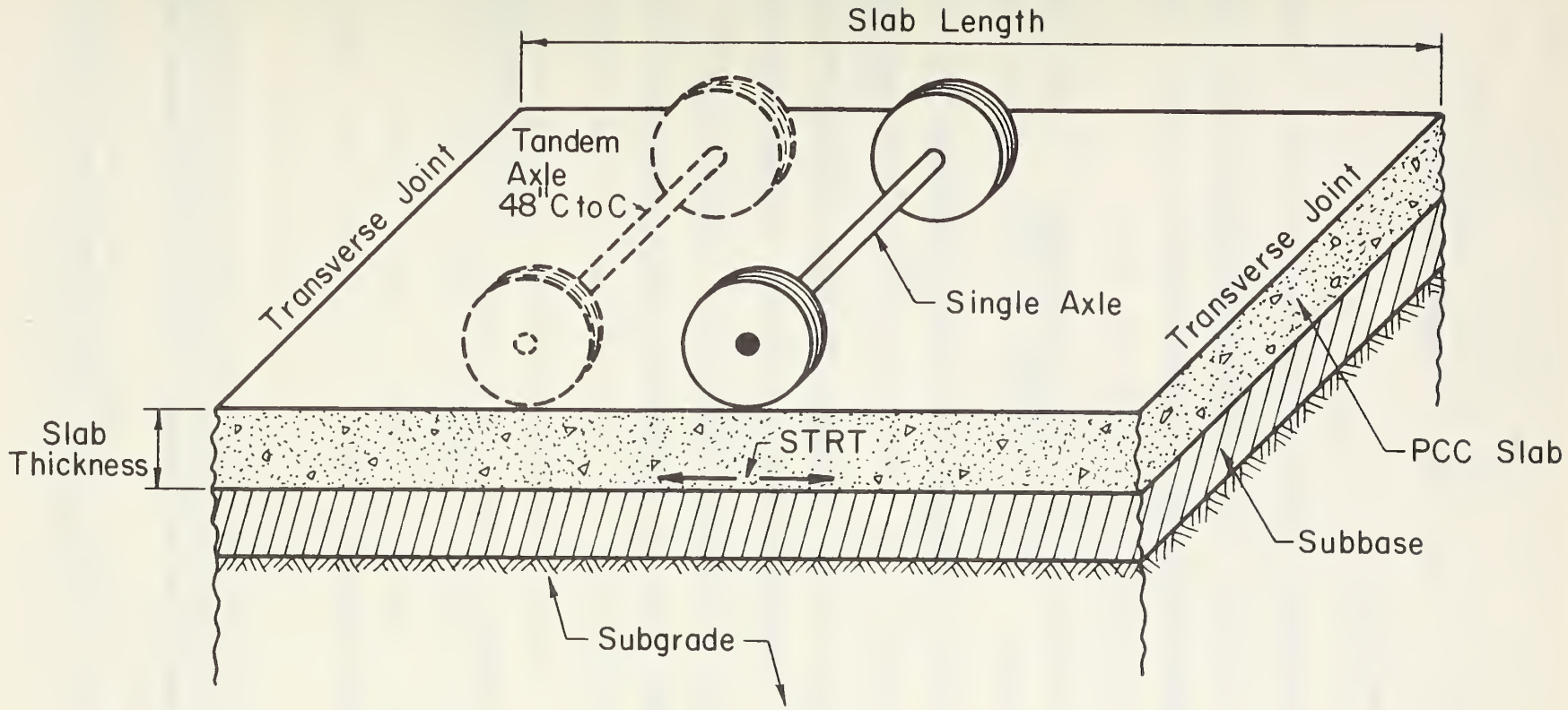


Figure 4.40 Illustration of Location of Loads and Stresses in PCC Slabs.

both load stress and slab curling (as discussed in Section 4.1). The stress models were derived using multiple stepwise regression techniques from a factorial of data obtained from the finite element program over a wide range of the design variables.

| | |
|---|---|
| Slab Thickness (H): | 8, 10, 14 ins. |
| Thermal Gradient (G): | -1.5, 0.0, +3.0°F/in. |
| Foundation Modulus (k): | 50, 200, 500 pci |
| Slab Length (L): | 15, 20, 25, 30 ft. |
| Erodability (ES): | 0, 12, 36, 60 ins. along slab edge |

The finite element computed stresses for all possible combinations of these factors are given in Tables 43-45. Individual equations were derived for load stress (STRL) and for thermal gradient curl stress (STRC) without traffic load. Results showed that the load and curl stresses could not be directly added to obtain the combined overall resulting stress (STRT). Therefore an adjustment factor, R, was derived to adjust the curl stress so that is could be added directly to obtain the correct total combined stress (STRT) which is used in the fatigue analysis. The total stress at the bottom of the slab edge with the load located at the edge is computed as follows:

$$STRT = STRL + (R)STRC \tag{4.15}$$

where

STRT = total resultant stress in the longitudinal direction at the bottom of the PCC slab edge when the wheel load is located at the slab edge (load is single axle or tandem axle), see Figure 4.40.

STRL = stress at bottom of PCC slab edge when load is located at slab edge (no thermal curling stress)

STRC = stress at bottom of PCC slab edge caused by curling of slab due to thermal gradient (no traffic load)

R = adjustment factor for STRC so that it can be combined with STRL to give correct STRT

The R ranges from about 0.8 to 1.5 depending on slab/foundation conditions.

The regression equations determined for these stresses are as follows:

Load Stress for single axle load:

$$STRL = [LOAD/(18.0H^2)][17.35783 + 0.78015ES - 0.05388H^3/k + 7.41722 \log_{10}(H^3/k)] \quad (4.16)$$

Load stress for tandem axle load:

$$STRL = [LOAD/(36.0H^2)][14.09599 + 0.10522ES - 0.09886H^3/k + 6.2339 \log_{10}(H^3/k) + 1.95266 (\log_{10}(H^3/k))^2 - 0.71963 \log_{10}(ES + 1.0)] \quad (4.17)$$

Curl stress:

$$STRC = [(G)(ET)/(5 \times 10^{-6})][0.006712k + 79.07391 \log_{10}k + 11.72690L - 0.00720kL - 3.22139L \log_{10}k - 0.06883LES - 0.59539ES \log_{10}k - 204.39477H/k - 38.08854L/H - 8.36842H \log_{10}k + 0.07151ESH + 0.95691LES \log_{10}k + 0.20845LH \log_{10}k + 0.00058LHk - 0.00201LES \log_{10}k] \quad (4.18)$$

R adjustment factor:

$$R = 0.48039 + 0.01401H - 0.00427ES - 0.27278G - 0.00403L + 0.19508 \log_{log}k + 0.45187G \log_{10}H - 0.00532G^2 + 0.01246GL - 0.00622GL \log_{10}k + 8.7872 \log_{10}(H^3/k)/H^2 + 0.00104GES - 0.11846G \log_{10}(H^3/k) + 0.07001 \log_{10}(ES + 1.0) - 0.01331G \quad (4.19)$$

where

LOAD = total load on single or tandem axle, pounds

H = PCC slab thickness, inches

G = thermal gradient through slab, °F/in.

k = modulus of foundation support (top of subbase, pci)

L = slab length, ft.

ES = erodability of support along slab edge, inches

ET = thermal coefficient of contraction of PCC/°F

Standard estimate of error based on 426 data points:

Single axle of STRL = 7.65 psi

Tandem axle of STRL = 4.59 psi

Curling stress STRC = 15.36 psi

Total combined stress STRT = 18.97 psi

Further verification of these equations was made by comparing the edge stress computed by the finite element program with the combined stress (STRT) computed using Equations 4.15 - 4.19 for 48 randomly selected slabs with varying H, G, k, L, ES and axle loads. Results of this comparison are shown in Figure 4.41. The standard error is 29.75 psi which, as expected, is higher than the 18.97 psi obtained using the data for which it was derived. However, the standard error is believed acceptable when compared to the other uncertainties involved.

A computer program, called JCP-1, was developed to compute the accumulated fatigue damage according to Equation 4.15 over the design life of the pavement. This data can be used to evaluate and design a plain jointed concrete pavement considering fatigue damage.

## 4.6 LIMITING FATIGUE CONSUMPTION

The fatigue analysis that has been developed is quite comprehensive in that it considers directly the effects of traffic loadings, thermal gradient through slab, joint spacing, loss of foundations support (i.e. pumping), and the increase in PCC strength over time. However, there are several

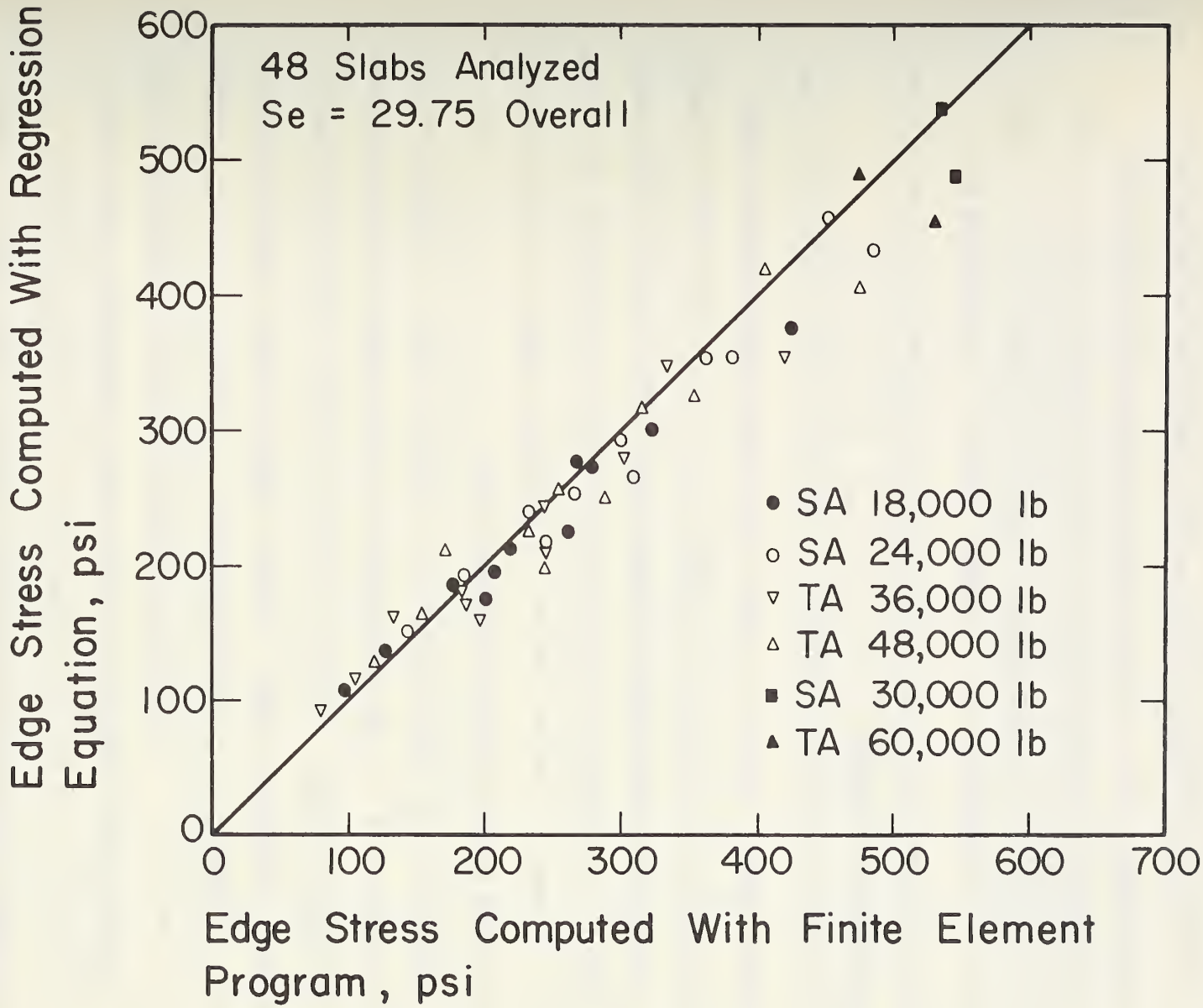


Figure 4.41. Comparison of Edge Stress Computed with Eqs. 4.15 and with the Finite Element Program for 48 Ramdom Slab/Load Conditions.

factors that are not considered due to insufficient information. One of the most important factors may be the use of PCC fatigue curves obtained from small beams to estimate the fatigue life prediction of large fully supported pavement slabs. Traffic loading conditions also differ considerably between laboratory and field. Other inadequacies could be cited, however, the point to be made is that the final accumulated fatigue "damage" based on Eq. 4.15 computed for a pavement slab must be correlated with measured slab cracking before a limiting fatigue consumption can be selected with confidence for design.

According to the Miner hypothesis, a material should fracture when the accumulated "damage" equals 1.0. Even if the Miner hypothesis were exactly correct, variability of material strengths, loads, and other properties would cause a variation in accumulated "damage" ranging from much less than 1.0 to much greater. For example, the PCC concrete laboratory data shown in Figure 4.35 shows a computed "damage" ranging from roughly $5 \times 10^{-4}$ to more than 1000 based on the mean fatigue curve.

Assuming that the Miner hypothesis is exactly correct, the use of a computed "damage" of 1.0 (or 100 percent) in design would result in a 50 percent chance of fatigue failure if no safety factors were applied to any of the input parameters. Hence a design "damage" of much less than 1.0 is essential to provide for a very low probability of fatigue cracking (or high design reliability). This limiting value may be different depending on the type of pavement under design (i.e. low volume or expressway), and in the present application it is for high volume heavily trafficked expressways.

The appropriate accumulated fatigue limiting "damage" for use in zero-maintenance design was determined as follows:

(1) Field data were collected from three sources:

(a) AASHO Road Test Sections on Loops 4, 5, and 6 which were under traffic for 2 years (1958-1960). Sections having excessive pumping were excluded (i.e. pumping index greater than 40 cubic ins./in. of slab). A total of 28 sections were included ranging in slab thickness of 8-12.5 ins.

(b) AASHO Road Test Sections that were left in-service after the end of the test and became incorporated as part of I-80. These sections were under regular mixed traffic from 1962 to 1974. Extensive measurements of distress were made periodically by the Illinois Department of Transportation. A total of 25 sections were included ranging in slab thickness from 8 to 12.5 ins.

(c) Twelve in-service projects located in the U.S. and Canada: New Jersey, Arizona, California (2), Michigan, Utah, Georgia, Colorado (2), Washington, Texas, and Ontario, Canada. These projects were high traffic volume freeways ranging in age from 6 to 34 years.

(2) The total accumulated fatigue "damage" from the opening of each project to traffic until the date of survey was computed using the computer program JCP-1 (or Eq. 4.15). The heaviest traveled truck lane was always used in the computations. A summary of this data along with other information for each project is given in Table 4.11.

(3) A plot of cracking index (ft./1000 $ft.^2$) versus total accumulated fatigue "damage" is shown in Figure 4.42. Results show that as computed fatigue "damage" increases to more than approximately $1 \times 10^{-4}$ the amount of observed transverse cracking occurring increases. Those projects having accumulated fatigue "damage" greater than $10^{-1}$ generally have large amounts of cracking. The abrupt increase of cracking after a long period of no cracking is typical of concrete pavement performance.

The relationship between slab cracking and computed fatigue "damage" indicates the following:

(a) A correlation exists between transverse slab cracking and computed fatigue "damage" in the slab. Fatigue damage is computed at the longitudinal

Table 4.11. Summary of Pavement and Computed Fatigue Damage Data.

| Project No. | Section, Location | Dates | Slab (in.) | PCC Mod.* Rupture-psi | k-value** (pci) | Jt. Spacing (ft.) | Transverse Cracking Index ft./1000 ft.$^2$ | Accumulated Fat. Damage*** |
|---|---|---|---|---|---|---|---|---|
| Loop 4 | 672, 688, 684, 652, 658 | 1958-1960 | 8 | 690 | 115 | 15 | 0 | $1.31 \times 10^{-4}$ |
| Loop 4 | 676, 702 690 | 1958-1960 | 9.5 | 690 | 115 | 15 | 0 | $1.75 \times 10^{-6}$ |
| Loop 5 | 548, 534 | 1958-1960 | 8 | 690 | 115 | 15 | 7 | $1.64 \times 10^{-2}$ |
| Loop 5 | 512, 542, 552, 528 | 1958-1960 | 9.5 | 690 | 115 | 15 | 1 | $7.95 \times 10^{-5}$ |
| Loop 5 | 530, 498 510 | 1958-1960 | 11 | 690 | 115 | 15 | 0 | $1.25 \times 10^{-6}$ |
| Loop 6 | 368, 390 376 | 1958-1960 | 9.5 | 690 | 115 | 15 | 4 | $2.37 \times 10^{-3}$ |
| Loop 6 | 378, 364, 398, 366, 388 | 1958-1960 | 11 | 690 | 115 | 15 | 0 | $1.87 \times 10^{-5}$ |
| Loop 6 | 396, 350, 380 | 1958-1960 | 12.5 | 690 | 115 | 15 | 0 | $4.78 \times 10^{-7}$ |
| JCP-1, 2, 3 | 672, 658, 652 | 1958-1974 | 8 | 690 | 115 | 15 | 20 | 29.86 |

* 28 day, 3rd Point Loading
** On top of Subbase-Mean of 9 lowest months.
*** Computed from Eq. 4.13.

Table 4.11. Summary of Pavement and Computed Fatigue Damage Data (Continued).

| Project No. | Section, Location | Dates | Slab (in.) | PCC Mod.* Rupture-psi | k-value** (pci) | Jt. Spacing (ft.) | Transverse Cracking Index ft./1000 ft.$^2$ | Accumulated Fat. Damage*** |
|---|---|---|---|---|---|---|---|---|
| JCP-4, 5, 6 | 676, 702 690 | 1958-1974 | 9.5 | 690 | 115 | 15 | 0 | $6.25 \times 10^{-3}$ |
| JCP-7, 8, 9, 10 | 528, 542, 512, 552 | 1958-1974 | 9.5 | 690 | 115 | 15 | 2 | $9.53 \times 10^{-5}$ |
| JCP-11, 12, 13, 14 | 376, 390 368, 352 | 1958-1974 | 9.5 | 690 | 115 | 15 | 6 | $8.62 \times 10^{-3}$ |
| JCP-15, 16, 17 | 530, 510, 498 | 1958-1974 | 11 | 690 | 115 | 15 | 0 | $1.71 \times 10^{-5}$ |
| JCP-18, 19, 20, 21, 22 | 364, 378, 498, 388, 398, 366 | 1958-1974 | 11 | 690 | 115 | 15 | 0 | $3.45 \times 10^{-5}$ |
| JCP-23, 24, 25 | 396, 350, 380 | 1958-1974 | 12.5 | 690 | 115 | 15 | 0 | $7.93 \times 10^{-7}$ |
| JCP-26 | WA | 1962-1974 | 9 | 700 | 192 | 15 | 0 | $1.52 \times 10^{-2}$ |
| JCP-27 | CA | 1955-1974 | 8 | 675 | 450 | 15 | 3 | 0.22 |
| JCP-28 | CA | 1954-1974 | 8 | 675 | 500 | 15 | 3 | 0.37 |

* 28 day, 3rd Point Loading
** On top of Subbase-Mean of 9 lowest months.
*** Computed from Eq. 4.13.

Table 4.11. Summary of Pavement and Computed Fatigue Damage Data (Continued).

| Project No. | Section, Location | Dates | Slab (in.) | PCC Mod.* Rupture-psi | k-value** (pci) | Jt. Spacing (ft.) | Transverse Cracking Index ft./1000 ft.$^2$ | Accumulated Fat. Damage*** |
|---|---|---|---|---|---|---|---|---|
| JCP-29 | TX | 1960-1974 | 10 | | | 15 | 0 | $3.69 \times 10^{-4}$ |
| JCP-30 | UT | 1965-1974 | 9 | 675 | 267 | 12-18 | 0 | $2.13 \times 10^{-2}$ |
| JCP-31 | AZ | 1960-1974 | 9 | 725 | 200 | 15 | 0 | $1.08 \times 10^{-2}$ |
| JCP-32 | NJ | 1949-1974 | 10 | 750 | 197 | 15 | 0 | $1.54 \times 10^{-3}$ |
| JCP-33 | GA | 1950-1974 | 8 | 707 | 206 | 30 | 7 | 1.38 |
| JCP-34 | CO | 1964-1975 | 8 | 707 | 353 | 12-19 | 17 | 3.98 |
| JCP-35 | CO | 1964-1975 | 8 | 707 | 367 | 15 | 0 | 0.36 |
| JCP-36 | MI | 1942-1976 | 10 | 600 | 115 | 25 | 30 | 71.42 |
| JCP-37 | Ontario | 1970-1976 | 9 | 650 | 400 | 12-19 | 5 | 0.85 |

* 28 day, 3rd Point Loading
** On top of Subbase-Mean of 9 lowest months.
*** Computed from Eq. 4.13

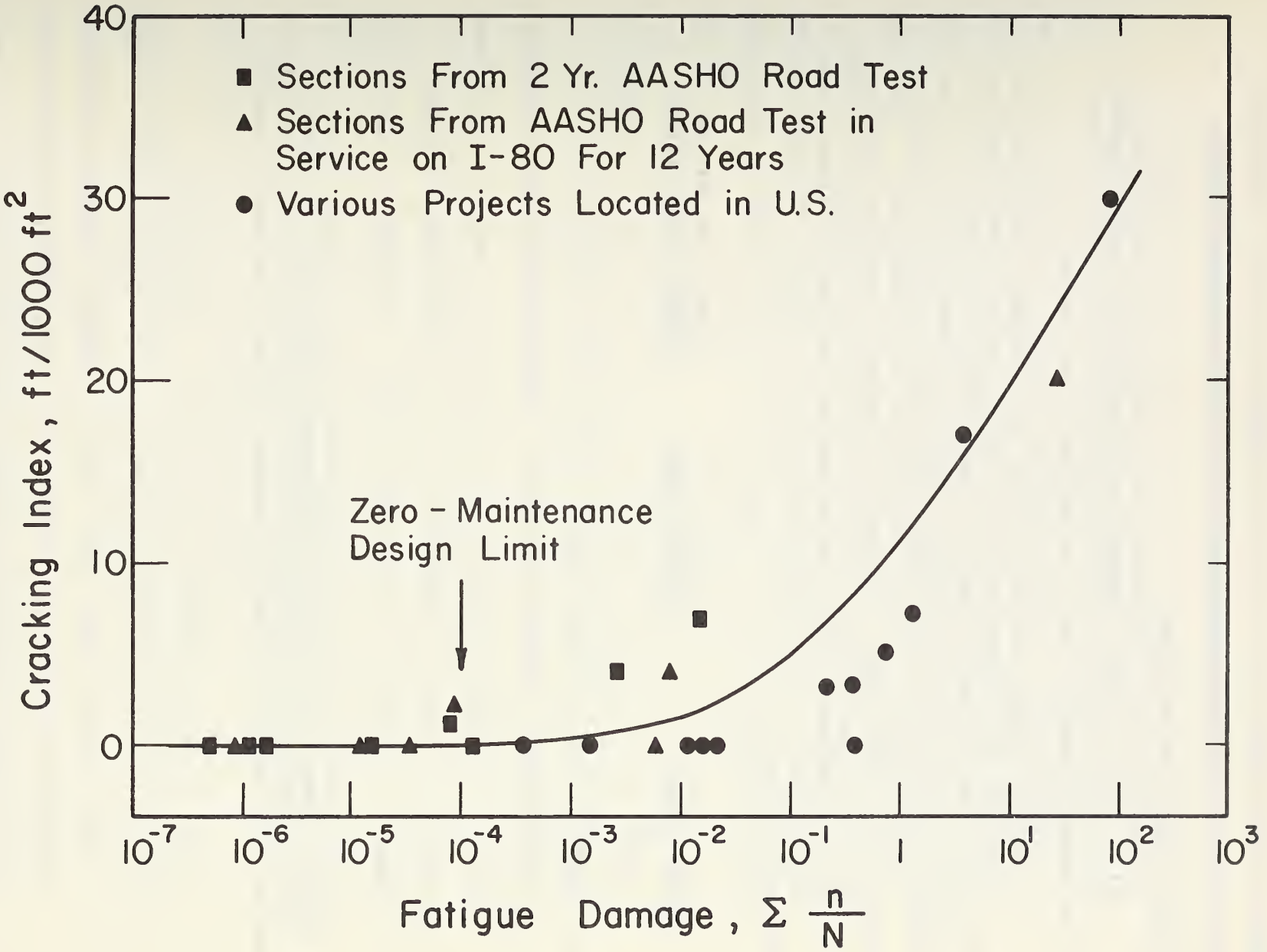


Figure 4.42. Effect of Fatigue "Damage" on Cracking of PCC Plain Jointed Concrete Pavements.

edge and hence should relate directly to transverse cracking. This high correlation provides reasonable verification of certain aspects of the fatigue computation procedure.

(b) A limiting fatigue "damage" can be selected for design depending on the amount of cracking that is acceptable in the pavement.

The fatigue "damage" design limit for zero-maintenance design must be chosen such that transverse cracking is very unlikely to occur. All projects having less than $10^{-4}$ damage either did not exhibit any cracking or only a very minor amount. The amounts of probable transverse cracking for various accumulated "damage" determined from the curve fit through the data is as follows:

| Fatigue Damage | (ft./1000 ft.$^2$) Cracking Index | (Example for L=15 ft.) Percent Slabs Cracked |
|---|---|---|
| $10^{-5}$ | 0 | 0 |
| $10^{-4}$ | 0 | 0 |
| $10^{-2}$ | 1.5 | 2 |
| 1 | 11 | 17 |
| 10 | 20 | 30 |
| 100 | 30 | 45 |

A limiting "damage" value for zero-maintenance design of $10^{-4}$ is chosen to provide a high reliability that the pavement slabs will not exhibit cracking.

# CHAPTER 5

# DESIGN OF JOINTS, SHOULDERS AND SUBSURFACE DRAINAGE

All components of the pavement must be designed as part of a system. The structural design of the slab and subbase should be coordinated with the joint, shoulder, and subsurface drainage design. These components must compliment the structural design so that the pavement can withstand both heavy traffic and severe environmental factors without the occurrence of distress. Many conventional pavement have adequate structural design, but due to inadequate consideration of joints, shoulders, and/or subsurface drainage premature distress and reduced maintenance-free life has occurred. Development of design criteria are provided for joints, shoulders, and subsurface drainage.

## 5.1 JOINTS

Joints are placed in plain jointed concrete pavements to control cracking and also for construction purposes. The major distresses related to joints as identified in Chapter 2 are (1) faulting (2) sealant damage and infiltration of incompressibles and moisture, and (3) increase in various distresses when joint spacing is increased. These distresses must be prevented to provide a maintenance-free pavement. Recommendations for minimizing their occurrence are presented. Excellent joint design and construction recommendations for other factors are provided in References 69 and 77.

5.1.1 Joint Faulting. The faulting of transverse joints in plain jointed concrete pavements is a very serious distress which leads to maintenance when roughness becomes excessive. Most faulting problems have occurred on non-doweled pavements but some has also occurred on doweled pavements. Two major field studies have been conducted to determine the

cause of faulting in non-doweled transverse contraction joints. Conclusions from the California study are as follows:

> "1. Faulting of PCC pavement joints is caused by an accumulation of build up of loose material under the slabs near the joints. This accumulation may occur only under the approach slab, or it may be a differential build up under both slabs with the thicker layer under the approach slab.
>
> 2. The build up is caused by violent water action on available loose or erodible materials that are beneath or adjacent to the slabs The water is moved backward (and probably transversely) by the fast depression of the curled or warped slabs under heavy wheel loads and by the suction caused by the release of load on the approach slab, which erodes and transports any loose materials.
>
> 3. The major sources of the buildup are the untreated shoulder material and the surface layer of the cement-treated base. Minor amounts may come from abrasion of the concrete joint interface and from material on the pavement surface moving downward through the joints." (Ref. 75).

The Georgia study concluded similarly:

> "The faulting occurring on the Georgia Interstate System is caused by the erosional effects produced by a combination of free water under the slab and the repeated passage of heavy axle loads across the joints. There is a loss of fine material from the top of the base on both the leave and approach side of the joint but this loss is more serious at the leave side. Some material is being redeposited under the approach side." (Ref. 74).

The degree of load transfer across a transverse joint and the ability of the joint to maintain sufficient load transfer is related to joint faulting. If a joint could maintain a high load transfer, joint deflection would be minimized and there would be no differential joint deflection between slabs, which would minimize backward pumping of fines as a load passed over the joint. Joint load transfer efficiency or effectiveness has been defined two ways. One definition is Eq. 4.2 and the other definition that is more generally used is as follows:

$$\text{Joint Effectiveness } (\%) = \frac{2\,d_1}{d_1 + d_2}\,100 \qquad (5.1)$$

where $d_1$ = deflection of unloaded slab

$d_2$ = deflection of loaded slab

Joint effectiveness or efficieicy depends on several factors including: joint opening, number of load applications, foundation support, wheel load applications, foundation support, wheel load, aggregate particle angularity, and the presence of mechanical load transfer devices (Refs. 71, 72, 77). Results obtained from laboratory, field and analytical studies are presented to show the effects of these factors.

1. Joint opening: The effectiveness of load transfer is significantly lost as joint opening increases as shown in Figure 5.1. The rate of loss is much greater when the joint contains no mechanical load transfer (i.e. dowels) as will be subsequently shown. Joint opening depends on several factors such as joint spacing, frictional resistance of subbase, PCC properties including thermal contraction and drying shrinkage, and moisture content and temperature of the slab. Variation in joint opening from joint to joint in a given pavement is high with a coefficient of variation of 40 percent computed on one project (Ref. 73). Despite the many complexities involved, mean joint opening over a yearly or daily time interval can be computed approximately using the following expression:

$$\Delta L = CL[\alpha\Delta T + \varepsilon] \qquad (5.2)$$

where

$\Delta L$ = joint opening caused by temperature change $\Delta T$ and drying shrinkage of PCC

$\alpha$ = thermal coefficient of contraction of PCC ($/^{\circ}F$)

(generally 5-6 x $10^{-6}/^{\circ}F$)(9-10.8 x $10^{-6}/^{\circ}C$)

$\varepsilon$ = drying shrinkage coefficient of PCC (approximately 0.50 to 2.50 x $10^{-4}$ in/in.) (cm/cm)

L = joint spacing (ins.)

$\Delta T$ = temperature range (for design use temperature at placement minus lowest mean minimum monthly temperature)

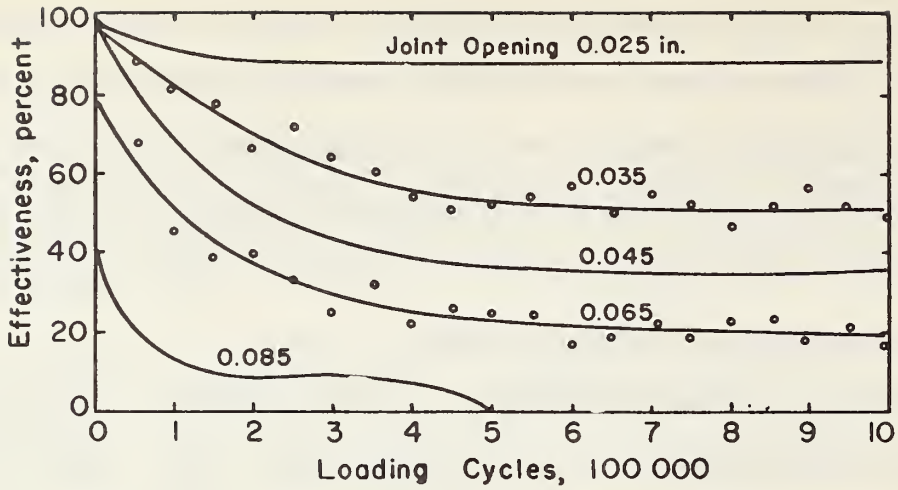


(a) Influence of joint opening on effectiveness (9 in. slab, 6 in. gravel subbase, k = 145 psi)

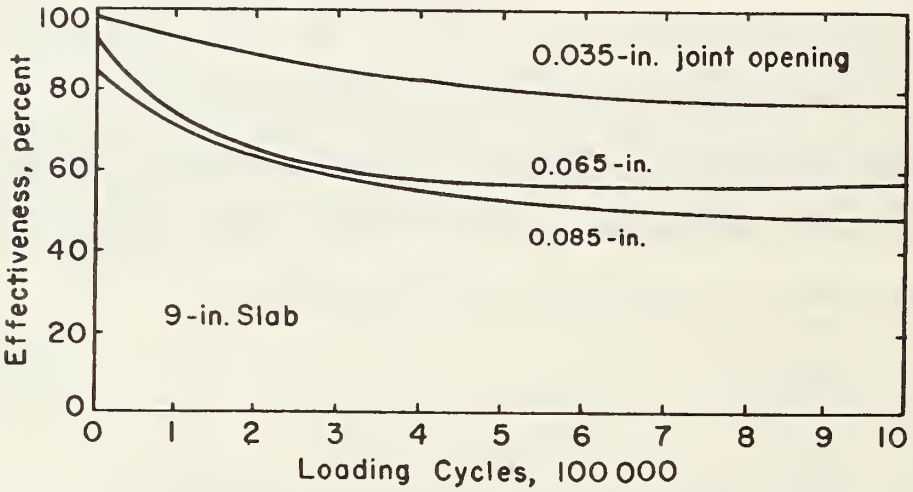


(b) Influence of joint opening on effectiveness (9 in. slab., cement stabilized subbase, k = 542 pci)

Figure 5.1. Joint load effectiveness for gravel and cement treated subbase for various joint openings (Ref. 71).

C = adjustment factor due to subbase/slab frictional restraint (0.65 for stabilized subbase, 0.80 for granular subbase.)

The recommended adjustment factor, C, and the drying shrinkage coefficient suggested were computed from limited field data from Utah (Ref. 73), Florida (Ref. 72), Michigan (Ref. 70), and California (Ref. 101).

Using typical values for slab and temperature drop, maximum joint openings are computed in Table 5.1. Values of joint openings during ten years of performance in seven states with joint spacing of 10 to 25 ft. (3-7.6m) range within the values shown in Table 5.1 (Ref. 70). However progressive opening up of joints due to infiltration of incompressibles would increase the joint width beyond these values.

Joint faulting is related to joint opening and joint effectiveness. Data from the Minnesota road test, for example, show that joint faulting of plain concrete pavements without dowels increases as joint spacing (and opening) increases from 15 to 30 ft. (4.6-9.1m) (Ref. 70). Joint opening in a given climate can be limited most easily through control of joint spacing and use of a stabilized subbase. Thus, if a maximum joint opening of 0.04 ins. (1.0mm) were considered as the limiting criteria, the yearly range in average daily temperature is 60°F (33°C) for a given region, and a stabilized subbase is used, the maximum allowable joint spacing computed from Eq. 5.2 is 12 ft. (3.7m). Of course not all joints open the same amount and this contributes to considerable variability in joint faulting.

2. Load applications: Joint effectiveness decreases as load applications are applied to a given joint in both laboratory and field studies (Refs. 71, 72). Even under heavy loadings most pavements do not fault until 5-10 years of service. The rate of decrease depends on many factors including joint opening, slab thickness, foundation support, load magnitude, mechanical load transfer,

Table 5.1. Computed maximum joint openings using Eq. 5.2 for a temperature drop of 60°F and drying shrinkage.

| | Joint Opening - ins. | | | |
|---|---|---|---|---|
| | Stabilized Subbase | | Granular Subbase | |
| Joint Spacing-ft. | Temp. | Temp. & Shrinkage | Temp. | Temp. & Shrinkage |
| 10 | .026 | .034 | .032 | .041 |
| 15 | .039 | .050 | .047 | .062 |
| 20 | .051 | .067 | .063 | .082 |
| 25 | .064 | .084 | .079 | .103 |
| 30 | .077 | .101 | .095 | .124 |

$\alpha = 5.5 \times 10^{-6}/°F$

$\Delta T = 60°F$

$\varepsilon = 1.0 \times 10^{-4}$

and type of aggregate (See Figures 5.1 and 5.2).

3. Slab Thickness and Foundation Support: Increased slab thickness and foundation support decreases the loss of joint effectiveness with repeated load applications as shown in Figures 5.1 and 5.2. This may be due to the reduced unit vertical shear across the joint face as the slab thickness and k-value are increased. The corner deflection under a load changes with slab thickness and foundation support as shown in Figure 5.3. As the k-value decreases below 200 pci (54 $MN/m^3$) the deflection increases rapidly. The less the deflection the less unit shear that must be transferred across the joint for a given load, and thus over a number of repeated load applications the joint load effectiveness remains higher.

4. Load Magnitude: As load magnitude increases the joint effectiveness decreases as shown in Figure 5.2 because deflection and unit shear transferred across the joint for every load application is increased.

5. Mechanical Load Transfer: Dowels improve the joint effectiveness significantly for relatively wide open joints as shown by some 12 year field results from Florida in Figure 5.4. Data from a recent Georgia study also indicate higher load effectiveness for doweled joints, particularly during cold weather (Ref. 78). The most significant effect of dowels is in reducing the faulting at transverse joints. Considerable evidence can be cited to show that the use of dowels causes a significant reduction in faulting over a similar joint without dowels. The most recent and comprehensive study was conducted by the Florida DOT where faulting was measured at seven test sites over a 12 year period. Both doweled and non-doweled plain jointed concrete pavements were located at most of the sites so that a direct comparison could be made. Histograms showing measured faulting for some of the test sites are given in Figures 5.5-5.6. Conclusions reached by Stelzenmuller, Smith, and Larsen are:

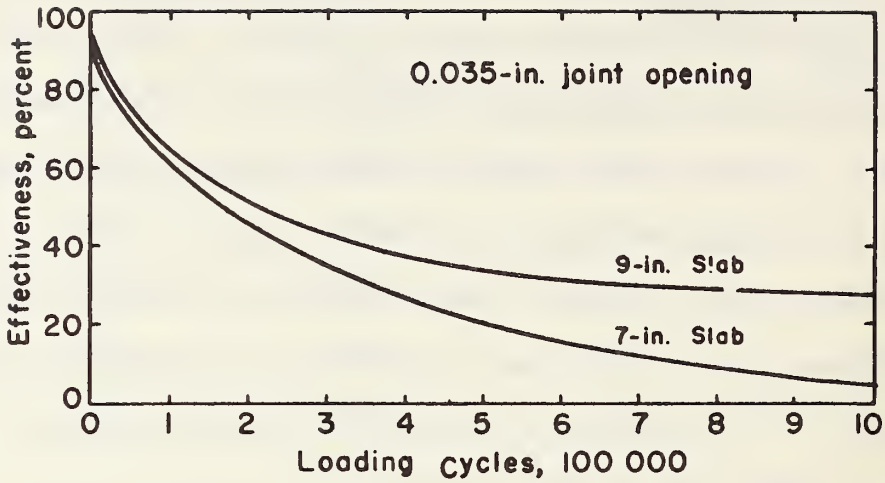


(a) Influence of slab thickness on effectiveness

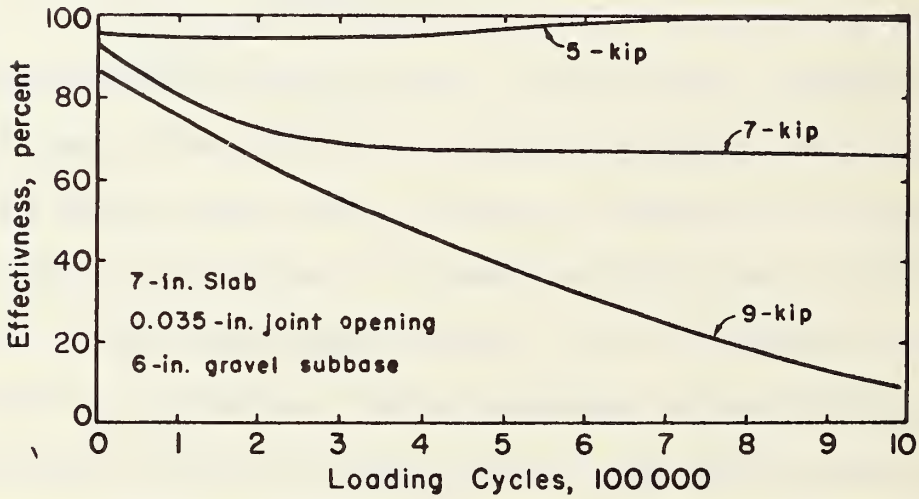


(b) Influence of wheel load on effectiveness

Figure 5.2. Joint load effectiveness (Ref. 71).

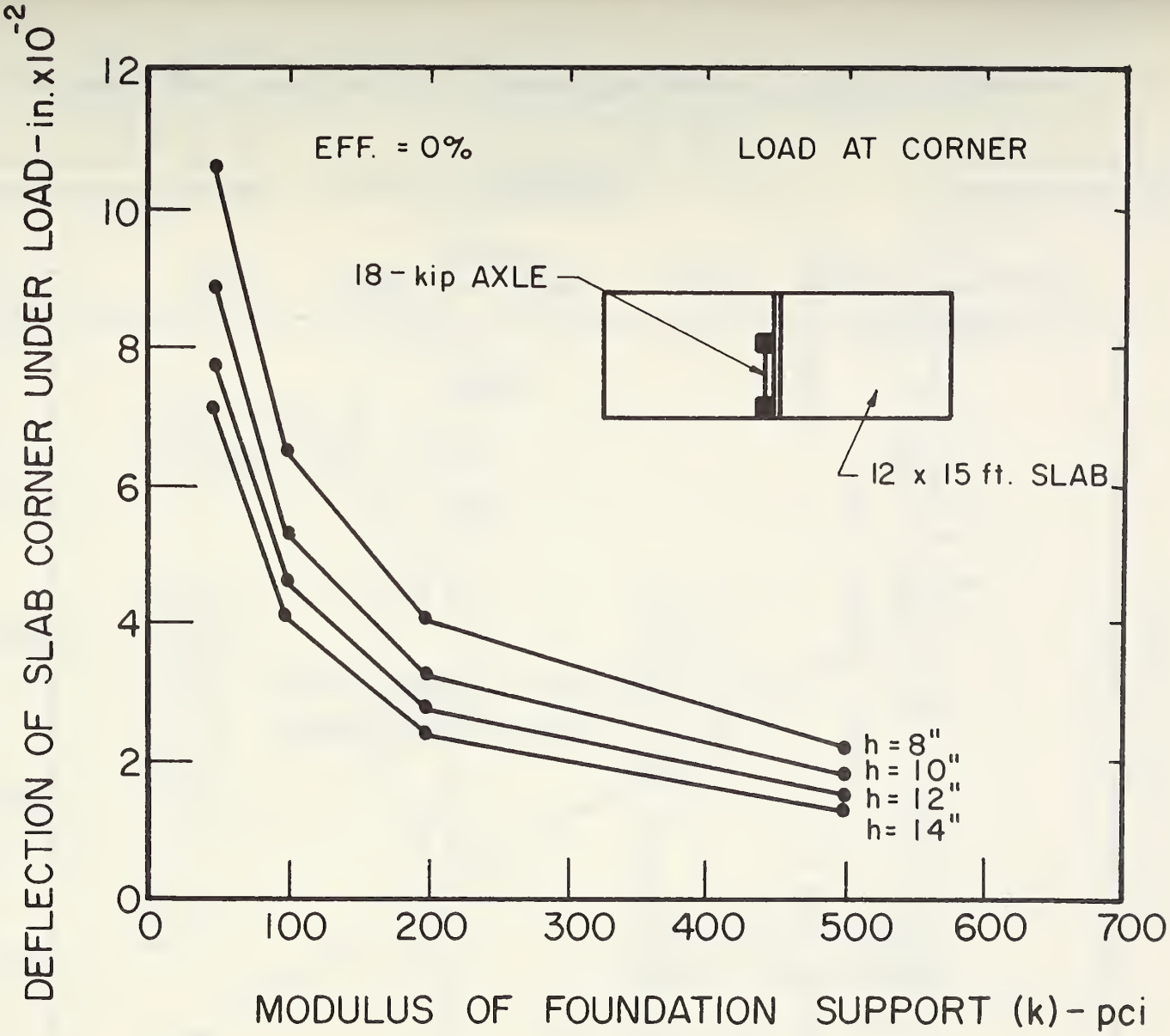


Figure 5.3. Influence of Slab Thickness and Foundation Support on Corner Deflection (computed with F.E. program).

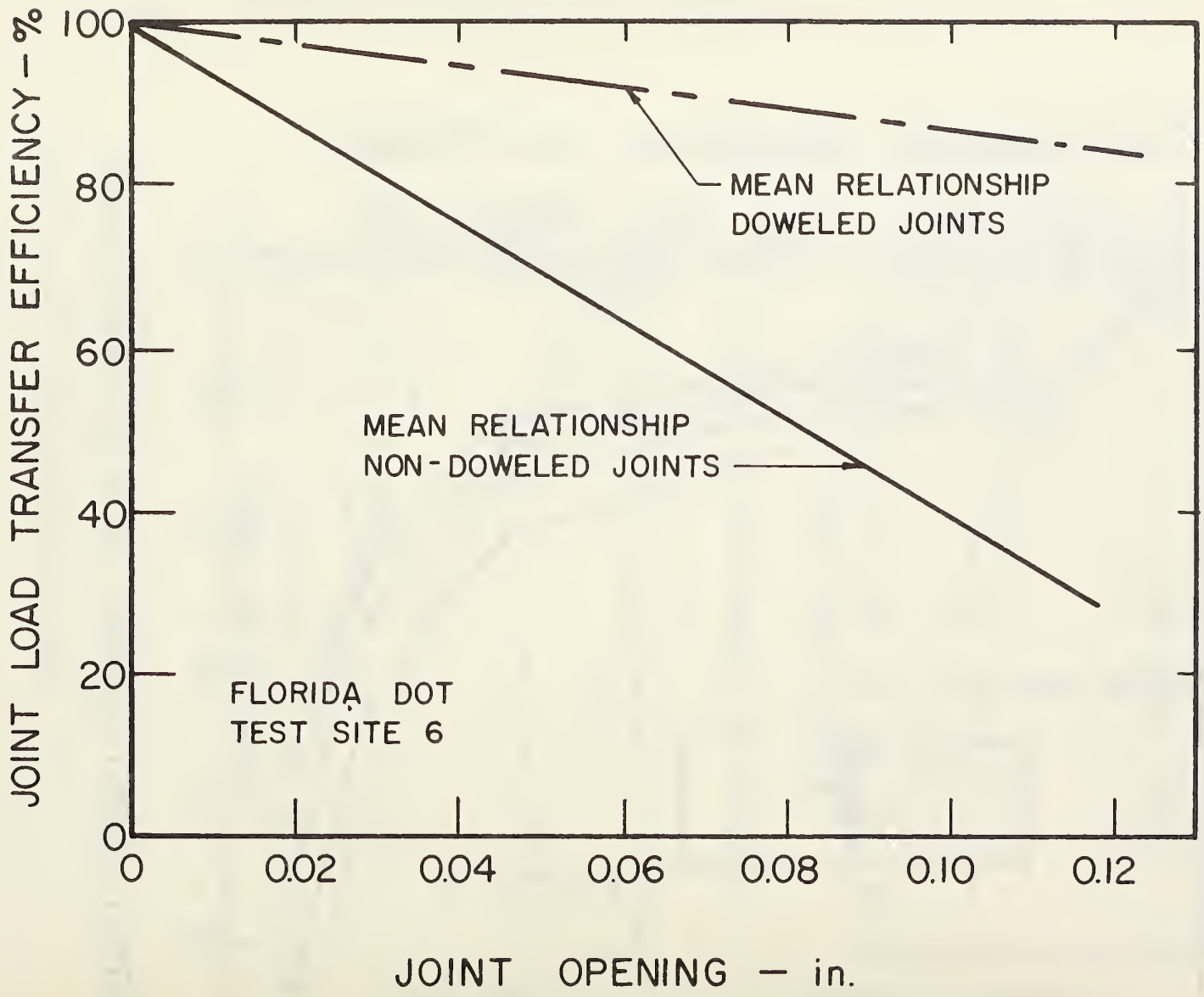


Figure 5.4. Influence of Mechanical Load Transfer Device on Joint Effectiveness After 12 Years of Service (Ref. 72).

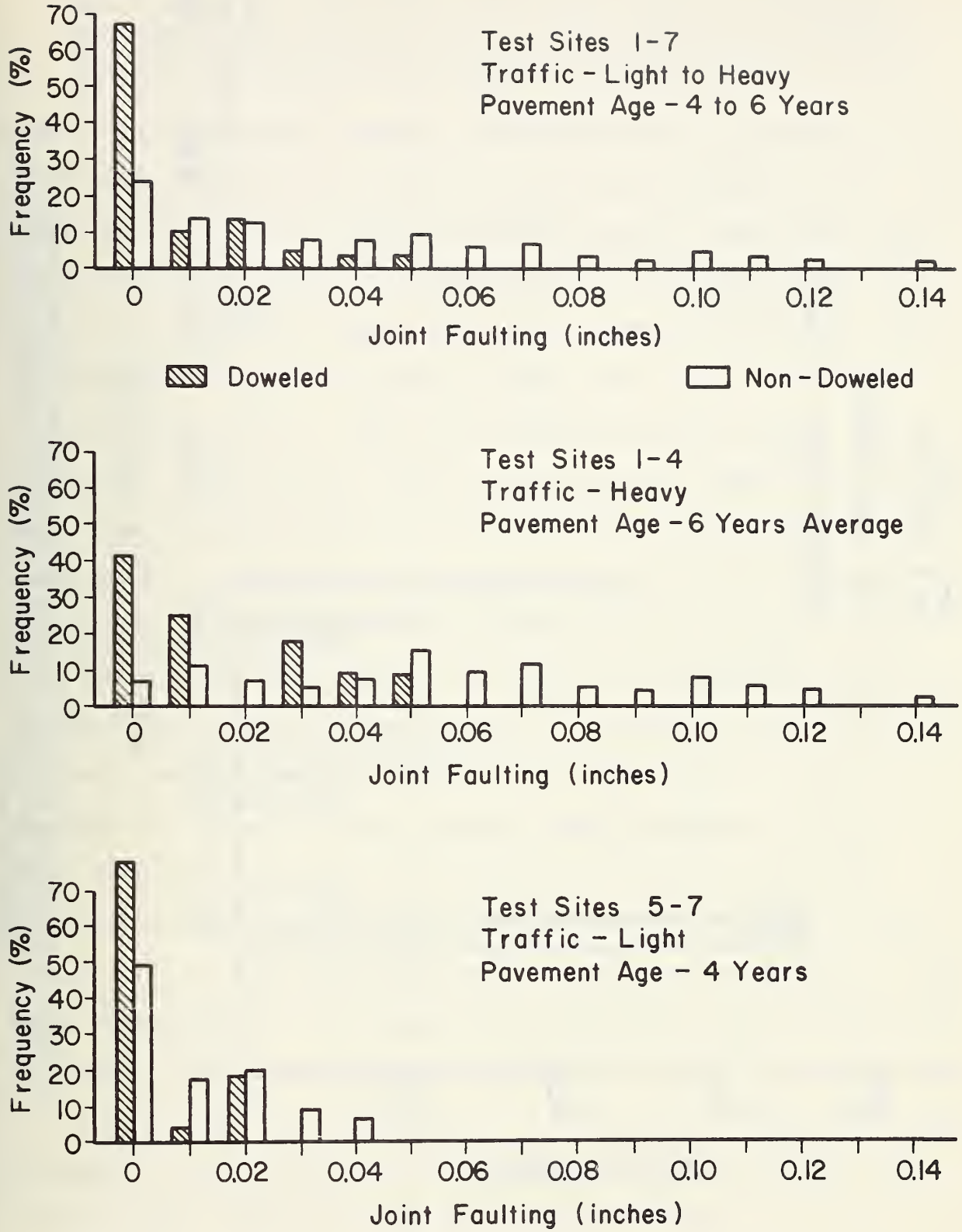


Figure 5.5. Comparison of Joint Faulting in Florida for Doweled and Non-doweled Joints.

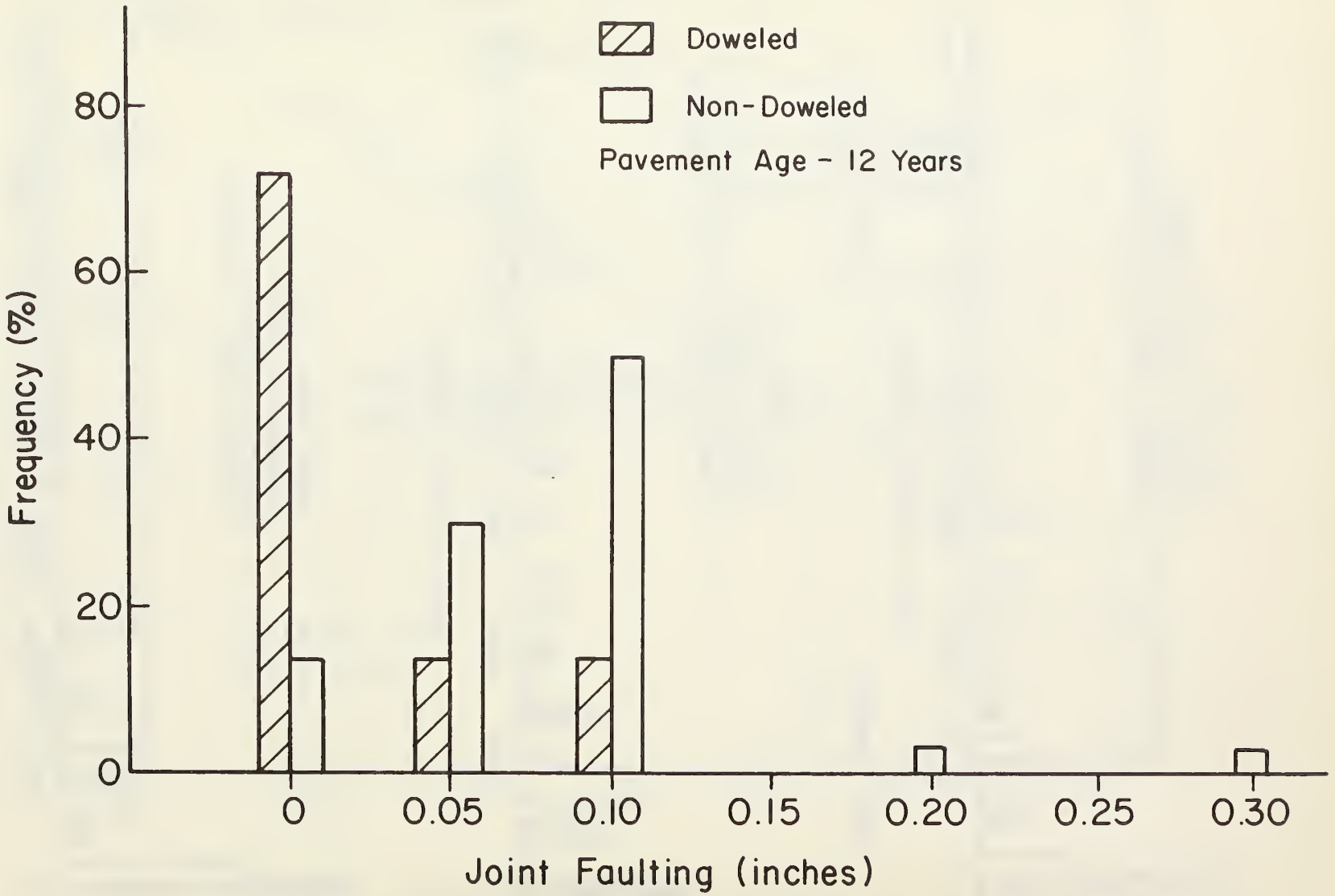


Figure 5.6 Comparison of Joint Faulting Between Doweled and Non-doweled Joints - Florida Test Sites 3, 6, and 7 - River Gravel and Crushed Stone Aggregate in PCC.

"It was found that doweled joints show less faulting than non-doweled joints and that dowels increase the effective load transfer when properly designed and installed. Aggregate interlock provides 40 percent or more load transfer during warm weather, but frequently less than 40 percent during cold weather. Dowels retard joint faulting better than aggregate interlock." (Ref. 72)

Results from the Michigan, Minnesota, and Missouri road tests (Ref. 70) indicate that doweled joints definitely fault less than non-doweled joints. Van Breemen concludes that for heavily trafficked pavements in New Jersey, load transfer devices are needed at transverse joints to avoid the faulting of those that open excessive amounts (Ref. 51). Studies in Georgia also show that dowels are effective in reducing faulting (Ref. 74).

Even though the use of dowels have definitely reduced faulting, there are several projects that had doweled joints, yet still showed serious faulting. Hence dowels are definitely not a panacea for prevention of faulting. A good example is the AASHO Road Test sections of plain jointed concrete pavement left in service on I-80 for 12 years as shown in Figure 5.7. The 8 in. (203mm) slabs showed very serious faulting, but faulting decreased with increased slab thickness and dowel diameter. The bearing stress on the concrete was computed using the Friberg analysis method (Ref. 76) and a plot of bearing stress caused by an 18-kip (80 kN) single axle load at the joint versus joint opening for each of the four slabs is shown in Figure 5.8. Mean joint faulting versus dowel concrete bearing stress is shown in Figure 5.9. There is a high correlation between bearing stress and faulting. These joints have been subjected to approximately 13-19 million 18-kip (80 kN) ESAL and there has been some pumping of the subbase.

5. Aggregates: Joint effectiveness is maintained at a higher level when the aggregate hardness and angularity is increased (Refs. 71 and 72). The effects are most significant after many load applications.

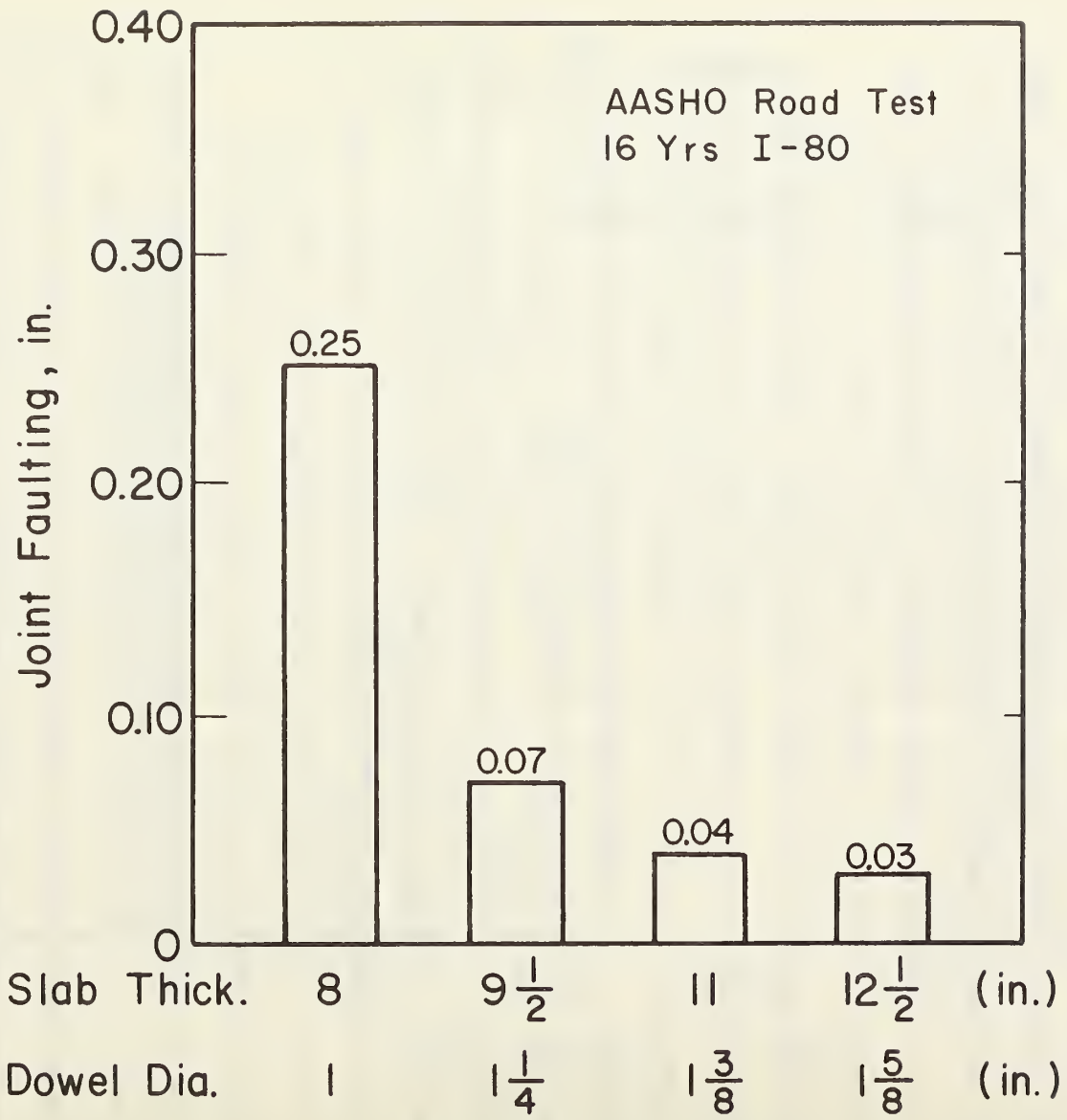


Figure 5.7. Joint Faulting on Plain Jointed Concrete AASHO Road Test Sections Left In-service on I-80.

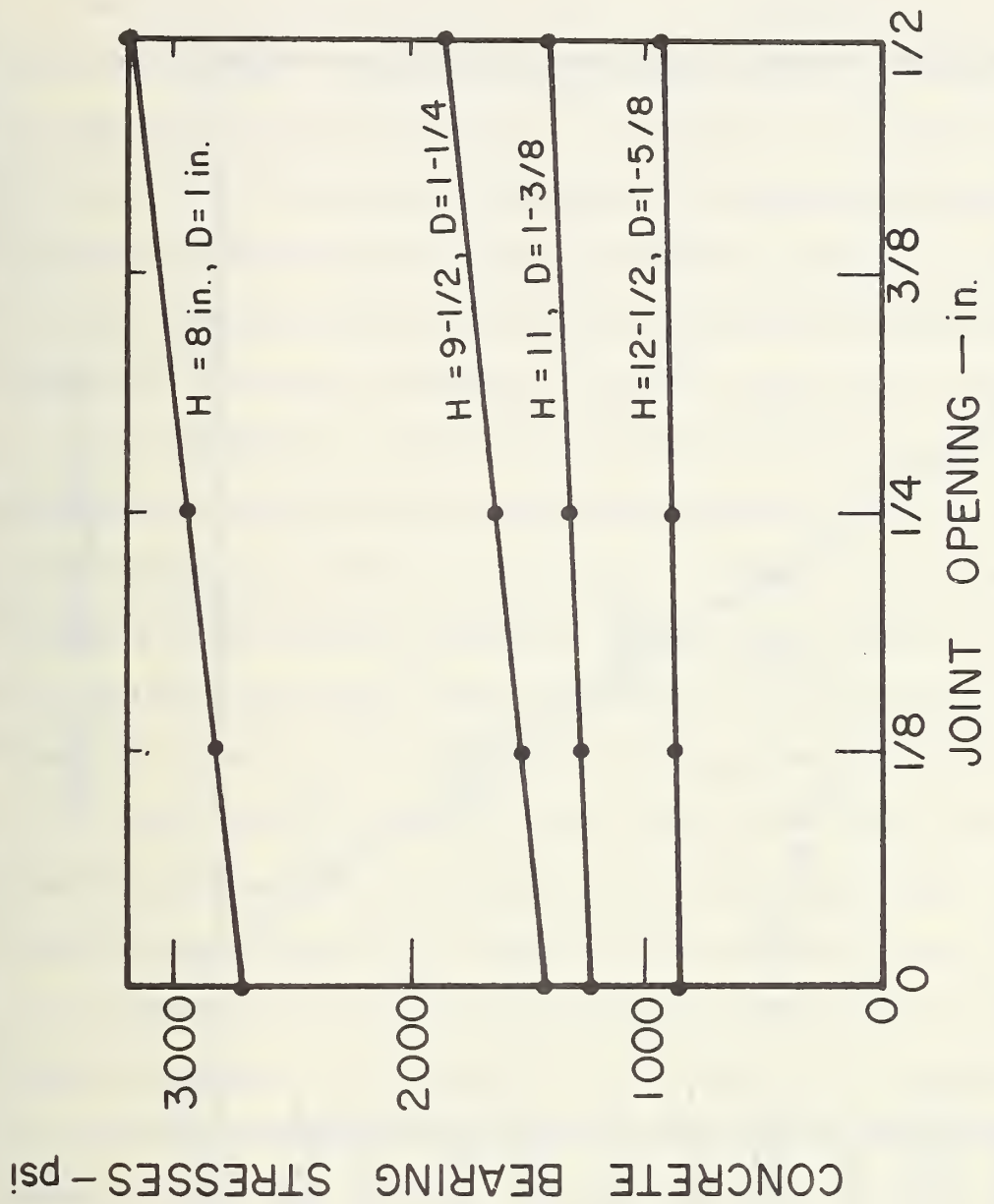


Figure 5.8. Computed Concrete Bearing Stress Under Dowels for JCP-1 to 25.

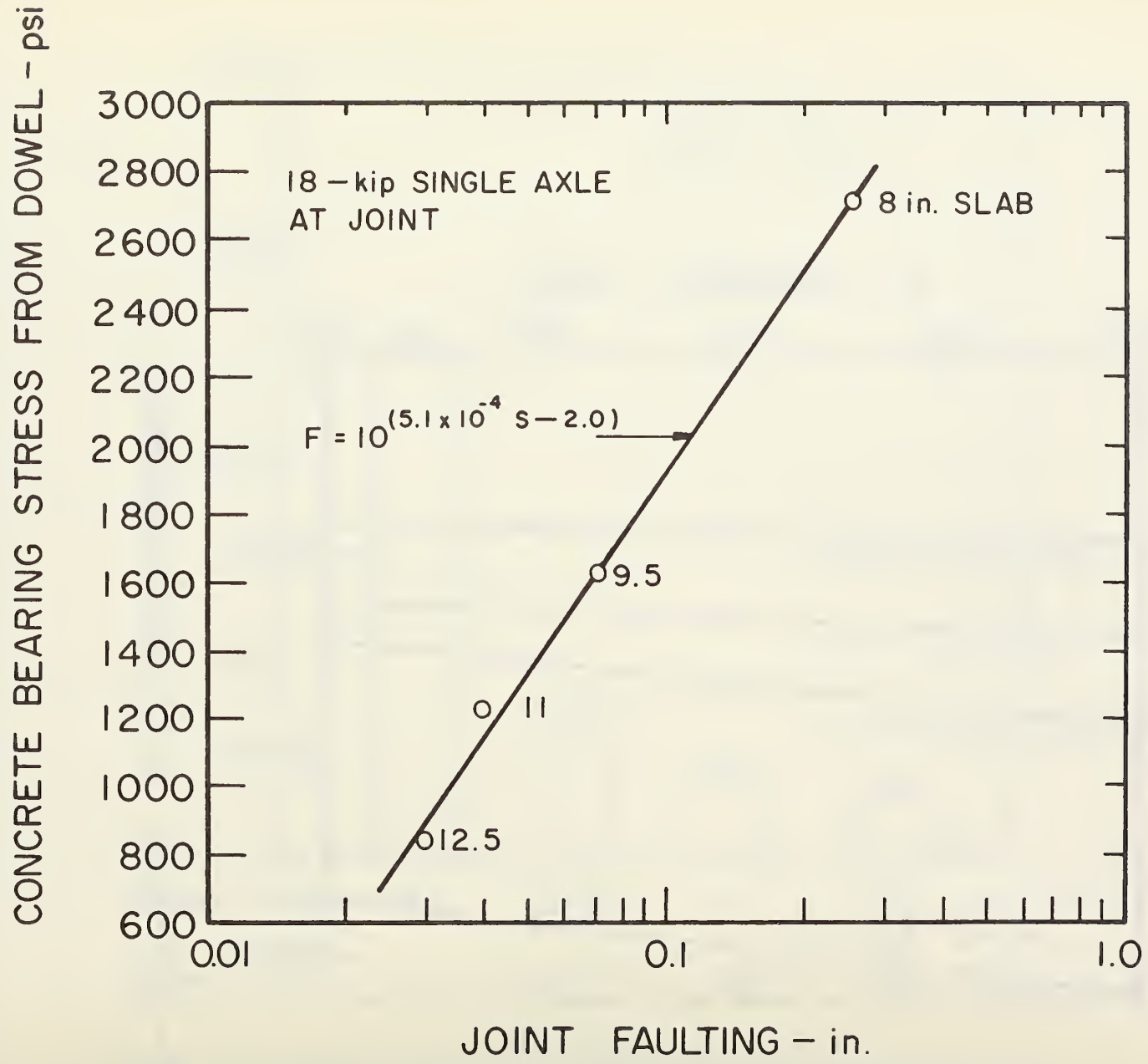


Figure 5.9. Concrete Bearing Stress under Dowel Bars versus Mean Joint Faulting for JCP-1 to 25 After Being Subjected to 13-19 Million 18-kip ESAL Over 16 Years.

Griffin concluded that prevention of faulting can be accomplished by (1) excluding free water from the subbase in the joint area, (2) selecting porous subbase materials or those not affected by erosion, and (3) making the load transfer device adequate (Ref. 79). Recommendations of Spellman, Woodstrom, and Neal from the California study include: (1) use of dowels, (2) shorter joint spacing (6-8 ft. ) (1.8-2.4m), (3) increased thickness of slab, (4) minimize water infiltration, (5) subsurface drainage, and (6) use a erosion-resistant subbase and shoulder materials (Ref. 75).

The following conclusions are made with regard to prevention of transverse joint faulting for pavements subjected to heavy track traffic:

1. A high degree of joint load transfer effectivness must be maintained throughout the design life through either aggregate interlock or both aggregate interlock and mechanical load transfer. The joint load transfer effectiveness must be maintained throughout the year, particularly in cold weather. Thus, maintaining adequate joint effectivness in colder climates using only aggregate interlock is not believed possible under heavy traffic.

2. Dowel bars of adequate size and spacing will greatly help to maintain joint effectiveness and reduce faulting even under heavy traffic if slab thickness and subbase support are adequate to limit concrete bearing stress.

3. Relatively short joint spacing must be used so that seasonal and daily joint opening can be kept within acceptable limits to maintain aggregate interlock. Based on laboratory and field studies an acceptable limit is approximately 0.03 in. (0.8mm). However, due to the large variation in joint openings there will be a large proportion of joints with openings greater than this limit even if the design opening is less than 0.03 in. Thus, aggregate interlock will be lost and faulting may occur at these joints if dowels are not provided.

4. An open graded drainage layer beneath the slab in wet climates will minimize free water and high water pressure beneath the slab. If the subbase is dense graded, it must be erosion resistant.

5. Joints should be adequately sealed to reduce water and incompressibles infiltration into the joint. This will reduce free water under the slab and prevent progressive joint opening.

6. Increased PCC slab thickness will increase the area of effective aggregate interlock and reduce joint deflection under load thereby improving long term joint effectiveness. It also will reduce concrete bearing stresses caused by dowels.

7. Increased slab foundation support will reduce joint deflection and hence increase long term joint effectivensss and reduce concrete bearing stress (minimum recommended is 200 pci (54 $MN/m^3$).

8. Provision of full depth PCC or asphalt concrete shoulders will minimize availability of pumpable material. PCC shoulders tied to the traffic lane will provide increased load transfer along the longitudinal joint and hence reduced deflection.

5.1.2 Joint Sealant Damage. The major problems commonly associated with the deterioration or damage of joint sealants include: (1) increased water infiltration causing significant free water beneath the slab, and subsequent pumping and other moisture problems, and (2) infiltration of incompressibles which may result in progressive joint opening (pavement growth), spalling, blowups and loss of load transfer. The interviews and field surveys of plain jointed concrete pavements, however, indicated that blowups and joint spalling rarely occured. Only two projects were observed to exhibit pavement growth (in New Jersey and Arizona) due to infiltration of incompressibles. Most states visited do not reseal joints on heavily trafficked pavement as evidenced by the fact that only a few of the pavements surveyed had resealed joints over time

periods of 6 to 30 years. Thus, it appears that some engineers are not much concerned about the deterioration of joint seals for short jointed plain concrete pavements. There are certainly many, however, that do feel that the joint seals are important. The degree to which joint faulting occurred because of infiltration of moisture and incompressibles is believed to be sig-cant on several of the projects visited. Recent studies have shown that with current sealant materials and practices it is impossible to keep moisture out of the pavement section (Refs. 82-86). If an open graded drainage layer is provided in "wet" areas and a non-erodable subbase is provided in "dry" areas the effect of moisture on faulting will be minimized. Thus, it is definitely desirable to provide a sealant that will at least minimize the infiltration of moisture and also prevent the intrusion of incompressibles.

Only the most durable sealants should be used for zero-maintenance design and the expected maximum joint opening and allowable sealant extensibility should be considered when selecting the sealant. Two general types of sealants are available: liquid and preformed. Field studies have shown that hot applied bituminous liquid sealants have a field life of only a few years and thus would not be suitable for long term performance (Refs. 2, 84, 87, 88). For example, a recent study by McBride and Decker (Ref. 88) shows the bituminous sealant had failed and significant infiltration of incompressibles occurred on pavements having a random joint spacing of 12-18 ft. (3.6-5.5m) and varying in age from 1-1/2 to 10 years (See Figure 2.15). However, the newer elastomer types (polysulfides, urethanes, polyvinyl chloride, etc.) may be capable of providing longer service lives (some companies are now providing a warranty for 10 years on these seals). Preformed sealants are available that have been shown to give 10+ years of acceptable service even on long jointed concrete pavements under heavy traffic. Figure 5.10a is a photo of a preformed seal in service on Highway 401 Toronto for 12 years (joint spacing is 56 ft. (17m),

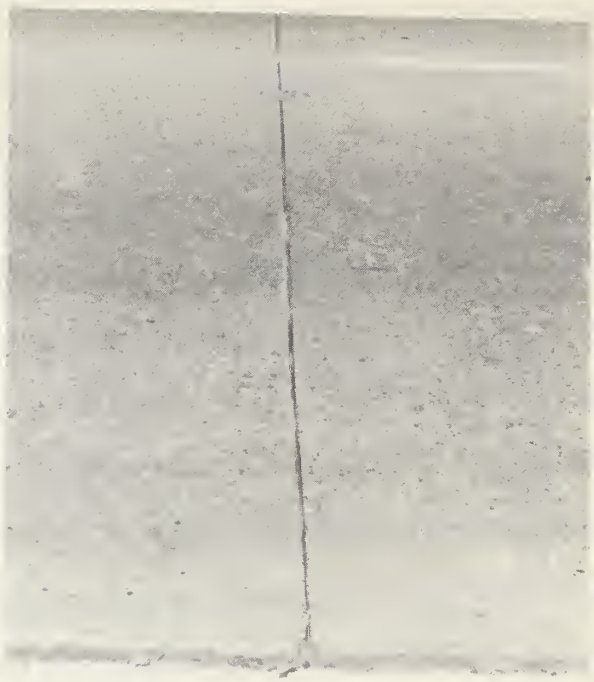

(a) Hwy 401, Toronto, Ontario, 12 years old,
joint spacing 56 ft, ADT 187,000

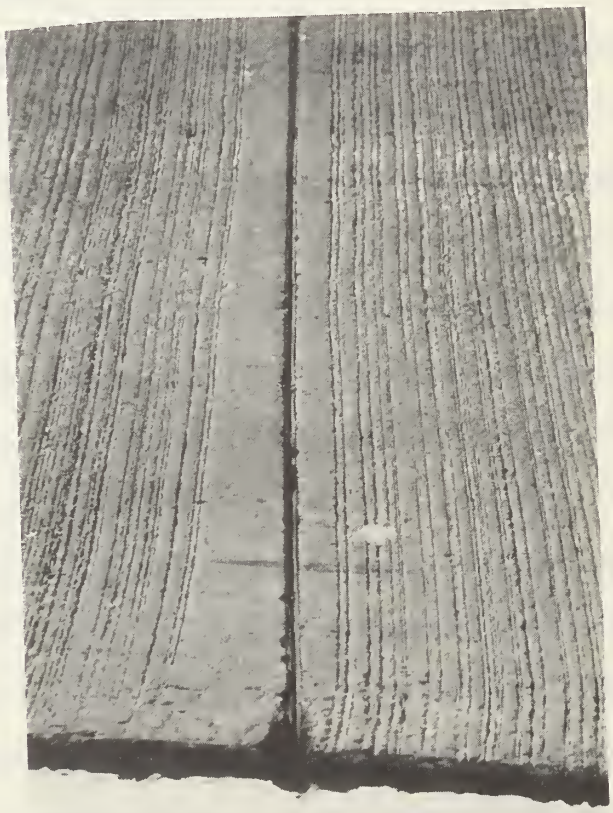

(b) Hwy 27, Toronto, Ontario, 6 years old,
Joint spacing 12-19 ft, ADT 80,000

Figure 5.10. Neopreme Preformed Compression Sealant In-Service

and Figure 5.10b shows a preformed seal on JCP-37 in Toronto in service for 6 years (joint spacing 12-19 ft. (3.6-5.8m), with very few signs of distress. Preformed compression sealant was the type most recommended to achieve the required long term performance needed. Preformed seals have been observed to do an excellent job of keeping out incompressibles over long time intervals, but are not completely water tight seals.

The liquid or preformed seal must be designed to accommodate joint movement. The elastomers have an expansion-compression range of about $\pm$ 20 percent at temperatures from -40°F to +180°F (-40 to 82°C). The preformed sealants are designed so that the seal will always be in compression. The preformed compression sealants should be selected so that it will always be compressed at least 20 percent in the sawed joint. The maximum allowed compression of the seal is 50 percent before a rubber on rubber situation is reached. Thus the seal working range is 20 to 50 percent (Refs. 88, 89, 90).

The required joint sawed width for a liquid sealant can be determined as follows:

Joint spacing = 15 ft. (4.6m)

Design temperature range = 100°F (55°C) (temperature at placement minus lowest mean minimum monthly temperature)

Stabilized subbase

Maximum allowed extension of sealant = 20%

Design joint movement (Eq. 5.2):

$$\Delta L = 0.65 \times 10 \text{ ft.} \times 12 \frac{\text{in}}{\text{ft}} [5.5 \times 10^{-6}/^{\circ}\text{F} \times 100^{\circ}\text{F} + 1.0 \times 10^{-4}]$$

$$= 0.076 \text{ ins. (1.9mm)}$$

$$\text{Min. joint sawed width} = \frac{0.076}{0.20} = 0.38 \text{ in. (9.7mm)}$$

Use reservior width = 0.5 in. (12.7mm)

The size of preformed seal and joint sawed width can be determined as follows:

$\Delta L$ = 0.076 in. (1.9mm)

Try 7/16 in. (11mm) width seal in a 1/4 in. (6.4mm) sawed joint and install in summer (joint would not be further compressed).

Check maximum Compression: $\frac{0.4375 - 0.25}{0.4375} \times 100 = 43\% < 50\%$ ok

Check minimum Compression: $\frac{0.4375 - (.25 + .076)}{0.4375} \times 100$

$= 25\% > 20\%$ ok

Working range of seal = 25 - 43% of uncompressed seal

In conclusion, while there is not yet a sealant available that can be guaranteed to last for 20 years, the minimum desired zero-maintenance design period, there are sealants that will definitely perform satisfactory for more than half of this time period. Considering the numerous heavily trafficked plain jointed concrete pavements that never receive joint maintenance, and the structural design being proposed for zero-maintenance pavements (thick slabs, subsurface drainage, dowel bars, stabilized subbase, stabilized shoulders, and short joint spacing), it is fairly certain that joint sealant maintenance will not be necessary for the rest of the design period should some of the joint sealant fail after 10-15 years.

5.13 Transverse Joint Spacing. This factor has a very significant effect on pavement performance. Decreasing transverse joint spacing has the following beneficial effects:

1. decreases thermal curl stress (Fig. 4.31)
2. decreases transverse cracking (Fig. 4.30)
3. decreases curling of slab upward at joint
4. decreases joint spalling (Fig. 5.11)
5. decreases seasonal and daily joint opening, and thus:
   - increases joint load transfer effectiveness.

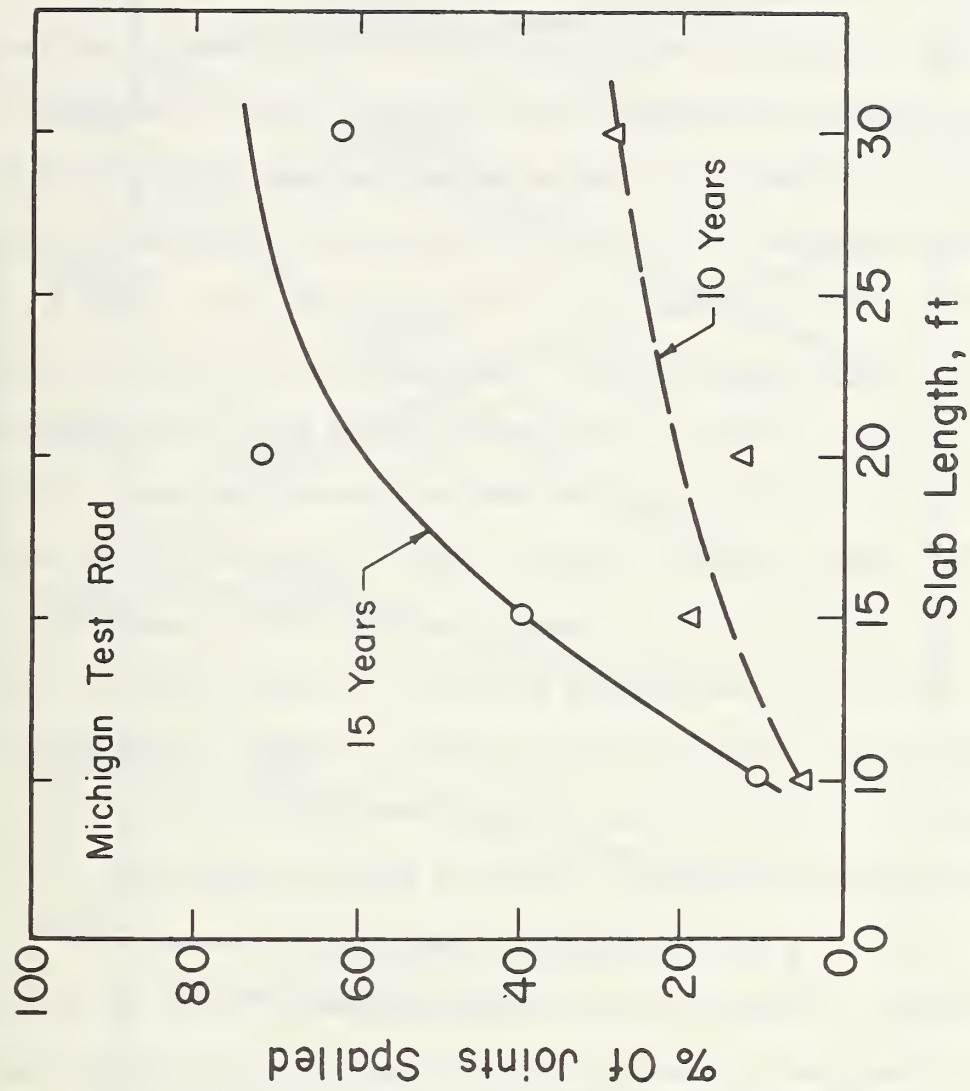


Figure 5.11. Effect of Joint Spacing on Spalling of Joints.

- reduces sealant extension

6. For spacings less than about 20 ft. (6.1m) increased slab thickness is beneficial in decreasing total stress from load and temperature gradients (Fig. 5.12).

Of course, to minimize construction cost it is desirable to increase the joint spacing, however, maintenance-free performance is of prime concern here. Based upon these considerations, the recommended maximum joint spacing for zero-maintenance pavements is 20 ft. but it is highly recommended to limit spacing to about 15-17 ft if dowels are used, and 12-15 ft. or less if they are not used.

5.14 Joint Load Transfer Device. Many types and varieties of mechanical load transfer devices (LTD) and joint configurations have been tested over the years. Nearly all of these have given poor performance and caused serious joint failure. Several pavement failures caused by proprietary lugs were observed during the field survey. Based on extensive field experience, round steel dowels have become the standard and nearly the only mechanical LTD used in current practice. There are also significant problems associated with dowels as determined from the interviews, field and laboratory studies: (1) corrosion, (2) providing proper size and spacing for the specific application, and (3) alignment.

1. Corrosion: Although the serious consequences of dowel corrosion have been known for many years, almost nothing has been done to prevent it until just the last few years. The most significant and perhaps first work to determine the effects of dowel corrosion and the subsequent development of corrosion proof dowels was by Van Breemen of the New Jersey Department of Transportation. Van Breemen first reported the effects of corrosion in New Jersey in 1945 (Ref. 81) and a comprehensive report on field and laboratory studies was published in 1955 (Ref. 80). Major findings from these studies are as follows:

1. Serious corrosion of carbon steel dowel bars occurred after only a few years in service. Most corrosion occurred in the joint space, but

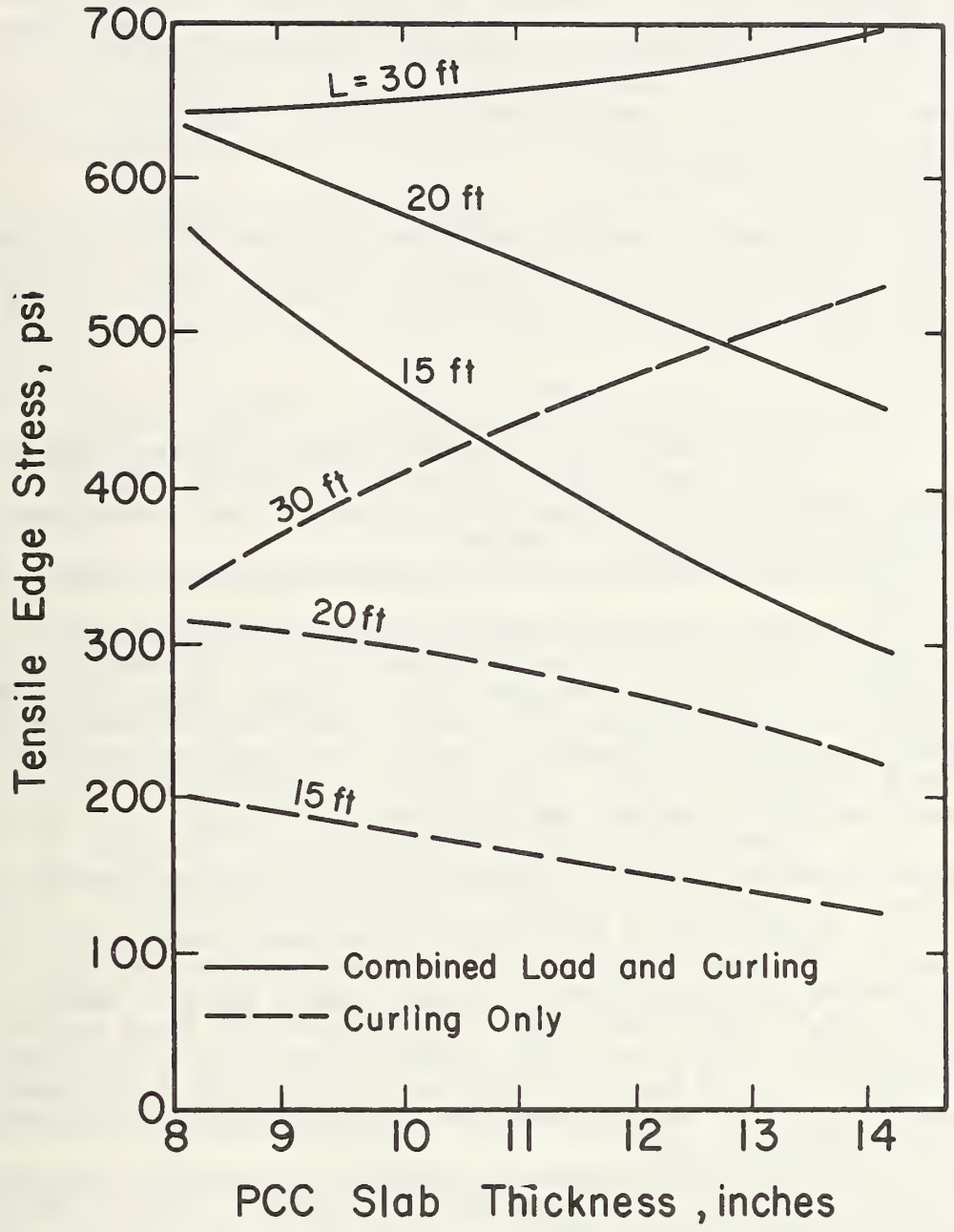


Figure 5.12. Effect of Joint Spacing and Slab Thickness of Curling and Combined Curling and Load on Edge Stress (computed with Finite Element Program).

extended for 3 inches or more on each side of the joint.

2. The corrosion resulted in a lock-up of the joint as verified by joint width change measurements and dowel pull out tests. The joint lock-up resulted in the forced opening of transverse cracks and rupturing the slab reinforcement. These cracks soon spalled and faulted. Some joints also showed distress (spalling and faulting).

3. Several experimental dowels to which had been applied various coatings and protection treatments were installed in pavements and evaluated after 8 years in service.

> "1. All of the dowels partly encased in Monel tubing ("monel" dowels) were still in practically perfect condition.
> 2. All of the ordinary hot-rolled carbon steel dowels were rusted in various amounts, ranging from minor to serious, regarldess of the kind of coating.
> 3. Hot-dipped galvanizing delayed but did not prevent rusting.
> 4. All of the various dowel coatings (which included red lead, white lead, tar paint, graphite paint, transmission oil, cylinder stock grease, and asphaltic oils, grades MC-2, SCO, and CC) had deteriorated to the extent that they are now practically worthless. Moreover, in numerous instances the coatings had disappeared entirely. Apparently the deterioration and loss has been due mainly to the action of water.
> 5. The enclosure of the sliding portion of the dowel in a sheet metal sleeve had no apparent effect on prolonging the life of the coating, at least to any appreciable extent.
> 6. In practically all instances, the exceptionally thick coatings of asphalt applied to the hot-rolled dowels on Route 25, Newark, had disappeared entirely, despite the fact that sheet metal sleeves were used in conjunction with these coatings. In addition to the loss of the coatings, the sleeves had almost completely rusted away, and there was considerable rusting and significant loss in section of the sliding portions of the dowels, and at the joint space.
> 7. Thick coatings apparently prevent seizure, but upon their disappearance there is a creation of clearance. This in turn permits the entrance of corrosive agents to the entire sliding portion of the dowel.
> 8. The back-and-forth movement of the dowel results in a certain amount of abrasion.
> 9. In practically all instances, the compressible material at the ends of the dowels was in a very wet condition.
> Judging from the conditions found, it appears probable that there are times, during rainy weather, when the joints are completely inundated and, in effect, functioning under water. There furthermore were strong indications in several instances that there was a slight vacancy under the dowel which served

as a channel to carry water clear to the end of the dowel. This vacancy was apparently the result of a slight slumping-away of the concrete, or the accumulation of a thin layer of water or air, underneath the dowel." (Ref. 80).

Additional tests with stainless steel coated dowels (both stainless steel encased tubing and solid stainless steel coatings) showed that "no rusting of the stainless steel tubing has occurred nor does there appear to be rusting of any consequence between the tubes" (Ref. 80). Based upon these results New Jersey has specified Monel or stainless steel protection (as alternatives) for their dowels since 1947 and have obtained excellent results. Joint lock-up was virtually eliminated in these pavements (Ref. 2). The dowel bar specification used by New Jersey is given in Figure 5.13.

To further verify the serious problems of dowel corrosion, two joints were removed from concrete slabs near Ottawa, Illinois by the Illinois Department of Transportation (IDOT) in June, 1975 and then tested at the University of Illinois to determine the extent of joint lock-up. The entire full lane width was removed as shown in Figure 5.14 from Section 382 of the original AASHO Road Test (now 17 years old and under heavy traffic on I-80) and from another section constructed in 1962 by IDOT. Two six foot wide sections of joint containing six dowels were pulled apart using hydraulic jacks and the axial tension load and joint opening carefully recorded. A plot of joint opening versus axial tensile force as is shown in Figure 5.15 for Section 382. A total of 30,000 lbs (133kN) was required to open the joing 0.1 inches (2.5mm) (approximately 5000 lbs (22kN)/dowel). Visual observation of the dowels showed significant corrosion at least 3 inches (76mm) on either side of the joint (Ref. 91). The other joint tested gave approximately the same results (Ref. 91). The pavement slabs on either side of the joints were 40 ft (12.2m) in length and contained highly spalled and faulted cracks, and the steel reinforcement had ruptured. These results closely parallel the New Jersey fundings. Approximately 5 tons/lane mile (44kN/km) of deicing slabs are used

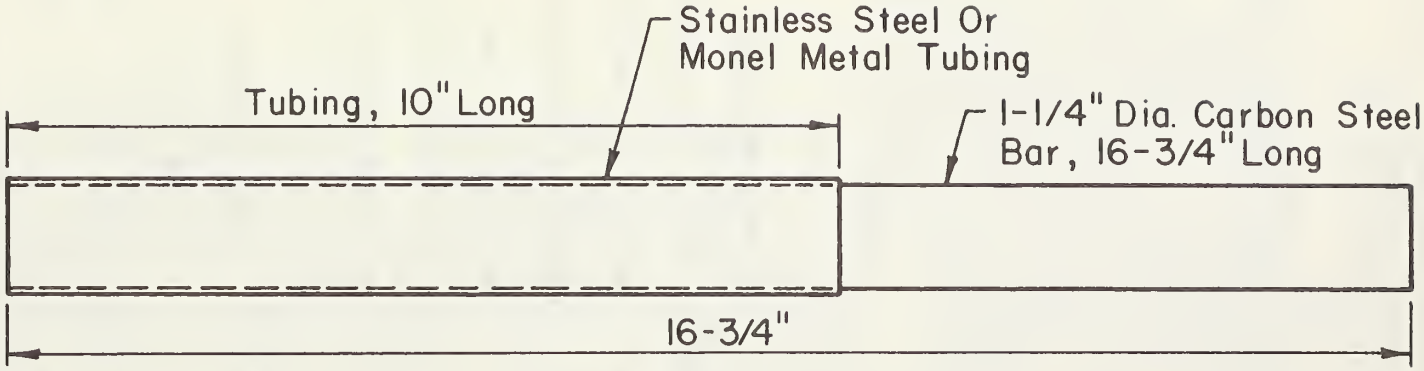


The dowels shall consist of either (a) 1-1/4" diameter solid stainless steel bars, (b) 1-1/4" diameter carbon steel bars encased in stainless steel or Monel metal, or (c) 1-1/4" diameter carbon steel bars that have been impregnated with chromium throughout their exposed surface. The stainless steel shall contain not less than 12 percent chromium. If encased in stainless steel or Monel metal, the thickness of the stainless steel or Monel shall be not less than .01 inches, and the tightness of fit shall be such as to preclude the occurrence of corrosion between the stainless steel or Monel and the underlying carbon steel. If rendered corrosion-resistant by impregnation with chromium, the layer of metal which has been so impregnated shall have (a) an average thickness of not less than .009 inch, (b) at no point a thickness of less than .008 inch, and (c) an average chromium content of not less than 20 percent, by weight. The Contractor shall furnish the Engineer with a certification showing that the means employed for rendering the dowels corrosion-resistant complies with the foregoing specification.

The dowels shall not vary in straightness throughout their length in excess of 1/32". The sliding portion of the dowel shall be of uniform cross section, free from burrs, projections, and any other irregularities that would interfere with free movement in the concrete.

Figure 5.13. Corrosion Proof Dowel Specified by New Jersey.

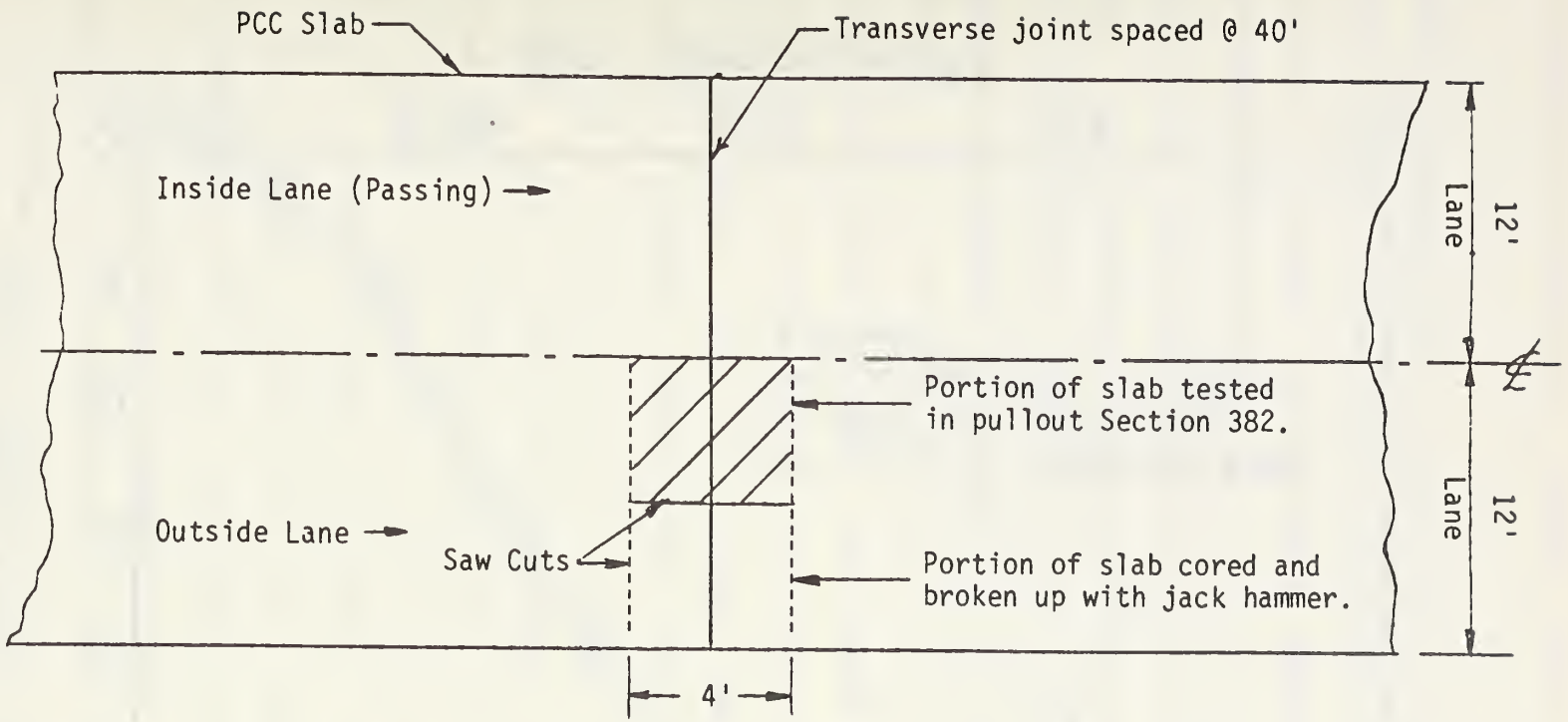


Figure 5.14. Location of slab tested from Section No. 382.

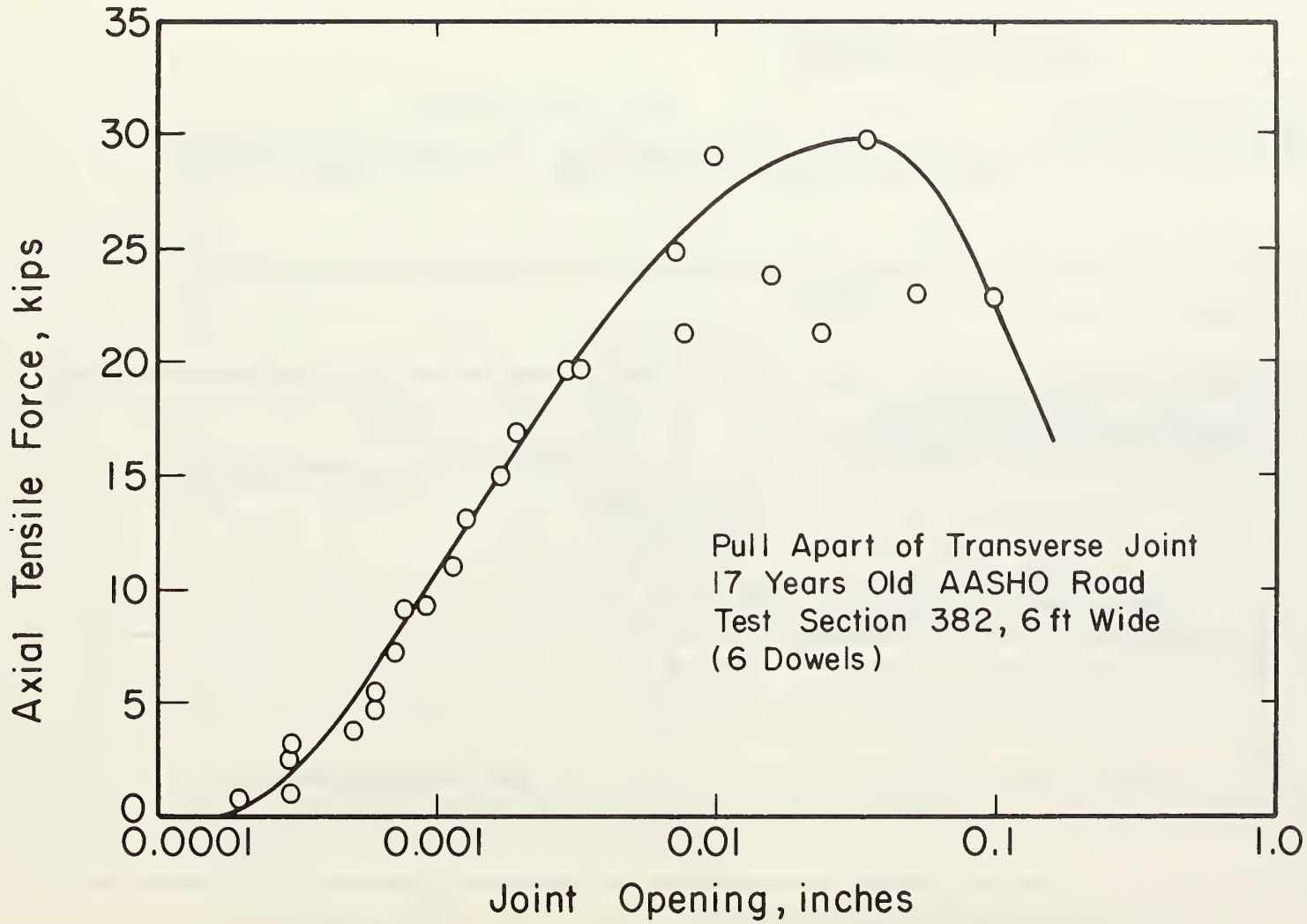


Figure 5.15. Joint Pull Apart Test Conducted at University of Illinois.

on this highway per year which has definitely contributed to the corrosion problem.

Additional studies on dowel corrosion and pull out tests were conducted by New York (Ref. 92). These results showed similar findings with regard to corrosion and joint lock-up. Therefore it is concluded that to prevent dowel corrosion and subsequent joint lock-up in areas where deicing salts are used (and possibly other areas where corrosion occurs), dowels must be corrosion resistant. Long term experience in New Jersey has shown that Monel metal or stainless steel coatings do provide non-corrosive dowels that allow adequate joint movement for pavements now in service nearly 30 year. Other corrosion resistant coatings are available, but without long term performance data as for the stainless of Monel clad dowel. These methods include pretreatment with various plastic coatings (Ref. 93) and fiberglass dowels.

2. Size and Spacing: The size and spacing of dowels currently used is based upon field, laboratory, and analystical studies. Dowels generally are spaced 12-15 ins. (205-381mm) and have a diameter of approximately 1/8 of the slab thickness. These criteria have generally been successful in preventing faulting but there are exceptions, particularly on heavily trafficked pavements (i.e. the previously discussed joints shown in Figure 5.7). The analytical dowel analysis and design procedure such as that of Friberg (Ref. 76) and ACI (Ref. 94) are based on providing sufficient strength to transfer one-half of the assumed pavement design wheel load across the joint with a safe bearing pressure between the dowel and the supporting concrete. Allowable bearing stress as recommended by the ACI and the computed bearing stress and mean joint faulting for the AASHO Road Test sections in-service on I-80 previously discussed are given in Table 5.2. These data show that even though the allowable bearing stress was not exceeded (the allowable stress is based on static failure criteria) considerable faulting still occurred even though the dowels were of

Table 5.2. Joint concrete bearing stress and faulting data.

| Slab Thickness (in) | Dowel Diameter (in) | Concrete Bearing Stress-psi * | Allowable Bearing Stress-psi ** | Mean Joint Faulting (in) |
|---|---|---|---|---|
| 8 | 1 | 2715 | 3000 | 0.25 |
| 9.5 | 1 1/4 | 1620 | 2751 | 0.07 |
| 11 | 1 3/8 | 1230 | 2625 | 0.04 |
| 12.5 | 1 5/8 | 840 | 2376 | 0.03 |

* Computed using Friberg Analysis (Ref. 94)

**Computed using $f'_{ci}$ = 3000 psi

the recommended size and spacing. This is probably the result of a concrete bearing fatigue failure phenomenon. This data may indicate that for heavy truck traffic (i.e. approximately 1 million 18-kip (80kN) ESAL/year/lane) the concrete allowable bearing stresses should be further reduced as indicated in Table 5.2. Further research in this area is clearly needed. One final and important point with regard to dowels is their required spacing on multilane pavements. The point at which joint faulting is most serious is the outside corner of the outer traffic lane. This is also the point at which critical dowel bearing stress occurs. On multilane pavement, faulting is much less on interior lanes thus it is believed that dowel spacing may be increased in these lanes. Truck travel is generally less on the interior lanes and there is significant load transfer across the longitudinal joint.

## 5.2 SHOULDERS

Shoulders must be designed to provide zero-maintenance performance, since repair of a shoulder failure usually requires closing of the adjacent traffic lane. Results from field studies indicate that the only shoulder types adjacent to jointed concrete pavements that have low maintenance performance are PCC and full depth asphalt concrete (AC) (Refs. 2, 95, 96, 97, 98, 99). Full depth asphalt concrete shoulders have shown generally good performance in the various states, but have required longitudinal joint maintenance often and have exhibited some separation and cracking at the longitudinal lane shoulder joint in freeze areas (Ref. 95). PCC shoulders have been observed to give over 10 years of maintenance-free performance in Illinois (with no sign of distress) and equal performance in other states over shorter time periods. Figure 5.16 shows a photo of a 10 year old PCC shoulder in Illinois located

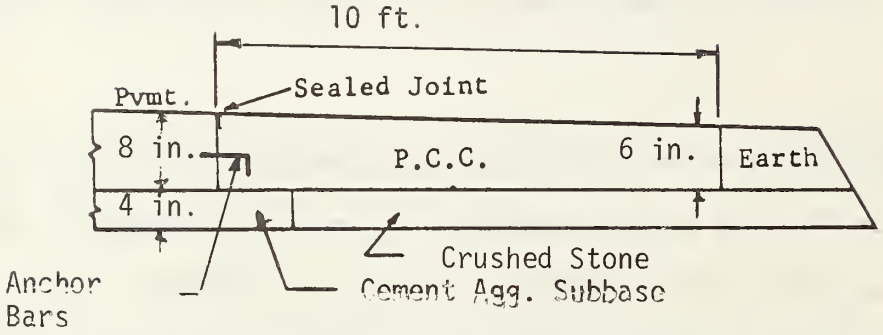


The longitudinal joint in half of each test section is sawed 1/2" wide by 3/4" deep and sealed with a hot-poured rubber-asphalt joint sealant.
Surface is transverse broomed. Dummy groove transverse joints at 20' intervals.
Rumble strips 6' wide @ 60' intervals.

Anchor Bars: No. 4 hooked bolts, 15 in. length turned into 2-in. snap off expanding end anchors set into the edge of slab at 30 in. intervals.

Figure 5.16. PCC shoulders on I-80 in Illinois, 10 years old.

on I-80, and Figure 5.17 shows an 11 year old PCC shoulder on I-74. Both have provided zero-maintenance performance. Recommendations from highway agency engineers indicated perference for PCC shoulders when the traffic lanes were PCC. However, full depth AC shoulders may provide maintenance-free performance in certain climatic regions where previous performance data are available.

5.2.1. PCC Shoulder Design. PCC shoulders, when tied to the lane slab, have the potential to reduce edge stress. Figure 5.18 was prepared using the finite element program to illustrate the effect of longitudinal joint efficiency. Even the small amount of load transfer obtained from tie bars may reduce critical edge stress as shown. The following recommendations are based upon results of field studies in Illinois and other states:

(a) Slab thickness - preferably equal to the mainline slab thickness at the longitudinal joint and continuing at the same thickness throughout. If taper is more economical, begin taper 24 inches from joint to a thickness of eight inches at the shoulder edge.

(b) Tie Bars - tie the shoulder to the mainline pavement by No. 4 or No. 5 deformed steel tie bars spaced at 30 inches on center.

(c) Transverse joint - space joints identical to the traffic lanes.

(d) Longitudinal joint - place at edge of traffic lane and seal (or preferably increase traffic lane width 1-2 ft. to decrease number of edge loads).

(e) Subbase - use same subbase as placed beneath PCC mainline pavement (See subsurface drainage, Section 5.3).

Further details on PCC shoulder design can be found in Reference 100.

5.2.2. Asphalt Concrete Shoulder Design. The following recommendations are based upon results of field studies in several states:

(a) Thickness - equal to slab thickness at the longitudinal traffic lane/shoulder joint for at least 24 inches and tapering to 10 inches at shoulder edge (edge must be of adequate thickness to prevent failure from parked trucks.

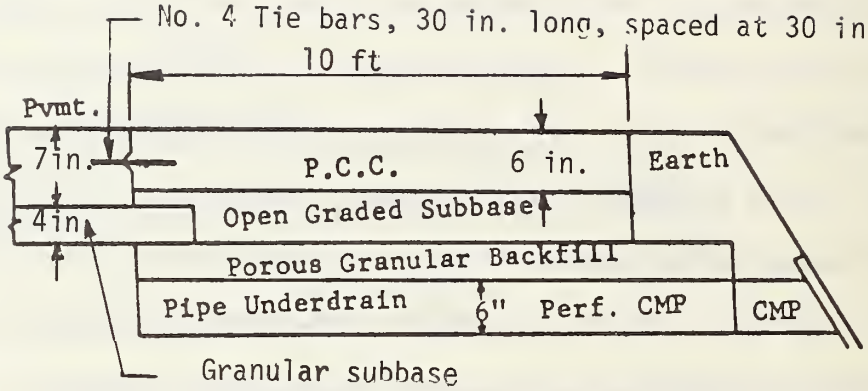


Longitudinal keyed joint

Rumble Strips: 4 ft wide groupings of corrugations 1 in. deep

Transverse joints spaced 10-20 ft.

Figure 5.17. PCC shoulders on I-74 in Illinois, 11 years old.

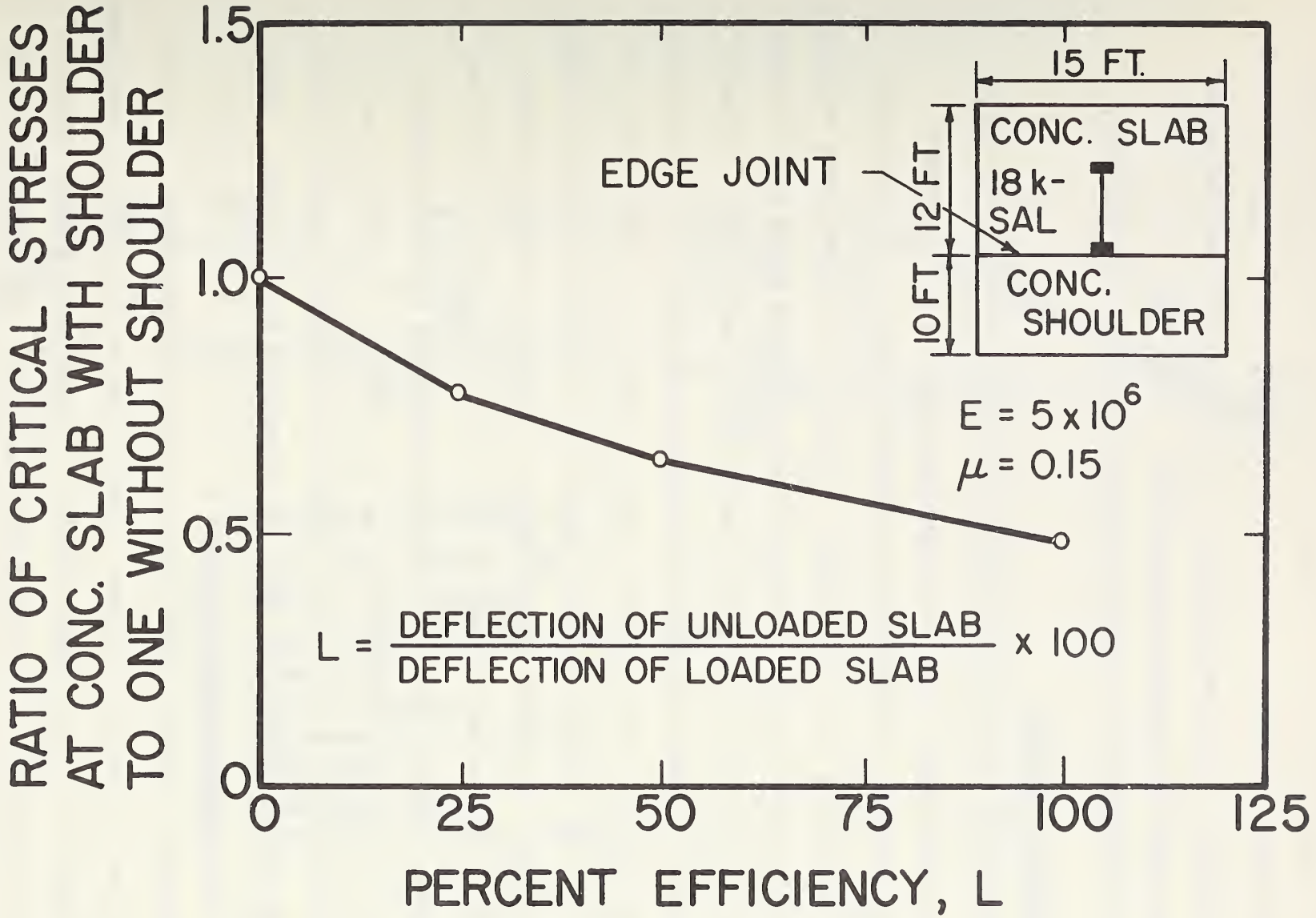


Figure 5.18. Effect of Concrete Shoulder on Critical Edge Stress for Varying Joint Load Transfer Efficiency.

(b) Longitudinal joint - saw cut a 1 inch square joint and fill with high type joint sealant.

(c) Subbase - use same subbase as is placed under PCC mainline pavement (See subsurface drainage, Section 5.3).

Further information on AC shoulder design can be found in Reference 95.

## 5.3 SUBSURFACE DRAINAGE

The presence of free water beneath the PCC slab can result in several distresses which would limit the maintenance-free life of the pavement. These distresses may include cracking, faulting, pumping, frost heave, and durability problems in PCC and subbase. Therefore, in regions where relatively high annual rainfalls exist, or where significant ground water exists, consideration should be given to providing subsurface drainage systems. The major components of a general subsurface drainage system are shown in Figure 5.19. The major purpose of the subsurface drainage system is to rapidly drain the roadbed to reduce the periods when the structure is exposed to excess moisture.

The general guidelines for the design of subsurface drainage systems, developed for the Federal Highway Administration by Cedergren (Ref. 85) are recommended. The basic procedure considers subsurface drainage layers as conveyors of water and considers in-flow rates from all significant sources. Seepage principles are then used to determine the permeability and thickness of a subsurface drainage layer that will accommodate the water flow. Hence, the drainage system is designed to have an out-flow rate equal to the rate of infiltration into the pavement during a one-hour design rainfall having a frequency of occurrence of one year. Theinfiltration rate of PCC is considered to be 0.50 to 0.67 of the total rainfall. This procedure, however, gives a drainage layer having a very high drainage capacity. This high capacity may not be required and a somewhat less porous drainage layer may be adequate, which would have greater stability in providing support for the PCC slab.

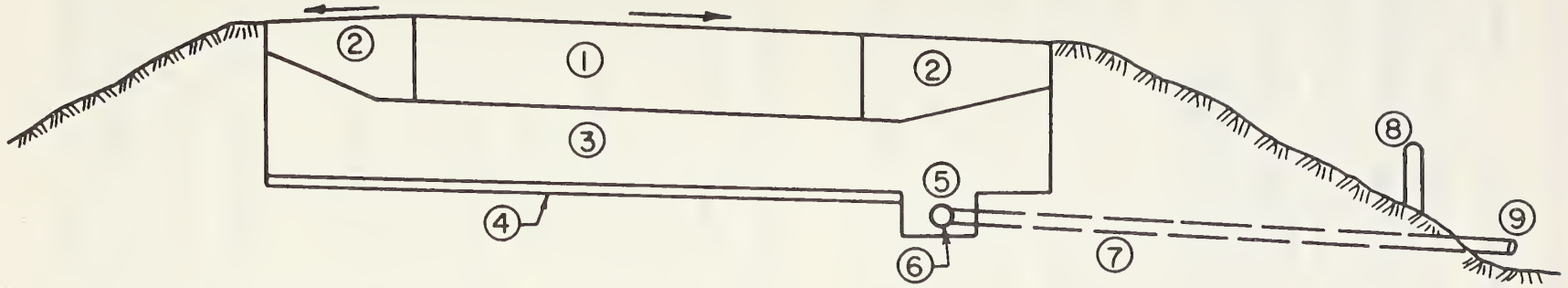


Description Of Components

① PCC Slab - Traffic Lanes
② PCC or AC Shoulders
③ Open Graded Subbase (Drainage Layer)
④ Filter Layer
⑤ Collector Trench
⑥ Perforated Collector Pipe
⑦ Outlet Pipe
⑧ Outlet Pipe Marker
⑨ Outlet Pipe Automatic Drainage Gate

Figure 5.19. Typical Subsurface Drainage System with Collector Pipe.

Pavements located in areas where subsurface moisture is not of sufficient magnitude to provide subsurface drainage should not, however, be constructed in a "bathtub". The subbase should be daylighted to provide for some lateral drainage in these areas. The subbase should be constructed with high quality asphalt or cement stabilized granular materials to provide an erosion proof subbase surface. Additional information on subsurface drainage is found in References 82, 83, 84, and 85.

# CHAPTER 6

# VERIFICATION OF DESIGN

## 6.1 DESIGN APPROACH AND COMPUTER PROGRAM

The structural design of zero-maintenance plain jointed concrete pavement involves two independent but complimentary approaches. It is based upon both a serviceability/performance analysis and a PCC slab fatigue analysis. Both approaches have distinct capabilities needed for structural design. The design recommended for construction must meet the limiting criteria of both approaches. Structural design consists of the selection of PCC slab thickness and strength, subbase type and thickness, and joint spacing. The design must be compatible with shoulder and subsurface drainage design. The general approach to design is shown in Figure 1.2.

The basic structural design philosophy to provide zero-maintenance plain jointed concrete pavements is to prevent linear (transverse) cracking of the slab and excessive pavement roughness caused by joint faulting and other factors such as slab settlement. The fatigue analysis provides a direct precedure that is used to prevent transverse cracking. The serviceability/performance analysis provides a direct procedure that is used to prevent the occurrence of excessive roughness as indicated by the serviceability index which is an estimator of the user's acceptability of the pavement.

Limiting criteria have been selected for zero-maintenance design for fatigue damage and for serviceability index as described in Chapters 3 and 4.

(a) Fatigue Damage: A maximum allowable fatigue damage (or DAMAGE) as accumulated monthly over the entire design analysis period at the slab

edge, midway between joints, is $10^{-4}$ as computed by Eq. 4.13. However, since this value is very small and inconvenient to use in design, it was multiplied by a scale factor of $10^{6}$ so that the limiting value is 100. This value was set based upon fatigue analyses of 37 in-service pavements ranging in age from 6 to 34 years to give a high reliability that linear cracking from fatigue would be prevented. The computed fatigue damage for each of these pavements, prior to any cracks that occurred, was greater than this specified limiting value.

(b) Terminal Serviceability: The terminal serviceability index selected is 3.0. This value was set based upon observations on the 37 in-service pavements. Use of this value along with a reduction in the modulus of rupture provides a high reliability that the pavement will not require maintenance due to excessive roughness over the design analysis period.

A computer program was written to provide fatigue and serviceability data for use in design. The program is designated: JCP-1 (Jointed Concrete Pavement - 1) and is written in FORTRAN computer language for the IBM-360 digital computer. The program can be adapted for usage on other computers with only minor modifications. The computer processing time for a complete design problem is about 12 seconds. The storage requirement for the program is 50,000 locations. An input guide, sample input/output, flow chart, and program listing is given in the Appendix. The designer must specify trial structural designs, determine the required inputs, run the JCP-1 computer program, and analyze the output fatigue and serviceability data. The program is written to analyze any number of slab thicknesses and provide outputs for each thickness, while holding all other inputs constant.

The designer can therefore examine a range of slab thicknesses for a given traffic, foundation support, and environment with only one run of the program.

A complete detailed example of zero-maintenance design is given in Chapter 6 of Volume II (Ref. 1).

## 6.2 STRUCTURAL DESIGN VERIFICATION

Complete verification of the design procedure requires construction of the recommended designs in various climatic regions and observation of their performance over the design maintenance-free life. In lieu of this costly and time consuming procedure, a reasonable verification can be obtained by comparing the design and performance of various plain jointed concrete projects with a zero-maintenance design of each project. The zero-maintenance design period would be set equal to the existing life of the project under consideration, the design inputs would include the as-built construction data and the traffic applied to the project since its construction. It is desirable to use projects that were not used in the development of the design procedure. Due to the limited funding and time available this was not possible. Thus, the 37 projects are used to provide a partial verification of the procedure. The following steps were followed for each project:

1. As-built construction data (material strength, joint design, thicknesses, etc) were obtained from the agency responsible for its construction. Traffic data over the life of the project were also obtained (See Chapters 2, 3, and 4).

2. The foundation including subbase and subgrade and the joint design were kept the same as the existing project, and all other necessary inputs

to the zero-maintenance design procedures determined.

3. The required slab thickness necessary to meet the fatigue damage and serviceability limiting design criteria were then obtained using the design procedure.

4. The new design slab thickness was compared with the actual slab thickness and performance of the pavement. Conclusions were made based upon this comparison.

A summary of results from each of the projects is given in Table 6.1, and a discussion of these results for selected projects is provided.

1. AASHO Road Test Site: Existing pavements are 16 years old with slab thicknesses of 8, 9.5, 11, and 12.5 ins. (203, 241, 279, 318 mm) and a transverse doweled joint spacing of 15 ft. (4.6 m). A summary of significant performance data are as follows:

| Slab | Cracking ($ft/1000\ ft^2$) | Joint Faulting | Final Serviceability Index |
|---|---|---|---|
| 8 in. | 20 | 0.25 in. | 1.7 |
| 9.5 | 3 | 0.07 | 3.1 |
| 11 | 0 | 0.04 | 3.3 |
| 12.5 | 0 | 0.03 | 3.6 |

The 8 and 9-1/2 inch (293, 241 mm) slabs received patching and crack repair. The thicker slabs did not require maintenance with the exception that some patching was also needed due to joint spalling caused by "D" cracking. The thickness of slab provided by the zero-maintenance design was 10.7 ins. (272 mm) with fatigue controlling the thickness. This pavement constructed over the existing foundation and having similar materials and joint design would not crack or fault and the serviceability index is

Table 6.1. Comparison of Zero-Maintenance Design with Original Design of Projects.

| Project No. and Location | Zero-Maintenance Design Slab Thick (in.) Fatigue | Zero-Maintenance Design Slab Thick (in.) Serviceability | Existing Slab Thick (in.) | ±ΔH (in.) | Did Existing Pavement Receive Maintenance? | Is Z.M. Design Adequate?* |
|---|---|---|---|---|---|---|
| 1-3, IL | 10.7 | 9.5 | 8 | +2.7 | Yes | Yes |
| 4-14, IL | 10.7 | 9.5 | 9.5 | +1.2 | Yes | Yes |
| 15-22, IL | 10.7 | 9.5 | 11 | -0.3 | No | Yes |
| 23-25, IL | 10.7 | 9.5 | 12.5 | -1.8 | No | Yes |
| 26, WA | 10.2 | <9.0 | 9 | +1.2 | No | Yes |
| 27, CA | 10.4 | 8.2 | 8 | +2.4 | Yes | Yes |
| 28, CA | 10.5 | 10.8 | 8 | +2.8 | No** | Yes |
| 29, TX | 10.4 | <9.0 | 10 | +0.4 | No | Yes |
| 30, UT | 10.5 | <9.0 | 9 | +1.5 | No | Yes |
| 31, AZ | 10.4 | 9.7 | 9 | +1.4 | No | Yes |
| 32, NJ | 10.8 | 12.1 | 10 | +2.1 | No** | Yes |
| 33, GA | 12.8*** | 10.4 | 8 | +4.8 | Yes | Yes |
| 34, CO | 10.8 | <8.0 | 8 | +2.8 | Yes | Yes |
| 35, CO | 10.0 | 8.0 | 8 | +2.0 | No | Yes |
| 36, MI | 14.1*** | 12.0 | 10 | +4.1 | Yes | Yes |
| 37, ONT | 11.6 | <9.0 | 9 | +2.6 | No | Yes |

*Additional components design for joints, subsurface drainage, subbase, and shoulders not shown here, but would follow recommendations given in design manual (Ref. 1).

**Pavement did not receive maintenance but was in need of maintenance.

***These slab thicknesses are very large because joint spacing was very long. Recommended maximum joint spacing is 17 ft (5 m). Design thickness would be much less at this joint spacing.

above 3.0 over the 16 year period. In addition, subsurface drainage is recommended since the project is located in a wet-freeze climate. Figure 6.1 shows slab cracking vs. slab thickness. Full depth asphalt or concrete shoulders are also recommended. Thus, the new design would be expected to provide maintenance-free performance over the 16 year period. A higher quality PCC must be provided, however, to prevent the spalling caused by "D" cracking.

2. JCP-27 and 28, California: These pavements both have 8 in. (203 mm) PCC slabs over 4 ins. (102 mm) of cement treated subbases, non-doweled joint spacing of 15 ft. (4.6 m), and they are both 20 years old. Both projects have significant faulting and some transverse cracking. JCP-27 has received some patching and crack filling maintenance, but JCP-28 is maintenance-free. However, both may require maintenance soon due to the joint faulting condition. It is interesting to note that JCP-28 was subjected to the heaviest traffic of any project surveyed (39 million 18 kip ESAL). The zero-maintenance design slab thickness is 10.4 and 10.8 ins. (264, 274 mm) for JCP-27 and 28, respectively. This increase in slab thickness would reduce joint faulting and transverse cracking on both projects, and should definitely provide maintenance-free performance over the 20 year period.

3. JCP-32, New Jersey: This project is 25 years old and its design consists of 10 in. (254 mm) PCC slab, 12 ins. (305 mm) granular non-pumping subbase, 15 ft. (4.6 m) transverse non-doweled joint spacing, and very high quality PCC. It has been subjected to very heavy traffic (i.e., 36 million 18-kip ESAL). The pavement has significant joint faulting but no cracking and the project has never received maintenance. The

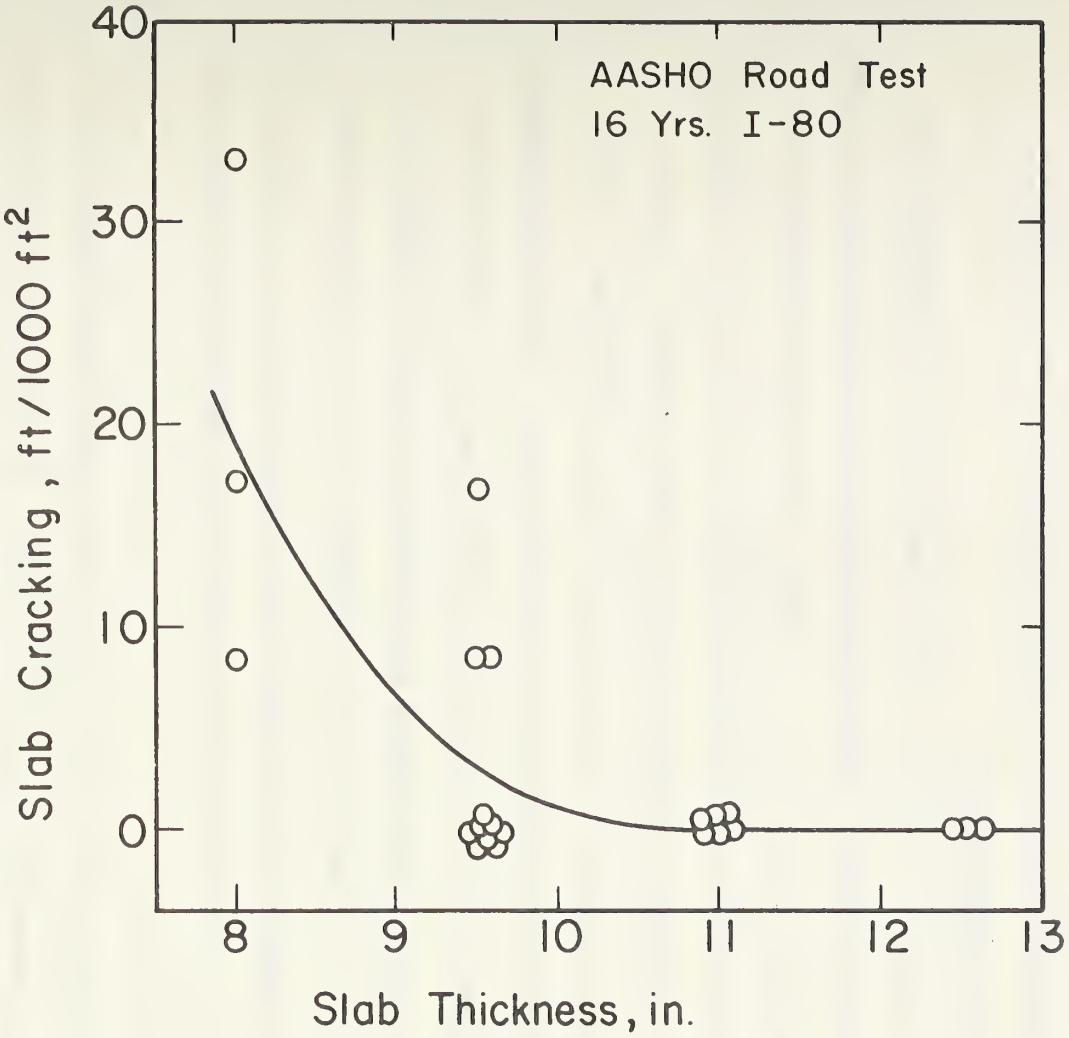


Figure 6.1. Effects of Slab Thickness on Slab Cracking.

zero-maintenance design slab thickness is 12.1 in. (307 mm) with serviceability criteria controlling the design. Dowel bars and subsurface drainage would be recommended for this project since it is located in a wet-freeze climate to prevent faulting. This thicker slab design, and other recommendations would be expected to provide maintenance-free performance over the 25 year design period.

4. JCP-34 and 35, Colorado: These two 10 year old projects have similar designs of 8 ins. (203 mm) PCC slab, granular subbase and subgrade, and non-doweled transverse joints. However, JCP-34 has a longer joint spacing (12-19 ft. [3.7-5.8 m]) than JCP-35 (15 ft. [9.6 m]). JCP-34 has considerable transverse cracking and some corner cracking, and also significant joint faulting and has received some maintenance. JCP-35 does not have any cracking and only minor faulting. The zero-maintenance slab thicknesses are 10.8 and 10.0 in. (274-254 mm) for JCP-34 and 35, respectively, with fatigue damage controlling the design. Dowel bars and a stabilized subbase are also recommended in this dry-freeze region. Thus, this recommended design should prevent both transverse cracking and joint faulting and provide zero-maintenance over the 10 year period, and probably much longer.

Other projects show similar results with the zero-maintenance slab design always exceeding the existing design. The long joint spacings on JCP-33 and 36 (30 and 25 ft. [9.1-7.6 m]) have a great effect on the zero-maintenance slab thickness. If joint spacing were reduced to 15 ft. (4.6 m), for example, design slab thickness as required by fatigue is much less. Overall, while it is desirable to obtain additional data for further verification, the available results show that the new design procedure gives

designs that exceed existing designs that have provided long term maintenance-free performance.

# CHAPTER 7

# CONCLUSIONS AND RECOMMENDATIONS

## 7.1 CONCLUSIONS

Comprehensive design procedures for heavily trafficked zero-maintenance plain jointed concrete pavements have been developed. This report (Vol. I) describes the field, laboratory and analytical studies upon which the procedures are based and provides research documentation. Based upon these results, a design manual was prepared (Vol. II) that contains all necessary procedures needed for actual design. A computer program designated JCP-1 was developed that is used to obtain fatigue damage and serviceability data for use in the structural design. The program is written in FORTRAN and is easily adaptable to most computers. The term "zero-maintenance" refers to the structural adequacy of the pavement lanes and shoulder. Thus, a "zero-maintenance" pavement would not require maintenance such as patching, joint repair, crack repair, grinding, and overlays.

1. Field surveys of several plain jointed concrete pavements revealed several that have given zero-maintenance performance over time periods ranging up to 25 years under very heavy traffic. Therefore, it is possible to achieve a "zero-maintenance" performance over long time periods. Several projects, however, exhibited distress that required maintenance. The following distress types commonly occurring in heavily trafficked plain jointed concrete pavements must be considered in design and thereby prevented: (1) joint faulting, (2) transverse cracking, (3) "D" cracking, (4) joint and corner spalling, (5) joint seal damage, (6) settlement of slabs, and (7) shoulder deterioration.

2. Comprehensive fatigue damage analysis procedures were developed that permit direct consideration of slab cracking. Stresses due to both traffic loading and thermal gradients are considered in the analysis through use of a finite element model. A fatigue damage limiting design criteria was determined from field data that provides a high reliability for preventing slab cracking.

3. A new serviceability/performance design model was derived for plain jointed concrete pavements. The new model was derived from performance data of 25 sections of the original AASHO Road Test that have been under heavy mixed traffic on I-80 since 1962. The performance model was "extended" using Westergaard's edge stress model and through the incorporation of a climatic factor. The serviceability/performance analysis provides consideration of various distress including joint faulting, slab cracking, settlement of slabs, spalling, etc.

4. Design recommendations were developed for joint spacing, load transfer, and sealants. These factors were found to have a major effect on pavement zero-maintenance life.

5. Use of full depth asphalt or concrete shoulders and subsurface drainage systems are strongly recommended.

6. An example design application is provided that describes the use of the procedure in detail. The economic justification for constructing a zero-maintenance pavement is presented along with an example in Volume II. The additional cost increment for constructing a zero-maintenance pavement over a conventional pavement is determined for two different geographic areas and two levels of traffic and found to vary from 12 to 24 percent.

7. Adequacy of the design procedures are assessed in terms of structural

sufficiency and also through a sensitivity analysis. The results show that the procedure provides designs that structurally exceed those of projects that have performed maintenance-free over long time periods and subject to heavy traffic.

8. The design procedures and results documented herein can be used for numerous purposes other than zero-maintenance design. The effect of the following variables on slab cracking and performance can be analyzed: slab thickness, concrete strength and variation, foundation support (subbase and subgrade including degree of saturation), lane width, lateral distribution of traffic, thermal gradients, traffic overloads, lane distribution of trucks, joint spacing and others.

## 7.2 RECOMMENDATIONS

The zero-maintenance pavement design procedures documented herein and in the design manual (Ref. 1) are ready for trial implementation. They have been partially verified and shown to give adequate pavement structures. Many additional findings related to the design of plain jointed concrete pavements are believed to be significant and useful in minimizing the occurrence of distress and thus reducing maintenance costs.

Trial implementation should proceed by selecting states that are willing to cooperate and are located in each of the four climatic regions. The state in consultation with FHWA and the project staff would select one or more heavily trafficked projects for consideration (either new designs or reconstructions). Zero-maintenance designs would then be developed by the state agency with the assistance of the project staff. The results would then be evaluated for adequacy by the state personnel, FHWA, and the Project staff. Any necessary modifications to the zero-maintenance design procedures be made so that it would be ready for implementation.

## REFERENCES


1. Darter, M. I., and E. J. Barenberg, "Design of Plain Jointed Concrete Pavements: Vol II - Design Manual," University of Illinois, Technical Report to Federal Highway Administration, June, 1977.

2. Darter, M. I. and E. J. Barenberg, "Zero-Maintenance Pavement: Results of Field Studies on the Performance Requirements and Capabilities of Conventional Pavement Systems," Technical Report prepared for Federal Highway Administration, University of Illinois at Urbana-Champaign, April, 1976.

3. Butler, B. C., Jr., "Traffic Warrants for Premium Pavement Requiring Reduced Maintenance," Vol. I, II, III, DOT-FH-11-8132, prepared for Federal Highway Administration, September, 1974.

4. Treybig, H. J., Hudson, W. R., and A. Abou-Ayyash, "Application of Slab Analysis Methods to Rigid Pavement Problems," Research Report 56-26, Center for Highway Research, The University of Texas at Austin, May, 1972.

5. Eberhardt, A. C. and J. L. Willmer, "Computer Program for the Finite Element Analysis of Concrete Airfield Pavements," Technical Report S-26, Construction Engineering Research Laboratory, 1973.

6. "The Multiple Wheel Load Elastic Layer Program," University of Illinois, Highway Pavements and Materials Group, Department of Civil Engineering.

7. "The Finite Element Program for Pavement Analysis - User's Manual," Department of Civil Engineering, University of Illinois, 1973.

8. Zienkiewicz, O. C., and Y. K. Cheung, The Finite Element Method in Structural and Continuum Mechanics, McGraw-Hill, 1967.

9. "The AASHO Road Test - Report 5 - Pavement Research," Special Report 51E, Highway Reserach Board, 1962.

10. Hudson, W. R., and F. H. Scrivner, "AASHO Road Test Principal Relationships - Performance with Stress, Rigid Pavements," Special Report 73, Highway Research Board, 1962.

11. Teller, L. W., and E. C. Southerland, "The Structural Design of Concrete Pavement," Part 1 - A Description of the Investgation, Public Roads, Vol. 16, No. 8, 1935.

12. Teller, L. W., and E. C. Southerland, "The Structural Design of Concrete Pavements," Part 2 - Observed Effects of Variations in Temperature and Moisture on the Size, Shape and Stress Resistance of Concrete Pavement Slabs, Public Roads, Vol. 16, No. 9, 1935.

13. Teller, L. W., and E. C. Southerland, "The Structural Design of Concrete Pavements," Part 3 - A Study of Concrete Pavement Cross Sections, Public Roads, Vol. 16, No. 10, 1935.

14. Teller, L. W., and E. C. Southerland, "The Structural Design of Concrete Pavements," Part 4 - A Study of the Structural Action of Several Types of Transverse and Longitudinal Joint Designs, Public Roads, Vol. 17, Nos. 7 and 8, 1936.

15. Teller, L. W., and E. C. Southerland, "The Structural Design of Concrete Pavements," Part 5 - An Experimental Study of the Westergaard Analysis of Stress Conditions in Concrete Pavement Slabs of Uniform Thickness, Public Roads, Vol. 23, No. 8, 1943.

16. Hatt, W. K., "Effect of Moisture on Concrete," Public Roads, Vol. 6, No. 1, March 1925; also Trans. ASCE, Vol. 84, 1926.

17. Westergaard, H. M., "Analysis of Stresses in Concrete Pavements Due to Variations in Temperature," Proc. Sixth Annual Meeting, Highway Research Board, 1927; also Public Roads, Vol. 8, No. 3, May, 1927.

18. Bradbury, R. D., Reinforced Concrete Pavements, Wire Reinforcement Institute, Washington, D. C., 1938.

19. Finney, E. A., and L. T. Oehler, "Final Report on Design Project, Michigan Test Road," Proc. Highway Research Board, Vol. 38, 1959.

20. Carsberg, E. C., and P. G. Velz, "Report on Experimental Project in Minnesota," Research Report 17-B, Highway Research Board, 1956.

21. "Concrete Manual," Seventh Edition, United States Dept. of the Interior, Bureau of Reclamation, Denver, CO, 1966.

22. Carlson, R. W., "Drying Shrinkage of Concrete as Affected by Many Factors," Proceedings, Vol. 38, Part II, ASTM, 1938.

23. Davis, R. E., "A Summary of Investigations of Volume Changes in Cements, Mortars, and Concretes Produced by Causes Other Than Stress," Proceedings, Vol. 30, Part I, ASTM, 1930.

24. Goldbeck, A. T., "Friction Tests for Concrete on Various Subbases," ACI Proceedings, Vol. 8, 1917.

25. Lin, T. Y., Design of Prestressed Concrete Structures, Wiley, Second Edition, New York, 1963.

26. Goldbeck, A. T., "Friction Tests of Concrete on Various Subbases," Public Roads, July, 1924.

27. Harr, M. E., and G. A. Leonards, "Warping Stresses and Deflections in Concrete Pavements," Proceedings, 38th Annual Meeting, 1959, Highway Research Board.

28. Wiseman, M. E. Harr, and G. A. Leonards, "Warping Stresses and Deflections in Concrete Pavements, Part II," presented at the 39th Annual Meeting, 1960, Highway Research Board.

29. Moore, J. H., with discussions by E. C. Sutherland and Warner Harwood, "Thickness of Concrete Pavements," Transactions, ASCE, Vol. 121, Paper No. 2834, 1956.

30. Miner, M. A., "Cumulative Damage in Fatigue," Transactions, Am. Soc. of Mechanical Engr., Vol. 67, 1945, pp. A159-A164.

31. Kelley, E. F., "Applications of the Results of Research to the Structural Design of Concrete Pavement," Public Roads, Vol. 20, No. 5, July, 1939.

32. Murcock, J. W., "A Critical Review of Research on Fatigue of Plain Concrete," Eng. Exp. Station, University of Illinois, Bulletin 476, 1965, 32 pp.

33. Nordby, G. M., "Fatigue of Concrete - A Review of Research," Proceedings, Am. Concrete Inst., Vol. 55, 1959, pp. 191-220.

34. Statens institute for byggnadsforskning. Rapport 22: 1969: Utmattning av betond och armerad betong. En litteraturoversikt. (Fatigue of plain and reinforced concrete. A survey of literature), by B. Westerberg. Stockholm, Sweden, Svensk Byggtjanst, 1969.

35. Hilsdorf, H. K., and Kesler, C. E., "Fatigue Strength of Concrete Under Varying Flexural Stresses," Proceedings, Am. Concrete Inst., Vol. 63, 1966, pp. 1059-1976.

36. Raithby, K. W., and Whiffin, A. C., "Failure of Plain Concrete Under Fatigue Loading - A Review of Current Knowledge," Road Research Laboratory, Report LR 231, Berkshire, England, 1968, 23 pp.

37. McCall, J. T., "Probability of Fatigue Failure of Plain Concrete," Proceedings, Am. Concrete Inst., Vol. 55, 1959, pp. 233-245.

38. Murdock, J. W., and Kesler, C. E., "Effect of Range of Stress on Fatigue Strength of Plain Concrete Beams," Proceedings, Am. Concrete Inst., Vol. 55,1959, pp. 221-231.

39. Ople, F. S., Jr., and C. L. Hulsbos, "Probable Fatigue Life of Plain Concrete with Stress Gradient," Proceedings, Am. Concrete Inst., Vol. 63, 1966, pp. 59-81.

40. Clemmer, H. F., "Fatigue of Concrete," Proceedings, Am. Soc. of Testing and Materials, Vol. 22, Part II, 1922, pp. 408-419.

41. Kesler, C. E., "Effect of Speed of Testing on Flexural Strength of Plain Concrete," Proceedings, Highway Research Board, Vol. 32, 1953, pp. 251-258.

42. Raithby, K. D., and J. W. Galloway, "Effects of Moisture Condition, Age, and Rate of Loading on Fatigue of Plain Concrete, SP-41, American Concrete Institute, 1974.

43. Ballinger, C. A., "Cumulative Fatigue Damage Characteristics of Plain Concrete," Highway Research Record No. 370, Highway Research Board, 1972.

44. Mills, . ., and . . Dawson. "Fatigue of Concrete," Highway Research Board Proceedings, Vol. , 1928.

45. Darter, M. I., and E. J. Barenberg, "Zero-Maintenance Pavement: Results of Field Studies on the Performance Requirements and Capabilities of Conventional Pavement Systems," Federal Highway Administration, Contract Number DOT-FH-11-8474, April 1976.

46. "The AASHO Road Test - Pavement Research," Special Report 61E, Highway Research Board, 1962.

47. Hveem, F. N., "Report on Experimental Project in California," Research Report 17-B, Highway Reserach Board, 1956.

48. Coons, H. C., "Report on Experimental Projection in Michigan," Research Report 17-B, Highway Research Board, 1956.

49. "Thickness Design for Concrete Pavements," Portland Cement Association, 1966.

50. Carsberg, E. C., and P. G. Velz, "Report on Experimental Project in Minnesota," Research Report 17-B, Highway Research Board, 1956.

51. "Road Test One - MD," Special Report 4, Highway Reserach Board, 1952.

52. Troxell, G. E., H. E. Davis, and J. W. Kelly, Composition and Properties of Concrete, 2nd Edition, McGraw-Hill, 1968.

53. Taragin, Asriel, "Lateral Placement of Trucks on Two Lane Highways and Four-Lane Divided Highways," Public Roads, Vol. 30, No. 3, August, 1958.

54. Emery, D. K., "A Preliminary Report on the Transverse Lane Displacement for Design Trucks on Rural Freeways," paper presented to the ASCE Pavement Design Speciality Conference, Atlanta, GA, June, 1975.

55. Dempsey, B. J., "A Heat Transfer Model for Evaluating Frost Action and Temperature-Related Effects in Multilayered Pavement Systems," Ph.D. Thesis, University of Illinois, Department of Civil Enginering, Urbana, Illinois, 1969.

56. Dempsey, B. J., and M. R. Thompson, "A Heat Transfer Model for Evaluating Frost Action and Temperature-Related Effects in Multilayered Pavement Systems, HRR NO. 342, HRB, 1970, pp. 39-56.

57. Van Breemen, W., "Current Design of Concrete Pavements in New Jersey," HRB Proceedings, Vol. 28, 1948.

58. "Structural Design of Portland Cement Concrete Pavements," Rev. Nov. 1970, Illinois Department of Transportation.

59. "Structural Design of the Roadbed," April 16, 1970, Planning Manual, California Department of Transportation.

60. AASHO Interim Guid for the Structural Desgin of Rigid Pavement Structures," Committee on Design, April, 1962.

61. "AASHO Interim Guide for Design of Pavement Structures," Washington, D. C., 20004, 1972.

62. McCullough, B. F., et. al., "Evaluation of AASHO Interim Guides for Design of Pavement Structures," NCHRP Report 128, Highway Research Board, 1972.

63. "Combined Average Annual Precipitation and Evaporation Map for the United States," compiled for the Federal Highway Administration, Robert G. Van Schooneveld, September, 1974.

64. Corps of Engineers, "Engineering and Design, Pavement Design for Frost Conditions," EM-1110-345-306, 1958.

65. Walker, R. S. and W. R. Hudson, "The Use of Spectral Estimates for Pavement Characterization," Research Report 156-2, CFHR, University of Texas, 1973.

66. Huang, Y. H., and S. T. Wang, "Finite Element Analysis of Concrete Slabs and Its Implications for Rigid Pavement Design," Highway Research Record 466, 1973.

67. Huang, Y. H., "Finite Element Analysis of Slabs on Elastic Solids," Transportation Engineering Journal of ASCE, Vol. 100, No. TE28, May 1974, pp. 403-416.

68. "Computer Program for Concrete Airport Pavement Design," Special Report, Portland Cement Association, 1968.

69. "Joint Design for Concrete Highway and Street Pavements," Portland Cement Association, 1975.

70. "Joint Spacing in Concrete Pavements," Highway Research Board, Research Airport 17-B, 1956.

71. Colley, B. E. and H. A. Humphrey, "Aggregate Interlock at Joints in Concrete Pavements," Highway Research Record No. 189, Highway Research Board, Washingtin, D. C., 1967.

72. Stelzenmulter, W. B., L. L. Smith, and T. J. Larson, "Load Transfer at Contraction Joints in Plain Portland Cement Concrete Pavements," Research Report 90-D, Florida Department of Transportation, April, 1973.

73. Darter, M. I., and W. B. Isakson, "Thermal Expansion and Contraction of Concrete Pavements in Utah," Interim Report, Project 915, Utah Department of Highways, 1970.

74. Gulden, Wouter, "Pavement Faulting Study," Final Report Project 7104, Georgia Department of Transportation, 1975.

75. Spellman, D. L., T. H. Woodstrom, and B. F. Neal, "Faulting of Portland Cement Concrete Pavements," Highway Research Record No. 407, Highway Research Board, 1972.

76. Friberg, B. F., "Design of Dowels in Transverse Joints of Concrete Pavements," Transactions, ASCE, Vol. 105, 1940.

77. "Design, Construction, and Maintenance of PCC Pavement Joints," Synthesis of Highway Practice No. 19, NCHRP, Washington, D. C., 1973.

78. "Evaluation of the Performance of Doweled Contraction Joints Placed on Three Types of Subbase Courses," Report No. 30, unpublished internal reports, Georgia Department of Transportation, February, 1974.

79. Griffin, H. W., "Transverse Joints in the Design of Heavy Duty Concrete Pavement," Proceedings HRB, Vol. 23, 1943.

80. Van Breeman, W., "Experimental Dowel Installations in New Jersey," Proc. HRB, Vol. 34, 1955.

81. Van Breeman, W., "Special Papers on the Pumping Action of Concrete Pavements," Research Reports No. 1D, Highway Research Board, 1945.

82. Cedergren, H. R., Drainage of Highway and Airfield Pavements, John Wiley & Sons, New York, 1974.

83. "Implementation Package for a Drainage Blanket in Highway Pavement Systems," Federal Highway Administration, May, 1972.

84. Barksdale, R. D., and R. G. Hicks, "Improved Pavement Shoulder Joint Design," Final Report NCHRP Project 14-3, June, 1975.

85. Cedergren, H. R., et al., "Guidelines for the Design of Subsurface Drainage Systems for Highway Structural Sections," Technical Report prepared for Federal Highway Administration, June, 1972.

86. Cedergren, H. R., "Methodology and Effectiveness of Drainage System for Airfield Pavements," Technical Report E-13, CERL, 1974.

87. Stromberg, F. J., and J. Weisner, "Inservice Behavior of Preformed Neoprene Joint Seals," Interim Report, Maryland State Highway Administration, 1972.

88. McBride, J. C., and M. S. Decker, "Performance Evaluation of Utah's Concrete Pavement Joint Seals," Final Report, Utah Department of Transportation, October, 1974.

89. Carlson, R. D., "Transverse Joint Construction and Sealing Practices," Research Report 20, New York State Department of Transportation, 1974.

90. "Evaluation of Preformed Elastomeric Pavement Joint Sealing Systems and Practices," NCHRP Research Results Digest 35, 1972.

91. Darter, M. I. and M. L. Hine, "PCC Joint Dowel Pullout Test Results," unpublished Report, Department of Civil Engineering, University of Illinois at Urbana-Champaign, 1975.

92. Bryden, J. E. and R. G. Phillips, "Performance of Transverse Joint Supports in Rigid Pavements," Research Report 12, New York State Department of Transportation, March, 1973.

93. Bryden, J. E., and R. G. Phillips, "New York's Experience with Plastic-Coated Dowels," Special Report 27, New York Department of Transportation, December, 1974.

94. "Structural Design Considerations for Pavement Joints," ACI Committee 325, ACI Journal, July, 1956.

95. Barksdale, R. D., and R. G. Hicks, "Improved Pavement Shoulder Joint Design," Final Report NCHRP Project 14-3, June, 1975, 151 pps.

96. Portigo, Josette M., "State of the Art Review of Paved Shoulders," paper presented at the 55th Annual Meeting of the Transportation Research Board, Washington, D. C., January, 1976.

97. Report of an Investigation on Potential Causes of Deterioration of the Shoulders on the Southwest Expressway, Professor E. J. Barenberg and Professor M. R. Thompson, Civil Engineering Department, University of Illinois, October 12, 1965.

98. Report No. 27, Portland Cement Concrete Shoulders (IHR-404), Illinois Divisions of Highways in cooperation with the U. S. Department of Transportation, Federal Highway Administration, and Bureau of Public Roads, July, 1970.

99. McKenzie, Lloyd J., Report No. 39, Experimental Paved Shoulders on Frost Susceptible Soils (IHR-404), Illinois DOT in cooperation with U. S. DOT and Federal Highway Administration.

100. "Concrete Shoulders." Portland Cement Association. 1975.

101. Spellman, D. L., J. H. Woodstrom, B. F. Neal, and P. E. Mason, "Recent Experimental PCC Pavements in California," Interim Report, California Division of Highways, Nov. 1072.

APPENDIX A

## A.1 INPUT GUIDE - JCP-1 PROGRAM

## ZERO-MAINTENANCE DESIGN OF PLAIN JOINTED CONCRETE PAVEMENT

### IDENTIFICATION OF PROBLEM

Three Cards

| 20A4 |
|---|
| 20A4 |
| 20A4 |

1 80

Enter descriptive identification of design project; date of run, project number, designer, etc. (Any or all of the cards may be left blank).

### DESIGN CRITERIA DATA

One Card

| F10.0 | F10.0 | F10.0 | F10.0 | I5 | |
|---|---|---|---|---|---|

1 10 20 30 40 45 80

DLIFE SIC PT OPEN KMONTH

DLIFE = Pavement zero-maintenance design life (years)

SIC = Initial serviceability index after construction

PT = Terminal serviceability index for zero-maintenance

OPEN = Time after PCC slab placement that pavement will be opened to traffic (years)

KMONTH = Month pavement will be opened to traffic (right justify) (Input 1 through 12 according to the following key: Jan=1, Feb=2, Mar=3, Apr=4, May=5, Jun=6, Jul=7 Aug=8, Sep=9, Oct=10, Nov=11, Dec=12)

### PRINTOUT DATA CONTROL

One Card

| 80I1 | |
|---|---|

1 DLIFE 80

Enter 1 in the columns that correspond to the years during which summary of fatigue and serviceability data will be printed.

One Card

| 80I1 |
|---|

1 DLIFE 80

Enter 1 in the columns that correspond to the years during which comprehensive fatigue output will be printed.

SLAB PROPERTIES DATA

One Card

| F5.0 | F5.0 | F5.0 | F5.0 | E10.3 | E10.3 | |
|---|---|---|---|---|---|---|

1 5 10 15 20 30 40 80
H L FF FCV ET E

H = Slab thickness - inches

L = Slab length - feet

FF = Mean PCC modulus of rupture (28 days) - psi

FCV = Coefficient of variation of PCC modulus of rupture - percent

ET = PCC coefficient of thermal expansion (per degree - F)

E = PCC modulus of elasticity (psi)

TRAFFIC DATA

One Card

| F10.0 | F10.0 | F10.0 | F10.0 | F10.0 | F10.0 | F10.0 | I5 | |
|---|---|---|---|---|---|---|---|---|

1 10 20 30 40 50 60 70 75 80
ADTI ADTF T LD DD A PC D

ADTI = Average daily traffic at beginning of design period - two direction

ADTF = Average daily traffic at end of design period - two direction

T = Percent trucks of ADT

LD = Percent trucks in heaviest traveled or design lane

DD = Percent direction distribution

SIX CARDS SET FOR EACH ADDITIONAL TRIAL PCC SLAB THICKNESS:

IDENTIFICATION OF PROBLEM

Three Cards (Same as first trial thickness).

| |
|---|
| 20A4 |
| 20A4 |
| 20A4 |

80

SLAB THICKNESS

One Card

| | |
|---|---|
| F5.0 | |

1 5 80

H

H = New Slab Thickness, inches

CONTROL DATA

One Card

| | |
|---|---|
| 80I1 | |

1 DLIFE 80

Enter 1 in the columns that correspond to the years during which summary of fatigue and serviceability data will be printed.

One Card

| | |
|---|---|
| 80I1 | |

1 DLIFE 80

Enter 1 in the columns that correspond to the years during which comprehensive fatigue output will be printed.

FINAL CARD OF DATA DECK

| |
|---|
| /* |

12 80

/* indicates end of data deck

A = Mean axles per truck

PC = Percent trucks during daylight

D = Mean distance from slab edge to outside of truck duals (in.) (right justify)

One Card

| I5 | I5 | |
|---|---|---|

1 5 10 80

KK KSAL

KK = Number of axle load distribution groups (single plus tandem) (right justify)

KSAL = Number of single axle load distribution groups (right justify)

As Many Cards As Needed

| F10.0 | F10.0 | F10.0 | F10.0 | F10.0 | F10.0 | F10.0 | F10.0 |
|---|---|---|---|---|---|---|---|
| F10.0 | F10.0 | F10.0 | F10.0 | F10.0 | F10.0 | F10.0 | F10.0 |

1 10 20 30 40 50 60 70 80

LOAD(I)

[LOAD(I), I=1,KK]

LOAD(I) = The highest value of each axle load distribution group (first enter single axle loads (KSAL) and then tandem axle loads)(pounds)

As Many Cards As Needed

| F10.0 | F10.0 | F10.0 | F10.0 | F10.0 | F10.0 | F10.0 | F10.0 |
|---|---|---|---|---|---|---|---|
| F10.0 | F10.0 | F10.0 | F10.0 | F10.0 | F10.0 | F10.0 | F10.0 |

1 10 20 30 40 50 60 70 80

DIST(I)

[DIST(I),I=1,KK]

DIST(I) = The percentage axle loads in each of the KK axle load groups input in the previous card (first enter single axle percentage and then tandem axle percentage)

One Card:

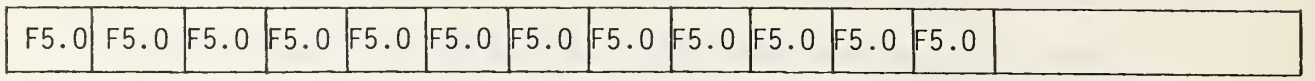


1 5 10 15 20 25 30 35 40 45 50 55 60 80

TRUKPC(I)

[TRUKPC(I),I=1,12]

TRUKPC(I) = The monthly truck percentage over year (enter percentage for first month pavement will be opened to traffic in Columns 1-5, 2nd month in Columns 6-10, etc.)

FOUNDATION SUPPORT DATA:

One Card:

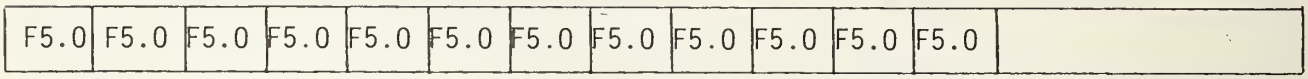


1 5 10 15 20 25 30 35 40 45 50 55 60 80

K(J)

[K(J),J=1,12]

K(J) = Modulus of foundation support (k-value at top of subbase) for each month in pci (enter k-value for first month pavement will be opened to traffic in Columns 1-5, 2nd month in Columns 6-10, etc.)

One Card:

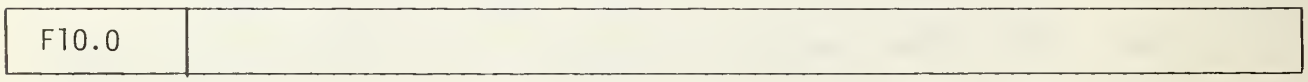


1 10 80

ERODEF

ERODEF = The amount of erodability of foundation at the end of design life in inches.

One Card:

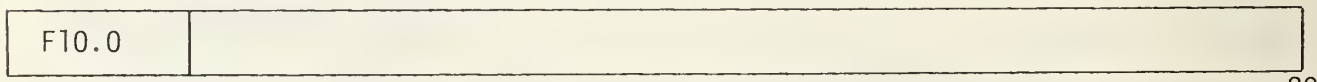


1 10 80

DK

DK = Design modulus of foundation support for serviceability/performance analysis in pci.

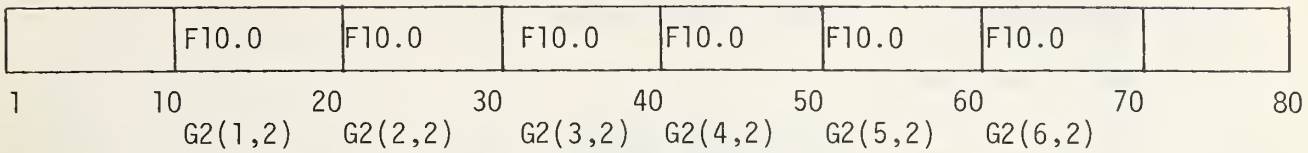


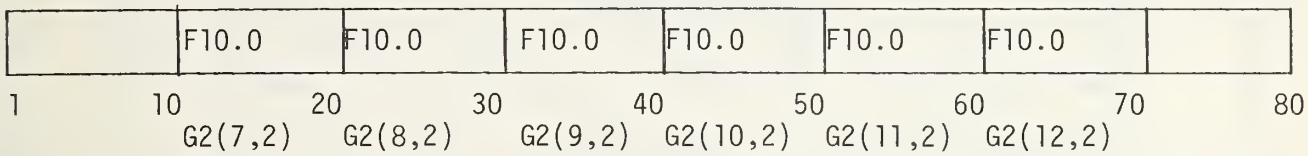


H2 = PCC slab thickness for relatively thick slab (usually 12 inches) - inches

G2(J,M) = Mean temperature gradients for slab of H2 thickness for each month, day, and night where
J = index for months
(J=1 for first month opened to traffic)
M = index for day (M=1) and night (M=2)

One Card

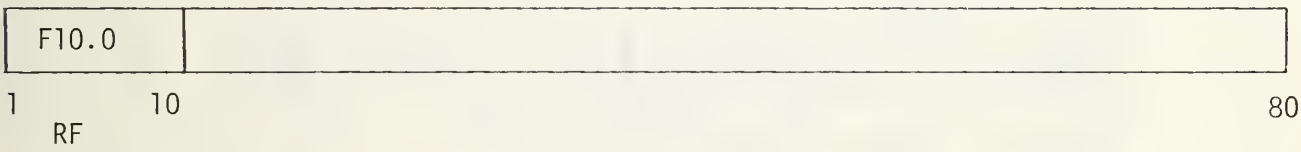


RF = Regional factor

The cards shown on the following page may be added for each additional PCC slab thickness to be analyzed:

ENVIRONMENTAL DATA (TWO SETS OF FOUR CARDS):

Set One - Four Cards

| F10.0 | F10.0 | F10.0 | F10.0 | F10.0 | F10.0 | F10.0 | |
|---|---|---|---|---|---|---|---|
| 1 | 10 | 20 | 30 | 40 | 50 | 60 | 70 80 |
| H1 | G1(1,1) | G1(2,1) | G1(3,1) | G1(4,1) | G1(5,1) | G1(6,1) | |

| | F10.0 | F10.0 | F10.0 | F10.0 | F10.0 | F10.0 | |
|---|---|---|---|---|---|---|---|
| 1 | 10 | 20 | 30 | 40 | 50 | 60 | 70 80 |
| | G1(7,1) | G1(8,1) | G1(9,1) | G1(10,1) | G1(11,1) | G1(12,1) | |

| | F10.0 | F10.0 | F10.0 | F10.0 | F10.0 | F10.0 | |
|---|---|---|---|---|---|---|---|
| 1 | 10 | 20 | 30 | 40 | 50 | 60 | 70 80 |
| | G1(1,2) | G1(2,2) | G1(3,2) | G1(4,2) | G1(5,2) | G1(6,2) | |

| | F10.0 | F10.0 | F10.0 | F10.0 | F10.0 | F10.0 | |
|---|---|---|---|---|---|---|---|
| 1 | 10 | 20 | 30 | 40 | 50 | 60 | 70 80 |
| | G1(7,2) | G1(8,2) | G1(9,2) | G1(10,2) | G1(11,2) | G1(12,2) | |

H1 = PCC slab thickness for relatively thin slab (usually 8 inches) - inches

G1(J,M) = Mean temperature gradients for slab of H1 thickness for each month, day, and night where
J = index for months
(J=1 for first month opened to traffic)
M = index for day (M=1) and night (M=2)

Set Two - Four Cards

| F10.0 | F10.0 | F10.0 | F10.0 | F10.0 | F10.0 | F10.0 | |
|---|---|---|---|---|---|---|---|
| 1 | 10 | 20 | 30 | 40 | 50 | 60 | 70 80 |
| H2 | G2(1,1) | G2(2,1) | G2(3,1) | G2(4,1) | G2(5,1) | G2(6,1) | |

| | F10.0 | F10.0 | F10.0 | F10.0 | F10.0 | F10.0 | |
|---|---|---|---|---|---|---|---|
| 1 | 10 | 20 | 30 | 40 | 50 | 60 | 70 80 |
| | G2(7,1) | G2(8,1) | G2(9,1) | G2(10,1) | G2(11,1) | G2(12,1) | |

IBM

FORTRAN Coding Form

GX28-7327-6 U/M 050** Printed in U.S.A.

PROGRAM: ZERO MAINTENANCE DESIGN - EXAMPLE PROBLEM (JCP-1) | PUNCHING INSTRUCTIONS | GRAPHIC | PAGE 1 OF 2

PROGRAMMER: M. I. DARTER | DATE: 2 JULY 1976 | PUNCH | CARD ELECTRO NUMBER*

| COMM. | STATEMENT NUMBER | CONT. | FORTRAN STATEMENT | IDENTIFICATION SEQUENCE |
|---|---|---|---|---|
| | | | (BLANK CARD) | |
| | | | ZERO-MAINTENANCE DESIGN -- EXAMPLE PROBLEM -- 9-INCH SLAB | |
| | | | (BLANK CARD) | |
| | | | 20.0 4.5 3.0 0.16 10 | |
| | | | 1 0001 0 0001 0 0001 0 0001 0 0001 | |
| | | | 0 0000 0 0000 0 0000 0 0000 0 0000 | |
| | | | 9.00 15.0 650. 12. 5.E-06 5.E+06 | |
| | | | 7 0000. 9 0000. 10. 60.0 50. 2.75 60. | 18 |
| | | | 32 14 | |
| | | | 3 0000. 7 0000. 8 0000. 12 0000. 16 0000. 18 0000. 20 0000. 22 000. | |
| | | | 24 0000. 26 0000. 28 000. 30 000. 32 000. 34 000. 6 000. 2 000. | |
| | | | 18 0000. 24 0000. 30 000. 32 000. 34 000. 36 000. 38 000. 40 000. | |
| | | | 42 0000. 44 0000. 46 000. 48 000. 50 000. 52 000. 54 000. 56 000. | |
| | | | 7.28 16.23 7.75 15.01 4.75 1.94 1.32 1.02 | |
| | | | 0.42 0.14 0.06 0.02 0.01 0.01 0.01 9.76 | |
| | | | 4.36 5.68 8.92 4.90 4.30 3.40 1.40 0.43 | |
| | | | 0.19 0.08 0.06 0.03 0.02 0.02 0.01 0.01 | |
| | | | 8.33 8.33 8.33 7.00 7.00 7.00 8.36 9.33 9.33 9.33 9.33 8.33 | |
| | | | 240. 224. 224. 500. 500. 135. 178. 190. 240. 240. 240. 240. | |
| | | | 13.0 | |
| | | | 212.0 | |
| | | | 8.0 0.88 0.72 0.57 0.45 0.32 0.86 | |
| | | | 1.59 1.46 1.58 2.08 1.73 1.34 | |
| | | | -0.80 -0.79 -0.50 -0.84 -0.78 -0.87 | |

*A standard card form, IBM electro 888157, is available for punching statements from this form.

**Number of forms per pad may vary slightly



Coded input data for example problem design (Four trial slab thicknesses are run with this input).

IBM

FORTRAN Coding Form

GX28-7327-6 U/M 050**
Printed in U.S.A.

PROGRAM ZERO MAINTENANCE DESIGN - EXAMPLE PROBLEM (JCP-1) | PUNCHING INSTRUCTIONS | GRAPHIC | PAGE 2 OF 2

PROGRAMMER M. I. D. | DATE 2 JULY 1976 | PUNCH | CARD ELECTRO NUMBER*

| COMM | STATEMENT NUMBER | CONT | FORTRAN STATEMENT | IDENTIFICATION SEQUENCE |
|---|---|---|---|---|
| | | | -0.62 -0.72 -0.90 -0.91 -1.00 -1.13 | |
| | 12.0 | | 0.56 0.43 0.40 0.27 0.18 0.59 | |
| | | | 1.11 0.99 1.88 1.54 1.32 0.92 | |
| | | | -0.62 -0.64 -0.37 -0.63 -0.57 -0.62 | |
| | | | -0.41 -0.49 -0.57 -0.54 -0.63 -0.83 | |
| | 1.0 | | | |
| | | | (BLANK CARD) | |
| | | | ZERO-MAINTENANCE DESIGN -- EXAMPLE PROBLEM -- 11-INCH SLAB | |
| | | | (BLANK CARD) | |
| | 11.00 | | | |
| | | | 10001 00001 00001 00001 | |
| | | | 00000 00000 00000 00000 | |
| | | | (BLANK CARD) | |
| | | | ZERO-MAINTENANCE DESIGN -- EXAMPLE PROBLEM -- 13-INCH SLAB | |
| | | | (BLANK CARD) | |
| | 13.00 | | | |
| | | | 10001 00001 00001 00001 | |
| | | | 10000 00000 00000 00000 | |
| | | | (BLANK CARD) | |
| | | | ZERO-MAINTENANCE DESIGN -- EXAMPLE PROBLEM -- 15-INCH SLAB | |
| | | | (BLANK CARD) | |
| | 15.00 | | | |
| | | | 10001 00001 00001 00001 | |
| | | | 00000 00000 00000 0000 0 | |

*A standard card form, IBM electro 888157, is available for punching statements from this form

**Number of forms per pad may vary slightly

A.3 FLOW CHART OF PROGRAM

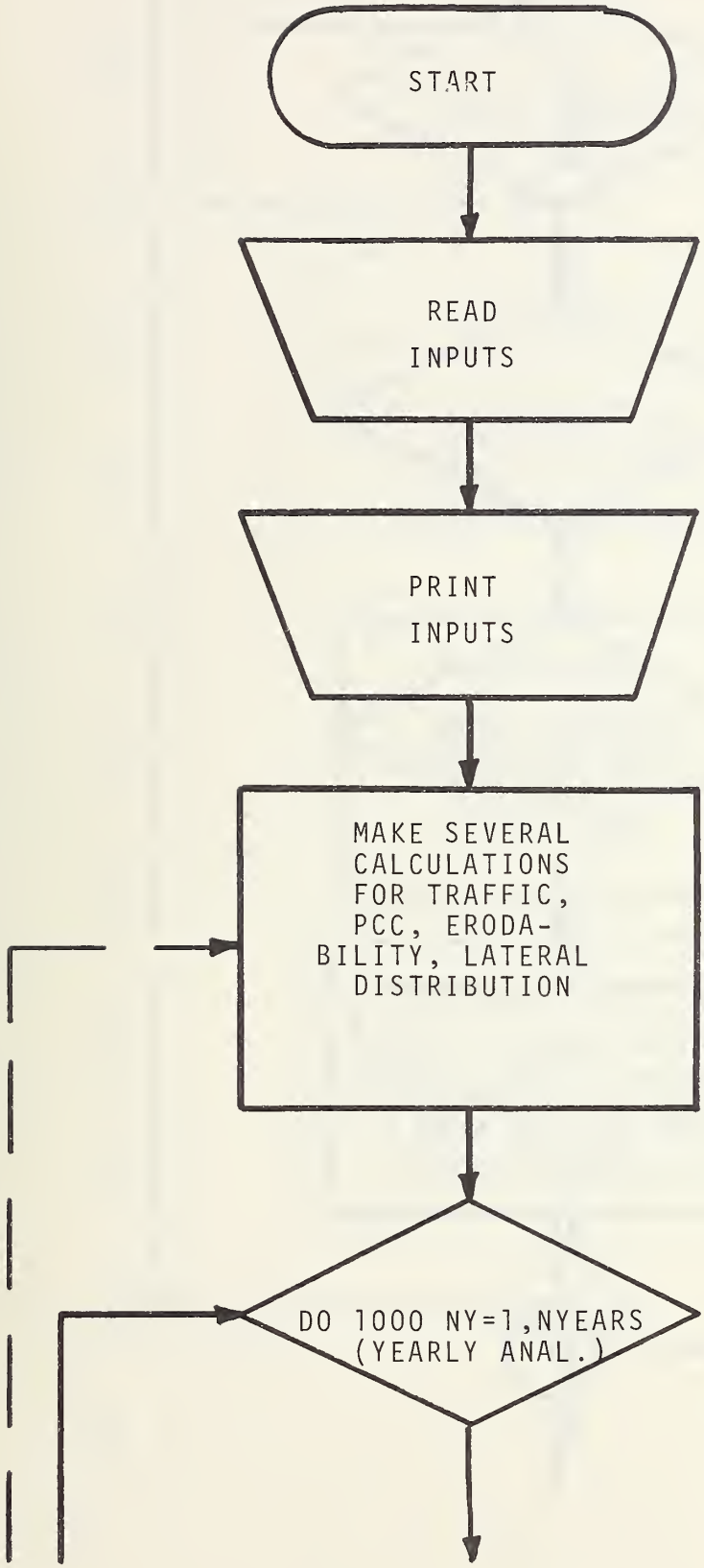

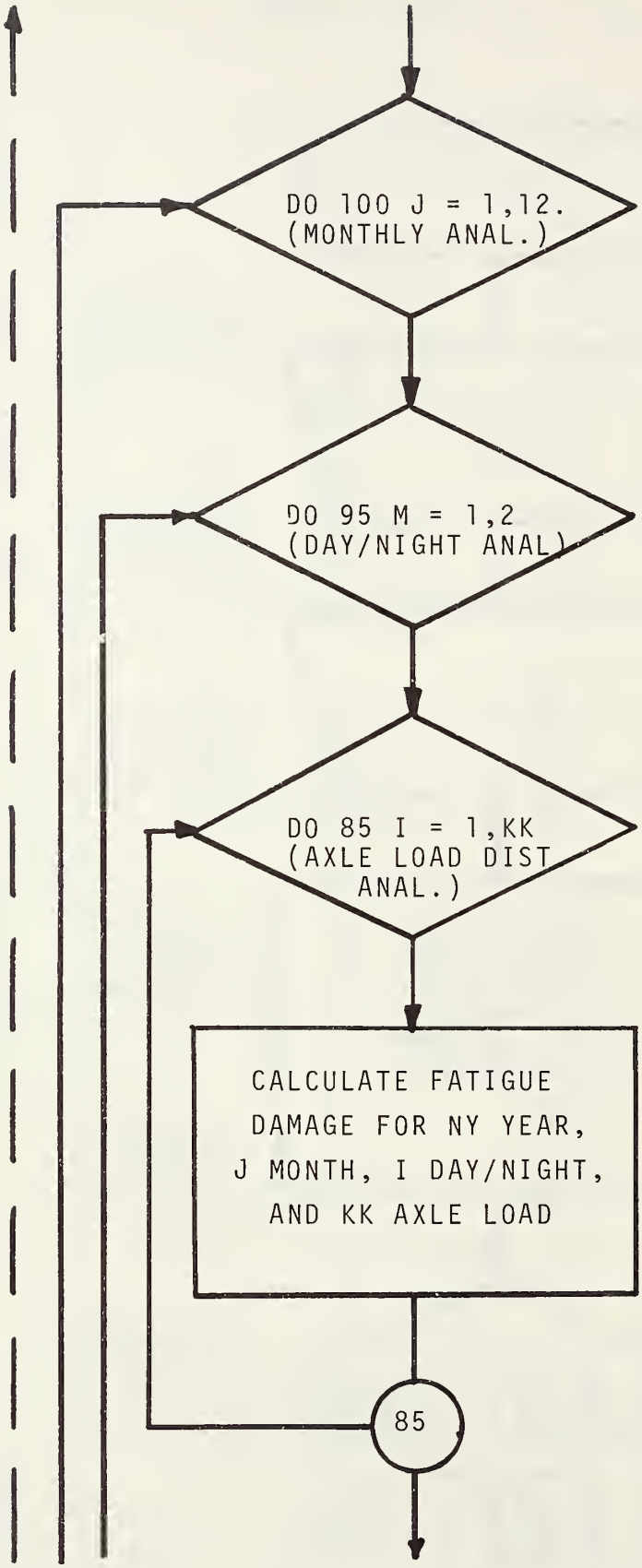
DO 100 J = 1,12.
(MONTHLY ANAL.)
DO 95 M = 1,2
(DAY/NIGHT ANAL)
DO 85 I = 1,KK
(AXLE LOAD DIST
ANAL.)
CALCULATE FATIGUE
DAMAGE FOR NY YEAR,
J MONTH, I DAY/NIGHT,
AND KK AXLE LOAD
85

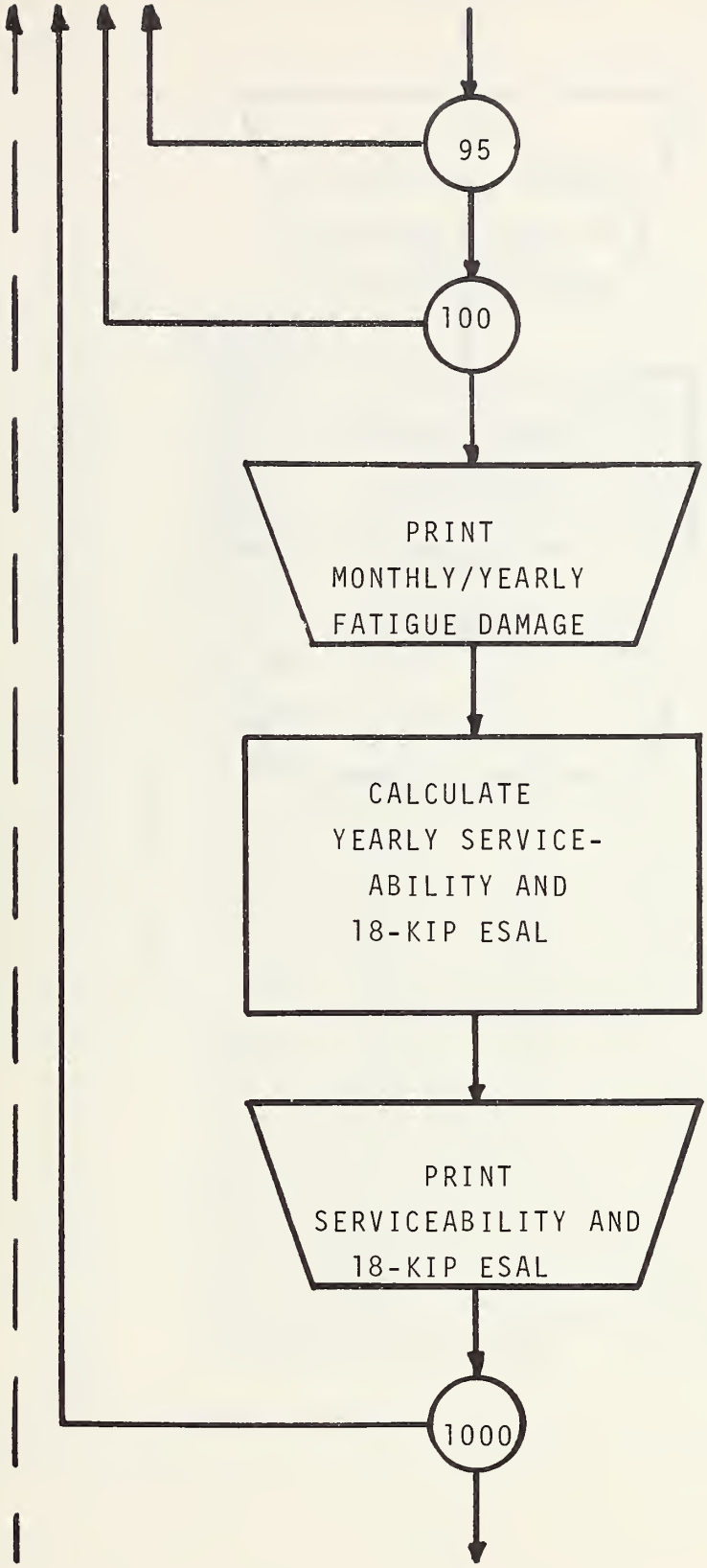
95
100
PRINT
MONTHLY/YEARLY
FATIGUE DAMAGE
CALCULATE
YEARLY SERVICE-
ABILITY AND
18-KIP ESAL
PRINT
SERVICEABILITY AND
18-KIP ESAL
1000

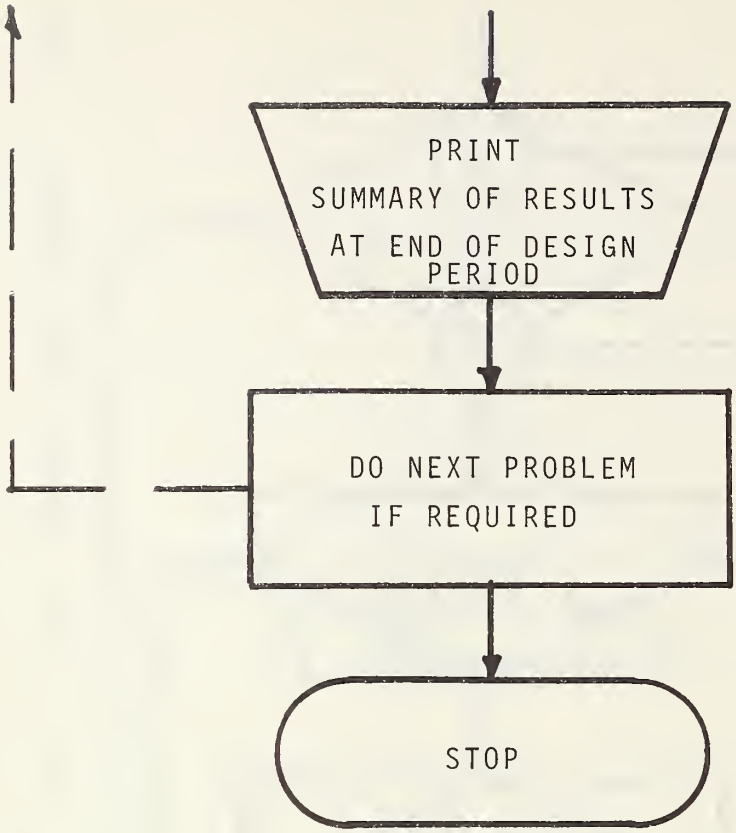
PRINT
SUMMARY OF RESULTS
AT END OF DESIGN
PERIOD
DO NEXT PROBLEM
IF REQUIRED
STOP

```
C*****************************************************************************
C*****************************************************************************
C*                                                                           *
C*                                                                           *
C*                              ZERO-MAINTENANCE                             *
C*                    PORTLAND CEMENT CONCRETE PLAIN JOINTED PAVEMENT        *
C*                                 DESIGN PROGRAM                            *
C*                                     JCP-1                                 *
C*                                                                           *
C*                                                                           *
C*****************************************************************************
C*****************************************************************************
C*                                                                           *
C*                                                                           *
C*                              PROGRAM NARRATIVE                            *
C*                                                                           *
C*       THIS PROGRAM COMPUTES DATA FOR USE IN DESIGNING ZERO-MAINTENANCE PLAIN*
C*   JOINTED CONCRETE PAVEMENTS.  THE PROGRAM INPUTS DESIGN CONSTRAINTS, TRAFFIC,
C*   MATERIALS, FOUNDATION SUPPORT, CLIMATIC, AND GEOMETRIC DATA RELATED TO THE *
C*   PROJECT UNDER DESIGN, AND OUTPUTS FATIGUE DAMAGE AND SERVICEABILITY-PERFOR-*
C*   MANCE DATA.  THE OUTPUT DATA CAN THEN BE USED TO SELECT APPROPRIATE       *
C*   STRUCTURAL THICKNESSES FOR ZERO-MAINTENANCE DESIGN.  THE TWO MAJOR PROGRAM *
C*   OUTPUTS ARE AS FOLLOWS.                                                   *
C*   (1)  FATIGUE DAMAGE--TOTAL FATIGUE DAMAGE AT THE EDGE OF THE PCC SLAB AS  *
C*   COMPUTED BY MINER'S ACCUMULATIVE DAMAGE HYPOTHESIS OCCURRING OVER THE LIFE *
C*   OF THE PAVEMENT.  BOTH TRAFFIC LOADS AND CURLING OF THE SLAB ARE CONSID-  *
C*   ERED.  MODELS DEVELOPED USING A FINITE ELEMENT SLAB PROGRAM ARE USED TO   *
C*   COMPUTE THE STRESSES.                                                     *
C*   (2)  SERVICEABILITY-PERFORMANCE-- THE LOSS OF SERVICEABILITY OVER TIME/   *
C*   TRAFFIC AND THE NUMBER OF EQUIVALENT 18,000 POUND SINGLE AXLE LOADS TO    *
C*   TERMINAL SERVICEABILITY FOR ZERO-MAINTENANCE DESIGN ARE COMPUTED. AN      *
C*   EMPIRICAL MODEL DEVELOPED FROM LONG TERM PERFORMANCE DATA FROM IS USED    *
C*   IN THIS COMPUTATION.                                                      *
C*       ACCUMULATED FATIGUE DAMAGE IS COMPUTED EVERY MONTH FROM THE OPENING   *
C*   OF THE PAVEMENT TO TRAFFIC TO THE END OF ITS DESIGN LIFE.  FATIGUE DAMAGE *
C*   IS ACCUMULATED MONTHLY OVER THE DESIGN LIFE.  THE MODULUS OF RUPTURE,     *
C*   ERODABILITY, AND TRAFFIC ALL VARY OVER THE DESIGN LIFE AND HENCE FATIGUE  *
C*   IS COMPUTED INCREMENTALLY ON A MONTHLY BASIS TO OBTAIN AN ACCURATE        *
C*   ESTIMATION.  SERVICEABILITY LOSS IS COMPUTED FOR EACH YEAR OF THE DESIGN  *
C*   LIFE. THESE DATA ARE THEN USED BY THE DESIGNER TO SELECT THE APPROPRIATE  *
C*   STRUCTURAL DESIGN FOR ZERO-MAINTENANCE PERFORMANCE.                       *
C*       THIS PROGRAM WAS WRITTEN BY DR. MICHAEL I. DARTER AT THE UNIVERSITY OF*
C*   ILLINOIS AT URBANA CHAMPAIGN, MAY 1976(REVISED NOVEMBER 1976).            *
C*                                                                           *
C*****************************************************************************
C
C   THE FOLLOWING LIST OF VARIABLES INCLUDES ALL VARIABLES USED IN
C   THE PROGRAM.  A '*' IN COLUMN 2 INDICATES THE VARIABLE IS AN INPUT.
C
C
C*  A               AXLE FACTOR, MEAN NUMBER OF AXLES PER TRUCK
C   ADT             AVERAGE DAILY TRAFFIC FOR A GIVEN MONTH, 2 DIRECTIONS
C*  ADTI            AVERAGE DAILY TRAFFIC AT BEGINNING OF DESIGN PERIOD, 2 DIREC-
C                   TIONS
```

```
C*  ADTF          AVERAGE DAILY TRAFFIC AT END OF DESIGN PERIOD, 2 DIRECTIONS
C   ALPHAM(24)    ALPHA CHARACTERS OF MONTHS, TO ADJUST FIRST MONTH OF STUDY
C   AXDAY         NUMBER OF TRUCK AXLES PER DAY IN DESIGN LANE
C   C(30)         TABLE OF VALUES CORRESPONDING TO PHI, C(PHI)=PROPORTION OF
C                 AXLE-LOADS THAT PASS WITHIN 6 INCHES OF SLAB EDGE
C   CO            =C(PHI)
C   CF            ADJUSTMENT FACTOR FOR MONTHLY TRUCK PERCENTAGE TO ADJUST FOR
C                 SEASONAL VARIATION OF TRUCK VOLUME
C   CON           =1 FOR SINGLE AXLE LOADS; =2 FOR TANDEM AXLE LOADS; USED WHEN
C                 COMPUTING DAMAGE
C*  D             MEAN DISTANCE FROM SLAB EDGE TO OUTSIDE OF TRUCK DUALS (IN)
C   DAMAGE        FATIGUE DAMAGE COMPUTED USING MINER'S HYPOTHESIS, FOR ONE
C                 MONTH (DAY OR NIGHT)
C   DAYTOT(2)     DAYTOT(1)=TOTAL DAMAGE FOR ONE YEAR DURING THE DAYTIME,
C                 DAYTOT(2)=TOTAL DAMAGE FOR ONE YEAR DURING THE NIGHTTIME
C*  DD            DIRECTIONAL DISTRIBUTION, PERCENT OF VEHICLES TRAVELING IN
C                 ONE DIRECTION ONLY
C*  DIST(40)      LOAD DISTRIBUTION TABLE, PERCENT FOR EACH LOAD RANGE
C   DISTF(40)     LOAD DISTRIBUTION TABLE, PROPORTION FOR EACH LOAD RANGE
C*  DK            DESIGN MODULUS OF FOUNDATION SUPPORT FOR SERVICEABILITY/
C                 PERFORMANCE ANALYSIS (PCI)
C*  DLIFE         ZERO-MAINTENANCE DESIGN LIFE (YEARS)
C   DMNTH2(12,2)  DMNTH2(I,1)=TOTAL DAMAGE FOR ONE MONTH DURING THE DAYTIME,
C                 DMNTH2(I,2)=TOTAL DAMAGE FOR ONE MONTH DURING THE NIGHTTIME
C   DMONTH(12)    TOTAL DAMAGE FOR ONE MONTH, DAY AND NIGHT COMBINED
C   DT(12,2)      MONTHLY AVERAGE TEMP. GRADIENTS (DAY & NIGHT); CALCULATED
C                 FOR SLAB THICKNESS UNDER ANALYSIS
C   DYEAR         TOTAL DAMAGE FOR ONE YEAR, DAY AND NIGHT COMBINED
C*  E             PCC MODULUS OF ELASTICITY,PSI
C   EF            AXLE LOAD EQUIVALENCE FACTOR
C   ERODE         ERODABILITY OF FOUNDATION FOR A GIVEN MONTH
C   ERODEI        ERODABILITY OF FOUNDATION (IN.) AT BEGINNING OF DESIGN PERIOD
C*  ERODEF        ERODABILITY OF FOUNDATION (IN.) AT END OF DESIGN PERIOD
C*  ET            COEF. OF THERMAL EXPANSION OF PCC, PER DEG-F
C   F28           MODULUS OF RUPTURE (FOR 28 DAYS) AFTER ADJUSTMENT FOR
C                 VARIABILITY
C   F             MODULUS OF RUPTURE FOR A GIVEN MONTH FOR USE IN COMPUTING
C                 FATIGUE DAMAGE
C   FA            RATIO OF MOD. OF RUPTURE AT A SPECIFIED TIME (F) TO MOD. OF
C                 RUPTURE AT 28-DAYS (FF)
C   FCONF         STANDARD NORMAL DEVIATE AT CONFIDENCE LEVEL OF 99 PERCENT,
C                 USED FOR CONCRETE MODULUS OF RUPTURE
C*  FCV           COEFFICIENT OF VARIATION OF PCC MOD. OF RUPTURE
C*  FF            MEAN MOD. OF RUP. (FOR 28 DAYS) BEFORE ADJUSTMENT FOR
C                 VARIABILITY
C   FSD           STANDARD DEVIATION OF FF
C*  G1(12,2)      SET OF THERMAL GRADIENTS FOR THINNEST SLAB, DEG-F/IN
C*  G2(12,2)      SET OF THERMAL GRADIENTS FOR THICKEST SLAB, DEG-F/IN
C*  H             PCC SLAB THICKNESS (IN)
C*  H1            THICKNESS FOR FIRST SET OF THERMAL GRADIENTS (FOR GETTING DT)
C*  H2            THICKNESS FOR SECOND SET OF THERMAL GRADIENTS (FOR DT)
C   I             USED ONLY IN ITERATIVE STATEMENTS
C*  ILIST         =1 FOR COMPREHENSIVE FATIGUE OUTPUT DATA FOR A GIVEN YEAR
C*  ISUM          =1 FOR SUMMARY OF FATIGUE DAMAGE FOR A GIVEN YEAR
```

```
C   J              USED IN ITERATIVE STATEMENTS FOR MONTH
C   JMONTH         =KMONTH+11, TWELFTH MONTH OF YEAR UNDER STUDY
C*  K(12)          MODULUS OF FOUNDATION SUPPORT FOR EACH MONTH (PCI)
C                  (ON TOP OF SUBBASE)
C*  KK             NUMBER OF INTERVALS IN LOAD DISTRIBUTION TABLE
C*  KMONTH         FIRST MONTH OF YEAR UNDER STUDY, FIRST MONTH PAVEMENT IS OPEN
C                  TO TRAFFIC
C*  KSAL           NUMBER OF SAL INTERVALS IN LOAD DISTRIBUTION TABLE
C   KSAL1          =KSAL+1; STARTING ELEMENT OF LOAD DIST FOR T.A.L.
C   KTAL           NUMBER OF TAL INTERVALS IN LOAD DISTRIBUTION TABLE
C*  L              PCC SLAB LENGTH (FT)
C*  LD             LANE DISTRIBUTION FOR COMPUTING AXDAY, PERCENT OF TRUCKS IN
C                  ONE DIRECTION IN DESIGN LANE
C*  LOAD(40)       VALUES OF LOADS IN LOAD DISTRIBUTION TABLE (POUNDS)
C   LOGN           LOG TO BASE 10 OF N
C   LRANGE(40)     LOWER END OF INTERVALS IN LOAD DISTRIBUTION TABLE
C   M              USED IN ITERATIVE STATEMENTS; =1 FOR DAY, =2 FOR NIGHT
C   N              ALLOWABLE LOAD APPLICATIONS TO FAILURE OF PCC, OBTAINED FROM
C                  FATIGUE CURVE
C   NAAL           NUMBER OF APPLIED AXLE LOADINGS FOR ONE MONTH (DAY OR NIGHT)
C                  PASSING WITHIN 6 INCHES OF SLAB EDGE
C   NTPD           NUMBER OF TRUCKS PER DAY
C   NY             USED IN ITERATIVE STATEMENTS FOR YEARLY CALCULATIONS
C   NYEARS         NUMBER OF YEARS FOR WHICH PROGRAM IS TO BE EXECUTED
C*  OPEN           TIME AFTER PCC SLAB PLACEMENT THAT PAVEMENT WILL BE OPENED TO
C                  TRAFFIC (YEARS)
C*  PC             PERCENT OF TRUCKS DURING THE DAY
C   PCP(M)         PROPORTION OF TRUCKS DURING THE DAY AND NIGHT. PCP(1)=PROPOR-
C                  TION DURING DAY, PCP(2)=PROPORTION DURING NIGHT
C   PHI            NORMAL STANDARD DEVIATE OF LATERAL-LOAD DISTRIBUTION
C   PN             PROBLEM NUMBER
C*  PT             TERMINAL SERVICEABILITY INDEX FOR ZERO-MAINTENANCE
C                  DESIGN
C   R              ADJUSTMENT FACTOR FOR CURL STRESS SO THAT IT MAY BE
C                  COMBINED WITH LOAD STRESS TO GIVE TOTAL STRESS IN SLAB
C                  UNDER LOAD
C   RA             RADIUS OF LOADED AREA (IN)
C*  RF             CLIMATIC REGIONAL FACTOR FOR USE IN SERVICEABILITY
C                  ANALYSIS
C   SI             SERVICEABILITY INDEX AT END OF YEAR UNDER STUDY
C*  SIC            INITIAL SERVICEABILITY INDEX AFTER CONSTRUCTION
C   SLE            SLOPE OF ERODABILITY LINE
C   SLOPE          SLOPE OF ADT LINE
C   SPE            SUM OF PRODUCTS OF LOAD EQUIVALENCY FACTORS AND PER-
C                  CENT LOADS WITHIN LOAD GROUP
C   STRC           CURL STRESS (PSI)
C   STRL           STRESS DUE TO LOAD AT EDGE OF SLAB (PSI)
C   STRT           TOTAL STRESS FOR LOAD AND CURL (PSI)
C   SUM1(12,2)     SUM1(I,1)=TOTAL DAMAGE FOR DESIGN PERIOD, MONTHLY, DURING THE
C                  DAYTIME, SUM1(I,2)=TOTAL DAMAGE FOR DESIGN PERIOD, MONTHLY,
C                  DURING THE NIGHTTIME
C   SUM2(12)       TOTAL DAMAGE FOR DESIGN PERIOD, MONTHLY, DAY & NIGHT COMBINED
C   SUM3(2)        SUM3(1)=TOTAL DAMAGE FOR DESIGN PERIOD DURING THE DAYTIME
C                  SUM3(2)=TOTAL DAMAGE FOR DESIGN PERIOD DURING THE NIGHTTIME
```

```
C   SUM4            TOTAL DAMAGE FOR DESIGN PERIOD, DAY & NIGHT COMBINED
C*  T               PERCENT OF TRUCKS IN ADT; USED FOR COMPUTING AXDAY
C   T2              TIME AFTER PCC SLAB WAS PLACED (YEARS)
C   TIME            MONTH WHICH IS UNDER STUDY, STARTING FROM THE FIRST MONTH
C                   PAVEMENT WAS OPEN TO TRAFFIC
C*  TITLE(20,3)     STRING FOR STORING TITLE, 3 CARDS, 80 COLUMNS EACH
C*  TRUKPC(12)      MONTHLY TRUCK PERCENTAGE OVER A YEAR TO ADJUST FOR SEASONAL
C                   TRUCK VOLUME CHANGES
C   TY              TIME IN YEARS FROM OPENING OF PAVEMENT TO TRAFFIC
C   W               NUMBER OF 18-KIP EQUIVALENT SINGLE AXLE LOAD
C                   APPLICATIONS ACCUMULATED TO END OF YEAR UNDER STUDY
C                   IN DESIGN LANE
C   WW              NUMBER OF 18-KIP SINGLE AXLE LOAD APPLICATIONS COMPUTED
C                   USING SERVICEABILITY/PERFORMANCE EQUATION FOR CHANGE
C                   IN SERVICEABILITY FROM  INITIAL TO SI
C   YI              Y-INTERCEPT OF ADT LINE
C   YTE             Y-INTERCEPT OF ERODABILITY LINE
C   YL              YEARS FOR WHICH YOU WANT COMPREHENSIVE FATIGUE OUTPUT DATA
C   YS              YEARS FOR WHICH YOU WANT SUMMARY OF FATIGUE DAMAGE
C
C
C*************************************************************************
C
0001          REAL SUM1(12,2),SUM2(12),SUM3(2)
0002          INTEGER PN
0003          REAL NTFD
0004          INTEGER ISUM(100),YS(100)
0005          INTEGER D
0006          INTEGER YL(100),ILIST(100),PHI
0007          REAL K(12),LOGN,N,LOAD(40),LD,L,NAAL,LRANGE(40)
0008          DIMENSION DMONTH(12), DT(12,2), DMNTH2(12,2), DIST(40), PCP(2),
             1     DISTP(40),TITLE(20,3),C(30),ALPHAM(23),
             2     TRUKPC(12), G1(12,2), G2(12,2), DAYTOT(2)
0009          DATA ALPHAM /3HJAN,3HFEB,3HMAR,3HAPR,3HMAY,3HJUN,3HJUL,3HAUG,
             1            3HSEP,3HOCT,3HNOV,3HDEC,3HJAN,3HFEB,3HMAR,3HAPR,
             2            3HMAY,3HJUN,3HJUL,3HAUG,3HSEP,3HOCT,3HNOV/
0010          DATA C /.4602, .4207, .3821, .3446, .3085, .2743, .2420,
             1     .2119, .1841, .1587, .1357, .1151, .0963, .0808, .0668,
             2     .0548, .0446, .0359, .0287, .0228, .0179, .0139, .0107,
             3     .0082, .0062, .0047, .0035, .0026, .0019, .0013/
C
C*************************************************************************
C
C   READ TITLE
0011          READ(5,500) ((TITLE(I,J),I=1,20),J=1,3)
C
C   WRITE PROBLEM NUMBER AND TITLE
0012          PN=1
0013          WRITE(6,600) PN,((TITLE(I,J),I=1,20),J=1,3)
C
C     PART I:
C   READ IN ALL DATA AND DO ALL CALCULATIONS WHICH WILL NOT CHANGE FROM YEAR
C   TO YEAR
C
```

```
      C   READ DESIGN CRITERIA - DESIGN LIFE, INITIAL SERVICEABILITY INDEX AFTER CON-
      C   STRUCTION, TERMINAL SERVICEABILITY INDEX FOR ZERO-MAINTENANCE, TIME AFTER
      C   SLAB PLACEMENT THAT PAVEMENT WILL BE OPENED TO TRAFFIC, AND MONTH PAVEMENT
      C   WILL BE OPENED TO TRAFFIC
0014        READ(5,530) DLIFE,SIC,PT,OPEN,KMONTH
      C
      C   IF DESIGN LIFE IS LESS THAN OR EQUAL TO ZERO, SET IT EQUAL TO ONE
0015        IF(DLIFE.LE.0) DLIFE=1.0
      C
      C   NUMBER OF YEARS FOR WHICH YOU WANT THE PROGRAM TO BE EXECUTED=DESIGN LIFE
0016        NYEARS=DLIFE
      C
      C   CHECK TO MAKE SURE THAT KMONTH IS BETWEEN 1 AND 12
0017        IF(KMONTH.LT.1) KMONTH=1
0018        IF(KMONTH.GT.12) KMONTH=12
      C
      C   WRITE OUT DESIGN CRITERIA
0019        WRITE(6,630) DLIFE,SIC,PT,OPEN,ALPHAM(KMONTH)
      C
      C   READ AND WRITE YEARS FOR WHICH SUMMARY OF FATIGUE DAMAGE AND SERVICEABILITY
      C   DATA WILL BE PRINTED. READ IN EITHER 0 OR 1 FOR EVERY YEAR OF DESIGN PERIOD,
      C   1=YES, 0=NO
0020        READ(5,704) (ISUM(I),I=1,NYEARS)
0021        J=0
0022        DO 450 I=1,NYEARS
0023        IF(ISUM(I).EQ.0) GO TO 450
0024        J=J+1
0025        YS(J)=I
0026      450 CONTINUE
0027        WRITE(6,706) (YS(I),I=1,J)
      C
      C   READ AND WRITE YEARS FOR WHICH YOU WANT COMPREHENSIVE FATIGUE OUTPUT DATA.
      C   READ IN EITHER 0 OR 1 FOR EVERY YEAR OF THE DESIGN PERIOD. 1=YES, 0=NO
0028        READ(5,704) (ILIST(I),I=1,NYEARS)
0029        J=0
0030        DO 402 I=1,NYEARS
0031        IF(ILIST(I).EQ.0) GO TO 402
0032        J=J+1
0033        YL(J)=I
0034      402 CONTINUE
0035        WRITE(6,705) (YL(I),I=1,J)
      C
      C   READ AND WRITE SLAB PROPERTIES - SLAB THICKNESS, SLAB LENGTH, MEAN MODULUS
      C   OF RUPTURE (28 DAYS) BEFORE ADJUSTMENT FOR VARIABILITY, COEFFICIENT OF
      C   VARIATION OF MODULUS OF RUPTURE, COEFFICIENT OF THERMAL EXPANSION, AND PCC
      C   MODULUS OF ELASTICITY
0036        READ(5,501) H,L,FF,FCV,ET,E
0037        WRITE(6,601) H,L,FF,FCV,ET,E
      C
      C   STANDARD NORMAL DEVIATE AT CONFIDENCE LEVEL OF 85% USED FOR CONCRETE MODULUS
      C   OF RUPTURE=1.03
0038        FCONF=1.03
      C
      C   ADJUST MODULUS OF RUPTURE TO ACCOUNT FOR VARIABILITY OF PCC
```

```
0039              FSD=FF*FCV/100.0
0040              F28=FF-FSD*FCONF
                C
                C   READ AND WRITE TRAFFIC DATA - AVERAGE DAILY TRAFFIC (ADT) AT BEGINNING OF
                C   DESIGN PERIOD, ADT AT END OF DESIGN PERIOD, PERCENT OF TRUCKS IN ADT,
                C   PERCENT OF TRUCKS IN DESIGN LANE, PERCENT DIRECTIONAL DISTRIBUTION, MEAN
                C   AXLES PER TRUCK, PERCENT TRUCKS DURING DAYLIGHT, MEAN DISTANCE FROM SLAB
                C   EDGE TO OUTSIDE OF TRUCK DUALS
0041              READ(5,502) ADTI,ADTF,T,LD,DD,A,PC,D
0042              WRITE(6,602) ADTI,ADTF,T,LD,DD,A,PC,D
                C
                C   CALCULATE SLOPE AND Y-INTERCEPT OF ADT LINE:
                C   INITIAL ADT AND FINAL ADT WERE READ IN, TIME FOR ADTI=0, TIME FOR ADTF IS
                C   THE END OF THE DESIGN PERIOD. ASSUME ADT IS A STRAIGHT-LINE FUNCTION OF
                C   TIME. THE SLOPE AND Y-INTERCEPT OF THE ADT LINE IS FOUND SO THAT ADT FOR ANY
                C   GIVEN TIME CAN BE CALCULATED LATER.
0043              SLOPE=(ADTF-ADTI)/DLIFE
0044              YI=ADTI
                C
                C   COMPUTE PROPORTION OF AXLE-LOADS THAT PASS WITHIN DS INCHES FROM SLAB EDGE:
                C   THE LATERAL LOAD DISTRIBUTION IS NORMAL WITH MEAN=D AND STANDARD DEVIATION=
                C   SIGMA. THE C TABLE IS USED TO DETERMINE THE PROPORTION OF WHEEL LOADS THAT
                C   PASS WITHIN DS FROM THE SLAB EDGE. FIRST SET SIGMA AND DS.
0045              SIGMA=10.0
0046              DS=6.0
                C
                C   NEXT COMPUTE PHI, WHICH IS A STANDARD NORMAL DEVIATE OF THE LATERAL LOAD
                C   DISTRIBUTION. THE VALUE OF PHI MUST BE MULTIPLIED BY 10 SO THAT IT CAN BE
                C   USED TO DETERMINE THE PROPORTION FROM THE C TABLE.
0047              PHI=(D-DS)*10.0/SIGMA
0048              IF(PHI.EQ.0) GO TO 400
                C
                C   FIND PROPORTION FROM C TABLE
                C   IF PHI=0, PROPORTION=0.5
0049              CD=C(PHI)
0050              GO TO 401
0051            400 CD=0.5000
0052            401 CONTINUE
                C
                C   CONVERT PERCENT OF TRUCKS DURING DAY TO A PROPORTION OF 1 AND COMPUTE PRO-
                C   PORTION OF TRUCKS DURING NIGHT
0053              PCP(1)=PC/100.0
0054              PCP(2)=1.0-PCP(1)
                C
                C   READ NUMBER OF INTERVALS IN LOAD DISTRIBUTION TABLE, NUMBER OF SAL INTERVALS
                C   IN LOAD DISTRIBUTION TABLE
0055              READ(5,503) KK,KSAL
                C
                C   COMPUTE NUMBER OF TAL INTERVALS IN LOAD DISTRIBUTION TABLE
0056              KTAL=KK-KSAL
                C
                C   WRITE NUMBER OF SAL INTERVALS, NUMBER OF TAL INTERVALS
0057              WRITE(6,603) KSAL,KTAL
                C
```

```
C   COMPUTE STARTING ELEMENT OF LOAD DISTRIBUTION FOR TAL AND TWELFTH MONTH OF
C   STUDY
0058        KSAL1=KSAL+1
0059        JMONTH=KMONTH+11
C
C   READ VALUES OF LOADS IN LOAD DISTRIBUTION TABLE AND PERCENT FOR EACH LOAD
0060        READ(5,504) (LOAD(I),I=1,KK)
0061        READ(5,504) (DIST(I),I=1,KK)
C
C   COMPUTE LOWER END OF INTERVALS IN LOAD DISTRIBUTION TABLE
0062        LRANGE(1)=0.0
0063        DO 16 I=2,KK
0064     16 LRANGE(I)=LOAD(I-1)+1
0065        LRANGE(KSAL1)=0.0
C
C   WRITE OUT LOAD DISTRIBUTION TABLE FOR SAL AND TAL
0066        WRITE(6,604) ((LRANGE(I),LOAD(I),DIST(I)),I=1,KSAL)
0067        WRITE(6,605) ((LRANGE(I),LOAD(I),DIST(I)),I=KSAL1,KK)
C
C   CONVERT PERCENT FOR EACH LOAD INTO PROPORTION OF 1
0068        DO 11 I=1,KK
0069     11 DIST(I)=DIST(I)/100.0
C
C   READ IN MONTHLY TRUCK PERCENTAGE
0070        READ(5,505) (TRUKPC(I),I=1,12)
C
C   WRITE OUT EACH MONTH OF YEAR (FROM MONTH PAVEMENT WAS OPEN) AND MONTHLY
C   TRUCK PERCENT
0071        WRITE(6,606) (ALPHAM(I),I=KMONTH,JMONTH),(TRUKPC(I),I=1,12)
C
C   READ AND WRITE MONTHLY FOUNDATION MODULUS
0072        READ (5,505) (K(J),J=1,12)
0073        WRITE(6,607) (ALPHAM(I),I=KMONTH,JMONTH), (K(J),J=1,12)
C
C   SET ERODABILITY AT BEGINNING OF DESIGN PERIOD AT ZERO, READ IN ERODABILITY
C   AT END OF DESIGN PERIOD, WRITE BOTH
0074        ERODEI=0.0
0075        READ(5,701) ERODEF
0076        WRITE(6,702) ERODEI,ERODEF
C
C   CALCULATE THE SLOPE AND Y-INTERCEPT OF THE ERODABILITY LINE:
C   INITIAL ERODABILITY WAS SET EQUAL TO ZERO, FINAL ERODABILITY WAS READ IN,
C   TIME FOR ERODEI=0, TIME FOR ERODEF IS THE END OF THE DESIGN PERIOD. GIVES
C   DATA TO PLOT ERODABILITY AS A STRAIGHT-LINE FUNCTION OF TIME.  THE SLOPE
C   AND Y-INTERCEPT OF THE ERODABILITY LINE WILL BE COMPUTED SO THAT
C   ERODABILITY CAN BE CALCULATED FOR ANY PARTICULAR TIME.
0077        SLE=(ERODEF-ERODEI)/DLIFE
0078        YIE=ERODEI
C
C   READ AND WRITE DESIGN MODULUS OF FOUNDATION SUPPORT FOR SERVICEABILITY/
C   PERFORMANCE ANALYSIS
0079        READ(5,701) DK
0080        WRITE(6,631) DK
C
```

```
                C   READ IN TEMPERATURE GRADIENTS FOR TWO DIFFERENT SLAB THICKNESSES FOR EACH
                C   MONTH, DAY AND NIGHT
0081                  READ(5,508) H1,((G1(J,M),J=1,12),M=1,2),H2,((G2(J,M),J=1,12),M=1,2
                     1)
                C
                C   CHECK TO MAKE SURE THAT 1ST AND 2ND SLAB THICKNESSES ARE NOT THE SAME
0082                  IF (H1 .NE. H2) GO TO 14
0083                  H2=H2+1.
0084                  PRINT 6061,H2
0085               14 CONTINUE
                C
                C   READ REGIONAL FACTOR
0086                  READ(5,701) RF
                C
                C   INTERPOLATE FROM THE TWO SETS OF TEMPERATURE GRADIENTS WHICH WERE READ IN TO
                C   FIND TEMPERATURE GRADIENTS FOR THE SLAB THICKNESS UNDER STUDY
0087                3000 DO 15 M=1,2
0088                     DO 15 J=1,12
0089               15 DT(J,M)=(H-H1)/(H2-H1)*(G2(J,M)-G1(J,M))+G1(J,M)
                C
                C   WRITE OUT THE TWO SETS OF TEMPERATURE GRADIENTS AND THE SET WHICH WAS JUST
                C   CALCULATED
0090                  WRITE(6,703) (ALPHAM(I),I=KMONTH,JMONTH),
                     1             H1,((G1(J,M),J=1,12),M=1,2),
                     2             H2,((G2(J,M),J=1,12),M=1,2),
                     3              H,((DT(J,M),J=1,12),M=1,2)
                C
                C   WRITE REGIONAL FACTOR
0091                  WRITE(6,632) RF
                C
                C   INITIALIZE SUMS FOR TOTAL DAMAGE FOR DESIGN PERIOD
0092                  SUM4=0.0
0093                  SUM3(1)=0.0
0094                  SUM3(2)=0.0
0095                  DO 430 J=1,12
0096                  SUM2(J)=0.0
0097                  DO 440 M=1,2
0098               440 SUM1(J,M)=0.0
0099               430 CONTINUE
                C
                C*****************************************************************************
                C
                C     PART II:
                C   ALL CALCULATIONS IN THIS PART OF THE PROGRAM WILL CHANGE FROM YEAR TO YEAR
                C
                C   INITIALIZE TIME AT ZERO
0100                  TIME=0.0
                C
                C   INITIALIZE TIME FOR FLEXURAL STRENGTH AT TIME PAVEMENT WAS OPENED TO TRAFFIC
0101                  T2=OPEN
                C
                C   DO THIS ENTIRE PART (UP TO STATEMENT 1000) FOR EACH YEAR
0102                  DO 1000 NY=1,NYEARS
                C
```

```
                C   INITIALIZE SUMS FOR YEAR, DAY AND NIGHT
0103                  DYEAR=0.
0104                  DAYTOT(1)=0.
0105                  DAYTOT(2)=0.
                C
                C   DO UP TO STATEMENT 100 FOR EACH MONTH
0106                  DO 100 J=1,12
                C
                C   INCREMENT MONTH
                C   TIME=1 FOR THE 1ST MONTH PAVEMENT WAS OPEN TO TRAFFIC
0107                  TIME=TIME+1.0
                C
                C   DIVIDE BY 12 TO FIND TIME IN YEARS
0108                  TY=TIME/12.0
                C
                C   IF YOU WANT DETAILED FATIGUE OUTPUT PRINTED, WRITE TITLE AND YEAR
0109                  IF(ILIST(NY).EQ.1) WRITE(6,629) NY
                C
                C   INITIALIZE SUM FOR MONTH
0110                  DMONTH(J)=0.
                C
                C   CALCULATE AVERAGE DAILY TRAFFIC FOR ONE MONTH: USE THE FORMULA Y=A*X+B
                C   WHERE Y=ADT, A=SLOPE, X=TIME, AND B=Y-INTERCEPT
0111                  ADT=(SLOPE*TY)+YI
                C
                C   CALCULATE NUMBER OF TRUCKS PER DAY IN ONE DIRECTION AND IN DESIGN LANE
0112                  NTPD=ADT*T/100.0*LD/100.0*DD/100.0
                C
                C   ADJUST NUMBER OF TRUCKS PER DAY FOR MONTHLY TRUCK PERCENT
0113                  CF=TRUKPC(J)*12.0/100.0
0114                  NTPD=NTPD*CF
                C
                C   CALCULATE NUMBER OF TRUCK AXLES PER DAY IN DESIGN LANE
0115                  AXDAY=NTPD*A
                C
                C   CALCULATE FLEXURAL STRENGTH (MODULUS OF RUPTURE): FA IS COMPUTED FROM A
                C   CURVE WHICH IS A FUNCTION OF TIME. HERE, TIME IS TAKEN AS TIME AFTER THE
                C   SLAB WAS PLACED.
0116                  FA= 1.22 + 0.17*ALOG10(T2) - 0.05*(ALOG10(T2))**2
0117                  F=FA*F28
0118                  T2=T2+(1.0/12.0)
                C
                C   CALCULATE ERODABILITY FOR ONE MONTH: USE THE FORMULA Y=A*X+B WHERE Y=ERODA-
                C   BILITY, A=SLOPE, X=TIME, AND B=Y-INTERCEPT.
0119                  ERODE=(SLE*TY)+YIE
                C
                C   DO UP TO STATEMENT 95 ONCE FOR DAY AND ONCE FOR NIGHT
0120                  DO 95 M=1,2
                C
                C   M=1 FOR DAY, M=2 FOR NIGHT
                C
                C   COMPUTE CURL STRESS FOR ONE MONTH, DAY OR NIGHT
0121                  STRC=DT(J,M)*ET/(5.*10.**(-6))*(0.06712*K(J)+79.07391*ALOG10(K(J))
                     1 +11.72690*L-0.0072*K(J)*L-3.22139*L*ALOG10(K(J))-0.06883*L*ERODE
```

```
                     2 -C.59539*ERODE*ALOG10(K(J))-204.39477*H/K(J)-38.C8854*L/H-8.36842
                     3 *H*ALOG10(K(J))+0.07151*ERODE*H+0.05691*L*ERODE*ALOG10(K(J))
                     4 +0.20845*L*H*ALOG10(K(J))+0.C0C58*L*H*K(J)-0.00201*L*ERODE*H
                     5 *ALOG10(K(J)))
               C
               C   COMPUTE RATIO R
0122                 R=0.48039+0.014C1*H-C.00427*ERODE-0.27278*DT(J,M)-0.C0403*L+
                     1 0.19508*ALOG10(K(J))+0.45187*DT(J,M)*ALOG10(H)-0.00532*DT(J,M)**2
                     2 +C.01246*DT(J,M)*L-C.C0622*DT(J,M)*L*ALOG10(K(J))+8.7872
                     3 *ALOG10((H**3)/K(J))/(H**2)+0.00104*DT(J,M)*ERODE-0.11846*DT(J,M)
                     4 *ALOG10((H**3)/K(J))+0.07001*ALOG10(ERODE+1.0)-0.01331*DT(J,M)
                     5 *ALOG10(ERODE+1.C)
               C
               C   INITIALIZE SUM FOR PERIOD OF DAY FOR ONE MONTH
0123                 DMNTH2(J,M)=0.0
               C
               C   SUM THE DAMAGE FOR ONE MONTH, DAY OR NIGHT, FOR ALL LOAD STRESSES (KK)
               C
0124                       DO 85 I=1,KK
0125                          IF (I .GT. KSAL) GO TO 90
               C
               C   LOAD STRESS EQUATION FOR SAL
0126                 STRL=LOAD(I)/(18.0*H**2)*(17.35783+0.07801*ERODE-0.05388*(H**3)/
                     1 K(J)+7.41722*ALOG10((H**3)/K(J)))
0127                       CON=1.C
0128                       GO TO 91
               C
               C   LOAD STRESS EQUATION FOR TAL
0129                90 STRL=LOAD(I)/(30.C*H**2)*(14.C9599+C.10522*ERODE-C.00886*(H**3)/
                     1 K(J)+6.2339*ALOG10((H**3)/K(J))+1.95266*(ALOG10((H**3)/K(J)))**2
                     2 -0.71963*ALOG10(ERODE+1.C))
0130                       CON=2.C
               C
               C   COMPUTE TOTAL STRESS FOR LOAD AND CURL
0131                91          STRT=STRL+STRC*R
               C
               C   COMPUTE ALLOWABLE LOAD APPLICATIONS TO FATIGUE FAILURE OF PCC SLAB
0132                       LOGN=16.81-17.61*STRT/F
0133                       IF (LOGN .LT. C.) LOGN=C.
0134                       N=10.**LOGN
               C
               C   COMPUTE NUMBER OF APPLIED AXLE LOADINGS DURING MONTH (DAY OR NIGHT)
0135                       NAAL=AXDAY*DISTP(I)*PCP(M)*3C.*CON*CD
               C
               C   COMPUTE DAMAGE
0136                       DAMAGE=NAAL/N
0137                 DAMAGE=DAMAGE*1C.**6.C
               C
               C   IF YOU WANT DETAILED FATIGUE ANALYSIS PRINTED, PRINT IT HERE
0138                       IF(ILIST(NY).EQ.1) PRINT 640,J,M,LOAD(I),STRL,STRC,R,
                     1        STRT,F,N,NAAL,DAMAGE
               C
               C   SUM DAMAGE FOR ONE MONTH, DAY OR NIGHT
0139                       DMNTH2(J,M)=DMNTH2(J,M)+DAMAGE
```

```
                C
0140               89          CONTINUE
                C
                C   SUM DAMAGE FOR ONE YEAR, DAY OR NIGHT
0141                       DAYTOT(M)=DAYTOT(M)+DMNTH2(J,M)
                C
                C   SUM DAMAGE FOR ONE MONTH, DAY AND NIGHT COMBINED
0142                       DMONTH(J)=DMONTH(J)+DMNTH2(J,M)
                C
                C   SUM DAMAGE FOR DESIGN PERIOD FOR A GIVEN MONTH, DAY OR NIGHT
0143                     SUM1(J,M)=SUM1(J,M)+DMNTH2(J,M)
                C
                C   SUM DAMAGE FOR DESIGN PERIOD FOR ALL MONTHS, DAY OR NIGHT
0144                     SUM3(M)=SUM3(M)+DMNTH2(J,M)
                C
0145               95       CONTINUE
                C
                C   SUM DAMAGE FOR ONE YEAR, DAY AND NIGHT COMBINED
0146                    DYEAR=DYEAR+DMONTH(J)
                C
                C   SUM DAMAGE FOR DESIGN PERIOD FOR A GIVEN MONTH, DAY AND NIGHT COMBINED
0147                     SUM2(J)=SUM2(J)+DMONTH(J)
                C
0148              100    CONTINUE
                C
                C   SUM DAMAGE FOR DESIGN PERIOD FOR ALL MONTHS, DAY AND NIGHT COMBINED
0149                     SUM4=SUM4+DYEAR
                C
                C*******************************************************************************
                C
                C   OUTPUT OF RESULTS FOR THE YEAR, IF DESIRED
0150                     IF(ISUM(NY).EQ.0) GO TO 1000
0151                     WRITE(6,600) PN,((TITLE(I,J),I=1,20),J=1,3)
0152                     WRITE(6,6000) NY
0153                     WRITE(6,610)  ((ALPHAM(J+KMONTH-1),(DMNTH2(J,M),M=1,2),DMONTH(J)),
                        1     J=1,12)
0154                     WRITE(6,611) (DAYTOT(M),M=1,2), NY, DYEAR
                C
                C   CALL SUBROUTINE SERV FOR SERVICEABILITY/PERFORMANCE ANALYSIS AT END OF YEAR
0155                     CALL SERV(H,KK,KSAL,LOAD,DTST,TY,A,DD,LD,T,SLOPE,YI,DK,E,SIC,PT,
                        1                 NY,RF,FF,W,SI,Y,FCV,FCONF)
0156                     IF(Y.LT.0.0) GO TO 63
0157                     IF(SI.LT.2.0) GO TO 63
0158                     WRITE(6,697) NY,SI,NY,W
0159               697 FORMAT(/1HO,55HRESULTS - SERVICEABILITY/PERFORMANCE OF JCP DESIGN
                       1LANE/8(1H*)//1HO,37HSERVICEABILITY INDEX AT END OF YEAR #,I3,1PE15
                       2.3/40H NUMBER OF ACCUMULATED 18-KIP EQUIVALENT/4X,
                       334HSINGLE AXLE LOADS AT END OF YEAR #,I3,1PE15.3)
0160                     GO TO 1000
0161                63 WRITE(6,64)
0162                64 FORMAT(/' ','DESIGN MESSAGE--SERVICEABILITY INDEX HAS DROPPED BELO
                       1W',/'                    3.0, STRUCTURE IS INADEQUATE')
                C
0163               1000 CONTINUE
```

```
                C
                C*************************************************************************
                C
                C   PRINT SUMMARY OF FATIGUE DATA AT END OF DESIGN PERIOD
0164                  WRITE(6,600) PN,((TITLE(I,J),I=1,20),J=1,3)
0165                  WRITE(6,6001)
0166                  WRITE(6,610) ((ALPHAM(J+KMONTH-1),(SUM1(J,M),M=1,2),SUM2(J)),
                     1      J=1,12)
0167                  WRITE(6,6002) (SUM3(M),M=1,2),SUM4
                C
                C*************************************************************************
                C
                C   CHECK IF SERVICEABILITY DATA HAS BEEN COMPUTED FOR LAST YEAR
                C   OF DESIGN LIFE, IF NOT COMPUTE IT
                C
0168                  IF(ISUM(NYEARS).EQ.1) GO TO 4000
0169                  NY=NYEARS
0170                  CALL SERV(H,KK,KSAL,LOAD,DIST,TY,A,DD,LD,T,SLOPE,YI,DK,E,SIC,PT,
                     1                NY,RF,FF,W,SI,Y,FCV,FCONF)
                C
                C*************************************************************************
                C   PRINT SUMMARY OF SERVICEABILITY DATA AT END OF DESIGN PERIOD
                C
0171                4000 IF(Y.LT.0.0) GO TO 176
0172                  IF(SI.LT.2.0) GO TO 176
0173                  WRITE(6,650) NY,SI,NY,W
0174                650 FORMAT(/1H0,55HRESULTS - SERVICEABILITY/PERFORMANCE OF JCP DESIGN
                     1LANE/8(1H*)//1H0,37HSERVICEABILITY INDEX AT END OF YEAR #,I3,1PE15
                     2.3/40H NUMBER OF ACCUMULATED 18-KIP EQUIVALENT/4X,
                     334HSINGLE AXLE LOADS AT END OF YEAR #,I3,1PE15.3)
0175                  GO TO 23
0176                176 WRITE(6,177)
0177                177 FORMAT(/' ',*DESIGN MESSAGE--SERVICEABILITY INDEX HAS DROPPED BELO
                     1W*,/'                    3.0, STRUCTURE IS INADEQUATE')
                C
                C*************************************************************************
                C
                C   DO THE NEXT PROBLEM:
                C
                C   READ THE NEW TITLE AND INCREMENT THE PROBLEM NUMBER. IF THERE ISN'T A NEXT
                C   PROBLEM, GO TO STOP
0178                 23 CONTINUE
0179                  READ(5,500,END=2000) ((TITLE(I,J),I=1,20),J=1,3)
0180                  PN=PN+1
                C
                C   WRITE PROBLEM NUMBER AND TITLE
0181                  WRITE(6,600) PN,((TITLE(I,J),I=1,20),J=1,3)
                C
                C   READ NEW SLAB THICKNESS
0182                  READ(5,707) H
                C
                C   WRITE DESIGN CRITERIA
0183                  WRITE(6,630) DLIFE,SIC,PT,OPEN,ALPHAM(KMONTH)
                C
```

```
C   READ AND WRITE YEARS FOR WHICH SUMMARY OF FATIGUE DAMAGE AND SERVICEABILITY
C   DATA WILL BE PRINTED. READ IN EITHER 0 OR 1 FOR EVERY YEAR OF DESIGN PERIOD,
C   1=YES, 0=NO
0184          READ(5,704) (ISUM(I),I=1,NYEARS)
0185          J=0
0186          DO 800 I=1,NYEARS
0187          IF(ISUM(I).EQ.0) GO TO 800
0188          J=J+1
0189          YS(J)=I
0190        800 CONTINUE
0191          WRITE(6,706) (YS(I),I=1,J)
C
C   READ AND WRITE YEARS FOR WHICH YOU WANT COMPREHENSIVE FATIGUE OUTPUT DATA.
C   READ IN EITHER 0 OR 1 FOR EVERY YEAR OF THE DESIGN PERIOD. 1=YES, 0=NO
0192          READ(5,704) (ILIST(I),I=1,NYEARS)
0193          J=0
0194          DO 801 I=1,NYEARS
0195          IF(ILIST(I).EQ.0) GO TO 801
0196          J=J+1
0197          YL(J)=I
0198        801 CONTINUE
0199          WRITE(6,705) (YL(I),I=1,J)
C
C   WRITE SLAB PROPERTIES, TRAFFIC DATA, FOUNDATION SUPPORT
0200          WRITE(6,601) H,L,FF,FCV,ET,E
0201          WRITE(6,602) ADTI,ADTF,T,LD,DD,A,PC,D
0202          WRITE(6,603) KSAL,KTAL
0203          WRITE(6,604) ((LRANGE(I),LOAD(I),DIST(I)),I=1,KSAL)
0204          WRITE(6,605) ((LRANGE(I),LOAD(I),DIST(I)),I=KSAL1,KK)
0205          WRITE(6,606) (ALPHAM(I),I=KMONTH,JMONTH),(TRUKPC(I),I=1,12)
0206          WRITE(6,607) (ALPHAM(I),I=KMONTH,JMONTH), (K(J),J=1,12)
0207          WRITE(6,702) ERODEI,ERODEF
0208          WRITE(6,631) DK
C
C   GO TO 3000 TO CALCULATE TEMPERATURE GRADIENTS FOR NEW SLAB THICKNESS, ETC.
0209          GO TO 3000
C
0210       2000 STOP
C
C*****************************************************************************
C
C   INPUT FORMATS
C
0211        500 FORMAT(20A4)
0212        530 FORMAT(4F10.0,I5)
0213        704 FORMAT(80I1)
0214        501 FORMAT(4F5.0,2E10.3)
0215        502 FORMAT(7F10.0,I5)
0216        503 FORMAT(2I5)
0217        504 FORMAT(8F10.0)
0218        505 FORMAT(12F5.0)
0219        506 FORMAT(7F10.4/10X,6F10.4/10X,6F10.4/10X,6F10.4/
               1       7F10.4/10X,6F10.4/10X,6F10.4/10X,6F10.4)
0220        701 FORMAT(F10.0)
```

```
0221          707 FORMAT(F5.0)
                C
                C*******************************************************************************
                C
                C   PRINT FORMATS FOR INPUT VALUES
                C
0222          600 FORMAT(1H1,T27,42H ZERO-MAINTENANCE PORTLAND CEMENT CONCRETE,/
                  1     T25,47H PLAIN JOINTED PAVEMENT DESIGN PROGRAM  (JCP-1),/
                  2     100(1H*)/1H0,10H PROBLEM #,I2,5X,20A4/13X,20A4/16X,20A4//
                  3     100(1H*))
0223          630 FORMAT(1H0,T40,10HINPUT DATA/T40,10(1H*)/
                  1     1H0,15HDESIGN CRITERIA/16(1H*)//3X,
                  2     46H PAVEMENT ZERO-MAINTENANCE DESIGN LIFE (YEARS),T60,F10.2/
                  3     3X,48H INITIAL SERVICEABILITY INDEX AFTER CONSTRUCTION,T60,
                  4     F10.2/3X,51H TERMINAL SERVICEABILITY INDEX FOR ZERO-MAINTENAN
                  5CE,  T60,F10.2/3X,44H TIME AFTER PCC SLAB PLACEMENT THAT PAVEMENT/
                  6     8X,34H WILL BE OPENED TO TRAFFIC (YEARS),T60,F10.2/
                  7     3X,41H MONTH PAVEMENT WILL BE OPENED TO TRAFFIC,T67,A3)
0224          700 FORMAT(3X,57H YEARS DURING WHICH SUMMARY OF FATIGUE AND SERVICEABI
                  1LITY/8X,22H DATA WILL BE PRINTED ,18(I2,1H,)/1X,43(I2,1H,)/1X,40(I
                  22,1H,),I3)
0225          705 FORMAT(/3X,53H YEARS DURING WHICH COMPREHENSIVE FATIGUE OUTPUT WIL
                  1L/8X,12H BE PRINTED ,21(I2,1H,)/1X,43(I2,1H,)/1X,35(I2,1H,),I3)
0226          601 FORMAT(/,1H0,15HSLAB PROPERTIES/16(1H*)//
                  1     3X,22H SLAB THICKNESS - INS.,T60,F10.2/
                  2     3X,18H SLAB LENGTH - FT.,T60,F10.2/
                  3     3X,44H MEAN PCC MODULUS OF RUPTURE (28-DAYS) - PSI,T60,F10.2/
                  4     3X,55H COEFFICIENT OF VARIATION OF PCC MODULUS OF RUPTURE - %
                  5,    T60,F10.2/3X,43H PCC COEF. OF THERMAL EXPANSION - PER DEG-F,
                  6     T60,1PE10.3/3X,26H PCC MODULUS OF ELASTICITY,T60,1PE10.3)
0227          602 FORMAT (/,1H0,7HTRAFFIC,/,8(1H*),//,3X,
                  1     52H AVERAGE DAILY TRAFFIC AT BEGINNING OF DESIGN PERIOD,T60,
                  2     F10.0/3X,46H AVERAGE DAILY TRAFFIC AT END OF DESIGN PERIOD,
                  3     T60,F10.0/3X,22H PERCENT TRUCKS OF ADT,T60,F10.2,/3X,
                  451H PERCENT TRUCKS IN HEAVIEST TRAVELED OR DESIGN LANE,T60,F10.2,/
                  5  3X,33H PERCENT DIRECTIONAL DISTRIBUTION,T60,F10.2,/,3X,
                  6     21H MEAN AXLES PER TRUCK,T60,F10.2,/,3X,
                  7     31H PERCENT TRUCKS DURING DAYLIGHT,T60,F10.2,/,3X,
                  8     60H MEAN DISTANCE FROM SLAB EDGE TO OUTSIDE OF TRUCK DUALS (I
                  9N),T65,I5)
0228          603 FORMAT(3X,37H NUMBER OF SINGLE AXLE LOAD INTERVALS,          T60,
                  1     I10,/3X,37H NUMBER OF TANDEM AXLE LOAD INTERVALS,T60,I10,/)
0229          604 FORMAT(28H1  S.A.L. DISTRIBUTION TABLE,/12X,12HWEIGHT RANGE,
                  1     6X,7HPERCENT,/14X,8H(POUNDS),/20(/,F17.0,2H -,F7.0,F10.2))
0230          605 FORMAT(/3X,26H T.A.L. DISTRIBUTION TABLE,/12X,12HWEIGHT RANGE,
                  1     6X,7HPERCENT,/14X,8H(POUNDS),/20(/,F17.0,2H -,F7.0,F10.2))
0231          606 FORMAT(/4X,24HMONTHLY TRUCK PERCENTAGE,/,8X,12(5X,A3),/,9X,12F8.2)
0232          607 FORMAT( /1H1,18HFOUNDATION SUPPORT,/,19(1H*),//,4X,
                  1     54HMODULUS OF FOUNDATION SUPPORT (K) FOR EACH MONTH - PCI,
                  2      /8X,12(5X,A3),/9X,12F8.0,//)
0233          702 FORMAT(3X,63H ERODABILITY OF FOUNDATION AT BEGINNING OF DESIGN PER
                  1IOD (INS.),T70, F5.2/3X,57H ERODABILITY OF FOUNDATION AT END OF DE
                  2SIGN PERIOD (INS.),T65,F10.2//)
0234          631 FORMAT(3X,45H DESIGN MODULUS OF FOUNDATION SUPPORT (K) FOR/
```

```
     1     6X,41HSERVICEABILITY/PERFORMANCE ANALYSIS - PCI,T65,F10.2//)
0235   703 FORMAT(14H ENVIRONMENTAL/14(1H*)//4X,
     1     55HPCC SLAB THERMAL GRADIENTS FOR EACH MONTH - DEG-F/INCH,
     2     //9X,12(5X,A3),//,2(4X,17HFOR THICKNESS OF ,F5.1,7H INCHES,
     3     /4X,3HDAY  ,12F8.2,/4X,5HNIGHT,12F8.2,//),4X,
     4     28HCALCULATED FOR THICKNESS OF ,F5.1,27H INCHES (BY INTERPOLA
     5TION),   /4X,3HDAY  ,12F8.2,/,4X,5HNIGHT,12F8.2///)
0236   632 FORMAT(3X,25H CLIMATIC REGIONAL FACTOR,T30,F10.2)
0237  6061 FORMAT('0',38H***** ERROR: H1=H2;  NOW H2=H1+1 *****)
      C
      C*******************************************************************************
      C
      C   OUTPUT FORMATS FOR RESULTS
      C
0238  6000 FORMAT(/1H0,10HFOR YEAR #,I3//69H RESULTS - ACCUMULATED FATIGUE DA
     1MAGE OF P.C.C. SLAB AT OUTSIDE EDGE/8(1H*))
0239   610 FORMAT(//2H0,12X,3HDAY,11X,5HNIGHT,10X,5HTOTAL,12(//,1X,A3,3(1PE15
     1.3)))
0240   611 FORMAT(/1H0,40HSUM OF FATIGUE DAMAGE FOR DAY LOADING IS,1PE15.3,
     1     /1H0,42HSUM OF FATIGUE DAMAGE FOR NIGHT LOADING IS,E13.3,
     2     /1H0,31HTOTAL FATIGUE DAMAGE FOR YEAR #,I3,3H IS,5X,E13.3)
0241   629 FORMAT(1H1,36H FATIGUE DAMAGE SUBTOTALS FOR YEAR #,I3//1X,5HMONTH,
     1     1X,3HD/N,2X,4HLOAD,6X,4HSTRL,6X,4HSTRC,10X,1HR,5X,4HSTRT,8X,
     2     1HF,12X,1HN,7X,4HNAAL,8X,6HDAMAGE/)
0242   640 FORMAT(1H ,I3,I5,F8.0,1P2E11.2,0PF10.4,1P4E11.3,1PE12.3)
0243  6001 FORMAT(/1H0,67HRESULTS - ACCUMULATED FATIGUE DAMAGE OF P.C.C. SLAB
     1 AT OUTSIDE EDGE,/,8(1H*),// 11X,25HSUMMARY FOR DESIGN PERIOD,/)
0244  6002 FORMAT(/1H0,40HSUM OF FATIGUE DAMAGE FOR DAY LOADING IS,1PE15.3,
     1     /1H0,42HSUM OF FATIGUE DAMAGE FOR NIGHT LOADING IS,E13.3,
     2     /1H0,41HTOTAL FATIGUE DAMAGE FOR DESIGN PERIOD IS,E14.3)
      C
      C*******************************************************************************
      C
0245        END
```

```
0001            SUBROUTINE SERV(H,KK,KSAL,LOAD,DIST,TY,A,DD,LD,T,SLOPE,YI,DK,E,
               1                SIC,PT,NY,PF,FF,W,SI,Y,FCV,FCONF)
                C
                C
0002              DIMENSION DIST(40)
0003              REAL L1,L2,LOG19,LOGEF,LW,LOGW,LD
0004              REAL LOAD(40)
                C
                C   CALCULATE EQUIVALENCY FACTORS CORRESPONDING TO AXLE TYPE AND LOAD, SLAB
                C   THICKNESS, AND TERMINAL SERVICEABILITY INDEX. SUM THE PRODUCT OF THE EQUIV-
                C   ALENCY FACTOR AND PERCENT AXLES IN EACH LOAD GROUP, AND CALL THIS SUM SPE.
                C
0005              B=1.0+3.63*19.0**5.2/((H+1.0)**8.46)
0006              G=ALOG10((4.5-PT)/3.0)
0007              GB=G/B
0008              LOG19=ALOG10(19.0)
0009              SPE=0.0
0010              DO 85 I=1,KK
0011              L1=LOAD(I)/1000.0
0012              IF(I.GT.KSAL) GO TO 90
0013              L2=1.0
0014              GO TO 91
0015             90 L2=2.0
0016             91 BI=1.0+(3.63*(L1+L2)**5.2)/(((H+1.0)**8.46)*(L2**3.52))
0017                LOGEF = 4.62*LOG19+G/BI+3.28*ALOG10(L2)-4.62*ALOG10(L1+L2)-GB
0018                EF=10.0**LOGEF
0019                EF = 1.0/EF
0020                SPE=SPE+(DIST(I)*EF)/100.
0021             85 CONTINUE
                C
                C   CALCULATE THE NUMBER OF EQUIVALENT 18,000 POUNDS SINGLE AXLE LOAD APPLICA-
                C   TIONS ACCUMULATED FROM THE TIME WHEN THE PAVEMENT WAS OPENED TO TRAFFIC TO
                C   THE END OF THE YEAR UNDER CONSIDERATION. CALL THIS VALUE W.
                C
0022              AADT=((SLOPE*TY+YI)+YI)/2.0
0023              W=AADT*A*DD/100.*TY*LD/100.*T/100.*365.*SPE
0024              Z=E/DK
0025              RA=7.0
0026              BB=SQRT(1.6*RA**2+H**2)-0.675*H
0027              RH=0.13879*H**2-6.59703
0028              B=30.64386*SQRT(H)-50.08820-3.77485*H
0029              SIF=1.9
0030              A1=SIF
0031              A2=SIC
0032              TOL=W*0.05
                C
                C   SOLVE BY TRIAL AND ERROR FOR THE SERVICEABILITY INDEX AT THE END OF THE YEAR
                C   UNDER CONSIDERATION. FIRST COMPUTE INITIAL VALUE FOR SI AND THEN ITERATE
                C   UNTIL THE SI COMPUTED GIVES THE CORRECT NUMBER OF EQUIVALENCIES ACCUMULATED
                C   TO THE END OF THE YEAR UNDER CONSIDERATION.  THE NUMBER OF EQUIVALENT LOAD
                C   APPLICATIONS TO REDUCE THE INITIAL SERVICEABILITY INDEX TO THE INDEX AT THE
                C   END OF THE YEAR UNDER CONSIDERATION IS COMPUTED USING THE NEW PERFORMANCE
                C   MODEL DEVELOPED USING LONG TERM PERFORMANCE DATA
                C
```

```
0033          101 SI=(A1+A2)/2.0
0034              Y=SI+(3.0/(2.71828**(-1.0*B/RH)+1.0))-SIC
0035              IF(Y.LT. 0.0) GO TO 92
0036              WW = ALOG10((RH*ALOG(3.0/Y-1.0) + B)*10.0**6.0)
0037              DMR=FF-(FF*FCV/100.)*FCONF
0038              LW=WW + (3.89256 - 0.70601*SI)*ALOG10(((DMR/690.)*(4.0*
                 1 ALOG10(8.78921*H**0.75/BB) + 0.359))/(4.0*ALOG10(Z**0.25*
                 1 0.54035*H**0.75/BB) + 0.359))
0039              WP=(10.0**LW)/RF
0040              IF(ABS(WP-W).LE.TOL) GO TO 92
0041              IF((WP-W).LT.0.0) GO TO 99
0042              A1=SI
0043              IF(A1.LT.2.0) GO TO 92
0044              GO TO 101
0045           99 A2=SI
0046              IF(A2.LT.2.0) GO TO 92
0047              GO TO 101
                C
0048           92 CONTINUE
0049              RETURN
0050              END
```



☆U.S. GOVERNMENT PRINTING OFFICE: 1978 O— 621-625/268 REGION 3-1

## FEDERALLY COORDINATED PROGRAM OF HIGHWAY RESEARCH AND DEVELOPMENT (FCP)

The Offices of Research and Development of the Federal Highway Administration are responsible for a broad program of research with resources including its own staff, contract programs, and a Federal-Aid program which is conducted by or through the State highway departments and which also finances the National Cooperative Highway Research Program managed by the Transportation Research Board. The Federally Coordinated Program of Highway Research and Development (FCP) is a carefully selected group of projects aimed at urgent, national problems, which concentrates these resources on these problems to obtain timely solutions. Virtually all of the available funds and staff resources are a part of the FCP, together with as much of the Federal-aid research funds of the States and the NCHRP resources as the States agree to devote to these projects.*

### *FCP Category Descriptions*

**1. Improved Highway Design and Operation for Safety**

Safety R&D addresses problems connected with the responsibilities of the Federal Highway Administration under the Highway Safety Act and includes investigation of appropriate design standards, roadside hardware, signing, and physical and scientific data for the formulation of improved safety regulations.

**2. Reduction of Traffic Congestion and Improved Operational Efficiency**

Traffic R&D is concerned with increasing the operational efficiency of existing highways by advancing technology, by improving designs for existing as well as new facilities, and by keeping the demand-capacity relationship in better balance through traffic management techniques such as bus and carpool preferential treatment, motorist information, and rerouting of traffic.

**3. Environmental Considerations in Highway Design, Location, Construction, and Operation**

Environmental R&D is directed toward identifying and evaluating highway elements which affect the quality of the human environment. The ultimate goals are reduction of adverse highway and traffic impacts, and protection and enhancement of the environment.

**4. Improved Materials Utilization and Durability**

Materials R&D is concerned with expanding the knowledge of materials properties and technology to fully utilize available naturally occurring materials, to develop extender or substitute materials for materials in short supply, and to devise procedures for converting industrial and other wastes into useful highway products. These activities are all directed toward the common goals of lowering the cost of highway construction and extending the period of maintenance-free operation.

**5. Improved Design to Reduce Costs, Extend Life Expectancy, and Insure Structural Safety**

Structural R&D is concerned with furthering the latest technological advances in structural designs, fabrication processes, and construction techniques, to provide safe, efficient highways at reasonable cost.

**6. Prototype Development and Implementation of Research**

This category is concerned with developing and transferring research and technology into practice, or, as it has been commonly identified, "technology transfer."

**7. Improved Technology for Highway Maintenance**

Maintenance R&D objectives include the development and application of new technology to improve management, to augment the utilization of resources, and to increase operational efficiency and safety in the maintenance of highway facilities.

---

* The complete 7-volume official statement of the FCP is available from the National Technical Information Service (NTIS), Springfield, Virginia 22161 (Order No. PB 242057, price $45 postpaid). Single copies of the introductory volume are obtainable without charge from Program Analysis (HRD-2), Offices of Research and Development, Federal Highway Administration, Washington, D.C. 20590.